Abstract

β-Diketonates for Chromatographic Analysis

A.C.Hunt

Three novel fluorinated, aromatic β-diketones, p-Methylbenzoyl-1,1,1-trifluoroacetone (p-Me-bta), Pentafluorobenzoyltrifluoroacetone (pfbtfa) and 1,1,1,2,2,3,3-heptafluoro-6-(pentafluorophenyl)-4,6-hexanedione (pfbhfh), based upon Benzoyl-1,1,1-trifluoroacetone (bta) have been synthesised, and the respective Group I, II, Ni, Cu, Zn, Pb, Cd and Hg chelates and complexes prepared. The solution stability, IR, UV and ^1H NMR spectroscopic, polarographic, thermal and vapour pressure properties of the chelates were systematically studied, and the conclusions derived applied to the gas and liquid chromatography of the metal chelates.

The β-diketones pfbtfa and pfbhfh and their respective metal chelates, though possessing fluoro-phenyl substitution, were shown nevertheless to behave spectroscopically, and polarographically in a manner similar to aliphatic - aliphatic terminally substituted β-diketones. Substituent effects in the β-diketonates were shown to operate equally on the oxygen atoms and the chelated metal ion. No evidence of a delocalised electron system within the chelate ring was observed. Physical parameters such as infra-red metal-oxygen bond stretch, polarographic half-wave potential and chelate methine proton resonance position, were linearly related to metal chelate solution stability constant.

The β-diketones were shown to impart insufficient thermal stability and volatility to the studied metals. Gas chromatography was only applied to the pfbtfa chelates, and proved largely unsuccessful. Liquid chromatography of the chelates confirmed the structural implications predicted from spectroscopic and polarographic studies.

TO MY MOTHER

β - Diketonates for Chromatographic Analysis

A thesis submitted to the Council for National Academic Awards in partial fulfilment of the degree of Doctor of Philosophy.

A.C.Hunt
Department of Physical Sciences
Trent Polytechnic, Nottingham.

June 1984

Abstract

β-Diketonates for Chromatographic Analysis

A.C.Hunt

Three novel fluorinated, aromatic β-diketones, p-Methylbenzoyl-1,1,1-trifluoroacetone (p-Me-bta), Pentafluorobenzoyltrifluoroacetone (pfbtfa) and 1,1,1,2,2,3,3-heptafluoro-6-(pentafluorophenyl)-4,6-hexanedione (pfbhfh), based upon Benzoyl-1,1,1-trifluoroacetone (bta) have been synthesised, and the respective Group I, II, Ni, Cu, Zn, Pb, Cd and Hg chelates and complexes prepared. The solution stability, IR, UV and ^1H NMR spectroscopic, polarographic, thermal and vapour pressure properties of the chelates were systematically studied, and the conclusions derived applied to the gas and liquid chromatography of the metal chelates.

The β-diketones pfbtfa and pfbhfh and their respective metal chelates, though possessing fluoro-phenyl substitution, were shown nevertheless to behave spectroscopically, and polarographically in a manner similar to aliphatic - aliphatic terminally substituted β-diketones. Substituent effects in the β-diketonates were shown to operate equally on the oxygen atoms and the chelated metal ion. No evidence of a delocalised electron system within the chelate ring was observed. Physical parameters such as infra-red metal-oxygen bond stretch, polarographic half-wave potential and chelate methine proton resonance position, were linearly related to metal chelate solution stability constant.

The β-diketones were shown to impart insufficient thermal stability and volatility to the studied metals. Gas chromatography was only applied to the pfbtfa chelates, and proved largely unsuccessful. Liquid chromatography of the chelates confirmed the structural implications predicted from spectroscopic and polarographic studies.

Acknowledgements

The author wishes to express his sincere thanks and gratitude to the following:

Dr's A. Braithwaite and F. Smith, Department of Physical Sciences, Trent Polytechnic, Nottingham, for their guidance, help and advice throughout the course of this thesis.

Upjohn Ltd. Crawley, West Sussex, and in particular Mr S. Isaac, for the use of computing facilities.

My wife Sonia, for her endless patience and encouragement, especially during preparation of the final draft.

DEO SOLI GLORIA

INDEX

PAGE

INTRODUCTION

SECTION 1

INTRODUCTION

1.1

The physiological effects of metal excess and deficiency

Biological and medicinal chemistry has shown that some 30 elements, eg; Sodium (Na), Potassium (K), Copper (Cu), Zinc (Zn), Iron (Fe), Magnesium (Mg), and Calcium (Ca) are essential for the maintainance of adequate health, both in plant life and 'in vivo'. Thus Zn, Mg and Ca are involved in DNA and RNA synthesis, and Fe and Cu are well established as being necessary for the transport of atmospheric oxygen to body tissue. Sodium and potassium are involved in the passage of ion-currents along nerve fibres, while Ca is known to be essential for the building of connective tissue.

The level of supply of essential trace elements to living organisms and plants is limited however to a fairly narrow range, deficiency or excess of supply causing symptomatic responses dependent upon both the time length and degree of excess or deficiency. Thus deficiency of Cu in man, causes both defective melanin production, due to a suppression of tyrosinase enzyme activity, and skeletal and vascular disorders, together with anaemia. Zinc deficiency results in anorexia and parakeratosis, and foetal abnormalities in rodents. Nickel (Ni) deficiency has been shown (1) to cause liver damage and dermatitis in chicken, and rats fed on a Ni deficient diet showed impaired growth and reproduction. In practice, many of the essential trace elements have multiple and inter-related biochemical roles, and though many of these roles are now identified, it is often difficult to correlate a metal deficiency with the known functions of that element. Probable causes of this difficulty are that as an element becomes deficient, it is not lost at a uniform rate at all the sites at which it functions. Further, the most dramatic consequences of deficiency, are sometimes an indirect result of the loss of activity of a trace metal dependent enzyme-mediated reaction. A good example of this situation is provided by excess Fe accumulation in the liver, resulting from a severe Cu deficiency.

Excess of metals in physiological systems is generally easier to observe. Symptoms arising from Lithium (Li) excess include nausia, cardiac arrythmias and renal failure. Abnormally high levels of Cu show especially in Wilsons desease, characterised by a progressive development of neurological disturbances such as tremor and rigidity. Impaired growth and cerebral disorders have also been attributed to Cu toxicity.

TABLE 1 lists the levels at which some trace elements are considered at normal, excess, and at deficient levels, in the average human diet (expressed in mg/day).

Other important areas of clinical nutrition still remain largely unexplored, either because ethical restraints hinder the common practice of the use of radioisotopes, or because certain clinical studies can not be made with existing technology and methods (2).

Not only do toxic effects result from an excess of those elements regarded as necessary to proper physiological health, but many other metals, arising from industry, have been shown to have marked toxic properties. The toxic effects of Lead (Pb) are well known, principally due to the frequent press given to the problems of lead in petrol. Lead exerts much of its activity through sulfhydryl inhibition, interaction with carboxyl and phosphoryl groups, and interference with haem synthesis. Cadmium (Cd) also inhibits sulfhydryl enzymes, and disrupts the pathways of oxidative phosphorylation, as well as causing damage to the liver, kidneys and teeth. Barium (Ba) is extremely toxic. The systemic action of Ba is characterised by an intense stimulation of muscles, vomiting, colic and haemorrage resulting from its action on the gastro-intestinal system. Motor disorders are observed and cardiac arrest and death frequently occur. Mercury (Hg) has also come to public prominance, following the Minimata disaster (3). In common with Pb and Cd, Hg has a great affinity for sulfhydryl groups, and also combines with phosphoryl, carboxyl, amine and amide groups. Mercuric ions also inhibit enzymes and precipitate proteins.

1.2

Metal pollution in aqueous media

The metals mentioned above, arising from street dust, industrial effluents, domestic waste and natural sources (volcanic action, erosion, etc.), collectively form a major source of metal input to surface waters. These waters are routed via sewerage treatment works in order to reduce the amount of metal discharged into rivers and sea water. The biological availability and toxic effects of metals, once in an aqueous body are dependent upon their chemical speciation, and the forms in which the metals now exist will determine their mobility and distribution, ie; whether they exist in solution, suspension or in association with bottom sediments. This in turn will influence the likelihood of the metals finding their way into the general public water supplies. Laboratory studies (4) have shown that humic and fulvic acids, the predominant forms of organic matter in effluent waters, are able to strongly bind to metals, forming high molecular weight complexes, which collect in the sludge deposits remaining after effluent treatment. Other studies (5) have shown that clay particles, present in sludges and soils, occlude heavy metals. It has been estimated (6), that 80% of metal pollutants entering a sewerage works are taken up by sludge materials during purification, the remaining 20% running off into water courses.

The exact composition of sludge deposits varies from area to area, but a typical sample, taken from the Beckton works in E. London, can be shown to be made up of two major components, metal content and organic matter. The metal content of Beckton sludge is shown in TABLE 2.

The organic matter in sludge is essentially that of β-humus, composed of humin, humic and fulvic acids. Humic substances are those materials produced in soils that are either yellow-brown or black in colour, acidic polydisperse substances of relatively high molecular weight. The group is divided into three classes differentiated by solubility in acid or alkali:

Fulvic acid	-	acid and alkali soluble	MW $\sim$ 1,000
Humic acid	-	acid insoluble	
		alkali soluble	MW $\sim$ 10,000
Humin substances	-	acid and alkali insoluble	MW $\sim$ 30,000

Fulvic acid

This is light brown in colour. The fraction appears to be lower in carbon and higher in oxygen content tnan the associated humic acid, and is therefore of usually high acidity. It is thought that phenol carboxylic acid units are held together by H-bonding. A suggested structure of Fulvic acid is shown below.

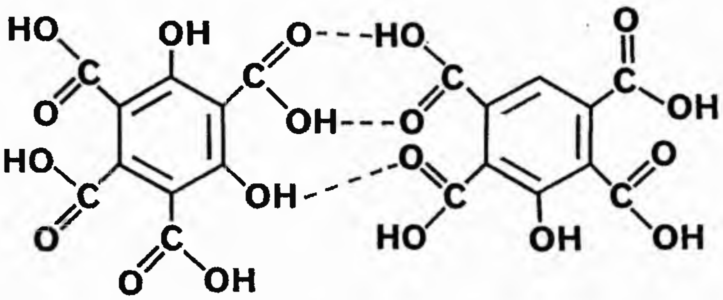

The relatively large inter-molecular spaces act as a trap for small organic molecules, such as alkanes, fatty acids and dialkylphthalates, as well as metal ions of the appropriate dimensions.

Humic acid

This is dark brown in colour, and consists of the following known components:

26%	Functional groups
15%	Single ring aromatics
10%	Amino acids
10%	Polycyclic aromatics
4%	Aliphatics

The basic structural unit of humic acid is thought to be:

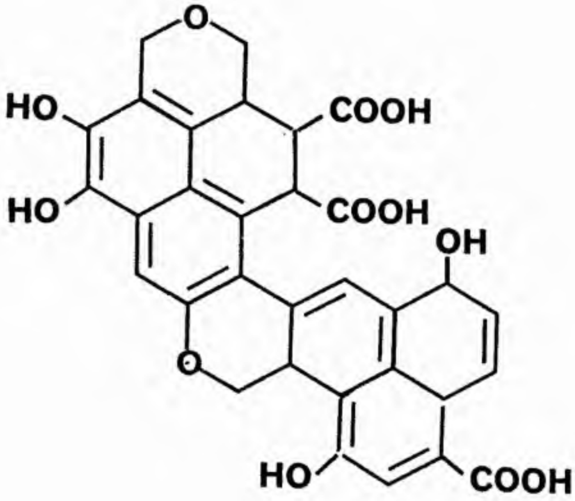

The disposal of sludge deposits from sewerage works has generally been achieved by four methods (7); incineration, sea disposal, land-fill and agricultural application. Incineration is too costly. Sea disposal, which has been carried out for some time, is now being severely restricted, due to impending EEC legislation. The third and fourth options of land-fill and using the sludge as a source of agricultural fertilizer accounted for some 15 million tonnes of sewerage sludge in 1980 (8) (almost half the total arising), at a cost of approximately £50 million. The advantage of sludge disposal on land is the close similarity between the organic matter in soil compared to sludge material. Fractionation of the organic matter in soil has shown (9) a composition by weight of:

45% Humin
30% Humic acids
20% Fulvic acids (including polysaccharides)
5% Resins, waxes, fats etc.

However, the associated metal ions bound into sludge severely limit the widespread use of sludge as a cheap source of agricultural nutrient. Field experiments (8,10), and a review (11) of common foodstuffs grown on soil enriched with known amounts of sludge have shown an unnacceptable degree of metal uptake from the soil, into the plant.

A comprehensive recent review (12) discusses the chemistry of toxic trace metals in the environment.

1.3

Methods of trace metal analysis

The increased need for rapid, accurate and sensitive means for the analysis of metals in sludges, and a variety of matrix forms, has therefore paralleled the growth in concern of the effect of toxic heavy metals upon the environment. A number of reviews have appeared in recent years detailing the available methods of trace element analysis, eg; polarographic (13), atomic absorption (14,15), colorimetric (16), ion-selective electrode (17) and activation analysis (18).

One of the severe practical difficulties in trace element analysis, is the physical or chemical separation necessary to isolate the elements of interest from the bulk sample matrix. Traditionally, extraction has been the method most utilised. However, as equipment detection limits and sensitivities have improved, together with a greater need for ultra-trace analysis, the potential sample losses become more and more important. Alternatives to extraction have therefore been investigated.

One method that has demonstrated high sensitivities and detection limits is that of chromatography, both Gas Chromatography (GC) and High Performance Liquid Chromatography (HPLC). However, few inorganic species are sufficiently volatile in themselves to allow successful GC, (where a vapour pressure of approximately 0.1mm Hg at column operating temperatures is regarded as the required volatility to allow the partition equilibria between the column stationary phase and the mobile phase). Methods have been developed therefore to bring the metal(s) under analysis into a suitable volatile form. One method of accomplishing this is by the direct volatilization of the trace elements in a sample.

1.3.1

Volatilisation techniques

Although the formation and volatilisation of a few inorganic species, such as H_2S, SiF_4, H_2SiF_6 and SeH_4 has been employed in some analytical applications, volatilisation of trace elements was truly established as a practical technique by Geilmann and co-workers (19-21). He defined the method as 'evaporation analysis', since an element was evaporated out of a matrix. TABLE 3 lists some examples of elements volatilised out from a sample non-volatile matrix.

The method has been extended by the use of reactions that lead to volatile derivatives, eg; by the use of halogens. TABLE 4 lists those elements that form volatile compounds with a reactant gas.

A number of different means may be used to achieve sample vapourisation.

1) A reactant gas may react with the trace elements alone to form the volatile compound, the non-volatile matrix remaining.
2) A reactant gas may react with the matrix, whereby the non-volatile trace elements are not vapourised.
3) A reactant gas may react with both matrix and trace elements to form volatile compounds.
4) A reactant gas reacts with both matrix and trace elements, but only the trace elements are volatilised.
5) A solid substance is used for the generation of volatile compounds.

The examples quoted in TABLE 3 are characteristic of the first type, although no reactive gases are used. A disadvantage of this method is that occluded trace elements are liable not to react with the passing gas stream. The second method is suitable for those elements that volatise in an O_2 stream, eg; Li, Na, Cd, Tl and Pb. In the third method, the separation of the volatile matrix from the trace elements of interest occurs at a later stage by, for example, desorption or fractional distillation. The advantage of this method is that the reaction is complete, the potential problems of the first method being eliminated. Applications of method 3 include the analysis of Al, Nb and Ta by chlorination of the sample matrix. The fourth method is limited in application, though is superior to the first method. The fifth method finds use in, for example, the addition of $NaBH_4$ to a matrix to form volatile hydrides, though there is a greater potential for sample contamination by this method.

Geilmann (19) and Heinrichs (20) have described in detail the apparatus necessary for element analysis be methods 1-4. Suitable gases for inducing volatilisation include inert gases (Ar, He), reactant gases (H_2O, O_2, H_2, CCl_4, HCl, F_2, Br_2 and HF), and complexing gases such as $AlCl_3$. The flow rate of gas over the sample matrix is not important, so long as it is high, but the use of high purity gases is essential. Thus the presence of O_2 or H_2O in chlorinating gases may lead to the formation of non-volatile oxides or partially volatile oxy-chlorides. Complex mixtures can be resolved by temperature programming, as commonly used in gas chromatography, and by the use of facilities for quickly switching gas flows. The reproducibility of element vapourisation has been checked by the use of radionuclides, in the same chemical state as the trace elements under study in the sample matrix. In practice, although there is no limit to the amount of sample that can be vapourised, eg; up to 5g (21), the sample needs to have as large a surface area as possible exposed to the passing gas stream. Further, the temperature should not be so high as to cause the sample matrix to melt, as volatile compounds would be liable to dissolve in the melt. However, this has been exploited by Bachmann (22), for the surface analysis of Ta in a melt of In.

Many elements, eg; Li, Na, K, Cs, Pt, Zn, Cd, Hg, Ga, Sn, Pb, Mg, Bi and Se can be determined by initially a direct vapourisation in an inert gas stream, or in an O_2 stream. (The high volatility of these elements is often the cause of sample losses by classical fusion methods, such as arc and spark spectroscopy). Geilmann and Hepp (23) separated Cd from Zn by this method, where CdO was reduced in an H_2 gas stream below 300°C, ZnO not being reduced at temperatures below 360°C. Following reduction of the CdO, the Cd was evaporated at a temperature at which ZnO was involatile.

In some cases, all the trace elements within a sample are volatilised at the same time or temperature. Spachidis (24) showed that analysis of the trace elements within a sample of Aluminium using HCl gas resulted in the trace elements all being volatilised at approximately 450°C. Even Na was partially evaporated, due to formation of the volatile complex $NaAlCl_4$. Following a second step in which the chlorides were condensed, the trace elements were resolved by a stream of Ar, so removing them from the $AlCl_3$ matrix. Spachidis (25) has utilised matrix volatilisation of Group I and II metal carbonates using Ar for the quality control of optical waveguide materials, where trace impurities of Cu, Cr, Co, Fe, Mn, Ni and V absorb light in the

900-1000nm range. Analysis of chemicals used in the manufacture of semi-conductors, particularly those used for MOS products, can also be achieved in this way (26).

Bachmann (21) found that alkali metals could be evaporated from biological materials with 90% recovery, and Tolg (27) determined As, Se and Cd in biological materials using an O_2 stream. Plutonium has been determined by Bachmann (28) by volatilisation, using $AlCl_3$ in a stream of Cl_2 and CCl_4, other elements such as alkali metals, which are also volatilised, being deposited along a thermal gradient. This method is much superior to the traditional method of extraction of Plutonium into Tributylphosphate (TBP).

The determination of anions is also possible using the volatilisation technique. Fluorine has been determined in rocks by Farzaneh and Troll (29), using the formation of H_2SiF_6, and by Burguera and Townsend (30) who utilised the formation of SiF_4. Chloride has been determined (31), by a similar method using HCl gas. Bachmann (32) determined HCl in air by the formation of volatile chromylchloride, prior to analysis of Cr by atomic absorption.

Following the volatilisation of trace elements from a sample matrix, a common method of separation is by gas chromatography. However, the development of GC applied to inorganic chemistry is not as advanced as traditional GC as applied to the analysis of organic compounds. Reasons for this include the lack of commercial gas chromatographic equipment operating at temperatures in excess of $500^{\circ}C$, and the difficulty in handling very hot, corrosive, oxidising and reducing gases. These difficulties notwithstanding, there are nevertheless advantages to be enjoyed in the use of GC for the analysis of inorganics:

1) Resolution of sample components is potentially good.
2) Multielement analysis is possible.
3) If using non-selective detectors, an element may be characterised by its retention time or volume.
4) If just one element is under consideration, the different speciations of that element may be determined.

TABLE 5 gives a brief comparison of inorganic to organic GC, the main differences being that organic GC is used for the analysis of compounds, while inorganic GC is used for the analysis of elements.

TABLE 6 lists some typical metal and metalloid separations achieved with high temperature GC. Jackwerth (33) and Skogerboe (34) have determined Ge, As, Sn and Sb via their hydrides. Bachmann (35) resolved a mixture of tetravalent metal chlorides on a NaCl stationary phase, over a temperature range of 200-900°C. Steffen (36) determined Os, Ir, Ru, Tc and Re by the GC of their volatile oxides.

To overcome the difficulties raised by the use of high temperatures, alternatives to the normal packed column have had to be found. Since most inorganic compounds react with metal surfaces at high temperature, all contact with exposed metals must be avoided. Rudolph (37) has described how a column can be made from fused quartz, where one end serves for on-column injection of the sample, thus avoiding the use of additional fittings. Problems can arise with the mobile phase, where the separation mechanisms occuring in the column can be affected. Thus the decomposition of a chloride resulting in non-volatile substances may occur, and be adsorbed onto the stationary phase, only to re-react with the mobile phase at a later point. This does have the advantage however that any impurities in the column are being constantly scavenged away.

TABLE 7 lists some of the stationary phases used in inorganic GC. Five groups are characterised:

(a) This group includes those stationary phases that are common to traditional GC, eg; silicone oils and squalane. Separation of low boiling point gases such as CO and H_2, $SiCl_4$, $GeCl_4$, $SnCl_4$, $TiCl_4$ and Hg compounds have been effected on these. Hamlin (38) separated a mixture of halogen oxides and interhalogen compounds on KEL-F 40 oil at 60°C. Pappas (39) separated a mixture of UF_6 and bromine fluorides on a perfluorinated alkane at 50°C.

(b) The second group consists of those substances known to have very large surface areas, such as Al_2O_3, silica gel, activated carbon, quartz, graphite and molecular sieves. With these packing materials gas-solid equilibria are involved. Agliulov (40) used silica gel for the analysis of organic impurities in commercial $GeCl_4$. Vlasov (41) performed a preparative scale separation of Ti and Fe chloride on the same adsorbent. Zvarova employed a glass capillary column for the analysis of rare earth (42) and actinide (43) chlorides.

(c) The third group comprises of solid metal salts, eg; NaCl, KCl, CsCl. These are common stationary phases for the analysis of chlorides as described above (35).

(d) The fourth group consists of liquid stationary phases of fused metal salts of low boiling point, usually as eutectic mixtures. TABLE 8 lists some inorganic and eutectic chlorides that are suitable as liquid stationary phases (44).

The choice of metal salt for a liquid stationary phase is subject to the same restrictions as that of conventional phases. It must be a liquid at the analytical temperature, it must not have an appreciable vapour pressure at this temperature, and it must be a solvent for the analytes, but must not react with them.

Juvet and Wachi (45) reported the first separation using this type of stationary phase, $TiCl_4$ and $SbCl_3$ were eluted at 240°C from a column packed with Sil-O-Cel impregnated with the eutectic $BiCl_3/PbCl_2$. Zado and Juvet (46) resolved a mixture of $NbCl_5$ and $TaCl_5$ at 444°C on LiCl/KCl, and again at 329°C on the eutectic $InCl_3/TlCl$.

(e) The final group consists of large surface area supports coated with inorganic salts. Bachmann (21) has reported the separation of interhalogen compounds on graphite coated with $HfCl_4$.

Having achieved separation, the problem of detection remains. Ellis et al (47,48) employed a gas density detector for the analysis of UF_6, Cl_2, Br_2, HF, ClF and BrF_5. This detector has the advantage that the detector sensing elements do not come into contact with any corrosive vapours. Spachidis (25) has described the coupling of a volatilisation apparatus with a number of detection systems, such as XRF, AA, MS and α-spectroscopy. For GC applications, an on-line coupling is usually necessitated, whereas for volatilisation alone, off-line coupling is possible, though some form of sample collection is needed. GC/MS, routine for the analysis of organic compounds, has not been much used for the analysis of inorganic compounds derived from volatilisation/GC because of the technological problems. Direct coupling to AA is only feasible when the volatile compound is released rapidly, otherwise broad peaks result, in which case the sample must be first trapped, by for example, condensation. This then has the disadvantage that the element analysis can only be carried out one element at a time. Similar restraints are liable upon other detection systems.

To overcome the use of high temperature for the GC of inorganic materials, methods of metal derivatisation, forming volatile compounds have therefore been studied. One such is the formation of organo-metallic compounds, where for the purpose of this thesis, an organo-metallic compound is defined as a compound in which there is a metal-carbon bond, frequently through π-bonds.

Tanikawa and Arakawa (49) were the first to undertake a systematic study of the use of GC for the analysis of ferrocenes. They used SE30, SE32, Apiezon L and PEG 6000 liquid stationary phases, with column temperatures of between 170-200°C. Nessmeyanov (50) studied the GC of ruthenocene and acetyl ruthenocene on polyethylene glycols, and Devyatykh (51) separated ethyl derivatives of dibenzenechromium on SE30 at 200°C. Longi and Mazzochi (52) attempted to separate a mixture of Sb, Sn, Pb, Al, Be, Zn and B alkyls on a liquid stationary phase of 85% paraffin, 15% triphenylamine. Good separation of $Sb(Et)_3$, $Sn(Et)_4$ and $Pb(Et)_4$ was obtained, but the other compounds were poorly eluted, with much tailing and poor resolution. Estes et al (53) determined volatile π- and carbonyl compounds of V, Cr, Mn, Fe, Co and Ni on a fused silica wall coated open tubular capillary column, using a microwave plasma emission detector.

Many organo-metallic compounds are not sufficiently volatile to be determined by GC. One method of overcoming this is to perform an on-column hydrolysis, using a micro-reactor, on the organo-metallic compound, and then to analyse for the resulting hydrocarbon. This has been applied to derivatives of Al by Dijkstra (54), and Hg and Mg by Guild (55). Dawson (56) developed a quantitative method for the analysis of Pb alkyls in petrol using SE30 and temperature programming between 20-90°C. However a disadvantage to Pb alkyl GC is the possibility of exchange reactions taking place on the column, between methyl and ethyl radicals of $Pb(Me)_4$ and $Pb(Et)_4$.

The GC of metal carbonyls has seen little work. Pommier and Guiochon (57) resolved Fe, Cr, Mo and W carbonyls on squalane and Apiezon L at 90°C, and Turkel'taub et al (58) have analysed tricarbonylcyclopentadienylmanganese on Apiezon L at 60°C.

Conclusion

In terms of the routine analysis of trace metals, the above methods are generally impracticable. Volatilisation requires the use of high temperatures and often the use of corrosive and reactive gases, with the subsequent difficulties in handling, as well as unusual, expensive and suitably modified GC and detection equipment. Metal derivatisation by the formation of organo-metallic compounds, is only really applicable to a limited number of elements, eg; Hg, Se, Pb, Sn, Ge, transition and platinum metals. Many of these compounds are also light, air, moisture and temperature sensitive, and so increase handling difficulties.

A method of metal derivatisation that is not affected by the above constraints is the formation of metal chelate compounds with 1,3-diketones.

1.3.2

Metal derivatisation via chelate compounds

1,3- β-diketones are conveniently prepared by the Claisen condensation of ketones with esters, using base catalysis. Hauser et al (59) have reviewed the preparation of β-diketones.

1,3-diketones exhibit keto-enol tautomerism:

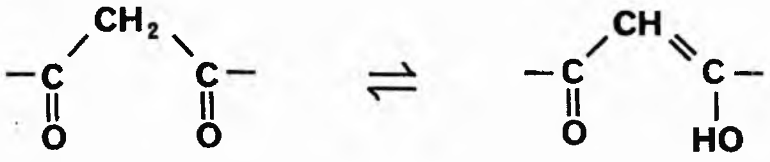

- where the enol form is stabilised by intra-molecular H-bonding. Under suitable conditions, the enolic hydrogen atom can be replaced by a cation, to form (usually) a chelate ring, thereby shifting the tautomeric equilibrium in favour of the enol form.

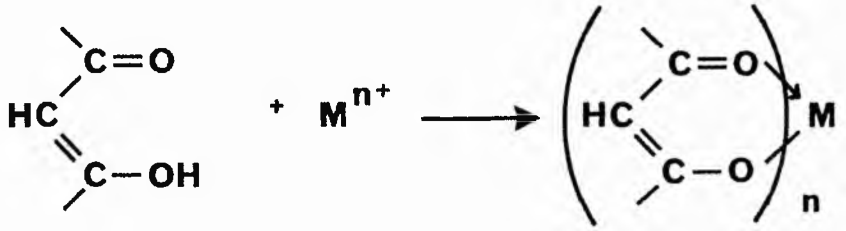

The ability of a 1,3-diketone to form such chelate compounds, is therefore influenced by the proportion of enol form in solution. The electronic and structural factors that determine enol contents have been investigated. Hammond et al (60) studied the properties of a series of 1,3-diketones, in which the steric requirements of the R groups in alkyl substituted acetylacetone were varied by progressive branching. It was shown that by increasing the branching of R, the enol content of a β-diketone increased, to the point where the 1,3-diketone dipivalylmethane (dpm) had no detectable diketo form:

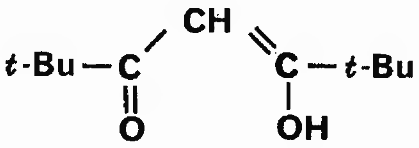

(dpm)

The variation in enol content was attributed to steric effects. Acetylacetone can adopt the configurations shown below:

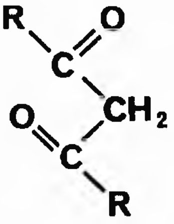

(i)

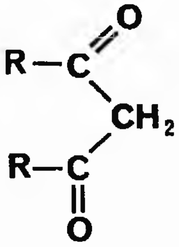

(ii)

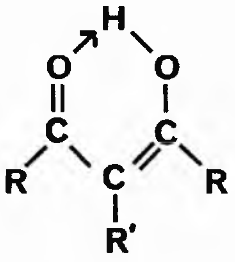

(iii)

- since these forms minimise dipole-dipole interactions. However, models of conformers (i) and (ii) for dpm indicate that much steric strain and electrostatic repulsion exists for the carbonyl moments, thus forcing the molecule into the enol conformer (iii). It would therefore be expected that substitution for hydrogen on the central carbon atom in (iii) would reduce enol content. Burdett and Rogers (61) have confirmed this prediction studying a range of β-ketoesters and β-diketones. They noted that bulky α-substituents caused a large reduction in enol content for such compounds. They also noted that terminal substitution of highly electronegative perfluoroalkyl groups such as CF_3, caused an enol increase, due to electron withdrawal from the region of the α-proton. Terminal aryl substitution to give for example, benzoylacetone (bza) and dibenzoylmethane (dbzm) and thenoyltrifluoroacetone was also observed to result in an enol increase. Electron withdrawal was again cited as the determining factor.

Keto-enol ratios have been determined by bromine titration (62-64), IR (65), UV (66) and refractive index measurements (67). However, none of these methods has been shown to be generally applicable for providing reliable quantitative information on keto-enol ratios.

Jarrett et al (68) showed that ^{1}H NMR provided an easy and accurate method of determining keto-enol ratios in 1,3-diketones. They determined enol contents of acetylacetone and 3-methylacetylacetone using this method. Springer et al (69) determined the enol content of 1,1,1,2,2,3,3-heptafluoro-3, 5-octanedione (fod), and Burdett and Fritz (70) determined the enol content of 1,1,1,2,2,6,6,7,7,7-decafluoro-3,5-heptanedione. Filler and Naqvi (71) studied enol contents of fluoro-β-ketoesters, and Reeves (72) studied the effect of solvent on the ^{1}H NMR spectra of acetylacetone solutions, and noted that the formation of solution complexes was the reason for variation in the observed resonances and enol content. TABLE 9 shows values of enol content of some β-diketones obtained by the NMR method.

β-1,3-diketones react with metals and metalloids, with the formation of M-O or M-C bonds, though both bonding types can occur.

With highly electropositive metals, such as the alkali metals, β-diketones act as monodentate ligands, forming salt-like compounds, where the metal and ligand exist as an ion-pair. Sidgwick and Brewer (73) have prepared acetylacetonates and benzoylacetonates of Na:

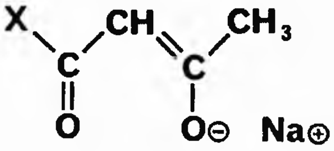

$X = CH_3, \phi$

The common mode of bonding is to form a six-membered ring, usually of high stability. Morgan et al (74) studied the general chemistry of a range of metal acetylacetonates:

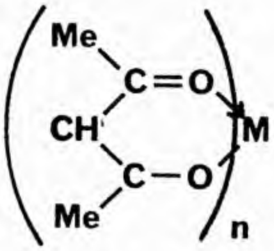

- where 'n' is the metal ion valency. For cases where the co-ordination number of a metal ion is double the metal ion valency, neutral molecules are formed, eg; Be(acac)$_2$, and Fe(acac)$_3$. If however, the co-ordination number is greater than the metal ion valency, the resulting chelate can act as a Lewis acid, achieving full co-ordination by intermolecular polymerisation, or by the formation of adducts,
eg; Ni(acac)$_2$.2H$_2$O.

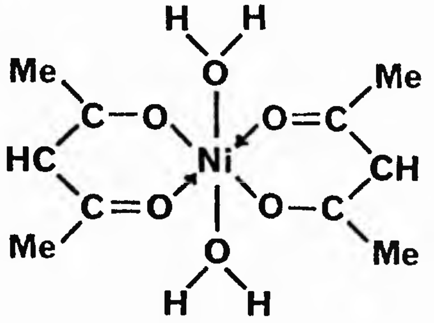

Other examples include $[Co(acac)_2]_4$ and $[Zn(acac)_2(NH_3)_2]$.

Metal-carbon (M-C) bonding occurs, for example in Se and Te β-diketone complexes. Dewar et al (75) reported the formation of three possible Se complexes with acetylacetone, the principal product (shown below), being obtained by reacting $SeCl_4$ with acetylacetone:

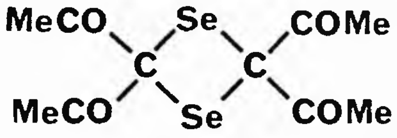

Confirmation of the above structure has been given by IR and ^1H NMR spectra (76), where ring proton vibrations, as shown for M-O bonded metal chelates were absent (see below).

Both M-O and M-C bonding has been proposed for β-diketone complexes of Hg. Bonati and Minghetti (77) proposed the structure:

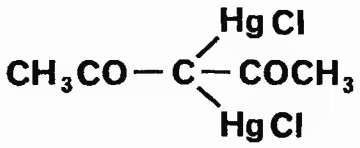

$$CH_3CO-C(HgCl)_2-COCH_3$$

- as the product of the reaction between mercuric chloride and acetylacetone. Thus the IR spectrum of the complex failed to show absorption bands in the region 1500-1600 cm^{-1}, expected if the complex were of a classical chelate ring type, but did however show a strong carbonyl band at 1685 cm^{-1}, and a Hg-C stretch band at approximately 500 cm^{-1}. No Hg-O stretch between 400-500 cm^{-1} was observed. The ^{1}H NMR spectrum of the complex showed one band at $\delta = 2.29$ ppm.

Other workers (78-80) have prepared 'Hg(11) acetylacetonates' and though IR spectra of the products, obtained by different synthetic routes were identical, analytical data were not reproducible. Bonati and Minghetti (77) suggested that the reason for this apparent discrepancy was due to the Hg complexes being either a mixture of variable proportions of insoluble C and O bonded complex, or an oligomeric molecule in which C and O bonded uni- and divalent acetylacetone residues are linked by Hg atoms.

Hammond et al (81) reported the preparation of $Hg(dpm)_2$, and on the basis of ^{1}H NMR and IR spectra assigned the structure:

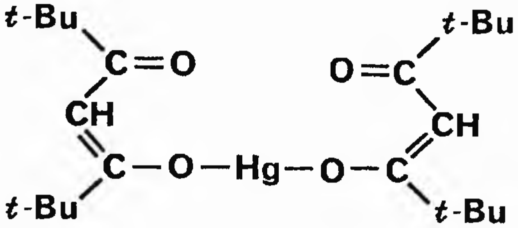

However, Bonati and Minghetti (77) suggested the type of fast exchange as shown between the forms:

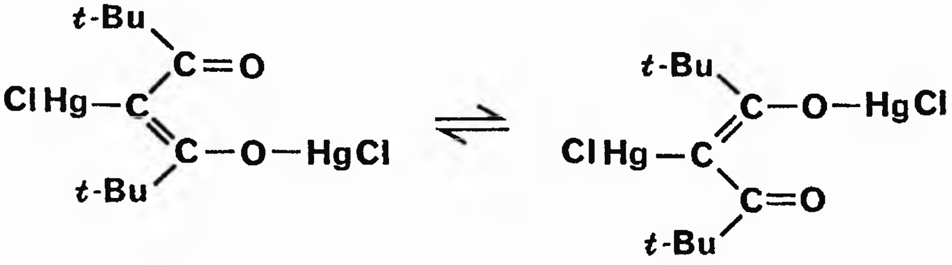

X-Ray diffraction analysis of dipivalylmethyl-mercury acetate (82), and bis(dipivalylmethyl)mercury (83) has confirmed both complexes to be C-Hg bonded. Allman et al (83) have reported the formation of diorganomercurials from the reaction of Hg(11) acetate with excess β-diketone. Fish (84) has reported similar products if a perfluoropropyl group is present in the diketone:

$$2\,RCOCH_2COR' + Hg(OAc)_2 \longrightarrow \left[RCOCH\,COR'\right]_2 Hg$$

It was also shown by ^1H NMR that the above complex exists as in a tautomeric equilibrium, according to:

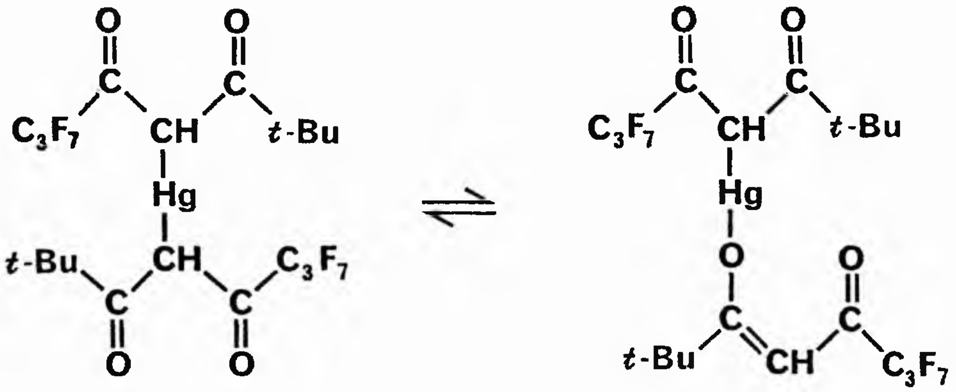

- and having equilibrium activation parameters of $\Delta H = 9.35 + 0.4$ KCal mol^{-1}, and $\Delta S = -3.45 + 1.6$ eu.

Complexes of the type Hg(L) with acetylacetone and benzoylacetone have been reported (85) but have not been successfully characterised.

1.4

The chromatographic analysis of metal chelates

1.4.1.a β-1,3-diketonates

The use of chromatographic methods for the quantitative analysis of metals, as their chelated derivatives, has only been explored during the last twenty years, and though Morgan and co-workers (86) noted that β-diketone ligands complexed with metals often resulted in the formation of significantly volatile compounds, it was not until 1955 that Lederer (87) suggested that separation of metal acetylacetonates might be possible by GC. In 1960, the first successful GC elution of metal acetylacetonates of Be, Al and Cr was achieved by Biermann and Gesser (88), although Duswalt (89) had reported the chromatography at an earlier date of Be, Sc and Zn acetylacetonates. Al and Cr acetylacetonates have been successfully eluted (90), as have chelates of V, Cu and Fe(111) (91). However, the range of applications of metal acetylacetonates to GC is limited, as most acetylacetonates are not sufficiently volatile to be eluted without decomposition. Sievers et al (92) demonstrated that the attempted GC of acetylacetonates of Zr, Hf, Co, Th and Ti at column temperatures of between 150-230^{o}C resulted in the decomposition of the metal chelates. It was shown that the decomposition of a metal chelate may itself lead to a volatile compound. Collection and examination of the eluate resulting from the GC of Co(111)acac showed that the peak was due to a decomposition product. The work of Charles et al (93), revealed that many acetylacetonates decomposed at 191^{o}C in a nitrogen atmosphere, giving the gaseous decomposition products acetone,

CO_2, CH_4 and acetylacetone (identified by mass spectrometry (94)). Moshier and Sievers (92) have therefore pointed out that a paper by Yamakawa et al (95), in which the GC of Co(111), Mn(11), Mg, Ca, Ba and Cd acetylacetonates was reported, may be incorrect, the chromatograms possibly being the result of decomposition products common to several of the complexes. MacDonald and Shannon (96) using mass spectrometry, have shown that many acetylacetonates polymerise in the vapour state, forming such species as $Ca_3(acac)_6$ and $Ca_2(acac)_4$. It is now realised that most acetylacetonates are not as volatile and thermally stable as was once thought, though certain metals, notably Be, Al and Cr can be quantitatively determined (97,98).

To improve chelate volatility and thermal stability, other 1,3-diketones have been investigated. Considerable attention has been given to the 1,3-diketones arising from substitution of fluorine atoms into the acac molecule, resulting in the development of the 1,3-diketone ligands trifluoroacetylacetone (tfa) and hexafluoroacetylacetone (hfa).

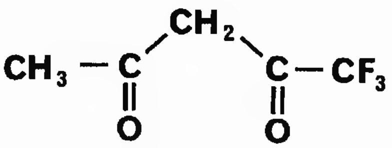

tfa

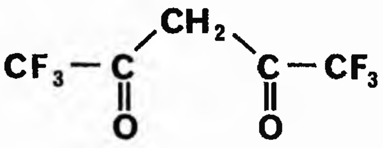

hfa

Metal chelates of these ligands have increased volatility, compared to the analogous acetylacetonates. Ross (99) demonstrated that on a column of 20% Dow Corning silicone fluid 710R, and using a nitrogen carrier gas, oven temperatures of 90, 162 and 215°C were required for the elution of Cr chelates of hfa, tfa and acac respectively, and again 90, 162 and 185°C for

Al chelates of these ligands. Sievers et al (100) compared elution temperatures of metal chelates of acac, tfa and hfa. Acetylacetonates of Be, Al, Cu and Cr were eluted at oven temperatures between 150-200°C, trifluoroacetylacetonates between 100-150°C, and Cr(111)hfa at 30°C. Goan et al (101) and Sievers (102) have shown that the thermal stability and volatility of Cr(111)hfa allows it to be steam distilled from water, and to be distilled unchanged from boiling concentrated H_2SO_4. Reasons for the increased volatility of fluorine substituted chelates are not clear, though several possible explanations have been proposed (92):

(a) A reduction in Van der Waals forces, and intermolecular H-bonding.

(b) Molecular models of octahedrally coordinated hexafluoroacetylacetonates, have shown that the majority of the chelate periphery is occupied by the 18 fluorine atoms, effectively encasing the central metal atom in a fluorocarbon cage, thus hindering close packing of the molecules in the crystal lattice.

(c) Fontaine (103) has suggested that the increased ease of elution of most hexafluoroacetylacetonates over trifluoroacetylacetonates is due to the hexafluoroacetylacetonates being less soluble in the stationary phase. The work of Wolf et al (104) supports this suggestion (see below).

Analytical applications based on the utilisation of fluorinated ligands are numerous. Sievers (102) resolved dl-Cr(111)hfa using a column of powdered d-quartz, and also reported (100) the resolution of cis and trans Cr(111)tfa on a silicone grease column.

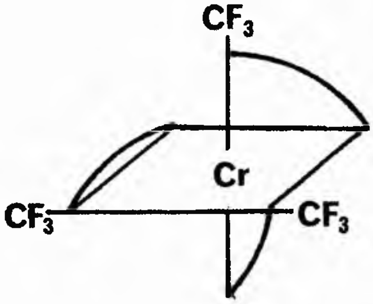
cis

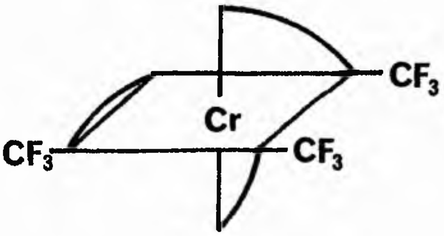
trans.

Ross and Wheeler (105) have determined Cr as the hexafluoroacetylacetonate, and Tanaka et al (106) have determined Cu, Al and Fe(111) on SE30 using hfa. Cartoni et al (107) have studied the ligand exchange equilibria between Al(111)acac and Al(111)hfa, and have also studied the metal-ligand equilibria occuring within a chromatographic column, using metal chelates as the stationary phase. Retention data was used to calculate equilibrium constants, free energies and entropies of reaction between a variety of ligands and their metal complexes. Wolf et al (104) studied the chromatographic thermodynamics of Al and Cr(111) chelates of tfa and hfa, and Cu, Pb, Cr(111), Fe(111) and Al chelates of 1,1,1,2,2,3,3-heptafluoro-7,7-dimethyloctane-4,6-dione (fod) in three different liquid stationary phases.

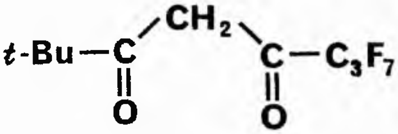

$$t\text{-Bu}-\underset{\underset{O}{\|}}{C}-CH_2-\underset{\underset{O}{\|}}{C}-C_3F_7$$

(fod)

Kownatski et al (108) studying Ca exchange in the human heart, reacted tfa with dried plasma and analysed for $Ca(tfa)_2$ using GC/MS. Hachey et al (2) have determined Fe(111) and

Cr(111) in plasma using a similar technique, and Hui et al (109) determined Cu in rat brain to nanogram levels. Cobalt has been determined in vitamin B12 and in liver extracts (110). Beryllium has been determined in air-borne dust (111), and lunar rocks (112), by reaction of the sample with tfa.

Sievers (113) has carried out a detailed survey of trifluoroacetylacetonates sufficiently volatile to be chromatographed. TABLE 10 lists the chelates investigated. Three classes of chelate are categorised:

(1) Class 1 includes those chelates that were successfully chromatographed, without any sample decomposition. Chromatograms of these chelates showed well defined peaks and were of reproducible retention time. Eluates were collected and examined, and it was shown that each chelate was eluted without decomposition. Complexes are listed in order of increasing retention time at 125°C on Dow Corning Silicone Oil 710. Class 1 chelates may be regarded as being suitable for routine quantitative analysis.

(2) For Class 2 chelates, well defined and reproducible peaks were recorded, condensed eluates showing no decomposition. However, it was noticed that a residue was present in the injection port, implying incomplete volatilisation of the sample.

(3) Class 3 metal chelates, for which only Nd(111)tfa is listed, includes those chelates that are not able to be chromatographed. At low temperatures, Nd(111)$_3$ remained in the injection port without volatilising. Increasing the temperature only resulted in decomposition of the chelate. At high temperatures, chromatograms were obtained, but these were shown to be due to decomposition products.

Practical difficulties also abound for hfa chelates. Schultz and Larsen (114) reported that hfa itself reacts readily with water, forming a solid tetrahydroxy compound:

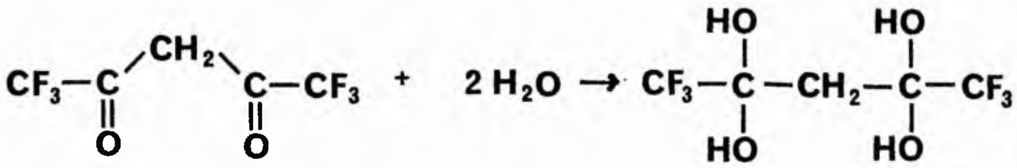

- which is a much poorer chelating agent compared to the anhydrous enol.

Norris (115) has reported that the hfa chelates of Fe(11), Co(11), Mn(11), Ni, Cu and Th(1V) can be prepared in aqueous solution, though hydrates are formed. However, many other metal hfa chelates, eg; Nb, Ti and Ta are moisture sensitive. For these reasons, the published literature on chelates of hfa is limited compared to the analogous trifluoroacetylacetonate literature.

Higher fluoroalkyl homologs of tfa have been prepared. Burgett and Fritz (70) reported the synthesis of 1,1,1,2,2,6,6,7,7,7-decafluoro-3,5-heptanedione (dfh) and the preparation of the respective Yttrium (70) and Cerium (116) group lanthanide chelates, prior to quantitative GC analysis.

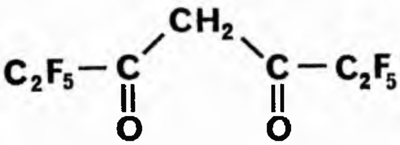

(dfh)

Smith et al (117) synthesised 1,1,1,5,5,6,6,6-octafluoro-2,4-hexanedione (ofh), and

1,1,1,5,5,6,6,7,7,7-decafluoro-2,4-heptanedione (dfd), and prepared their respective Zr, Hf and Cr(111) chelates, in anhydrous conditions. No significant improvement in chelate retention behaviour was observed over the analogous hfa chelates.

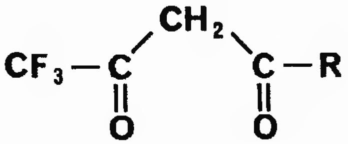

R = C_2F_5 (ofh)
R = C_3F_7 (dfd)

To extend the range of metal chelates capable of undergoing GC analysis, other 1,3-diketones have been investigated, and though there are potentially many possible ligands, only a few have shown sufficient chelate volatility to justify further study. One such is the 1,3-diketone 2,2,6,6-tetramethyl-3, 5-heptanedione (commonly refered to as dipivalylmethane (dpm)), where the bulky t-butyl groups encase the central chelated metal ion, and so prevent solvation effects such as the formation of hydrates.

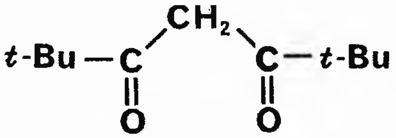

(dpm)

Berg et al (118,119) have reported on the volatility and fractional sublimation of a range of di, tri and tetravalent chelates of this ligand. They showed that dpm chelates possessed volatilities similar to those of the corresponding acetylacetonates, but less than those of the analogous chelates of tfa and hfa. Eisentraut et al (120) prepared and investigated dpm chelates of Sc, Yb and a range of lanthanides, and showed that the retention volumes on Apiezon greases varied regularly with the ionic radius of the coordinated metal. A feature of interest in dpm chelates is the surprisingly high volatility and thermal stability of the alkali metal complexes. Hammond (81) demonstrated that the alkali metal chelates of dpm could be purified by sublimation, without decomposition, and that they were soluble in organic solvents, when it would normally be expected that such complexes to dissolve only in polar solvents. Schwarberg (121) eluted Mg, Ca, Sr and Ba dipivalylmethanates on Apiezon L on a packed column when injected singly, but could not resolve a mixture of the chelates due to the proposed formation of a mixed metal polymeric species.

Fluorinated derivatives of dpm have been investigated. Three ligands that have received much study being 1,1,1-trifluoro acetylpivalylmethane (tpm), 1,1,1,2,2-pentafluoro-6,6-dimethylheptane-3,5-dione (ppm), and 1,1,1,2,2,3,3-heptafluoro-7,7-dimethyloctane-4,6-dione (fod) (122,123).

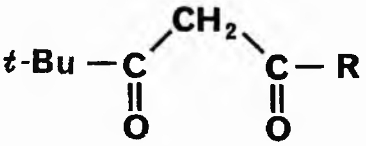

R = CF_3 (tpm)
R = C_2F_5 (ppm)
R = C_3F_7 (fod)

Belcher et al (122) have described the synthesis of these ligands, and have shown (122,123) that alkali metal chelates of these ligands are sufficiently volatile and thermally stable for

GC analysis, though mixtures of the chelates could not be resolved. They also studied the chromatography of the Pb chelates of the above ligands, but noted that quantitative results were not possible due to sample adsorption onto the stationary phase. Tanaka et al (124) have prepared Sc, Yb and rare earth chelates of tpm, and showed that they could be eluted without decomposition on SE 30. In common with $Nd(tfa)_3$ (115), $Nd(tpm)_3$ was not eluted without decomposition. The same workers (106) have determined Cu, Fe(111) and Al chelates of tpm on SE 30, as have Uden and Jenkins (125). Hachey et al (2) determined Mg and Ca, and their isotopic ratios in plasma by GC/MS of their ppm and fod chelates respectively. Springer et al (69) determined 15 rare earth fod chelates, and showed them to be more volatile than any other known lanthanide chelate. Ross et al (126) resolved cis and trans isomers of $Co(fod)_3$.

For the quantitative analysis of metals, different detector systems have been evaluated for their sensitivity and selectivity towards the eluted metal chelates.

The thermal conductivity detector (TCD) has been applied with success to the analysis of metal chelates (89,100,113,127). The conductivity cell is robust, and has the advantage that it is non-destructive upon the analyte, allowing collection of the eluates to be made, in order to check that no sample decomposition has occured, within the column. However, by modern GC standards, the TDC is only moderately sensitive, detection of metal being limited to the range 10^{-4} - 10^{-8}g (113).

The flame ionisation detector (FID) is more sensitive than the TCD, but has the disadvantage of being destructive upon the sample eluates, though stream splitting devices may be fitted to overcome this problem. The electron capture detector (ECD) has been used for the detection of metal chelates of acac, tfa and hfa (128,129), and Belcher et al (130) have used the FID for the determination of Group (11) chelates of tpm, ppm and fod. However, Hill and Gesser (129) reported that the substitution of fluorine atoms into a chelate decreased the FID response.

Precisely the opposite is observed for the detection of fluorinated metal chelates by ECD (99). The principle of operation of the ECD, whereby a ^{63}Ni source emits β particles, makes the detector particularly suitable for compounds containing either electronegative groups, eg; halogens, or a delocalised π-system. Fluorinated metal chelates possess both these properties, the chelate ring being proposed to contain some form of π-electron system. ECD is therefore the most sensitive of the detectors for the analysis of fluorinated metal chelates. Ross (99) has determined minimum detectable quantities (MDQ) of Al and Cr(111) chelates of acac, tfa and hfa. TABLE 11 gives a comparison of detection limits obtained, though the definition of MDQ (ratio of eluate signal to average base line noise level, S/N) was not the same in each case. Albert (128) has compared minimum detectable quantities of selected chelates, obtained on the FID and ECD detectors. TABLE 12 shows results obtained (in moles, S/N2).

Fujinaga et al (131) have noted a relationship between the response of the ECD and the electronic spectra maxima of fluorinated chelates. The difference in λmax between the chelate and the parent 1,3-diketone is related to the energy level of the lowest unoccupied molecular orbital, which also determines the electron affinity of the chelate to the emitted electrons from the ECD source.

Sucre and Jennings (132) using SE 30 on a wall coated open tubular fused silica column, determined minimum detectable quantities of selected trifluoroacetylacetonates, (S/N2), as shown in TABLE 13. They noted that the detection limits were comparable to previously reported values (112,128). Using the same column, MDQ values of Ni and Co chelates of diethyldithiocarbamate (DDTC) and di(trifluoroethyl) dithiocarbamate (DFDTC) were determined (S/N2) with the ECD, flameless nitrogen/phosphorous and flame photometric detectors. TABLE 14 compares results obtained.

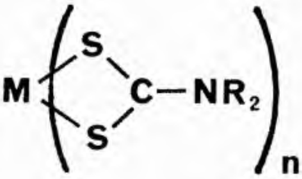

R = Et (DDTC)
R = CF_3CH_2 (DFDTC)

MDQ values of Zn, Ni and Pd di(isopropyl)dithiophoshates (DIDP) were also determined on the nitrogen /phosphorous, and flame photometric detectors.

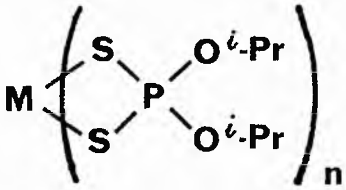

(DIDP)

Juvet and Durbin (133) have used the flame photometric detector for the analysis of metal complexes.

Other detectors that have been employed for the analysis of metal chelates and volatile organo-metallic compounds include thermionic emission (100), argon ionisation (88), microwave plasma emission (53,134), mass spectrometry (2,108) and dc arc plasma (135).

To extend the possibility of metal chelate analysis by GC, emphasis in recent years has been on the development of alternative ligands to 1,3-diketones. One approach has been to substitute alternative donor atoms in the β-diketone chain, in place of oxygen. Common alternatives are sulphur and nitrogen giving β-thioketones and β-ketoamines (also known as β-iminoketones). An advantage of this substitution is that S and N donors in a ligand are often able to chelate to a better extent than O atoms towards certain metals. Thus metals that have considerable class 'B' character (136), such as the Ni group (Ni, Pd, Pt) (where class 'B' metals form stable complexes with ligands whose donor atoms are derived from the third and subsequent rows of the periodic table), form more stable chelates with the second or subsequent donor atoms in the groups; $N \ll P < As < Sb$ and $O \ll S < Se < Te$. Increased thermal stability of monothio-acacs therefore, for example, would be expected over the analogous β-diketones. Other approaches have been to alter the β-diketone backbone to give, for example, alicyclic β-1,3-diketones and salicylaldimines.

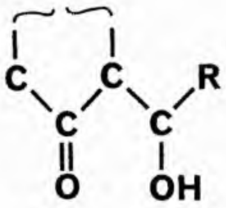

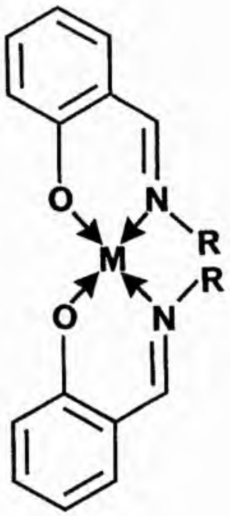

1.4.1.b

β-Thioketonates

The advantage of *β*-thioketones as chelating agents is that structural changes resulting from replacement of O by S are minimal. The compounds can be prepared by the action of H_2S on *β*-diketones. Fromm (137) reacted acetylacetone with hydrogen sulphide in an attempt to form monothioacetylacetone. However, the major product was shown to be the di-thioacetylacetone dimer:

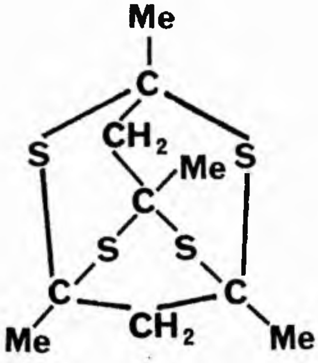

Reyes (138) attempted a similar reaction to prepare ethylthiobenzoylacetate. Livingstone et al (139,140) prepared a variety of substituted monothiodiketones. A drawback to the use of H_2S for such preparations is the formation of by-products similar to the dithioacac dimer. To limit the replacement of both oxygen atoms in the diketone, dilute solutions of the diketone must be used. Chaston (141) has shown that the amount of HCl catalyst necessary to form the monothiodiketone is related to the enol concentration of the *β*-diketone. TABLE 15 lists the range of HCl concentrations necessary.

A second method of preparation, employed by Uhlemann (142) and Yokoyama (143) involves the Claisen condensation of thieno and thio esters with ketones.

$$RCOCH_3 + R'C(S)OMe \longrightarrow R'C(S)CH_2COR + MeOH$$

$$RCOCH_3 + R'C(S)SMe \longrightarrow R'C(S)CH_2COR + MeSH$$

Monothiodiketones exist in tautomeric forms similar to β-diketones.

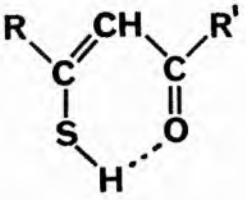

cis-thioenol

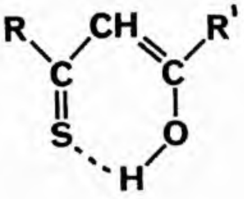

cis-enol

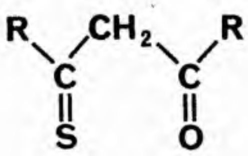

cis-thioxo

There has been much confusion in the literature concerning the tautomeric nature of monothioketones. Klose (144), Reyes (138) and Arnold (145) have shown by NMR that monothio-β-diketones exist predominantly in the enol form, there being no evidence of any $-CH_2-$ signal. However Chaston et al (142) using mass spectrometry, and Duus and Lawesson (146), concluded that they exist as the H-bonded thioenol tautomer. Belcher et al (147) examined monothio-acac, monothio-acetylpivalylmethane and monothio-tfa by IR, UV and NMR spectroscopy and concluded that monothio-tfa exists as the H-bonded enol tautomer, and that monothio-acac and monothio-apm exist predominantly as the H-bonded thioenol with some H-enol present.

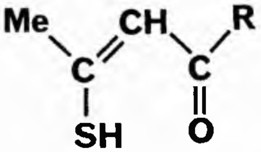

R = Me monothio-acac

R = ^{t}Bu monothio-acetylpivalylmethane

R = CF_3 monothio-tfa

The preparation and properties of a number of β-thioketones and their metal chelates has been reveiwed (141, 148, 149). TABLE 16 shows some of the common monothiodiketones used in metal chelate GC.

Belcher et al (147) studied the chromatography of monothio-tfa chelates on a range of polar and non-polar stationary phases. Detection limits of these chelates were determined on 2.5% Apiezon L using the FID detector. TABLE 17 lists results obtained.

Belcher et al (147, 150) have also shown that Co(11)monothio-acac but not Co(111)monothio-acac can be chromatographed, and that Co(111)monothio-tfa but not Co(11)monothio-tfa can be chromatographed. Improvements in technique and instrumentation may therefore be expected to aid the simultaneous determination of Co(11) and Co(111). Ho et al (151) have shown that Cu(11) chelates of β-thiodiketones are liable to reduction to the Cu(1) state, the resultant complexes being too involatile for GC applications. Uden and Henderson (152) have pointed out that this property of copper thioketonates suggests a useful method for the determination of trace amounts of metals in copper matrix, whereby the copper is first converted to the involatile Cu(1) state. Barrat et al (153) have determined trace amounts of Ni in instant tea and in margarine by the formation of the monothio-tfa chelate.

1.4.1.c

β-Ketoaminates

β-Ketoamines may be prepared with bi- or tetra-dentate functionalities. Bi-dentate ligands can be prepared by the reaction of ammonia or primary amines on 1,3-diketones, tetra-dentate ligands being formed by reaction of 2 moles β-diketone with the relevant diamine:

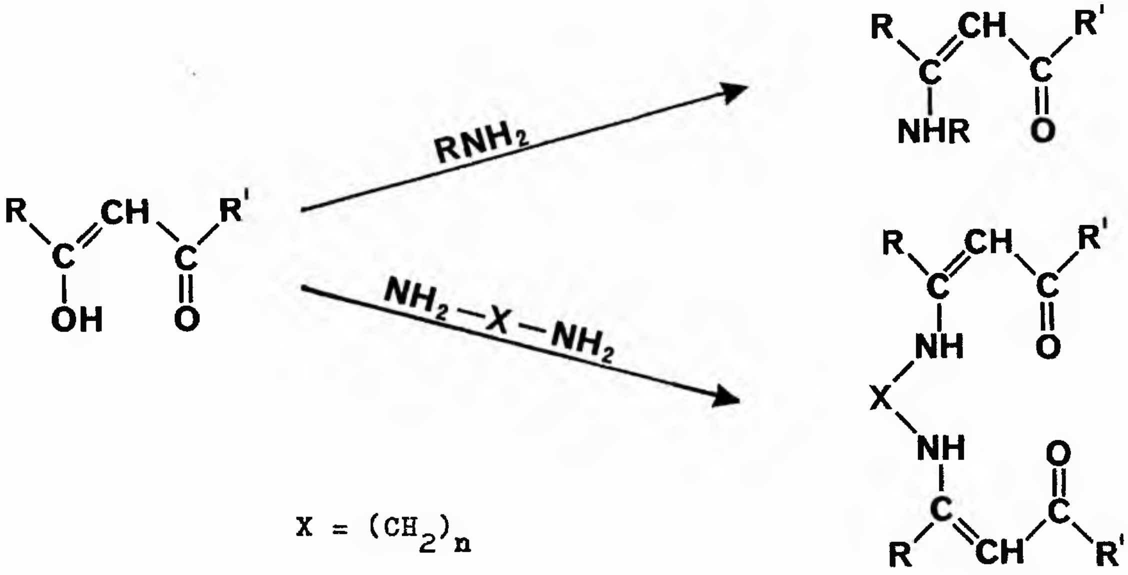

$X = (CH_2)_n$

Cromwell (154) has reviewed the methods of preparation of β-ketoamines.

The application of bi-dentate β-ketoaminates to GC is limited. Holm et al (155) have shown that the stability of Ni group metals (Ni, Pd, Pt), complexed with N-alkyl substituted ligands is low, especially with respect to hydrolysis. Parees (156) has pointed out some problems liable to be encountered with bi-dentate β-ketoamines.

(1) The chelates are labile, often releasing free ligand even under mild thermal conditions, resulting that metal exchange may

occur in heated GC injection ports, and/or at GC/MS interfaces. (2) The possibility of formation of mixed chelates (resulting from possible ligand hydrolysis), having one β-diketone and one β-ketoamine per molecule is significant. This problem is particularly notable for copper β-ketoaminates.

TABLE 18 lists some common bi-dentate β-ketoamines that have been used for metal GC analysis.

Successful application of β-ketoaminates is mainly limited to ligands with no N-alkyl substitution. Miyazaki et al (157) showed that $Ni(ap)_2$ alone, amongst a range of Ni and Cu β-ketoaminates, showed sufficient stability for quantitative chromatography. Belcher et al (158) studying Ni, Cu, Pd and Pt chelates of H(atfa) showed that the Ni and Cu chelates were quantitatively resolved.

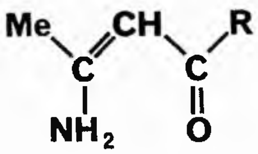

R = Me Amino-acac (ap)
R = CF_3 Amino-tfa (atfa)

However, though few bi-dentate ligands were found to be truly applicable to GC analysis, it became evident that the tetra-dentate β-ketoamine ligands showed much promise. TABLE 19 lists some common tetra-dentate ligands used in metal GC analysis.

Despite the close structural similarity to bi-dentate chelates, tetra-dentate β-ketoaminates show increased thermal and solution stability, as would be expected from the additional presence of a stabilizing five-membered ring. However, chelate volatility is reduced compared to the analogous bi-dentate chelates. Both fluorinated and non-fluorinated tetra-dentate chelates have been investigated, and it has been shown (158) that the volatility order is surprisingly reversed, non-fluorinated β-ketoaminates being more volatile than the fluoro-derivatives, in contrast with the situation found for β-diketones and β-thioketones.

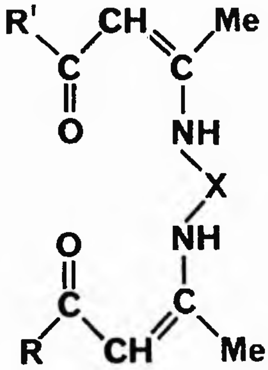

Belcher et al (158, 159) studied Ni, Cu, Pd and Pt chelates of H_2(en-$acac_2$), (R = R' = Me, X = $(CH_2)_2$) and H_2(en-tfa_2) (R = R' = CF_3, X = $(CH_2)_2$), and showed linear quantitation to the nanogram level. Uden and Blessel (160) resolved the two isomeric forms of Ni, Cu and Pd chelates of H_2(bn-tfa_2) (R = R' = CF_3, X = CH(Me) - CH(Me)), and showed that the chelates were of sufficient stability to be quantitatively determined. Uden and Henderson (161) determined Ni, Cu and Pd chelates of H_2(en-$acac_2$) and H_2(pn-$acac_2$) (R = R' = Me, X = CH(Me) - CH_2).

Dilli and Patsalides (162) successfully chromatographed tetra-dentate β-ketoaminates of VO(11), thus extending the potential range of metal speciation analysis.

To exploit the advantage of halogenated compound detection by ECD, and at the same time maintaining chelate volatility, Belcher et al (163) and Clark (164) developed mixed fluoro- and non-fluorinated tetra-dentate ligands, eg; H_2(en-acac-tfa). Results show that these ligands do indeed form chelates of suitable thermal stability and volatility. Isomeric chelates of H_2(bn-acac-tfa) have been resolved (164).

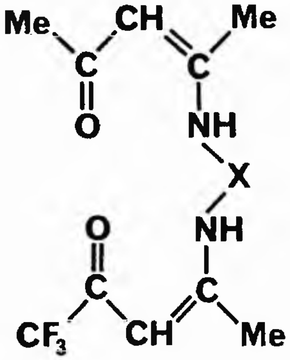

X = en, bn

Uden et al (165) compared the response of the ECD to bi-dentate and tetra-dentate β-ketoaminates, and showed linearity over three orders of magnitude, with detection limits of 4-8pg Ni.

1.4.1.d

Other ligand systems

Other ligand systems that have been employed for the gas chromatographic analysis of metals include salicylaldimines, dialkyldithiophosphates, dialkyldithiocarbamates and porphyrins.

Uden and Waldman (166) reported the chromatography of Ni, Cu and Zn salicylaldiminates. The thermal stability of such complexes is however a limiting factor in their GC analysis. Cardwell et al (167) chromatographed Cr, Ni, Zn, Pd, Pt and Rh dialkyldithiophosphates, and Sucre and Jennings (132) studied the chromatography of Se, Zn, Cd, Cu, Ni and Co diethyldithiocarbamates, and Ni, Zn and Pd chelates of di(isopropyl)dithiophosphates using glass capillary columns. They concluded that best results were obtained on short, highly inert, fused silica columns coated with non-retentive liquid stationary phases, such as SE30.

The GC of metal-porphyrin complexes has been studied, using very high pressures and polarisable organic compounds (such as CCl_2F_2) as carrier gas. Karayannis and Corwin (168) determined Mg, Ni, Cu and VO(11) etioporphyrins on a resin stationary phase. The same workers (169) also studied metal-porphyrin complexes of Co(11), Co(111), Mn, Zn, Pt, Pd, Ag(11), Fe(111) and Ti(1V). Detectors used were spectrophotometric fitted with flow cells, conventional GC detectors being unsuitable, due to the very high pressures involved.

1.4.2

High performance liquid chromatography of metal chelates

The above discussion on the GC analysis of metal chelates, leads to the conclusion that the method is only applicable to a few ligand systems, mainly those with a high degree of fluorine substitution, due to the overriding restriction that most metal chelates do not possess sufficient thermal stability and volatility at normal GC operating temperatures. This being so, solution chromatographic methods of metal chelate analysis have been evaluated.

Traditionally, cation-exchange chromatography has been employed for the analysis of metal ions, and has been extensively reviewed (170). Trace metal analysis has also been performed by TLC, and has been reviewed (171). However, these methods yield results that are only semi-quantitative in nature.

Though HPLC has been used for the rapid analysis of organic compounds, particularly those arising from a biochemical origin, the analysis of inorganic material is comparatively recent. Although some separations of organo-metallic complexes had been achieved (172), it was Huber et al (173) who were the first to apply HPLC to the analysis of metal chelate compounds. Using liquid-liquid chromatography, they resolved acac and tfa chelates of Be, Al, Cr(111), Fe(111), Co(11), Co(111), Ni, Cu, Zn, Zr and Ru using a ternary solvent system of H_2O/2,2,4-trimethylpentane/EtOH. Since that first report, HPLC has been used for the analysis of β-diketonates (173, 174), dithizonates (175, 176), β-ketoaminates (174, 177) and dithiocarbamates (178-183).

Much attention has been given to the use of adsorbent materials, such as silica and alumina, for the HPLC analysis of chelates, where the available literature on the TLC, eg; (171), of metal chelates can be readily translated to HPLC. Liska et al (180-182) studied the chromatography of a range of metal chelates of DDTC on silica columns. The dependence of column capacity ratios (k') on mobile phase polarity, and the effect of alkyl substitution in DDTC upon the elution behaviour of the chelates was investigated (where k' = the ratio number of moles solute in the stationary phase to the eluent phase). The formation of mixed ligand complexes within the column was observed when mixtures were injected. Edward-Inatimi et al (178) determined Ni, Cu, Mn, Co and Pb in standard steel samples via their DDTC chelates, and compared their results with certified values (obtained by AA), and showed good agreement. Tollinche and Risby (174) undertook a detailed study of the use of liquid-solid chromatography for the separation of metal chelates. Alumina, silica, bonded phases and open-pore polyurethane columns were used, with a variety of mobile phases, to study the chromatography of Ru, Rh, Al and transition metal chelates of acac, tfa, fod, dpm, pn-tfa and en-tfa. They concluded that silica columns were the most generally applicable to metal chelate analysis. They also showed that only those mobile phases with solvent strengths of $\epsilon < 0.32$ were able to resolve cis and trans Cr(111), Co(111), Ru and Rh chelates of tfa, whereas solvent strengths approaching $\epsilon = 0.0$ were required to resolve $Co(fod)_3$ and $Cr(fod)_3$. Walters (184) resolved cis and trans isomers of Cr(111) and Co(111) chelates of bza, dpm and tfa. Hilliard and Freiser (185) and Hambali and Haddad (186) separated a range of metal 8-hydroxyquinolates on silica.

Reverse phase liquid chromatography, where a non-polar stationary phase is used in conjunction with a polar mobile phase, has been applied to metal chelate analysis. A common means of achieving such phases is to attach alkylsilane groups (often octadecyl) to the silica support. Other groups have been bonded to silica, and the use of such bonded phases has been reviewed by Majors (187), and by Rehak et al (188).

Gaetani et al (177) attempted the liquid-liquid chromatography of Co(11), Ni, Cu and Pd chelates of en-acac, and en-bza, and showed that the Ni and Cu chelates were successfully resolved on two different columns, and that Pd was resolved from Cu, but not from Ni. UV detector response at 254nm to Ni and Cu en-acac was shown to be linear over two ranges of concentration (0.5 - 5 and 25 - 250ng metal injected), with detection limits of 0.2 and 0.5ng respectively, using Micropak CH column and a mobile phase of MeOH/borate buffer (pH 10), 70/30 mix. Tollinche and Risby (174) studied the reverse phase chromatography of Al, Cr(111) and Cu chelates of acac and tfa with H_2O/CH_3COOH and $MeOH/H_2O$ mobile phases on a Zipax C18 column. However, no major improvements over separations achieved using silica columns were observed. Hansen and Seivers (189) have reported similar results. Uden et al (190) separated Ni and Cu chelates of en-acac on Partisil ODS using H_2O/CH_3CN 60/40 mix. Schwedt (191) determined Cr(111) and Cr(V1) in water by reaction of the species with ammonium pyrollidinedithiocarbamate, using an RP8 column with CH_3CN/H_2O 70/30 mobile phase. Tande (179) performed a similar separation of Cr(111) and Cr(V1) by reverse phase separation of their respective DDTC chelates.

Chemically bonded phases have been developed for liquid-solid adsorption chromatography, where specific functions have been bonded to the supporting material, for the selective retention of certain metal ions. Hill (192) prepared an 8-hydroxyquinoline substituted silica column for the selective removal and concentration of Cu, Zn and other metals of environmental interest, from salt solutions of high ionic strength. Baumann et al (193) coupled dithizone to carboxymethyl cellulose for the extraction of trace metals from solution. Haas et al (194) prepared silica columns bonded with the fluorinated and non-fluorinated substituents $C_6F_5(CH_2)_3SiCl_3$, $C_6H_5(CH_2)_3SiCl_3$ and $CF_3(CF_2)_7(CH_2)_2SiCl_3$, and showed that phases with partially fluorinated ligands, showed entirely different chromatographic properties to the analogous non-fluorinated phases. Thus silica bound with the pentafluorophenyl-3-n-propyl grouping had higher k' values and a better selectivity for aromatic hydrocarbons, than the phenyl-3-n-propyl group. However, the stationary phase with the fluorinated carbon chain was shown to be less useful than silica bonded with n-decyltrichlorosilane, and was suggested to be due to a different contact area between the grouping and the solute.

1.5

Physical and spectroscopic studies of metal 1,3-diketonates

The chelation of a metal to a β-diketone, results in the formation of a six-membered metallocyclic ring. The electronic nature of this ring has been a subject of considerable debate in the literature for some years. Numerous X-ray diffraction studies (195) have shown that the acac portion of the chelate ring is almost planar, with M-O, C-O and C-C bonds of equal lengths, indicating some form of enolate resonance:

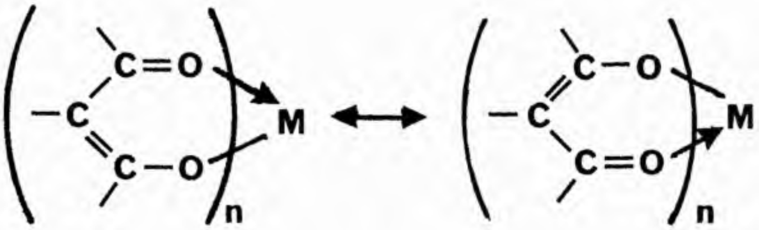

Calvin and Wilson (196) postulated a benzenoid-type nature to the chelate ring, on the basis of stability constant data for the copper chelate of ethylacetoacetate. Work done by Colman et al (197-199) confirmed this, by performing a variety of classical electrophilic substitution reactions, such as nitration, acylation, etc., on the chelate ring.

In order to understand better the electronic nature and structure of metal chelates, and their consequent effects upon such properties as volatility, and thermal and solution stability, a number of physical and spectroscopic techniques have been used, such as UV, IR, NMR, TGA and polarography.

1.5.1

Electronic Spectroscopy

The electronic spectra of metal 1,3-diketonates has received considerable attention. Particular emphasis has been given to the study of the effects of terminal substitution in the β-diketone, upon the pseudo-aromatic character of the chelate ring.

Belford et al (200) and Holm and Cotton (201) studied the electronic spectra of metal acetylacetonates, and assigned the band appearing at 288nm, in Na(acac) (in EtOH), to a ligand $\pi-\pi^*$ transition. However, no correlation was found between the variation of the position of this band, and the ionic charge on the metal ion. Both workers suggested therefore that the benzenoid structure proposed by Calvin and Wilson (196):

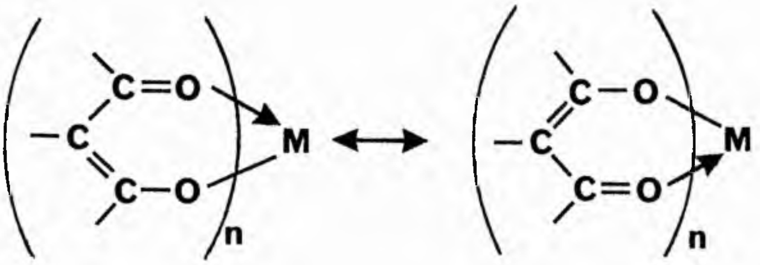

- should be modified into one in which π-delocalisation occurs independently of the metal.

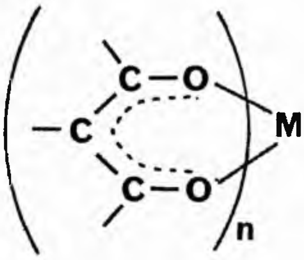

- a study of the $\pi-\pi^*$ absorption maxima thus being a measure of the extent of π electron delocalisation in the chelate ring, and hence it's stability.

The electronic spectra of transition metal chelates is generally quite different to those of non transition metal chelates, due to the interaction of the metal d-orbitals with anti-bonding orbitals on the ligand, causing a splitting of the $\pi-\pi^*$ band. Fackler (202) assigned the 250nm in $Cu(acac)_2$ to electron transfer from a ligand orbital to a metal antibonding orbital, and the band at 296nm to a $\pi-\pi^*$ transition. Singh and Sahai (203,204) studied the absorption spectra of a range of transition metal β-diketonates. They noted that if the chelate ring possessed sufficient aromatic character, the $\pi-\pi^*$ transition of the ligand in various α,ω-substituted metal β-diketonates, would be expected to shift in a manner similar to the spectral shifts reported by Matesen (205) for substituted benzenes. They also observed that ω-halogen substitution caused a shift of λmax to longer wavelength in the $\pi-\pi^*$ band, and it was suggested that an increase in π-delocalisation was the cause of this effect. Wish and Bolomey (206) studied the electronic spectra of phenyl substitutec acetylacetonates of Al, Cu and Pd, and noted that a shift to lower energy occured for all transitions. This was attributed to a dominance of the phenyl ring resonance effect over the weaker inductive effect. Thus the $\pi-\pi^*$ absorption band shifts to lower energy in the order M(acac) > M(bza) > M(dbzm).

Sasaki (207) has reported similar shifts when methyl is replaced by a furyl ring in acetylacetonates.

1.5.2

Nuclear magnetic resonance

If the chelate ring possessed some form of benzenoid character, as suggested by Calvin and Wilson (196), ^1H NMR spectra would be expected to reveal proton resonances similar to those found for olefinic or benzenoid protons, for the ring H atom.

Holm and Cotton (201) were the first to study metal chelates by NMR. They studied the ^1H NMR spectra of ten metal acetylacetonates in CCl_4 solution, and noted that the chemical shifts for the methine proton were close to those obtained for organic compound olefinic protons, and were approximately independant of the size, charge and π-bonding ability of the metal ion. They concluded that the position of the methine resonance could not be considered evidence for an aromatic ring, as resonance shifts of the methine proton relative to acetylacetone, were much less than the shift observed between benzene and acetylacetone. These conclusions have been supported by other workers (208-210).

Pinnavaia and Fay (211) and Chattoraj et al (212) recorded ^1H and ^{19}F NMR of some tetravalent metal chelates of acac, tfa and hfa in $CDCl_3$ and CCl_4. It was demonstrated that the introduction of the electronegative CF_3 caused a downfield shift in ^1H resonance. TABLE 20 lists the observed resonances. However, the downfield shift of the methine proton was probably more to do with the introduction of the electronegative CF_3 groups, than any increasing benzenoid character in the chelate ring.

Eaton (213) studied the ^{1}H NMR spectra of a range of paramagnetic acetylacetonates. Proton resonances and line widths were obtained, and were discussed in terms of the effect of metal ion upon proton resonances. It was shown that electron spin was partially delocalised from the metal ion to the ligand, resulting in the carbon atom bearing the proposed olefinic proton, suffering a large negative spin density leading to a shift to low field. Resonances were not obtained for Cu and VO(11) acetylacetonates, and it was suggested that these ions did not possess relaxation times of a sufficiently short enough duration, to allow spectra to be recorded. Linck and Sievers (209) studied the effect of solvent upon the resonance positions of a range of Al β-diketonates, and showed a Van der Waals contribution to the chemical shift-solvent effect. Proton shift downfield was enhanced by increasing the atomic number of the atoms in the solvent, due to an interaction of the electrons of the solute with the nuclei of the solvent, the interaction being the larger, the greater the charge on the solvent nuclei.

Metal chelate stereochemistry has been studied by NMR. Raban et al (214) studied the stereochemical consequences of ionic type bonding in alkali metal acetylacetonates, and showed that the alkali metal complexes existed primarily in the Z,Z and E,Z forms:

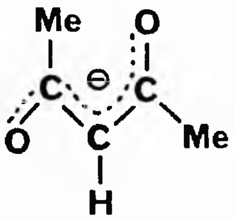

E,Z

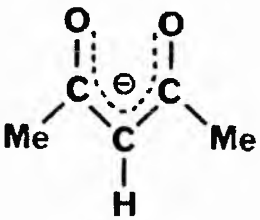

Z,Z

-where the Z,Z form is a chelated ion-pair, the E,Z form being dissociated. They showed that the amount of chelation decreased with increasing ionic radius of the metal ion, ie; Li > Na > K. Brittain (215), studying Group (11) acetylacetonates, showed that though the chelates produced the expected proton resonances, $Mg(acac)_2$ showed the presence of unsymmetrical isomers, the proportions of which were solvent dependent. Barabas et al (216) have shown that phenyl substitution in acetylacetone, to form benzoylacetone and dibenzoylmethane, resulted in these groups being co-planar with the chelate ring, though substitution of ϕ, CO and CH_3CO at the 3-position was shown (217) to give two π systems, non-coplanar to each other, and therefore not able to be conjugated to each other. Hammel and Smith (218) and Trestianu (219) have confirmed these results.

Fay and Piper (220) studied cis and trans benzoylacetonates of a range of trivalent metals, and noted that no resonance shifts were observed for the paramagnetic Cr(111), Mn(11) and Fe(111) chelates.

1.5.3

Infrared spectroscopy

Infra-red (IR) spectra provide information on the nature of the carbonyl groups and the strength of the metal-oxygen bond in the chelate ring. Particular emphasis has therefore been placed on the assignments of the ν(C-O), ν(C-C) and ν(M-O) stretching bands in the IR spectrum of a metal chelate.

Much confusion existed in the literature for some time with the assignments of the above stretching modes. Initially, Lecomte (221) studying metal acetylacetonates, observed two bands in the 1300-1600 cm^{-1} region, the higher frequency band being assigned to ν(C-O) and the lower to ν(C-C). Bellamy and Branch (222) attributed the 1580 and 1520 cm^{-1} bands in metal acacs to ν(C-O) and ν(C-C) respectively. Holtzclaw and Collman (223) observed similar bands in a variety of Cu chelates, and suggested that the double bond character of the C=C in the chelate ring was rather weak. However, Nakamoto et al (224,225), on the basis of force constant calculations, reversed these assignments, and was supported by Mikami et al (226), though some coupling of the two modes was suggested. The debate was settled by Pinchas et al (227) who studied the spectra of ^{13}C and ^{18}O labelled acetylacetonates of Cr(111) and Mn(111), and demonstrated that the band occuring at approximately 1570 cm^{-1} was significantly affected by ^{18}O labelling, whereas the band at 1515 cm^{-1} was little affected by the change in oxygen isotope. They therefore demonstrated that the earlier workers (221-223) were correct. Behnke and Nakamoto (228,229) have since confirmed the results of Pinchas using ^2H-substituted metal chelates.

Holtzclaw and Collman (223) have suggested that the position of ν(C-O) depends on four factors:

(a) The relative electron density of the σ-bonds, this being generally controlled by the electronegativity of the terminal groups attached to the carbonyl functionalities.
(b) The masses of the terminal groups attached to the carbonyl groups.
(c) The interaction of the carbonyl groups with the neighbouring metal p or d orbitals.
(d) The mass of the chelated metal ion.

A strong M-O bond is assumed to weaken the double bond character of the adjoining C=O group, this being reflected in higher values of ν(M-O) for stable chelates such as $Cu(acac)_2$, compared to weaker chelates, eg; Na(acac), and in lowered values of ν(C-O) relative to ν(C-O) in the parent H-bonded enol.

Substituent effects upon the positions of the above stretching modes have been studied by Nakamoto et al (225). IR spectra of Ni and Cu chelates of acac, tfa and hfa showed that successive replacement of the methyl groups by CF_3, caused a shift in ν(C-O) and ν(C-C) to higher frequency, and ν(M-O) to lower frequency. These observations are in accordance with electronic bonding theory, whereby the inductive effect of the CF_3 group strengthens the C-O and C=C bonds, and weakens the M-O bond, by drawing electron density away from the metal ion, and into the chelate ring, Joshi and Pathak (230,231) studied the IR spectra of a large number of fluorinated metal chelates, and confirmed these trends. It was also observed that phenyl substitution for methyl caused a shift in ν(M-O) to higher frequency, though the shift in ν(C-O) was irregular. Calculations performed on Ni and Cu benzoylmethanates, showed that phenyl substitution slightly increased the C=C and M-O stretch force constants, due to interaction with the pseudo-aromatic metallocycle according to the resonance structures:

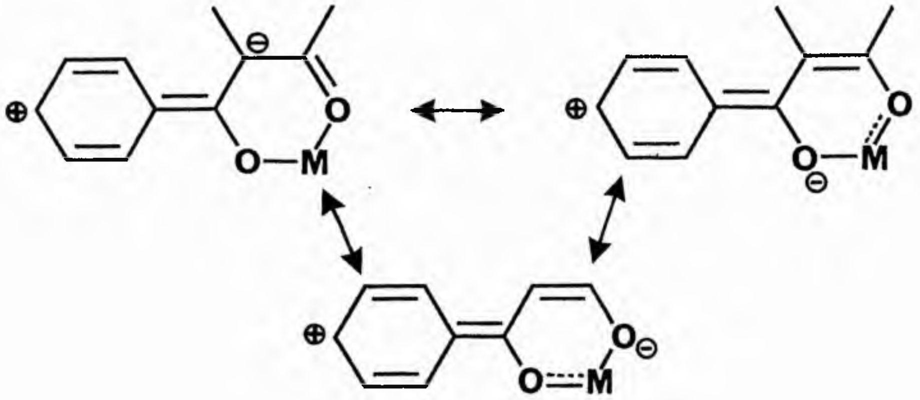

These structures indicate that due to the mesomeric effect of the phenyl group, the negative charge on the oxygen atoms increases, bringing about a strengthening of the σ as well as to some extent the π-character of the M-O bond. Group (11) metals, which cannot form π-bonds, would therefore be expected to show a smaller shift in ν(M-O) compared to transition metal chelates. TABLE 21 lists values of ν(C-O), ν(C-C) and ν(M-O) obtained for a range of substituted acetylacetonates.

West and Riley (232) studied the IR spectra of eighteen metal acetylacetonates, including those of the alkali metals. Spectra showed that coordinate covalent bonding is less important for Group (1) metals, compared to polyvalent metals, the alkali metal derivatives behaving as salts:

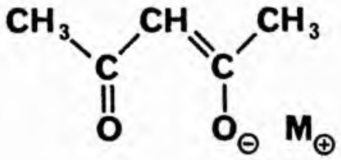

- this being due to the alkali metals being weakly polarising, and reluctant to act as electron acceptors. Values of ν(C-O) decreased for the alkali metal in the order Cs > K > Na > Li. Sidgwick and Brewer (73) have shown that Na(bza) has the properties of a salt, eg; being readily soluble in polar solvents, and having a high melting point. However, when recrystallised from aqueous EtOH, a dihydrated species was formed, soluble in both benzene and toluene. Studying anhydrous and hydrated Na and K chelates of acac, bza and salicylaldehyde, Boschmann (233) showed that there was no difference in the position of ν(C-O), implying that hydration had no effect on M-O and C-O bond strengths. Solubility of the hydrated complexes in non-polar solvents was therefore explained in terms of the structure:

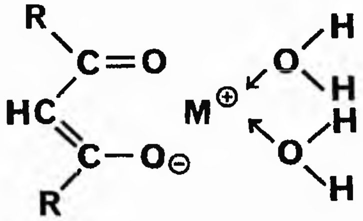

- where the charged metal ion is shielded from the external solvent by the water molecules.

Attempts have been made to correlate the position of ν(C-O) with chelate stability. IR studies on keto-enol equilibria, have indicated that the parent 1,3-diketone is capable of forming a resonance stabilised intra-molecular H-bond of considerable strength. This results in a large shift of ν(C-O), whereas it has been shown (234) that 'normal' H-bonding rarely produces shifts of more than 10 cm^{-1}. Bellamy and Branch (235) showed that the position of ν(C-O) in an unchelated β-diketone ligand was directly related to the double bond character of the ligand enol form. However, studying a range of divalent metal acetylacetonates, they found (222) that the position of ν(C-O) was not dependent on the double bond strength of the ligand enol form. No frequency-stability relationship could therefore be determined in terms of ν(C-O).

1.5.4

Solution stabilities of metal 1,3-diketonates

For a compound to undergo successful solution analysis, as in HPLC, a necessary requirement is that the compound be stable in that solution. Much work has therefore been directed to the determination of chelate stability constants (or formation constants). Prior to these however, the acid dissociation constants of the ligands must be known.

Calvin and Wilson (196) were the first to attempt such calculations using potentiometric means, and noted that due to the insolubility of the β-diketone ligand, and the resultant chelates, measurements were necessarily performed in aqueous dioxan mixtures. They carried out a quantitative survey of the effect of structural factors upon the stability of a range of copper chelates of substituted acetylacetone and o-hydroxy aromatic aldehydes. Eidenoff (236) calculated dissociation constants of acetylacetone, ethylacetoacetate and benzoylacetone in aqueous ethanol solutions.

However, the use of mixed solvents implies that values of pK_a so obtained, are expressed in terms of concentration only, the true thermodynamic activities of the species in solution being affected by the organic component in solution. The results of Calvin and Wilson (196) and Eidenoff (236) are therefore almost certainly in error. Van Uitert and Haas (237), using the dilute solution activity coefficient data for HCl in water-dioxan, obtained by Harned and Owen (238), were able to calculate approximate thermodynamic pK_a values for a range of

β-diketones in aqueous dioxan solutions. Block and McIntyre (239) extended this work by eliminating the need of using successive approximations, and showed that true thermodynamic constants were able to be calculated for aqueous solutions. Goldberg (240) combined the methods of Van Uitert and Haas (237) and Block and McIntyre (239), and calculated pK_a and formation constant data for acetylacetone and $Ni(acac)_2$ in 75% dioxan H_2O solution. Fernelius et al (241) calculated relative stabilities of alkali metal dibenzoylmethanates, and showed that chelate stability increased in the order $Li > Na > K > Cs$. Similar trends have been observed by Raban et al (204), from ^1H NMR data. Fernelius et al (242,243) showed that the general order of chelate stability of divalent metal ions chelated with β-diketones containing two terminal aromatic groups was:

$Ba > Sr > Ca > Mg > Cd > Mn > Pb > Zn > Co = Fe = Ni > Cu = Be$

Uhlemann and Frank (244) calculated dissociation constants of mesitoylacetone, mesitoylbenzoylmethane and dimesitoylmethane and the stability constants of their respective Cu, Ni, Zn and Be chelates.

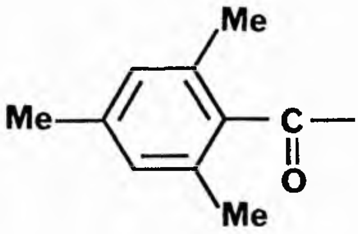

Mesitoyl

Comparison of the results with the analogous benzoylacetonates and dibenzoylacetonates, showed that substitution of mesityl for phenyl caused a decrease in chelate stability, and was explained in terms of resonance interactions between the chelate ring and its substituents. Steric effects, as opposed to electronic effects upon chelate stability have been investigated by Gutter and Hammond (245). Formation constants of Cu, Ni, Co(ll), Mn(ll) and Mg chelates of acac, diisobutyrylmethane (dibm) and dipivalylmethane (dpm) were calculated.

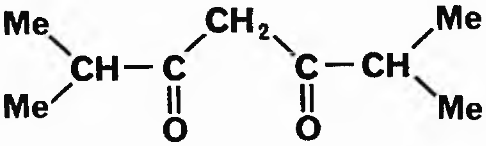

(dibm)

Correlation of the results indicated that the second formation constants of $Cu(dibm)_2$ and $Cu(dpm)_2$ were low, with large separation factors between the first and second formation constants. This indicated that the increasing bulk of the ligands acts to reduce overall chelate stability. Small separation factors were obtained for the non-square-planar complexes.

Fernelius et al (246) showed that the first formation constants of some tri- and tetravalent acetylacetonates increased in the order:

La(lll) < Nd(lll) < Sm(lll) < Y(lll) < Sc(lll) < In(lll) <
Th(lV) < Ga(lll) < Fe(lll)

-and showed that plots of log(1st formation constant) varied linearly with electronegativity, atomic number and the third ionisation constant of each metal.

Relative solution stabilities of metal chelates can be determined by DC polarography, using a dropping mercury electrode, a study of the polarographic behaviour of metal chelates reflecting the comparative solution stabilities to reduction of the metal chelates, assuming some form of π-electron delocalisation in the chelate ring. However, though half-wave potentials are not a strict quantitative measure of chelate stability under irreversible conditions, (the situation found for most divalent metal chelate reductions - where an irreversible reduction is one where the electrode potential is not strictly defined by the Nernst equation), they nevertheless provide a reasonable basis for the relative comparison of solution chelate stability to reduction. Thus, an increasingly negative value for $E_{\frac{1}{2}}$, or a greater difference in $E_{\frac{1}{2}}$ between the reduced chelate and the free solvated metal ion, reflects an M-O bond becoming more covalent in character, indicating increased chelate ring stability.

Lindvedt et al (247) studied the polarography of a range of fluoro- and non-fluorinated Cu chelates in 75% Dioxane-H_2O, and concluded that by classifying the chelates into aliphatic substituted, aromatic substituted and aliphatic and aromatic substituted groupings, a good correlation between $E_{\frac{1}{2}}$ and stability could be obtained. TABLE 22 lists values of $E_{\frac{1}{2}}$ obtained, and also lists some chelate stability constants, as determined by Van Uitert (248). Available data shows that the $E_{\frac{1}{2}}$ values follow the formation constants fairly regularly. The relative ease of reduction of aromatic substituted chelates has been explained by Handy and Lindvedt (249) as being due to the aromatic substituents providing a low energy path for electron transfer through the chelate π-system. This has been supported by Larson and Iwamoto (250), who suggested that the ease of reduction of metal ions in benzonitrile, as opposed to unconjugated nitriles, was due to electron transfer through a bridge mechanism to the nitrile conjugated system. Taube (251) has suggested a similar mechanism for the reaction between Cr(11) and $(NH_4)_5Co\text{-}(_2OC\text{-}CH{=}CH\text{-}COOH)^{2-}$. It is therefore believed that the chelate ring π-system acts as a bridge for electron transfer prior to reduction of the Cu ion. Chelates that have both aromatic and aliphatic substitution show less marked correlations between $E_{\frac{1}{2}}$ and stability, though trends are still apparent. $Cu(acac)_2$ is reduced at -0.502v, while the more stable $Cu(bza)_2$ (from absolute measurements (196)) is reduced approximately 0.1v more positive. These observations suggest therefore that stability comparisons between chelates can only be made between like substituted chelates, no simple relationship being apparent between unlike substituted chelates.

Patterson and Holm (252), studying substituent effects upon the polarographic reduction of Ru(111) chelates, noted that as the number and type of electron releasing substituents decreased, the value of $E_{\frac{1}{2}}$ became more positive, indicating a reduced character in the chelate ring resulting in lowered stability. TABLE 23 lists values of $E_{\frac{1}{2}}$ obtained.

Handy and Lindvedt (249) studied reduction potentials and substituent effects of a series of Cr(111) chelates in DMSO and dioxan-H_2O. They noted that substituent effects were additive on the value of $E_{\frac{1}{2}}$, and were determined by the nature of the polarising ability of the respective substituent. A good correlation between $E_{\frac{1}{2}}$ and the sum of the Hammett polar substituent constants was shown.

From the above discussion, the following general conclusions can be made concerning the stability of metal chelates in solution.

1) Introduction of electronegative CF_3 groups into the

β-diketone chain, lowers chelate stability, by drawing electron density away from the M-O bond.

2) Introduction of an aryl group into the β-diketone chain, increases chelate solution stability, due to the increased π-delocalisation effected by the presence of an adjacent conjugating π-system.

3) Substitution of methyl onto phenyl reduces chelate stability, due to the +I effect methyl group decreasing π-delocalisation in the chelate ring.

1.5.5

Thermal stabilities and vapour pressures of metal 1,3-diketonates

The above discussion has been concerned with the stability of metal chelates in solution, for HPLC applications. However, for GC applications, the thermal stability and the precise relationship between chelate volatility and temperature needs to be quantified.

Charles and Pawlikowski (93) studied the thermal stability of twentythree metal acetylacetonates by measuring the increase in pressure in an enclosed system, caused by the dissociation of the chelates maintained isothermally at 191°C. They noted that no general correlation could be made between the thermal dissociation of the chelates, and various parameters of the metal ion, such as cation size and charge. In some limited groups however, some trends were observable. Thus the thermal stability of the alkali metal compounds decreased with increasing atomic number, while the reverse was observed for the alkaline earth metal chelates.

Eisentraut and Sievers (253) have reported that thermogravimetric analysis (TGA) can compare the relative volatilities of a group of chelates, as well as directly showing their respective thermal stabilities. They showed that the order of volatility of rare earth dipivalylmethanates paralleled the order of ease of elution of these chelates from non-polar liquid stationary phases (120). They also showed that a series of Cr(111) chelates of the general form:

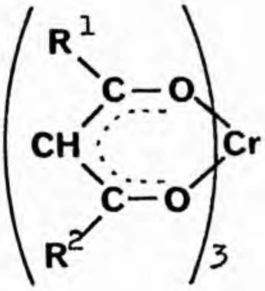

R^1	R^2	
CF_3	CF_3	A
CF_3	C_3F_7	B
C_3F_7	^tBu	C
CH_3	CF_3	D
^tBu	^tBu	E
CH_3	CH_3	F
(3-Bromo) CH_3	CH_3	G
CH_3	C_6H_5	H

-were vapourised in the order A, B, C, D, E, F, G, H. The 3-bromo-substituted acetylacetonate decomposed above 250°C. These results were compared with Al chelates of acac, tfa, hfa and fod, and mixed ligand acac/hfa complexes. The order of vapourisation was as expected, with $Al(fod)_3$ being vapourised close to $Al(tfa)_3$, but before $Al(acac)_3$. Belcher et al (122) have used TGA to study the relative volatilities of Group (1), (11) and Pb perfluoropivalylmethanates, and noted a significant difference in volatility between the various fluorinated chelates. They also showed (130) that Group (11) metal chelates of the same ligands were vapourised in the order Mg, Ca, Sr, Ba. Berg et al (254) have also studied the effect of substituent groups on chelate volatility. β-thioketones and β-ketoaminates have been studied by TGA. Belcher et al (147) studied Pd, Pt and transition metal monothio-trifluoroacetylacetonates and showed them to be of good thermal stability and volatility. From a discussion of metal class 'A' and 'B' character (136), Belcher et al showed that S atom donors provided more stable Ni group chelates than the respective β-diketones, and also showed in a comparison of Cu chelates of acac, tfa, fod, monothio-acac, monothio-tfa, amino-acac and the tetradentate ligands bis(acac)ethylenediimine and bis(trifluoroacac)ethylenediimine, a general chelate volatility of:

fluorinated β-diketonates $>$ fluorinated β-ketoaminates $>$ non-fluorinated β-ketoaminates, non-fluorinated tetradentate aminates $>$ fluorinated tetradentate aminates. Nickel chelates showed that the fluorinated monothio-diketonates and β-ketoaminates were the most volatile, followed by their non-fluorinated analogues, the tetradentate Ni chelates being the least volatile. Similar trends were shown for the Pd and Pt chelates of the above ligand systems.

Utsunamiya (255) studied the thermogravimetry of a range of Al, Ga and In β-diketonates, and showed that substitution of an aryl group, such as phenyl, furyl or thienyl, decreased chelate volatility, though thermal stabilities were not greatly affected, excepting the chelates of benzoylacetone and dibenzoylmethane.

Precise measurement of chelate vapour pressures was undertaken by Berg and Truemper (254,256) who studied the Be, Ni, Cu, Co(11), Al and Fe(111) chelates of acac, bza and benzoyltrifluoroacetone (bta), using an isoteniscopic technique as described by Smith and Menzies (257), and modified by Booth and Halbedel (258). From the measured vapour pressure data, they were able to calculate molar heats of vapourisation, using the Clausius-Clapeyron equation:

$$\ln(p) = -\frac{\Delta H}{RT} + \frac{\Delta S}{R}$$

where: p = vapour pressure

ΔH = Molar heat of vapourisation

ΔS = Molar entropy of vapourisation

R = Gas constant

T = Temperature K

-plots of the equation showing comparative vapour pressure-temperature characteristics of the chelates. Wood and Jones (259,260) used the technique to determine vapour pressures of acac and dibenzoylmethane chelates of selected transition metals, and Schweitzer (261) determined volatilities and vapour pressures of a range of Pb β-diketonates.

Wolf et al (104) and Frankhauser (262) however, have pointed out some of the inherent problems in the use of the isoteniscopic method, eg; vapours of the metal chelate analyte come into contact with mercury, and dissolve in it to some extent. Shulstad (263) therefore, employed a sensitive quartz spiral Bourdon guage to determine the vapour pressures of Al and Cr(111) chelates of acac, tfa and hfa. Sicre et al (264) measured vapour pressures of lanthanide dipivalylmethanates and showed that chelate volatility increased with lanthanide atomic number, due to the well known lanthanide contraction effect. Wolf et al (104) using the same technique, measured the vapour pressures of Cr(111) and Rh(111) chelates of hfa, and fod chelates of Cu, Cr(111), Fe(111), Al and Pd. Results showed the hexafluoroacetylacetonates to be more volatile than the fod chelates, and the fod chelates to be of comparable volatility to trifluoroacetylacetonates (253). It was also shown that the bis-square-planar fod chelates of Cu and Pd had vapour pressures less than the tris-fod chelates.

Swain and Karraker (265) utilised a modified Knudsen effusion method, whereby a continuous record of sample weight was made using an automatically recording microbalance, this procedure allowing measurement of the loss in weight of a vapourising substance through a calibrated orifice. Vapour pressures and thermodynamic quantities were calculated for lanthanide fod chelates. They also measured (266) vapour pressures of dipivalylmethanates of U and Th, as well as U, Th, Np and Pu chelates of fod.

Wiedemann (267) used thermogravimetry for the determination of vapour pressures of some selected organic compounds, where the usual thermogravimetric sample holder was replaced by an effusion cell. Results for benzoic acid agreed well with accepted literature values, though comparison of the vapour pressures of the other compounds with literature values was difficult, due to the different pressure ranges over which the measurements were taken. Ashcroft (268) dispensed with the effusion cell in favour of the normal thermogravimetric crucible, and determined ΔH of transition metal chelates of acac and various organic compounds, values comparing well with literature values. He noted that thermogravimetry yielded vapour pressure data at lower temperatures than by other techniques.

Fujinaga et al (269-271) have demonstrated that the extent of thermal decomposition of lanthanide chelates of tfa and hfa within a GC column can be reduced by a technique they termed 'Gas chromatography with ligand vapour as carrier additive', in which a chelate's parent 1,3-diketone vapour was added to the carrier gas in order to suppress thermal decomposition of the chelate. It was shown (271) that by the use of this technique, conventional thermogravimetric analysis with a dynamic gas flow over the sample allowed calculation of vapour pressures and thermodynamic data of lanthanide tfa and hfa chelates, both in the absence and presence of the parent 1,3-diketone additive. An advantage of this method, is that the conditions under which vapour pressures are calculated, approximate GC conditions to a better extent than the previous above mentioned methods, where vapour pressures had been determined 'in vacuo'.

Attempts have been made to correlate calculated thermodynamic data to chelate volatility. Swain and Karraker (266) suggested that changes in vapour pressure in rare earth fod chelates might be due to differences in ΔS, though Berg and Truemper (256) stated that such a correlation was not possible, and suggested a complex relationship between molecular structure and volatility.

From the above discussion, the following generalisations can now be made regarding substituent effects upon chelate volatility and thermal stability:

1) Volatile 1,3-diketonates of most metals can be prepared.
2) The volatility and thermal stability of many 1,3-diketonates is increased by fluorine substitution for hydrogen in the β-diketone terminal groups.
3) Chelate solvation effects are reduced for ligands that contain bulky terminal groups such as t-butyl.
4) Volatility of lanthanide chelates increases with atomic number.
5) Substitution of an aryl group, such as phenyl, furyl or thienyl, for a methyl group in the 1,3-diketone decreases

chelate volatility.

6) Substitution of a group, other than hydrogen, in the 3-position of the chelate ring reduces volatility and thermal stability.

1.6

General conclusions regarding the chromatographic analysis of metal chelates.

Depending on the choice of either gas or liquid chromatography, a number of contrary factors can affect the success of any attempted analysis of metal chelate compounds.

If HPLC analysis is the medium of choice, chelates derived from non-fluorinated, aryl substituted β-diketones are preferable, due to the increased solution stability that such chelates possess compared to fluorinated chelates.

If gas chromatography is to be utilised, fluorinated chelates are essential, in order to impart increased chelate volatility and thermal stability. Aryl substitution is not preferable due to the lowered volatility and thermal stability imparted to the resultant chelates.

For the work undertaken for the purpose of this thesis, a compromise between the above constraints was sought. This led to the design and synthesis of novel, heavily fluorinated, aryl substituted β-diketones, with the following objectives in mind:

1) Fluorinated β-diketones to be used for GC purposes, not only to aid in chelate volatility, but also in increased detection limits with respect to electron capture detection.
2) Aryl substitution to be incorporated into the β-diketone chain, in order to enhance chelate solution stability, and

therefore aid HPLC analysis.

For these reasons, a range of β-diketone ligands based on benzoylacetone (bza) and benzoyl-1,1,1-trifluoroacetone (bta) were prepared.

SECTION 2

EXPERIMENTAL, RESULTS AND DISCUSSION

2.1

Thesis objectives

The choice and use of fluorinated aromatic β-diketones for the derivatisation of metals prior to GC and HPLC analysis, was suggested by three independently documented areas of research.

1) High MW organic compounds of biochemical origin have been successfully determined by gas chromatography using ECD detection and prior derivatisation with halocompounds. Koshy et al (289) employed o-(2,3,4,5,6-pentafluorobenzyl)hydroxylamine hydrochloride for the GC/ECD determination of keto-steroids. It was shown that the use of this reagent led to increased sensitivity and detection limits of testosterones, progesterone and androsterone, compared to the use of heptafluorobutyrate derivatives. Nambara (290) used pentafluorobenzylhydroxylamine as a derivatising agent for the GC analysis of dehydroepiandrosterones.

2) Pentafluorophenyl derivatives have been employed (291) for the analysis of organo-metallic Ge, Hg, Sn, Cd and Pb complexes by liquid-solid chromatography.

3) Stephen (292) showed that the alkali metal complexes of 1-(dodecafluorobicyclo(2,2,1)heptan-1-yl)-4,4,4-trifluorobutan-2,4-dione (dtb) were soluble in ether solutions, and were sublimable.

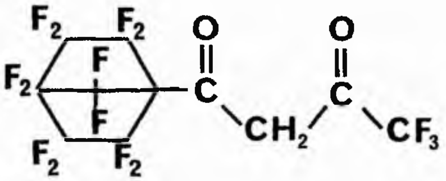

(dtb)

It was therefore considered of value to attempt to extend the use of fluorinated phenyl substituted β-diketones to the analysis of metals as their chelated derivatives. Prior to gas and/or liquid analysis of such chelates however, stability data would be required with respect to solid, solution and thermal constraints. Initially therefore, following synthesis and chelation of a range of novel fluorinated, aromatic β-diketones, absolute metal chelate solution (or formation) constants would be obtained. The correlation of such constants with spectroscopic, electrochemical and physical data derived from the chelates would then be statistically examined. Metal chelate thermal stability data, together with quantitative information on metal chelate vapour pressure - temperature characteristics would also be obtained.

From the solution and thermal stability and vapour pressure data obtained, predictions would be made with regard to the use and potential of such chelates to gas and liquid chromatography. These predictions would then be tested on a variety of chromatographic column materials and under varied conditions.

2.2 Synthesis of β-diketones and metal chelates

2.2.a Reagent Suppliers

Reagents used for the preparation of β-diketone ligands and their respective metal chelates were obtained from the following suppliers:

Fluorochem Ltd., Glossop, Derbys.

Ethyl trifluoroacetate
Ethyl heptafluorobutyrate
Pentafluoroacetophenone
Trifluoroacetylacetone
Hexafluoroacetylacetone

Aldrich Ltd., Gillingham, Dorset.

p-methylacetophenone
Acetylacetone
Benzoylacetone
Dipivalylmethane

Lancaster Synthesis. Lancaster, Lancs.

Benzoyl-1,1,1-trifluoroacetone

BDH Chemicals Ltd., Poole, Dorset.

2-Thenoyl-1,1,1-trifluoroacetone

Mercuric acetate

Fisons Ltd., Loughborough, Leics.

Alkali metals,

Mg, Ca, Sr, Ba, Ni, Cu, Zn, Pb and Cd

as the respective nitrates, AR grade.

Solvents were of SLR, AR and HPLC grade as appropriate.

2.2.b

Preparation of polyfluorinated β-diketone ligands

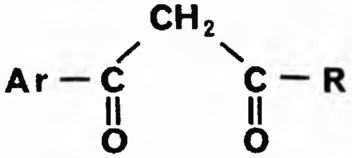

The β-diketones pentafluorophenyltrifluoroacetone (pfbtfa) (Ar = C_6F_5, R = CF_3), 1,1,1,2,2,3,3-heptafluoro-6-(pentafluorophenyl)-4,6-hexanedione (pfbhfh) (Ar = C_6F_5, R = C_3F_7) and p-methylbenzoyl-1,1,1-trifluoroacetone (p-Me-bta) (Ar = p-Me-ϕ R = CF_3) were synthesised by the classical Claisen condensation technique using sodium hydride as the base catalyst.

Synthesis of Pentafluorophenyltrifluoroacetone

Into a two-necked round bottom flask was placed sodium hydride (1.5g, 62 mmole, 80% in mineral oil), and ethyl trifluoroacetate (21.3g, 150 mmole) in 100 ml sodium dried ether. A solution of pentafluoroacetophenone (10.5g, 50 mmole) in sodium dried ether was then added slowly over a period of 45 minutes, the reaction being held under reflux for a further hour. The residual sodium hydride was destroyed with ethanol (2 ml) and then extracted with 2 X 100 ml 0.1 M HCl, in order to destroy any sodium - ligand complex formed. After washing (2 X 100 ml water) and drying (Na_2SO_4), the ether was removed in vacuo.

The pfbtfa ligand was extracted as its copper chelate by washing with ethanolic copper (II) acetate solution. After removing the solvent in vacuo, the copper chelate was extracted into $CHCl_3$, and washed with 3 X 100 ml water. After drying (Na_2SO_4), the $CHCl_3$ was removed in vacuo, and the copper chelate recovered. The chelate was washed with n-hexane to remove non-chelated impurities, and dried at 100^oC for three hours. The free ligand was then liberated by destroying the copper chelate with 5.0 M HNO_3, and extracting the β-diketone into $CHCl_3$. After washing (2 X 100 ml) and drying (Na_2SO_4), the $CHCl_3$ was removed in vacuo and the β-diketone recovered. Final purification was achieved by reduced pressure distillation to give a colourless liquid (5.7g, 37%), b.p. 80 - 84^oC at 1.5 mm Hg; ν_{max} (film) 1642, 1600, 1280, 1205, 1030, 825, 641 cm^{-1}; $\delta(CDCl_3)$ 6.30 (1H, s, CH), 13.97 (1H, s, OH); λ_{max} (MeOH) 309 nm, ϵ_{max} 15,400 $dm^3\ mol^{-1}\ cm^{-1}$.

Synthesis of 1,1,1,2,2,3,3-heptafluoro-6-(pentafluorophenyl)-4,6-hexanedione

The β-diketone pfbhfh was synthesised in like manner (vide supra) using ethyl heptafluorobutyrate (36.3g, 150 mmole) the product being isolated via the respective nickel chelate as a colourless liquid (8.1g, 40%), b.p. 73 - 77^oC at 0.2 mm Hg; ν_{max} (film) 1640, 1600, 1350, 1125, 750 cm^{-1}; $\delta(CDCl_3)$ 6.39 (1H, s, CH), 13.89 (1H, s, OH); λ_{max} (MeOH) 314 nm, ϵ_{max} 13,300 $dm^3\ mol^{-1}\ cm^{-1}$.

Elemental analysis for pfbtfa, pfbhfh and the synthetic precursor pentafluoroacetophenone showed significant variation from the calculated theoretical values. This was accounted for by difficulties in determining fluorine content of the samples (293). ^{1}H NMR spectra of the β-diketones (vide infra) however were according to the expected resonance pattern, no evidence for sample impurities being observed.

Synthesis of p-methylbenzoyl-1,1,1-trifluoroacetone

The β-diketone p-Me-bta was synthesised by reaction of p-methylacetophenone (6.7g, 50 mmole) with ethyl trifluoroacetate (21.3g, 150 mmole). The product was isolated via the copper chelate as off-white crystals (6.3g, 55%), b.p. 96 - 100°C at 1.3 mm Hg (Found: C, 57.2; H, 3.88; F, 24.5%. $C_{11}H_9O_2F_3$ requires C, 57.4; H, 3.91; F, 24.8%); ν_{max} (film) 1685, 1610, 1270, 815 cm^{-1}; δ ($CDCl_3$) 2.43 (3H, s, CH_3), 6.50 (1H, s, CH), 7.19 - 7.87 (4H, m, aryl), 14.62 (1H, s, OH); λ_{max} (MeOH) 327 nm, ϵ_{max} 9,000 dm^3 mol^{-1} cm^{-1}.

Attempts were made to prepare the β-diketone pentafluorophenylbenzoylacetone (Ar = C_6F_5, R = CH_3), both from the reaction of pentafluoroacetophenone with methyl acetate, and by reaction of ethyl pentafluorobenzoate with acetone. However both synthetic routes proved unsuccessfull, despite variation of experimental conditions and choice of base catalyst, eg; NaH, Na, NaOEt, NaOMe, $NaNH_2$.

Benzoyl-1,1,1-trifluoroacetone (bta) (Ar = C_6H_5, R = CF_3), a homologue to the above β-diketones, was used without further purification (m.p. 39 - 40°C, lit. 40°C).

The following β-diketone ligands were also used for comparative purposes, and were used without further purification: acetylacetone (acac), trifluoroacetylacetone (tfa), hexafluoroacetylacetone (hfa), dipivalylmethane (dpm), benzoylacetone (bza) and 2-Thenoyl-1,1,1-trifluoroacetone (tta).

2.2.c

Preparation of metal - ligand complexes

Alkali metal complexes

Alkali metal complexes of p-Me-bta, bta, pfbtfa and pfbhfh were prepared by direct reaction of freshly cut metal with the appropiate β-diketone in dry n-hexane solution. The reaction mixture was gently refluxed for approximately three hours, excess metal removed, and the powdered product washed with dry n-hexane, and dried at 60°C for three hours.

Group II, Ni, Cu, Zn, Pd, Cd and Hg chelates

β-diketonates of the Group II metals, Ni, Cu, Zn, Pb, Cd and Hg, with the exception of Ca(pfbhfh)$_2$, were all prepared by addition of a methanolic solution of the respective ligand to an aqueous solution of the metal nitrate containing an excess of sodium acetate. The resultant precipitate was filtered off at the pump, washed with water and n-hexane, and recrystallised from aqueous methanol. The chelates were then dried at 60°C for three hours. Isolation of Ca(pfbhfh)$_2$ was not possible, despite variation of the preparative conditions.

Transition metal chelates of acac, tfa, hfa, bza and tta used for comparative purposes, were prepared by established procedures (92), and recrystallised from aqueous methanol.

Metal content analysis of the chelates and complexes was performed by flame photometry (for the alkali metals), and by atomic absorption for the divalent metals. TABLES 24 a, b, c and d list relevant analytical data obtained.

2.2.d

Mercury - β-diketone complexes

The mercury complexes of p-Me-bta, bta, pfbtfa and pfbhfh are of particular interest. As previously discussed, Chapter 1.3.2, reaction of mercury salts with β-diketones does not usually occur with the formation of a classical chelate ring, but rather with the formation of Hg-C bonds. As expected therefore, the mercury complexes of the four studied ligands showed a variety of structural forms, as deduced from metal content anaysis and spectroscopic information.

Hg - p-Me-bta complex

Reaction of a solution of mercuric acetate containing excess sodium acetate in water, with methanolic p-Me-bta produced a white precipitate m.p. 104°C (Found: Hg, 44.24%; $C_{24}H_{18}O_6F_6Hg_2$ requires Hg, 43.74%); ν_{max} (KBr) 2870, 1710, 1418, 1350, 763, 510, 455 cm^{-1}; δ(^{6}D-acetone) 7.1 - 7.9 (8H, m, aryl), 3.31 (1H, s, CH), 2.44 (3H, s, CH_3), 2.37 (6H, s, CH_3); λ_{max} (MeOH) 261 nm, ϵ_{max} 22,100 dm^3 mol^{-1} cm^{-1}.

It is interesting to note that the IR spectrum of this complex showed no broad band at approximately 1600 cm^{-1}, indicative of a chelated carbonyl group as found in a classical chelate ring. CH stretch bands were however observed at 2870 and 763 cm^{-1} respectively, the bands at 1418 and 1350 cm^{-1} being typical of an acetyl group. The analytical data is therefore consistent with the proposed structure:

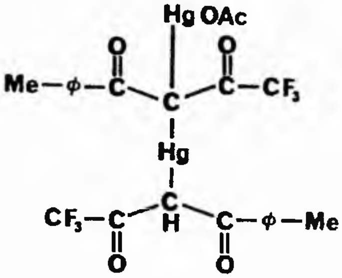

Hg - bta complex

Reaction of aqueous mercuric acetate containing an excess of sodium acetate, with methanolic bta solution resulted in a white precipitate m.p. 167^{o}C; ν_{max} (KBr) 1715, 1395, 890, 790, 504 cm^{-1}; δ(^{6}D-acetone) 7.5 - 8.1 (10H, m, aryl), 6.31 (1H, s, CH); λ_{max} (MeOH) 249 nm.

In common with the Hg - p-Me-bta complex, the IR spectrum did not show a broad band at 1600 cm^{-1}, therefore negating the possibility of a chelate ring. However, no evidence of an acetyl group could be observed. The aryl integral height was equivalent to ten protons, ie; two phenyl rings, but only one proton assigned to an olefinic proton was observed. A Hg-C stretch band at 504 cm^{-1} was observed, but no Hg-O stretch band was evidenced. The possible structures that can be drawn for the Hg - bta complex from the above information, could not be rationalised with the metal content analysis for this complex. It was further noticed that the complex was difficult to dissolve in a range of common solvents, eg; $CHCl_3$, DMSO, CCl_4.

These observations therefore suggest that the Hg - bta complex is polymeric, multiple bta residues being linked by mercury atoms. Bonati and Minghetti (77) drew similar conclusions from a study of the complex derived from reaction of mercuric acetate with acetylacetone.

Hg - pfbtfa complex

Reaction of aqueous mercuric acetate containing an excess of sodium acetate with methanolic pfbtfa produced a white precipitate m.p. 158°C (Found: Hg, 24.91% $C_{20}H_2O_4F_{16}Hg$ requires Hg, 24.75%); ν_{max} (KBr) 1724, 1412, 770, 500, cm^{-1}; δ(^{6}D-acetone) 3.34 (2H, s, CH); λ_{max} (MeOH) 312 nm, ϵ_{max} 25,100 dm^3 mol^{-1} cm^{-1}.

Again no chelated carbonyl absorption band was observed at 1600 cm^{-1}, ruling out the possibility of a chelate ring. The proton resonance at δ = 3.34 ppm, and the CH out-of-plane stretch band at 770 cm^{-1} indicate the presence of an Ar-CO-CH-C grouping. These facts plus the Hg-C stretch band at 500 cm^{-1}, indicate the proposed structure:

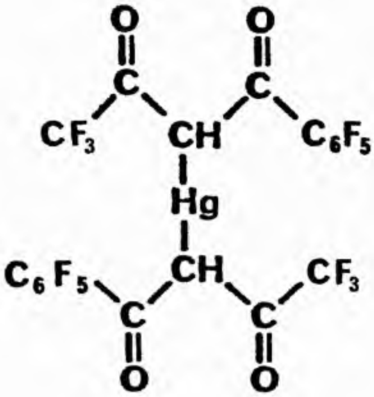

Hg - pfbhfh complex

Reaction of aqueous mercuric acetate containing an excess of sodium acetate with methanolic pfbhfh produced a white precipitate, m.p. 138°C (Found: Hg, 19.63%; $C_{24}H_{2}O_{4}F_{24}Hg$ requires Hg, 19.85%); ν_{max} (KBr) 2995, 1714, 770, 505 cm^{-1}; δ (^{6}D-acetone) 3.18 (2H, s, CH); λ_{max} (MeOH) 314 nm, ϵ_{max} 17,200 dm^{3} mol^{-1} cm^{-1}.

The spectroscopic data for the Hg - pfbhfh complex parallels that of the Hg - pfbtfa complex, the data being consistent with the proposed structure:

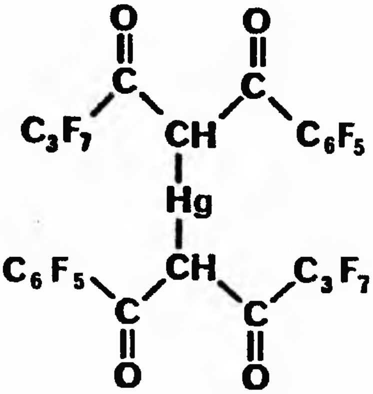

As previously described, Chapter 1.3.2, the mercury derivative of fod exists in the structural isomeric forms (84):

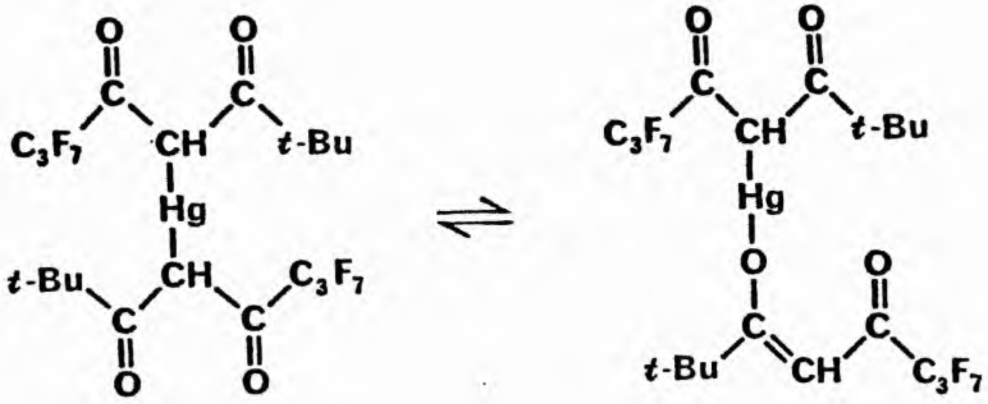

It has been suggested that the inductive effect of the perfluoro group aids the formation of the Hg-O bonded isomer, by increasing the $\sigma - \pi$ conjugation within the complex. However, ^{1}H NMR spectra for the Hg - pfbhfh complex suggests no isomerisation (on the NMR time scale), no olefinic proton indicative of the Hg-O bonded isomer being observed.

2.3

Determination of ligand association constants and absolute metal chelate stability constants

Introduction

In order to study and quantify the effect of varying fluoro-substitution in the β-diketone chain, and to correlate these effects with spectroscopic and electrochemical data, it was necessary to obtain the acid dissociation constants of the β-diketone ligands and formation constants of the metal chelates. However, because of the poor solubility of the metal chelates in wholly aqueous systems, dioxan-H_2O mixtures were employed. Such solvent compositions however complicate the ready calculation of thermodynamic data due to the variation in ionic activity coefficients in non-aqueous media. The calculation of β-diketone acid dissociation constants and chelate stability constants was therefore performed using the methods of Van Uitert (237) and Block and McIntyre (239), as modified by Goldberg (240). The mathematical justification for the method is given below.

2.3.a

Acid association constants

The β-diketones enolise in solution to an extent dependent on the solvent medium, according to:

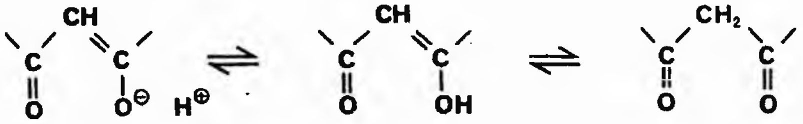

For the reaction in which a proton reacts with the enolate anion (L^-), the following equations may be defined:

$$H^+ + L^- = HL$$

$$Q_H = \frac{[HL]}{[H^+]\,[L^-]} \qquad (1)$$

$$K_H = Q_H \cdot \frac{\gamma_{HL}}{\gamma_{H^+}\,\gamma_{L^-}} \qquad (2)$$

- where Q_H and K_H are the concentration and thermodynamic association constants, and that γ_x is the activity coefficient of component x. Assuming the neutral species HL to have an activity coefficient of unity, and that $\gamma_{H^+} = \gamma_{L^-}$, then:

$$K_H = Q_H / \gamma_{\pm}^2 \qquad (3)$$

Now let $\bar{n}_H$ = Average number of hydrogen ions bound per enolate anion. Then:

$$\bar{n}_H = \frac{[HL]}{[L^-] + [HL]}$$

substituting for $[HL]$ (equation 1):

$$\bar{n}_H = \frac{Q_H [H^+] [L^-]}{[L^-] + Q_H [H^+] [L^-]}$$

$$\therefore \quad \bar{n}_H = \frac{Q_H [H^+]}{1 + Q_H [H^+]}$$

Also let $\bar{n}_H$ = (bound hydrogen)/(total ligand concentration), and bound hydrogen = total H^+ - reacted H^+ - dissociated H^+

$$\therefore \quad \bar{n}_H = \frac{C_{HL} - C_{OH} - [H^+] + [OH^-]}{C_{HL}}$$

where the use of brackets [ ] denotes concentrations, and C_x denotes stoichiometric concentrations of component x.

Now the experimentally observed pH will differ from the true hydrogen ion concentration in solution $[H^+]$, by a factor appropiate the presence of the organic component in solution (ie; dioxan), and the influence of the other ionic species. Van Uitert (237) has shown that this correction is of the form:

$$-\log [H^+] = B + \log(U_H) - \log(1/\gamma_{\pm})$$

where B = Experimentally observed pH

$\log(U_H)$ = Correction for the difference between the experimental pH and the activity of H^+ in dioxan-H_2O of known composition.

$\log(1/\gamma_{\pm})$ = Activity coefficient correction to ion concentrations in solution.

From values of $\bar{n}_H$ and $[H^+]$ the value of Q_H can be calculated, according to the equation:

$$Q_H = \frac{\bar{n}_H}{(1 - \bar{n}_H)\,[H^+]}$$

Rearrangement of equation (3) then allows calculation of K_H, the thermodynamic association constant.

$$\log K_H = \log Q_H + 2\log(1/\gamma_{\pm})$$

A computer program was written (Appendix 1) to calculate values of $\bar{n}_H$, $[H^+]$ and K_H during the course of the necessary pH titration, incorporating appropiate values of $\log(U_H)$ and $\log(1/\gamma_{\pm})$ into the calculation sequence.

Metal chelate formation constants

The formation of a chelate from divalent metal ion M^{2+} and enolate anion L^-, can be considered in terms of the stepwise formation constants K_1 and K_2:

$$M^{2+} + L^- \rightleftharpoons ML^+$$
$$ML^+ + L^- \rightleftharpoons ML_2$$

where:

$$K_1 = \frac{[ML^+]}{[M^{2+}]\,[L^-]}\,\frac{\gamma_{ML^+}}{\gamma_{M^{2+}}\,\gamma_{L^-}} = \frac{Q_1}{\gamma_\pm^2}$$

$$K_2 = \frac{[ML_2]}{[ML^+]\,[L^-]}\,\frac{\gamma_{ML_2}}{\gamma_{ML^+}\,\gamma_{L^-}} = \frac{Q_2}{\gamma_\pm^2}$$

assuming (according to the Debye-Huckel theory) that:

$$\gamma_{ML_2} = 1 \quad \text{and} \quad \gamma_{M^{2+}} = \gamma_\pm^2$$

and that:

$$\gamma_{ML^+} = \gamma_{L^-} = \gamma_\pm$$

Q_n being the respective concentration stepwise stability constant.

Now let $\bar{n}$ = the average number of enolate anions bound per metal ion:

$$\therefore \quad \bar{n} = \frac{[ML^+] + 2\,[ML_2]}{[M^{2+}] + [ML^+] + [ML_2]}$$

substituting for $[ML^+]$ and $[ML_2]$:

$$= \frac{\Omega_1\,[M^{2+}][L^-] + 2\Omega_1\Omega_2\,[M^{2+}][L^-]^2}{[M^{2+}] + \Omega_1\,[M^{2+}][L^-] + \Omega_1\Omega_2\,[M^{2+}][L^-]^2}$$

and eliminating $[M^{2+}]$:

$$= \frac{\Omega_1\,[L^-] + 2\Omega_1\Omega_2\,[L^-]^2}{1 + \Omega_1\,[L^-] + \Omega_1\Omega_2\,[L^-]^2}$$

Now the concentration of free enolate anoin $[L^-]$ is given by:

$$[L^-] = \frac{C_{HL} - C_{OH} - [H^+]}{\Omega_H\,[H^+]}$$

The average number of anions bound per metal ion is then given by:

$$\bar{n} = \frac{C_{HL} - [HL] - [L^-]}{C_m}$$

Substituting for HL (equation 1), and factorising:

$$\bar{n} = \frac{C_{HL} - (Q_H [H^+] + 1)[L^-]}{C_m}$$

A second computer program was written (Appendix 2) to calculate values of $\bar{n}$ and $[L^-]$ during the course of the necessary pH titration, again taking into account the change in solution volume plus appropiate values of $\log(U_H)$ and $\log(1/\gamma\pm)$.

From the results, plots of $\bar{n}$ against pL were made (where $pL = -\log[L^-]$), values of pL being read off the graphs at $\bar{n} = 0.5$ and $\bar{n} = 1.5$ such that:

at $\bar{n} = 0.5$ $\qquad Q_1 = 1/[L^-]_{1/2}$

at $\bar{n} = 1.5$ $\qquad Q_2 = 1/[L^-]_{3/2}$

To convert the concentration formation constants into the respective thermodynamic constants, values of Q_n were corrected by the appropiate activity coefficients, according to the equation:

$$\log K_n = \log Q_n + 2\log(1/\gamma\pm)$$

The overall thermodynamic metal chelate stability constant is then given by:

$$\beta = K_1K_2$$

2.3.b

Experimental

The pK_a values for p-Me-bta, bta, pfbtfa and pfbhfh were obtained in solutions of varying mole fraction (f_2) dioxan (equivalent to 45 - 82%) dioxan content) by potentiometric titration using an Orion Research 611 pH meter. The dioxan was purified by established procedures (294). A combined glass and calomel reference electrode, with temperature sensor was used, 100 cm^3 solutions of dioxan-H_2O containing approximately 0.5 mmole ligand, being titrated against standardised 1.0 M tetramethyl - ammonium hydroxide (Aldrich Ltd.). The pH meter was initially calibrated at pH 4.0 and 7.0 for pfbtfa and pfbhfh, and calibrated again at pH 7.0 and 9.2 for p-Me-bta and bta.

Stability constants of the chelates of the studied metals were obtained in like manner, using a Pye Unicam PW 9418 pH meter, the reaction solution containing metal nitrate such that the chelating ligand was present in at least a 3:1 molar excess over the metal ion. The apparatus was again initially calibrated at pH 7.0 and 4.0. All titrations were performed at 20°C. As a check on the method and calculation procedure, the pK_a of dipivalylmethane (dpm) and 2-Thenoyl-1,1,1-trifluoroacetone (tta), two β-diketones differing widely in known acid strength, were initially determined.

Results and Discussion

Values of pK_a for dpm and tta were determined as 15.58 ± 0.36 and 9.05 ± 0.07 in 75% dioxan-H_2O, and agree well with literature values of 15.71 and 9.10 (294, 248).

Values of pK_a for p-Me-bta, bta, pfbtfa and pfbhfh at varying mole fraction (f_2) dioxan content are shown in TABLE 25 and graphically in FIG 1. Using a computer program to apply regression analysis to the data, correlations of 0.997, 0.999, 0.998 (significant at greater than 99.0%, four data points) for p-Me-bta, bta, pfbtfa, and 0.999 (significant at greater than 95.0%, three data points) for pfbhfh were calculated. TABLE 26 lists calculated values to the constants 'a' and 'b' from the regression equation:

$$pK_a = a + b\,(f_2)$$

The good linear correlation of the pK_a - f_2 data, indicates that little change in keto - enol equilibria is occuring for the β-diketones in the different dioxan-H_2O solutions. Results indicate that in 75% dioxan-H_2O, the observed values of pK_a for the ligands are approximately four pK_a units larger than the extrapolated values in pure water (f_2 = 0.0). Further, results indicate that ligand basicity increases according to the order:

pfbhfh < pfbtfa < bta < p-Me-bta

- at all dioxan mole fraction contents. Data for p-Me-bta and bta in each dioxan-H_2O solution indicates that p-methyl substitution in the benzoyl functionality serves to decrease ligand acidity, due to the increased inductive effect of the p-methyl substituent increasing the basicity of the oxygen atoms. Study of the calculated slopes of the pK_a - f_2 regression equation ('b'), together with the associated error function indicates that within experimental error, solvent effects promoting the basicity of p-Me-bta over bta are only minimal. Further, the calculated intercepts of the pK_a - f_2 data (where the intercept predicts the extrapolated theoretical ligand pK_a in pure water, assuming no change in ligand tautomeric equilibria) indicates that within experimental error, the pK_a of p-Me-bta and bta are approximately the same. Comparison of the results for bta and pfbtfa in each dioxan-H_2O solution indicates that pentafluorophenyl substitution for phenyl increases ligand acidity by approximately 3.5 pK_a units. This is due to the inductive effect of the fluorination upon the phenyl ring, the resonance of the phenyl ring with the enolic ring being reduced. This has the effect of withdrawing electron density away from the O-H bond, therefore rendering the enolic proton more acidic. A further fluorination from pfbtfa to pfbhfh increases ligand acidity again.

The large difference in the observed pK_a values of the four β-diketones can also be accounted for by resonance interactions within the molecules. ^{1}H NMR studies of the four β-diketones (vide infra) demonstrate that in p-Me-bta and bta, resonance between the phenyl ring and the enolic ring occurs. This resonance imparts a greater basic character to the β-diketone ligand. In pfbtfa and pfbhfh no resonance occurs, due to the sterically large pentafluorophenyl ring hindering coplanarity with the enolic ring. This therefore has the additional effect, along with the higher fluorine content, of decreasing the stability of the system and therefore increasing β-diketone ligand acidity. The observed pK_a trend for pfbtfa and pfbhfh in all dioxan-H_2O solutions is in keeping with the expected increase in ligand acidity with increasing fluorination.

FIGS 2 - 13 show formation constant curves obtained for Mg, Ca, Sr, Ba, Ni, Cu, Zn, Pb and Cd with the four studied ligands, in 75% dioxan-H_2O. TABLES 27 - 30 show calculated values of $\log K_1$, $\log K_2$ and $\log\beta$ (where $\beta = K_1.K_2$, the overall thermodynamic metal chelate formation constant) for the studied metal chelates, derived from the formation curves at $\bar{n} = 0.5$ and 1.5 respectively. Results indicate that for p-Me-bta and bta, a general order of stability exists of:

$$Ba < Sr < Ca < Mg < Cd < Pb < Zn < Ni < Cu$$

For chelates of pfbtfa and pfbhfh however, a stability order of:

$$Ca < Ba < Sr < Cd < Mg < Pb < Zn < Cu < Ni$$

- is seen to operate. Study of TABLES 29 & 30 shows that the difference in the relative positions of the calcium chelates of pfbtfa and pfbhfh in the two sequences is that a value for log K_2 (and hence log β) could not be computed, because $\bar{n}$ (the average number of enolate anions bound per metal ion) did not rise to 1.5. FIGS 4&5 show that for $Ca(pfbtfa)_2$ and $Ca(pfbhfh)_2$, $\bar{n}$ only reached 1.4 and 1.34 respectively. It is interesting to note that where $\bar{n}$ did nor rise to 1.5, isolation of the solid metal chelate, from reaction of the buffered metal salt with alcoholic ligand was achieved with low yield for $Ca(pfbtfa)_2$ and for $Ca(pfbhfh)_2$ not possible. The formation constant curve for $Ca(p\text{-}Me\text{-}bta)_2$, FIG 2, also shows that at values of $\bar{n}$ greater than 1.5, the stability of the complex in solution apparently dropped. Again the yield of $Ca(p\text{-}Me\text{-}bta)_2$ compared to the yield of the respective Mg, Sr and Ba chelates was low. It is also worthy of note that the value of logβ for $Ni(pfbhfh)_2$ is higher than $Cu(pfbhfh)_2$, the only situation presented here, where a nickel chelate has a higher stability constant than the respective copper chelate in 75% dioxan-H_2O. Again, the nickel chelate of pfbhfh was noticeably easier to prepare and isolate than the copper chelate. ^1H NMR and polarographic studies (vide infra) of the copper chelates of the pentafluorophenyl substituted β-diketones, demonstrate a greater susceptibility of the copper chelates to stability change by introduction of polyfluoroalkyl substitution, compared to the phenyl substituted β-diketones. It is suggested therefore that the high degree of fluorination the $Cu(pfbhfh)_2$ molecule is sufficient to lower the stability of the chelate to below that of the nickel chelate.

An attempt was made to determine formation constants of the alkali metal - β-diketone complexes. However, calculated values of $\bar{n}_{max}$ did not exceed $\bar{n} = 0.2$, values of K_1 therefore not being obtained. However, since alkali metal - ligand complexes were in fact isolated, this observation must suggest a lower limit to which the potentiometric method is able to determine such solution stability constants.

Assuming that the ligand acidity constants reflect the substituent electronic effects operating in the β-diketone molecule, and that the same factors influence metal chelate stability, a plot of these two functions against each other would therefore be expected to show a high degree of correlation. FIGS 14 & 15 show such plots for the Group II and remaining divalent metals, and show that metal chelate stability increases with increasing ligand basicity. Applying regression analysis to the experimental data, correlation coefficients of 0.990 (significant at 99.0%), 0.987, 0.986, 0.986 and 0.983 (significant at greater than 95.0%) were calculated for Cu, Ni, Zn, Pb and Cd, and 0.972, 0.950 and 0.951 for Mg, Sr and Ba respectively, significant at greater than 95.0% (four data points each plot). A correlation could not be calculated for the calcium chelates, as only two data points were available. It is also to be noticed that the slopes of the $\log\beta$ - pK_a lines increase in the order:

$$Ba < Sr < Mg < Cd < Pb < Zn < Ni < Cu$$

- and reflect the increasing ability of each metal ion to be chelated. One can thus conclude that the same electronic effects that affect ligand acidity also influence metal chelate stability, ie; increasing fluorination in the β-diketone chain, causes electron withdrawl from the region of the donor oxygen atoms in the β-diketone, due to the electronegative fluorine weakening the O-H and M-O bonds respectively. Further confirmation of these trends is shown in FIG 16, which shows a plot of overall stability constant for the copper chelates against ligand pK_a, including in the plot chelate data for acac, tfa, hfa, acetylpivalylmethane (apm), dbzm and bza, as determined by Van Uitert (248). The plot shows excellent linear agreement of the data of Van Uitert with the data presented here, a calculated correlation of 0.915 (10 data points), significant at greater than 99.9% being obtained.

2.4

^{1}H NMR Studies

Experimental

^{1}H NMR spectra of p-Me-bta, bta, pfbtfa and pfbhfh and their chelated derivatives, were obtained on Hitachi - Perkin Elmer R-24B and JEOL FX60Q FT NMR spectrometers, operating at 60 MHz, using $CDCl_3$, CCl_4 and ^{6}D-acetone solvents. All proton resonances were measured with respect to a TMS internal standard.

Results and Discussion

FIGS 17 & 18 show resonance spectra for p-Me-bta, bta, pfbtfa and pfbhfh. TABLE 31 lists observed resonance positions for the methine and enolic proton of the studied β-diketones in all three solvents. Results show that the methine proton resonance positions for p-Me-bta and bta are very similar in all three solvents. Substitution of pentafluorophenyl for phenyl in bta to form pfbtfa causes an upfield shift of approximately 0.25 ppm in each solvent. This upfield shift of the methine proton is due to the decreased resonance interaction of the phenyl ring with the chelate ring, attributable to fluoro-substitution on the phenyl ring. This has the effect of weakening the C=C bond in the enolic ring, thus increasing the shielding around the methine proton. It could be argued that a long range anisotropic effect from the pentafluorophenyl ring is instrumental to some extent upon the observed methine proton shift. If the phenyl ring were coplanar with the chelate ring, any anisotropic effect from the pentafluorophenyl ring would be expected to deshield the methine proton. This however is not observed, and it can therefore be concluded that the dominant effect is the increased shielding around the methine proton. It is more likely however that the pentafluorophenyl ring twists away from coplanarity with the chelate ring, in order to minimise steric interactions. Substitution of C_3F_7 for CF_3 in pfbtfa to form pfbhfh results in a small downfield shift, and is due to the additional inductive effect of the extra fluorination strengthening the C=C bond, thereby causing a decrease in shielding around the methine proton. An observable trend among the four studied ligands in all three solvent systems is therefore seen, such that methine proton resonances occur in order of increasing δ according to the order:

$$\text{pfbtfa} < \text{pfbhfh} < \text{p-Me-bta} < \text{bta}$$

Assuming that the amount of shielding around the methine proton is related to the acid strength of the enolic hydrogen atom (a not unreasonable assumption considering the two protons are in tautomeric relation to each other), a plot of methine proton resonance position of the β-diketone against the pK_a of that β-diketone (as measured in 75% dioxan-H_2O) would be expected to show some degree of correlation. FIG 19 shows such a plot, the plot also including methine proton resonance-pK_a data for acac, tfa, hfa, bza, tta and dbzm as determined by Van Uitert and Lintvedt and Holtzclaw (248, 295), in order to better observe the trends present. It can be seen that the data falls into three distinct groups, appropiate to whether the β-diketone ligand possesses aromatic - aromatic, aromatic - aliphatic or aliphatic - aliphatic terminal substitution or not. Good correlation exists for the line comprising data points for pfbtfa, pfbhfh, acac, tfa and hfa ($r = 0.973$ significant at greater than 99.0%, five data points), data for p-Me-bta, bta, bza and tta falling as a separate line ($r = 0.973$ significant at greater than 95.0%, four data points). Dibenzoylmethane (dbzm) with two aromatic terminal substituents falls as a separate point on what would be a third line. The data points for pfbtfa and pfbhfh suggest therefore that the two ligands apparently 'behave' as aliphatic - aliphatic substituted ligands, even though the pentafluorophenyl substituent would be thought to be aromatic in nature. As previously indicated, steric interactions probably force the pentafluorophenyl ring away from coplanarity with the enolic ring, little or no resonance with the enolic ring occuring. The lower methine proton resonance positions of the two phenyl substituted ligands (p-Me-bta and bta), evidence coplanarity of the phenyl ring with the enolic ring. This coplanarity results in resonance between the two π systems, and therefore contributes toward the observed downfield shift. It can therefore be concluded that although the acid strength of a β-diketone can generally be related to the amount of shielding around the β-diketone methine proton, and hence the olefinic - aromatic nature of this proton, strict equivalence between these two functions for any β-diketone is not possible. Rather correlation can only be predicted for certain classes of β-diketone, of a similar substitution type.

Resonance positions of the enolic proton of the β-diketones (in $CDCl_3$) as shown in FIGS 17 & 18 show the following general trend:

pfbhfh < pfbtfa < p-Me-bta < bta

Comparison of the enolic proton resonance data for pfbtfa and bta indicates that the substitution of pentafluorophenyl for phenyl in bta increases the apparent shielding around the enolic proton, an upfield shift of some 0.9 ppm occuring. Substitution of C_3F_7 for CF_3 in pfbtfa results in an upfield shift of 0.08 ppm. Lintvedt and Holtzclaw (295) have suggested that the substitution trifluoromethyl for methyl in acetylacetone causes an increase in the shielding of the enolic proton. This was attributed to a strengthening of the C=O bond and a weakening of the O-H bond, the enolic proton therefore being shielded to a greater extent by its own electron cloud. The substitution of C_3F_7 in going from pfbtfa - pfbhfh would therefore be expected to show another upfield shift of the enolic proton. Data presented here demonstrates that this does occur, the enolic proton therefore being shielded by the increase in polyfluoroalkyl substitution, though admittedly the changes are very slight. Substitution of the p-methyl group in bta to form p-Me-bta occurs with an upfield shift of the enolic proton of approximately 0.2 ppm, and can be explained by the increased resonance of the aromatic ring with the enolic ring. This resonance increases the electron density on the oxygen atoms, resulting in a shorter O-H bond, the enolic proton therefore being better shielded. The increased basicity of p-Me-bta over bta supports this hypothesis.

Examination of the observed line widths of the enolic proton resonances reveals sharp bands for pfbtfa, pfbhfh, and bta (3.6, 7.4 and 5.6 Hz respectively, measured at half peak height), a broad band for p-Me-bta (28.2 Hz) being obtained. These observations can be explained in terms of the likely position of the enolic proton between the two oxygen atoms. Assuming the situation where the electron density on the two oxygen atoms in the β-diketone is similar, it can be argued that the enolic proton would take up a symmetrical orientation between the oxygen atoms. This being so, a sharp enolic resonance peak would result from the presence of electron withdrawing and/or groups that enhanced the resonance in the enolic ring. With bta, these two effects would result in a near symmetrical disposition of the enolic hydrogen atom between the two oxygen atoms, hence a sharp enolic resonance band. The broad enolic band observed for p-Me-bta must indicate therefore that the enolic proton is non-symmetrical about the two oxygen atoms. It is suggested that the increased resonance from the p-methyl substituent increases the electron density on the adjacent carbonyl oxygen. This has the result of drawing the enolic proton closer to the carbonyl group, and decreasing the potential of a symmetrical O-H-O arrangement. Thus:

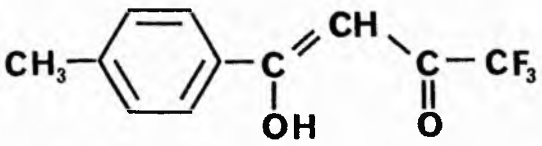

With pfbtfa and pfbhfh, non-coplanarity of the pentafluorophenyl ring with the enolic ring exists as explained previously. With the consequent absence of aromatic - enolic ring resonance, it is likely therefore that the enolic hydrogen atom is situated on the carbonyl group adjacent to the perfluoroalkyl group. Thus:

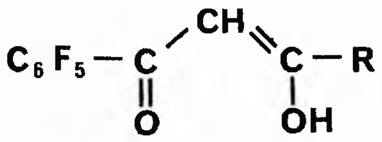

The observed increased basicity of p-Me-bta over bta, and the increased acidity of pfbhfh over pfbtfa, is in keeping with these suggestions.

Enol contents of p-Me-bta, bta, pfbtfa and pfbhfh were determined in the three studied solvents by comparison of half the intensity of the keto form methylene resonance peak, to the intensity of the enol methine proton resonance peak. For such determinations, at least four resonance scans were made over the relevant region, at slow scan speed, an average intensity value being computed. Enol contents as determined by this method indicated that in $CDCl_3$, CCl_4 and ^{6}D-acetone, all four studied β-diketones were completely enolised, no methylene proton resonance, indicative of the keto form being observed. These observations therefore demonstrate that the phenyl and polyfluoroalkyl sustituents favour the formation of the enol form.

^{1}H NMR spectra of the metal chelates derived from p-Me-bta, bta, pfbtfa and pfbhfh were obtained in ^{6}D-acetone due to solubility constraints, the resonance position of the chelate ring methine proton being noted. All spectra were simple and well defined, and in accordance with the expected resonance pattern, no evidence for inter-molecular polymerisation in solution, as found for Ni(acac)$_2$ (213), being observed. TABLE 32 lists values of δ recorded, and it can be seen that in all cases, the methine proton resonances were shifted upfield (ie; to lower δ) relative to the parent β-diketone, indicating an apparent reduction in the olefinic character of the metallocycle proton. Similar observations have been noted by Smith and Thawaites studying the ^{1}H NMR spectra of a range of metal acetylacetonates (208). The following trends are observable from the experimental data:

1) The alkali metal - β-diketone complexes, show methine proton resonance positions in the order:

$$K < Na < Li$$

This therefore indicates a reduction in olefinic character of the methine proton as the complexed metal ion increases in size. Raban et al (214) have shown that Li(acac) exists almost completely in the chelated form in solution, the degree of chelation amongst the alkali metal derivatives of acac decreasing in the order:

$$Li > Na > K$$

It is therefore likely that a similar situation prevails with the alkali metal complexes of p-Me-bta, bta, pfbtfa and pfbhfh.

2) Methine proton resonance positions of the Group II metal chelates within each ligand series are fairly similar, resonance positions being observed in the order:

$$Ba < Sr < Ca < Mg$$

- again as in the case of the alkali metal complexes, indicating a decreasing olefinic character to the chelate ring hydrogen, as the chelated metal ion increases in size.

3) Methine proton resonances for the nickel and copper chelates of the four β-diketone ligands were not observed. This therefore indicated the chelated nickel and copper ions to be in the paramagnetic state, complete collapse of the resonance signal therefore occuring (at the operating temperature of the spectrometer). The zinc chelates of the four ligands are concluded to be diamagnetic on the basis that methine proton resonances were observed. It is of interest to note that the zinc chelates showed methine proton resonances at the highest observed δ values within each ligand system (ie; the least shifted upfield from the parent enol form), and therefore indicate an increased degree of olefinic character to the metallocycle proton to the other studied metal chelates, and therefore qualitatively a more stable ring system.

4) Metal chelates of lead and cadmium show methine proton resonance positions comparable to the Group II metal chelates.

5) ^1H NMR spectra of the mercury - β-diketone complexes do not evidence an olefinic ring proton, and have been discussed above - Chapter 2.2.c.

Since the resonance position of the methine proton is related to the amount of shielding around that proton, and the amount of shielding itself is affected by the strength of the adjacent metal - oxygen bond (a strong M-O bond depleting the electron density around the region of the C-O bond), a plot of the metal chelate methine proton resonance position against the stability constant of that chelate would be expected to show some kind of relationship. FIG 20 shows a plot of these two functions for the studied metal chelates. It can be seen that the experimental data falls into two sets of approximately parallel lines appropiate to the phenyl and pentafluorophenyl substituted β-diketone ligands. The greater slope of the pentafluorophenyl substituted β-diketonates indicates that the electronic nature of the methine proton is more susceptible to change with chelated metal ion than with the respective phenyl substituted β-diketonates. A general stability - methine proton resonance relationship can therefore be seen within each ligand series. The good correlation of the pfbtfa chelate data ($r = 0.983$) allows the estimation of a value of $\log\beta$ for $Ca(pfbtfa)_2$ (the original formation constant curve not allowing ready calculation of $\log K_2$). Interpolation of the methine proton resonance data for $Ca(pfbtfa)_2$ from the regression plot of the pfbtfa data therefore reveals a value of $\log\beta = 10.73$ for $Ca(pfbtfa)_2$. The resonance position of the methine proton - stability relationship is however seen to be only valid within a particular ligand system, though qualitatively the more stable chelates do have a greater resonance position. This general stability relationship concluded is in contrast with the conclusions of Holm and Cotton (201), who stated that the shifts observed for a range of acetylacetonates were approximately independent of the nature of the chelated ion. The results presented here therefore imply that metal chelate stability increases with the olefinic nature of the ring proton. The observed proton resonances do not indicate any benzenoid or delocalised electron system in the chelate ring, as the observed methine resonances are well removed from typical aromatic proton resonances. The effect of increasing fluorination in the β-diketone backbone does indicate some alteration of the electronic properties of the chelate ring however. The fact that all methine proton resonances are shifted upfield from the parent enol form, indicates that any electron delocalisation contribution to the resonance position due due to metallocycle formation, is probably masked by a dominating effect to displace resonances to higher field.

2.5

Polarographic studies

Experimental

Polarography of the transition metal chelates of p-Me-bta, bta, pfbtfa, pfbhfh, acac, tfa, hfa, bza and tta was performed using a Parc EG & G Model 303 dropping mercury electrode (DME), the dispensed mercury drop size being set at 'medium'. Scanning voltages were generated at 10 mV sec^{-1} by a Princeton Applied Research Model 384 polarographic analyser, using the Normal Pulse Polarography mode. Polarographic waves were recorded against an Ag/AgCl reference electrode on a Princeton Applied Research RE 0082 X-Y digital recorder. Using the Model 384 analyser, polarograms were recorded both as real-time plots and as a first derivative, in order to accurately locate $E\frac{1}{2}$ potentials. The Normal Pulse mode was selected for this study, as the technique has a considerable sensitivity advantage over the classical (sampled) DC mode. (Although Differential Pulse Polarography is more sensitive again, the derivative maximum obtained is not strictly equal to $E\frac{1}{2}$, as the calculated derivative function is a second derivative, the real-time DPP plot being already a differential). Sample chelates were present at approximately 10^{-3} M in a solvent composition of 75% dioxan-H_2O, containing KNO_3 base electrolyte at 0.1 M. Polarograms were obtained at $20^{\circ}C$ under an atmosphere of N_2, the samples solutions having been degassed with N_2 for ten minutes previously.

Results and Discussion

Typical polarograms, that of $Cu(p\text{-}Me\text{-}bta)_2$ and $Zn(bza)_2$, are shown in FIG 21, TABLE 33 listing experimentally obtained values of $E\frac{1}{2}$ for the nickel, copper and zinc chelates. In all cases,irreversible waves were observed, as determined from the slope of the real-time polarogram, chelate reduction occuring via a one-step process.

FIG 22 shows a plot of $E\frac{1}{2}$: $\log\beta$ for the copper chelates, good correlation of the data points for pfbtfa, pfbhfh, acac, tfa and hfa, (ie; the aliphatic - aliphatic terminally substituted chelates),($r = 0.979$ significant at greater than 99.0%, five data points), being obtained. The correlation of the pfbtfa and pfbhfh copper chelate data points with acac, tfa and hfa chelate data, indicates that the pentafluorophenyl group 'behaves' as an aliphatic substituent. These observations parallel a similar conclusion already noted from ^1H NMR studies above. Data for chelates of p-Me-bta, bta, bza and tta (ie; the aliphatic - aromatic terminally substituted chelates), fall as a separate group, with a large degree of scatter. These trends therefore indicate that there is a general $E\frac{1}{2}$: stability order for the copper chelates, the more stable chelates being progressively harder to reduce, a more negative potential being required. However the trends can only be regarded as qualitative in nature, and applicable only to chelates of a similar substitution type. Similar conclusions we were drawn by Lintvedt et al (247), from a polarographic study of copper β-diketonates, though with a different cell arrangement.

Assuming the metal chelates to possess similar geometries for a given metal ion and each therefore to contain a common redox active centre, the mechanism of reduction of the metal chelate at the DME may be assumed to be identical for a given metal series. In this case, linear free energy relationships (ie; the Hammett equation) may be correlated with reduction potentials. The Hammett equation equates a kinetic rate constant with substituent effect. Since half wave potentials are a function of the logarathmic rate constants of the electrode process, such an $E\frac{1}{2}$: Hammett substituent effect correlation is fully justified.

Study of the general structure of a metal chelate:

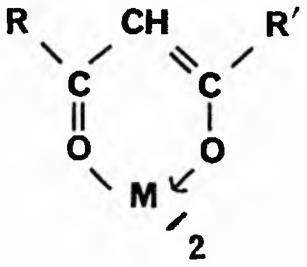

reveals that the substituent groups R and R' are meta with respect to the metal ion, and ortho and para to the chelating oxygen atoms. Accordingly, plots of $E\frac{1}{2}$ versus the sums of the Hammett σ_m and σ_p values for the studied copper chelates were made, and are shown in FIG 23. Calculated correlations of $r_m = 0.874$ (significant at greater than 99.0%, seven data points), and $r_p = 0.908$ (significant at greater than 99.0%, eight data points) were obtained, with calculated slopes of $\rho_m = 0.223 \pm 0.005$ and $\rho_p = 0.169 \pm 0.032$ respectively.

The data points for Cu(pfbhfh)$_2$ and Cu(p-Me-bta)$_2$ in the σ_m plot, and the data point for Cu(pfbhfh)$_2$ in the σ_p plot are not shown as relevant σ_x values for C_3F_7, and p-Me-ϕ were not available from the literature. However, the good correlation of the $E\frac{1}{2}$: σ_x data, assuming ortho effects to be negligible, allows estimation of σ_x values for these substituents. Interpolation of the $E\frac{1}{2}$ data for Cu(pfbhfh)$_2$ (-0.08 V) and Cu(p-Me-bta)$_2$ (-0.230 V) to the calculated $E\frac{1}{2}$: σ_x regression equations, values of C_3F_7 σ_m = 1.15 and p-Me-ϕ σ_m = 0.26, and C_3F_7 σ_p = 1.26 are calculated. It is interesting to note that Lintvedt et al (247) only plotted $E\frac{1}{2}$: $\Sigma\sigma_m$ for the aliphatic - aliphatic terminally substituted copper chelates, stating that correlation of aliphatic - aromatic and aromatic - aromatic terminally substituted chelates was not possible. A re-examination of their data however, plotting $\Sigma\sigma_m$ and $\Sigma\sigma_p$ for all their substituted chelates, where σ_x values were available from the literature, shows good correlation for both σ_m and σ_p plots (r_m = 0.876, twentythree data points, and r_p = 0.948, thirteen data points, both significant at greater than 99.9%).

FIG 24 shows plots of $\Sigma\sigma_x$: $E\frac{1}{2}$ for the studied nickel chelates. Using the calculated σ_x values for p-Me-ϕ and C_3F_7 as obtained above, correlations of r_p = 0.859 and r_m = 0.877 (eight data points each, significant at greater than 99.0%) are obtained, with calculated slopes of ρ_m = 0.083 ± 0.039 and ρ_p = 0.063 ± 0.030 respectively.

FIG 25 shows plots of $\Sigma\sigma_x$: $E\frac{1}{2}$ for the studied zinc chelates. The plots show a large degree of scatter, calculated correlations of r_p = 0.679 and r_m = 0.639 (eight data points each, significant at greater than only 90.0%) being obtained, with calculated slopes of $\rho_m = 0.068 \pm 0.043$ and $\rho_p = 0.056 \pm 0.033$ respectively. The poor correlation of the zinc $E\frac{1}{2}$ data with $\Sigma\sigma_x$ values, implies that variations in the mechanism of reduction may be occuring. This may be accounted for by differing structures of the zinc chelates.

Handy and Lintvedt (249) in a polarographic study of tris-β-diketonates of Cr(III) concluded that a plot of $\Sigma\sigma_p : E\frac{1}{2}$ for five chelates showed better correlation than the equivalent $\Sigma\sigma_m : E\frac{1}{2}$ plot. A statistical re-examination of their data however again concludes that at the 99.0% confidence limit, good correlation is observed for both the $\Sigma\sigma_m$ and $\Sigma\sigma_p$ plots ($r_m = 0.984$, $r_p = 0.987$, five data points).

The correlation results presented here, both for the studied copper and nickel chelates, together with the re-examined data of Lintvedt et al (247) and Handy and Lintvedt (249) all suggest therefore, that exact differentiation of where the substituent electronic effects are operating in the chelate ring is not possible. Rather the results suggest that the substituent effects are experienced both at the donor oxygen atoms, and the chelated metal ion. Further, the close significance of the two zinc correlations seems to confirm the conclusions from the copper and nickel study, that substituent effects operate equally on the oxygen and metal atoms.

The calculated slopes of the $E\frac{1}{2} : \Sigma\sigma_x$ data for each metal chelate series (equal to ρ - the Hammett equation reaction constant) are seen to be positive in each case. This therefore confirms that the electrode reaction (ie; metal chelate reduction) is facilitated by electron withdrawing groups attached to the β-diketone backbone. Thus heavily fluorinated chelates, such as the pfbhfh series, are significantly easier to reduce than those chelates that contain electron donating groups, eg; the acetylacetonates. The magnitude of the calculated slope is also a measure of the susceptibility to reduction of the chelates from the polar substituent effects. It is seen that the slope value for the copper chelate series is approximately fourfold that of the nickel and zinc chelates. The copper chelates are therefore demonstrated to be more liable to changes in solution thermodynamic stability by changes in terminal substituent, than the corresponding nickel and zinc chelates.

These results therefore follow the general metal chelate stability trend within the p-Me-bta, bta, pfbtfa and pfbhfh β-diketonates, as previously demonstrated by ^1H NMR studies, and the lower solution stability of $Cu(pfbhfh)_2$ compared to $Ni(pfbhfh)_2$.

2.6

Ultra-violet studies

Experimental

UV spectra of p-Me-bta, bta, pfbtfa and pfbhfh and their chelated derivatives, and that of tfa for comparative purposes, were obtained in AR methanol, and recorded on a Perkin Elmer Model 552 UV - visible spectrometer over the range 190 - 400 nm.

Results and Discussion

Spectra for p-Me-bta, bta, pfbtfa and pfbhfh are shown in FIGS 26 & 27, spectra for $Cu(pfbhfh)_2$ and $Ni(pfbtfa)_2$ as representative of the metal chelates being shown in FIG 28. TABLES 34 - 36 list the experimentally determined values of λ_{max} and ϵ_{max} for the ligands and metal chelates.

Spectra for the free ligands all show absorption bands in order of increasing λ_{max} according to:

$$\text{pfbtfa} < \text{pfbhfh} < \text{bta} < \text{p-Me-bta}$$

In comparison with tfa, substitution of pentafluorophenyl for methyl in tfa to form pfbtfa is seen to cause a red shift of 13 nm, substitution of phenyl for methyl to form bta causing a red shift of 28 nm. The effect of p-methyl substitution in bta to form p-Me-bta causes a small red shift of 3 nm. All the β-diketone absorption maxima in the region 290 - 330 nm are due to a $\pi - \pi^*$ transition within the enol form. The β-diketones bta and p-Me-bta show further absorption bands at approximately 255 nm, due to the presence of the phenyl ring in the molecule.

Spectra for the studied metal chelates and complexes were observed to be symmetrical in all cases, chelation of the metals to the ligands occuring with the following general trends:

1) Alkali metal complexes of p-Me-bta, bta, pfbtfa and pfbhfh show absorption and extinction maxima similar to the respective free ligands.
2) Chelation of the Group II metals to the four ligands occurs with minor changes to the respective position of λ_{max}, compared to the free ligand.
3) For each ligand series, the transition metal chelates show positions of λ_{max} in the order:

   $$Zn < Cu < Ni$$

   – while the respective values of ϵ_{max} decrease in the order:

   $$Ni < Cu < Zn$$

4) For lead and cadmium chelates of the four ligands, the lead chelate always occurs at the higher λ_{max}.
5) The respective zinc chelate of each ligand has the largest absorption maximum of the chelates within each ligand series.
6) Mercury complexes of the four ligands show positions of λ_{max} similar to the free ligands.

Similar trends have been noted by previous workers studying a range of acetylacetonates (201). No obvious correlation could be drawn between chelate λ_{max} and ϵ_{max}, and chelate solution stability and methine proton resonance data.

Analytically, the potential use of the studied ligands as useful complexing agents for the spectrophotometric analysis of mono and divalent metals can only be judged as moderate, based upon the experimentally observed values of ϵ_{max}.

Beers Law study of $Cu(pfbhfh)_2$, $Ni(pfbtfa)_2$, $Zn(pfbhfh)_2$, $Pb(p\text{-}Me\text{-}bta)_2$ and $Cd(bta)_2$ in MeOH as representative of the studied metals and β-diketone ligands, show linearity up to the following concentrations:

$Cu(pfbhfh)_2$ 8.5 ppm, $Ni(pfbtfa)_2$ 4.0 ppm, $Zn(pfbhfh)_2$ 5.8 ppm, $Pb(p\text{-}Me\text{-}bta)_2$ 19.7 ppm and $Cd(bta)_2$ 10.0 ppm.

2.7

Infra-red studies

Experimental

Infra-red spectra of p-Me-bta, bta, pfbtfa and pfbhfh were recorded on a Perkin Elmer 157G IR spectrometer over the range 4000 - 625 cm^{-1}. Infra-red spectra of the respective metal chelates and complexes were obtained on a Perkin Elmer 683 IR spectrometer, over the range 4000 - 200 cm^{-1}. Chelate spectra were recorded in KBr disks, the parent β-diketone spectra being recorded on NaCl plates.

Results and Discussion

Infra-red spectra of p-Me-bta, bta, pfbtfa and pfbhfh are shown in FIGS 29 & 30. Spectra for pfbtfa and pfbhfh indicate tautomerisation of the β-diketones in the pure state, two carbonyl stretch bands being observed, the broad band at approximately 1600 cm^{-1} being due to the intramolecular hydrogen bonded carbonyl:

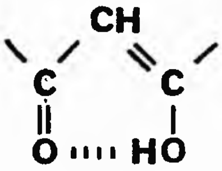

- the absorption band for the non-hydrogen bonded keto form being observed at approximately 1640 cm^{-1}. Only one band, at 1610 and 1605 cm^{-1} respectively, was observed for p-Me-bta and bta, indicating complete enolisation of the β-diketones in the solid state. The effect of p-methyl substitution in bta to form p-Me-bta is seen to shift ν(C-O) to higher frequency. This is in accord with results from ^{1}H NMR above, the increased resonance interaction of the phenyl ring with the enolic ring increasing electron density on the carbonyl group. Substitution of pentafluorophenyl for phenyl in bta to form pfbtfa shifts the enol form carbonyl absorption to lower frequency, due to the decreased resonance interaction of the phenyl ring with the enolic ring. The further fluorination increase from pfbtfa to pfbhfh lowers ν(C-O) for the enol form again, as expected from inductive effects.

FIG 31 shows spectra of $Cu(pfbtfa)_2$ and $Zn(pfbhfh)_2$ as representative of the studied metal chelates. The observed positions of ν(C-O) for the studied metal chelates, and ν(M-O) for the transition metal chelates are given in TABLES 37 & 38, and show the following general trends:

1) The position of ν(C-O) within each ligand series increases in the order:

   Ni,Cu,Zn,Pb,Cd < Group I < Group II metals

2) The transition metal chelates show positions of ν(M-O) in the order:

   p-Me-bta > bta > pfbtfa > pfbhfh

   This order is as expected, the electronegative fluorinated substituents withdrawing electron density away from the carbonyl group, and hence weakening the M-O bond strength.

3) For chelates of a particular ligand system, the position of ν(M-O) decreases in the order:

Cu > Ni > Zn

In common with previous workers (222), no obvious trend in metal chelate stability with the position of ν(C-O) could be correlated. As previously mentioned however (Chapter 1.5.3), the formation of a strong metal-oxygen bond in the chelate ring depletes the electron content of the adjacent carbonyl group, this effect being characterised by a decrease of ν(C-O) and an increase in the value of ν(M-O). To test the validity that the position of ν(M-O) therefore reflects the metal - oxygen bond strength, and hence the stability of the metal chelate, FIG 32 shows a plot of ν(M-O) against nickel, copper and zinc solution metal chelate stability constant. The plots show good linear correlation with calculated correlations of 0.993 (significant at greater than 99.0%), 0.975 and 0.976 (significant at greater than 95.0%) for nickel, copper and zinc chelates respectively (four data points each). Further confirmation of these trends is shown in FIG 33 which shows a plot of ν(M-O) : logβ for the copper chelates alone, including ν(M-O) data for acac, tfa, hfa, bza and dbzm, as determined by Nakamoto et al (225). A calculated correlation of 0.964 (nine data points, significant at greater than 99.9%) is obtained.

Plots for the lead, cadmium and Group II chelates are not shown due to the difficulty in identifying the position of ν(M-O) in the infra-red spectrum.

2.8 Chelate thermal stability and vapour pressure studies

Experimental

The thermal stability and vapour pressures of the metal chelates of p-Me-bta, bta, pfbtfa and pfbhfh were determined on a Stanton Redcroft 'Massflow' thermogravimetric analyser.

The experimental procedure involved following the loss in weight of an accurately weighed (ca. 20 mg) sample of chelate, over the temperature range 20 - 400°C. Samples were held under an atmosphere of dried nitrogen, at a flow rate of 50 ml min^{-1}. The apparatus was calibrated to determine its temperature rise - time characteristic, and was calculated as 5.3 ± 0.2 °C min^{-1} (6 replicates).

Results and Discussion

From the thermograms obtained, the percentage loss in weight with temperature for each chelate was calculated, and are shown in FIGS 34 - 49. From the figures the thermal stability of each metal chelate can be observed, thermally stable chelates giving smooth thermograms approaching 100% weight loss. Conversely chelates that have poor thermal stability show an early break in the thermogram, indicating thermal degradation of the chelate. It was seen that in such cases, a substantial darkened deposit was obtained in the sample crucible upon recovery at the end of the thermogravimetric run. Study of the thermograms reveals that all chelates underwent varying degrees of thermal decomposition, the following general trends being noted:

1) Thermal stability of the alkali metal complexes increased in the order:

$$\text{p-Me-bta} < \text{pfbhfh} < \text{bta} < \text{pfbtfa}$$

- the stability order of the individual metals within each ligand series being K < Na < Li, though with pfbhfh an order of K < Li < Na was observed.

2) Chelates of the alkaline earth metals showed poor thermal stability excepting Mg and Ba chelates of pfbtfa, due to the comparative weakness of the M-O bond, there being no metal d-orbital participation in the metal - ligand bonding.

3) Thermograms for the transition metal chelates of p-Me-bta, bta and pfbhfh revealed chelates of comparative thermal stability, chelates of pfbtfa showing weight losses of approximately 80% before the onset of thermal decomposition.

4) Lead and cadmium chelates of p-Me-bta showed very poor thermal stability, chelates with bta, pfbtfa and $Cd(pfbhfh)_2$ showing better stabilities. $Pb(pfbhfh)_2$ showed a weight loss of approximately 90% before thermal decomposition.

5) Mercury complexes of all four ligands showed a distinct break in each thermogram in the region 160 - 170°C, indicating some kind of decomposition. Each complex then showed further weight loss, greater than that observed for the corresponding lead and cadmium chelates.

The results demonstrate that the studied metal chelates and complexes of p-Me-bta, bta, pfbtfa and pfbhfh possess generally poor thermal stability, certainly less than the respective tfa and hfa chelates (eg; 104, 158), and therefore unsuitable for gas chromatographic applications.

Determination of metal chelate vapour pressures

From the experimentally obtained thermograms, and using an expanded scale plot of the temperature range over which chelate vapourisation began, the slope of the curve at various temperature intervals was calculated. Fujinaga et al (271) have shown that a semi-quantitative measure of chelate vapour pressure can be obtained from the thermogram, from the equation:

$$p = \frac{18,700 \, . \, a}{MF}$$

where:

p = chelate vapour pressure (mm Hg)
M = chelate molar mass
F = gas flow rate
a = rate of chelate weight loss (mg min^{-1})

- any self cooling of the sample crucible due to sample evaporation being assumed negligible, and the chelate vapour assumed monomeric. Chelate vapour pressures so calculated were then plotted against temperature according to the general form of the Clausius - Clapeyron equation:

$$\ln(p) = -\frac{\Delta H}{RT} + \frac{\Delta S}{R}$$

where ΔH = Enthalpy of vapourisation
ΔS = Entropy of vapourisation
R = Gas constant
T = Absolute temperature

The validity of the experimental and calculation procedure was first checked by determining ΔH for $Al(acac)_3$, a calculated value of 23.43 ± 2.66 KCal mol^{-1} agreeing well with a literature value of 23.95 KCal mol^{-1} (104) being obtained.

FIGS 50 - 65 show Clausius - Clapeyron plots for the studied metal chelates and complexes. The advantage of displaying the calculated vapour pressure data in this form, compared to the thermogravimetric curve FIGS 34 - 49, is that the comparative volatilities of the chelates can be immediately ascertained. From the figures, the following observations can be made:

1) Whereas the alkali metal thermograms showed a general thermal stability order of $Li > Na > K$, alkali metal complex volatility, FIGS 50, 54, 58 & 62 shows an order of $K > Na > Li$ for all four ligand systems.
2) Group II metals chelated with p-Me-bta and bta showed the expected volatility order of $Mg > Ca > Sr > Ba$, chelate volatility decreasing with increasing atomic weight and ionic size of the chelated metal ion. However the pentafluorophenyl substituted chelates showed a chelate volatility order of $Ca > Sr > Ba > Mg$.

Reasons for this change in volatility order are not clear. However it could be argued that the smaller ionic radius of Mg^{2+} coupled with the lack of coplanarity of the pentafluorophenyl ring with the chelate ring, leads to steric interactions within the molecule. However the solution stability data for the pfbtfa and pfbhfh chelates does not apparently support such a hypothesis.

3) For the remaining divalent metals, chelate volatility within each ligand system was according to the order:

p-Me-bta : Hg > Pb > Cd > Zn > Cu > Ni
bta : Hg > Pb > Zn > Cu > Ni > Cd
pfbtfa : Hg > Pb > Zn > Cu > Ni > Cd
pfbhfh : Hg > Pb > Cd > Cu > Zn > Ni

FIGS 50 - 65 serve to show how chelate volatility alters for the different metals within each ligand series. It would be useful however, to study also which ligand produces the most volatile chelate where the chelated metal ion is held constant. Accordingly, FIGS 66 - 78 show the comparative effect of change in ligand upon the volatility of a particular metal. Study of the figures indicates that metal volatility for each ligand is in the order:

Li : bta < p-Me-bta < pfbtfa < pfbhfh
Na : bta < p-Me-bta < pfbhfh < pfbtfa
K : pfbhfh < p-Me-bta < bta < pfbtfa

Mg : pfbhfh < p-Me-bta < bta < pfbtfa
Ca : p-Me-bta < bta < pfbtfa
Sr : p-Me-bta < bta < pfbhfh < pfbtfa
Ba : p-Me-bta < bta < pfbhfh < pfbtfa
Ni : p-Me-bta < bta < pfbhfh < pfbtfa
Cu : p-Me-bta < bta < pfbhfh < pfbtfa
Zn : p-Me-bta < bta < pfbhfh < pfbtfa
Pb : bta < pfbhfh < p-Me-bta < pfbtfa
Cd : bta < pfbtfa < pfbhfh < p-Me-bta
Hg : p-Me-bta < pfbhfh < pfbtfa < bta

By subjecting the vapour pressure - temperature data to a least squares regression analysis, values of ΔH and ΔS together with the associated error, obtained from the slope and intercept respectively, were calculated for each metal chelate, and are shown in TABLES 39 & 40. The raw data was initially manually plotted, in order to confirm valid temperature limits for the computation of ΔH and ΔS. This procedure showed negligible curvature of the data over the measured temperature interval.

The concept of chelate volatility must be approached with caution, in respect to the fact that in comparing the volatilities of two compounds,one compound may have a higher vapour pressure than another at one particular temperature, but may show a lower vapour pressure at some other temperature. Accordingly for this thesis, volatility is expressed in terms of the temperature required to achieve a stated vapour pressure. TABLE 41 shows the calculated temperatures at which a chelate vapour pressure of 0.1 mm Hg ($\ln(p) = -2.30$) was attained.

(It has been previously noted, Chapter 1.3, that a minimum vapour pressure of approximately 0.1 mm Hg would be necessary for successfull gas chromatography). Comparison of the results from TABLE 41 and FIGS 50 - 65 with calculated vapour pressures of lanthanide chelates of tfa, hfa and fod (264 - 266, 271), indicates that lanthanide chelates of fod achieved a vapour pressure of 0.1 mm Hg approximately 80°C lower than the pfbtfa chelates, and approximately 100°C lower than the pfbhfh chelates. Lanthanide chelates of tfa and hfa achieved 0.1 mm Hg pressures some 60°C lower than the pfbtfa chelates, and some 80°C lower than the pfbhfh chelates. Further comparison with the data of Wolf et al (104), indicates that the copper chelates of hfa and fod achieved vapour pressures of 0.1 mm Hg approximately 80°C lower than the pfbtfa chelates, and approximately 120°C lower than the pfbhfh chelates. These results suggest therefore that the pfbtfa and pfbhfh chelates are considerably less volatile than the above mentioned lanthanide chelates, and that oven and injector block temperatures of around 200°C would be required to perform gas chromatography of the chelates.

A disconcerting feature of the determined values of ΔH and ΔS, TABLES 39 & 40, is that no obvious correlation can be made between these values and chelate volatility, aside from the obvious fact that increased values of ΔH indicate a more rapid increase in chelate vapour pressur over the measured temperature range. It can be noted qualitatively however, that increased values of ΔH generally indicate a less thermally stable chelate. Similar conclusions were drawn by Berg and Truemper (256), studying the volatilities of a range of transition metal β-diketonates.

Combining the results of metal chelate thermal stability and volatility, the following general conclusions can be made therefore with regard to the potential use of the studied fluorinated ligands to divalent metal gas chromatographic analysis:

1) Fluorination of the phenyl ring, eg; bta - pfbtfa, generally improved chelate volatility and thermal stability as would be expected. However the thermal stability increase was still not sufficient to allow complete vapourisation of the pfbtfa chelates.
2) Increasing the extent of fluorination from pfbtfa - pfbhfh, decreased thermal stability and volatility. This was presumed due to the increased mass effect in the chelate molecule, overriding any benefit accrued by the further fluorination increase.
3) The comparative effect of change in ligand upon volatility of a particular metal (FIGS 66 - 78), indicated that pfbtfa produced the most volatile range of chelates.
4) Calculated chelate vapour pressures however, indicated that even for the pfbtfa chelates, temperatures in excess of 190°C would be required to attempt gas chromatographic analysis.

2.9

General conclusions from physical studies of the β-diketones and metal chelates

Collating the solution, electrochemical, spectroscopic and thermal data discussed above, the following conclusions can be made with regard to the β-diketones p-Me-bta, bta, pfbtfa and pfbhfh, and their chelated derivatives.

1) β-diketone acid strength increases in the order:

p-Me-bta $<$ bta $<$ pfbtfa $<$ pfbhfh

The observed sequence is in keeping with the increase in fluorination across the ligand series, and the decreasing basic character of the β-diketone oxygen atoms.

2) Metal chelate solution stability decreases with β-diketone ligand in the order:

p-Me-bta $>$ bta $>$ pfbtfa $>$ pfbhfh

- in accord with the increase in ligand acid strength. The implied low formation constants of the Group I metal complexes, indicates considerable chelate hydrolysis in aqueous systems.

3) ^{1}H NMR spectra of the β-diketone ligands indicates that in both p-Me-bta and bta, the phenyl ring is coplanar with the enolic ring. The pentafluorophenyl ring is shown to be non-coplanar with the enolic ring due to steric interaction.

4) The non-coplanarity of the pentafluorophenyl ring, and the consequent lack of resonance with the enolic - chelate ring, results in pfbtfa and pfbhfh 'behaving' as if they were aliphatic - aliphatic terminally substituted β-diketones.

5) ^{1}H NMR spectra of the studied metal chelates and complexes do not evidence the existence of an aromatic delocalised electron system within the chelate ring. Rather the ring proton is olefinic in type.

6) Polarographic studies of the metal chelates indicate that substituent effects operate equally on the chelated metal ion and the donor oxygen atoms within the molecule. Values of $E\frac{1}{2}$ are linearly related to substituent effect, and are linearly related to solution stability.

7) Thermal stability and vapour pressure studies indicate that pfbtfa is the most favourable ligand to perform metal chelate gas chromatography. However the temperatures required ($>190^\circ$C), may present problems related to thermal decomposition.

SECTION 3

CHROMATOGRAPHIC STUDIES

3.1 Gas Chromatographic studies

Thermogravimetric studies previously discussed have concluded that of the four β-diketones p-Me-bta, bta, pfbtfa and pfbhfh, only pfbtfa produced metal chelates of sufficient volatility to attempt GC analysis, though the thermal stability of the chelates was less than ideal. Accordingly a brief study of the gas chromatography of the metal chelates was only applied to the divalent metal chelates of pfbtfa.

Experimental

Gas chromatography of the divalent metal chelates of pfbtfa was investigated with both packed and capillary columns, using a Perkin Elmer F17 GC fitted with pulsed ECD (^{63}Ni) detector.

For packed column studies, the detector signal was monitored on a Servoscribe RE 541 chart recorder. The injection port temperature selected was a compromise between the two constraints of raising the injection port to a temperature sufficient to induce rapid sample volatilisation, but not so high as to cause appreciable sample thermal degradation. Oxygen free, dried nitrogen was used as carrier gas. The following packed columns were investigated:

6' 10% SE 30 on Supasorb 60 - 80
6' 5% OV 1 on Supasorb 60 - 80
6' 2½% OV 17 on Chromosorb G 80 - 100

All columns were conditioned at 150°C overnight before use. Flow rates were measured at the detector outlet via a bubble soapmeter against a stopwatch.

Capillary chromatography was performed using a 25 m wall coated open tubular (WCOT) vitreous silica column (0.2 mm id), coated with SE 30 (SGE Ltd. Milton Keynes, UK). The F17 was retained for this study, but modified to accept the capillary column by being fitted with a 'Unijector' multi-purpose injection system (SGE Ltd.), set in the 'splitter' mode. In this mode, the amount of sample injected was reduced to an amount within the capacity of the column. For this study a split ratio (the ratio of the gas volume flow through the column to the flow out of the splitter valve) of 1 : 62 was used. Carrier gas flow through the column was determined at a mean linear velocity of 25.7 cm sec^{-1}, with a detector purge flow of 48 ml min^{-1}. To cope with the higher column efficiency of the capillary column over the packed columns, the Servoscribe recorder was replaced with a Hewlett Packard 3390A Reporting Integrator.

For both the packed and capillary column studies, the ECD detector was set at pulse 6 (equivalent to 1 µsec pulses of 45 V at 8 KHz).

The retention behaviour of the pfbtfa chelates was examined by individual injections of the chelates in AR MeOH.

Results and Discussion

Preliminary elution experiments with the pfbtfa chelates were performed on the packed columns at oven temperatures in excess of 200°C. The chelates were shown to elute on the 10% SE 30, 5% OV 1 and 2.5% OV 17 columns, though retention times of the chelates were similar within each studied column. Inspection of the glass liners in the injection port evidenced some residue, indicating incomplete volatilisation or thermal decomposition of the chelates. FIG 79 shows chromatograms of $Mg(pfbtfa)_2$ obtained at 205 and 235°C on the SE 30 and OV 17 columns, with carrier gas flows of 40 and 70 ml min^{-1} respectively, and an injector/detector block temperature of 250°C. Calculated column efficiencies for the pfbtfa chelates were determined as approximately 63 and 30 theoretical plates for the SE 30 and OV 17 columns respectively (34 and 16 plates per metre).

Study of the pfbtfa chelates on the SE 30 coated capillary column, showed all chelates to be again eluted with similar retention times, over a range of studied oven temperatures. FIG 80 shows chromatograms of $Ni(pfbtfa)_2$ obtained at 130°C, with an injector/detector block temperature of 225°C. Calculated column efficiencies for eg; nickel and copper chelates of pfbtfa at 130°C were determined as 34,286 and 38,472 theoretical plates (1,371 and 1,529 plates per metre).

TABLE 42 lists minimum detected quantities (MDQ) of the pfbtfa chelates, determined at 130°C with an injector/detector block temperature of 225°C. MDQ is defined as the minimum quantity of solute required to achieve a detector response twice the average base line noise level. FIG 81 shows a typical MDQ chromatogram, that of $Zn(pfbtfa)_2$.

Conclusions from GC studies

1) The identical retention behaviour of the pfbtfa chelates would seem to imply that the pfbtfa ligand is sterically so large, that the column surface 'sees' a similar solute, irrespective of the chelated metal ion. Electronic effects within the chelate ring as demonstrated previously by polarographic and spectroscopic studies, do not appear to be significant at the chelate periphery. Chromatographic resolution of chelate mixtures therefore proved unsuccessful.
2) The retention behaviour of the pfbtfa chelates would classify the chelates as Class II according to the sequence of Sievers (113), ie; chelates that are capable of gas chromatographic analysis, but show evidence of thermal decomposition and/or incomplete volatilisation. It may be possible that the chelates underwent thermal decomposition within the injection port and/or column, the analyte actually detected being the parent β-diketone or some other decomposition product. Unfortunately, a GC - mass spectrometer system was not available to follow up this aspect of the work. Definitive identification of the column effluents was therefore not achieved.
3) MDQ values of the pfbtfa chelates, TABLE 42, indicates that the high degree of fluorination within the pfbtfa molecule promotes the ready detection of the chelates with the ECD detector. MDQ values for divalent metal chelates of pfbtfa are comparable to those for chelates of tfa as determined by Sucre and Jennings (132).

Suggestions for future work

1) Difficult resolutions of isomeric olefins have been achieved on columns impregnated with Ag(1) salts (296). ^1H NMR studies of the chelates have shown the ring proton to be olefinic in nature. It might well be possible to resolve the studied metal chelates with such a system therefore. Unfortunately, time did not allow such an investigation to be performed for this thesis.

2) No attempt was made to fully optimise the capabilities of the capillary column, eg; investigating the effect of helium or hydrogen gas, and determination of optimum carrier gas velocities.

3) Study of the use of on-column injection of the metal chelates. Such a technique is especially useful for thermally unstable compounds. Unfortunately, the 'Unijector' injection system utilised did not allow for the potential of on-column injection.

3.2 High Performance Liquid Chromatographic studies

Experimental

HPLC analysis of the divalent metal chelates of p-Me-bta, bta, pfbtfa and pfbhfh, was performed on two separate HPLC systems. Firstly a Pye Unicam unit comprising PU 4010 pump, Rheodyne injection valve fitted with 20 µl loop, LCXP solvent gradient programmer, and PU 4020 variable wavelength UV detector. Detector output was plotted on a Hewlett Packard 3390A reporting integrator. Secondly a Spectra Physics system, comprising SP 8100 pump fitted with autosampler and 10 µl loop, SP 8370 UV detector at 254 nm, detector output being plotted on a SP 4100 computing integrator. Where variable wavelength detection was required, a Pye Unicam LC-UV detector was used. Samples (ca. 1 mmole) were made in methanol (reverse phase) or dichloromethane (normal phase chromatography). Solvents used were of HPLC or AR grade, supplied by Fisons Ltd. Loughborough.

The elution behaviour of the chelates was observed on a variety of prepacked analytical columns as listed below:

1. 250 mm 10µ Spherisorb ODS
2. 250 mm 5µ Zorbax ODS
3. 250 mm 5µ Zorbax C8
4. 250 mm 10µ Spectra Physics RP8
5. 250 mm 5µ Lichrosorb Si 60
6. 200 mm 5µ Hewlett Packard Si 100

Results and discussion

Initial studies were performed at ambient temperatures using the reverse phase columns and binary solvent mixtures comprising either MeOH, MeCN or THF in conjunction with water as the polar modifier. Single injections of each metal chelate of each ligand system were studied, the retention behaviour of each chelate being noted.

With Spherisorb ODS, chelates of p-Me-bta and bta eluted with good peak shape with a mobile phase of 100% THF. With 100% MeCN, the copper chelates were irreversibly absorbed, and with 100% MeOH, both nickel and copper chelates of p-Me-bta and bta were irreversibly absorbed. All other chelates of p-Me-bta and bta were eluted satisfactorily, with good peak shape but with similar retention times within each mobile phase system. The retention behaviour of the pfbhfh chelates with a range of binary organo-aqueous solvents also showed all chelates to be eluted with similar retention times within each solvent mixture. With the pfbtfa chelates, differences in retention were noted however for the Ca and Ba, Cd and Hg pfbtfa chelate pairs. FIG 82 shows chromatograms obtained for the resolution of these chelate pairs using 60/40 MeOH/H_2O.

With Zorbax ODS and 100% THF and 100% MeCN, good peak shape was observed with identical retention times within each mobile phase for all p-Me-bta and bta chelates. With 100% MeOH however, tailing was observed for the copper chelates of p-Me-bta and bta. The remaining chelates all showed extremely broad bands and/or irreversible absorption.

The chelates of pfbtfa and pfbhfh however eluted as well defined peaks down to solvent strengths of $\epsilon = 1.56$ (ie; 60/40 MeOH/H_2O). With the C8 and RP8 columns, partition/retention mechanisms with the chelates were less strong as expected, though overall a similar pattern of retention behaviour was observed.

The variation in retention behaviour of the p-Me-bta and bta chelates on the Spherisorb ODS to the remaining reverse phase columns can be explained by differing particle shape, surface coverage of the hydrocarbon and the degree of end-capping performed on the column. This sort of variation is unfortunately a common occurence among columns derived from different sources, at the present state of column packing and preparation technology.

Spectroscopic and electrochemical studies of the metal chelates previously discussed have concluded that pfbtfa and pfbhfh 'behave' as aliphatic-aliphatic substituted systems. To study whether this behaviour would be carried through to the chromatographic properties of the chelates, a short study was performed on the retention behaviour of the copper chelates of bza, tta, acac, tfa and hfa, in conjunction with the studied copper chelates. With Zorbax ODS and 100% MeOH, significant differences in retention were noted between the copper chelates of p-Me-bta, bta, tta and bza. However considerable tailing was observed. Copper chelates of acac, tfa, hfa, pfbtfa and pfbhfh were eluted as sharp bands of similar retention time. With 100% THF and 100% MeCN, good peak shapes with identical retention times were observed for all copper chelates. Similar results were observed with the 5μ Zorbax C8 column. The fact that the p-Me-bta, bta, bza and tta copper chelates (ie; the aromatic - aliphatic terminally substituted chelates) eluted as broad bands with considerable tailing (with MeOH), and the pfbtfa and pfbhfh copper chelates, along with the aliphatic - aliphatic terminally substituted copper chelates eluting as sharp, well defined peaks, would therefore confirm the predictions concluded from spectroscopic and electrochemical studies presented previously. Thus pfbtfa and pfbhfh 'behave' as aliphatic - aliphatic substituted systems, due to the sterically large pentafluorophenyl ring not allowing coplanarity to be achieved with the chelate ring.

As binary solvent systems were shown not to be very promising toward the potential resolution of the studied metal chelates, attention was then addressed toward a ternary solvent system, comprising varying proportions of MeOH/MeCN/H_2O. Methanol and acetonitrile were the two organic components of choice, as these two solvents comprised solvents from selectivity Groups II and VI (solvent selectivity triangle, Snyder (297)), and represent two solvents that differ widely in selectivity. THF though a stronger solvent than both MeOH and MeCN (in reverse phase systems), was not selected as its selectivity was intermediate between MeOH and MeCN.

Using various mixtures of the three solvents, the retention behaviour of the chelates was investigated on the Zorbax ODS and C8/RP8 columns.

Individual injections of p-Me-bta and bta chelates again eluted as broad tailing bands, and though retention times were significantly different, the bands were again considered too broad to attempt resolution of a chelate mixture. Chelates of pfbtfa and pfbhfh eluted as sharp bands of good peak shape.

Normal phase chelate elution experiments with the 5 and 10μ silica columns, were performed using various binary mixtures of dichloromethane, chloroform, diethyl ether, hexane, methanol and acetonitrile.

Using the 5μ Si 60 and Si 100 columns, and mobile phases of 100% MeOH and MeCN, all chelates were eluted as sharp bands, close to the respective column void volume (determined via an injection of CCl_4). These observations imply little or no retention of the chelates on the columns. With 100% dichloromethane, the nickel and copper chelates of p-Me-bta and bta were irreversibly adsorbed. The remaining chelates of p-Me-bta and bta showed evidence of adsorption, very broad bands being obtained. Solvent strength had to be increased to $\epsilon = 0.33$ (eg; 98/2 dichloromethane/MeOH) in order to elute the chelates of p-Me-bta and bta satisfactorily. Chelates of pfbtfa and pfbhfh eluted satisfactorily, with similar retention times within each mobile phase system, including 100% dichloromethane. Decreasing solvent strength using mixtures of dichloromethane/hexane, increased pfbtfa and pfbhfh chelate retention as expected. However retention times were again similar within each ligand/mobile phase system. Chelates of pfbtfa and pfbhfh were irreversibly adsorbed at strengths of less than $\epsilon = 0.28$.

Snyder (298) has suggested that in normal phase systems, the solute adsorption energy (ie; in qualitative terms the increase in solute retention) increases with the planarity of the solute molecule. Such a model is apparently confirmed by the range p-Me-bta and bta chelates studied. Thus it can be argued that the increase in p-Me-bta and bta chelate adsorption arises from the phenyl - chelate ring resonance increasing the electron density on the oxygen donor atoms. Assuming the chelated metal ion to be screened by its surrounding ligands, chelate adsorption onto the silica surface must therefore occur via hydrogen bonding from the β-diketone oxygen atoms to the surface silica hydroxyl groups. This suggestion is supported by the fact that one oxygen atom in the β-diketone possesses the free electron pairs necessary for such bonding (174). The pfbtfa and pfbhfh ligands, which do not allow coplanarity to be achieved between the pentafluorophenyl substituent and the chelate ring, would therefore decrease the potential for hydrogen bonding through the oxygen atoms. Hydrogen bonding could be visualised to occur through the peripheral fluorine atoms and the silica surface, but not to the same extent as postulated for the p-Me-bta and bta chelated systems.

Finally in a further attempt to achieve chelate resolution, a study was made using non - aqueous reverse phase (NARP) chromatography. Such systems have been demonstrated to be of value for the resolution of isomeric aromatic and olefinic hydrocarbons (299). Using Zorbax ODS and various binary mixtures of dichloromethane/THF, good peak shapes were obtained for all chelates, though again similar retention times were recorded within each ligand - mobile phase system combination. With Zorbax ODS and various binary mixtures of dichloromethane/

MeOH, significant differences in retention were observed between the aliphatic - aliphatic terminally substituted chelates, though peaks were broad. Aliphatic - aliphatic terminally substituted chelates including the pfbtfa and pfbhfh were eluted as sharp bands, with similar retention within each studied mobile phase combination. Differences in retention behaviour of the chelates with dichloromethane/THF and dichloromethane/MeOH are explained in terms of solvent strength, THF being a considerably stronger solvent than MeOH in reverse phase systems. Similar results were obtained with the C8 and RP8 columns.

Conclusions from HPLC studies

Overall, the application of p-Me-bta, bta, pfbta and pfbhfh toward the potential resolution of the studied divalent metal chelates was poor. With the p-Me-bta and bta chelates, the partition and adsorption mechanisms occuring within the columns were too strong, resulting (certainly for the weaker solvents) in the chelates eluting as broad tailing bands. The pfbtfa and pfbhfh chelates however eluted as sharp bands, similar in retention behaviour to aliphatic - aliphatic terminally substituted chelates such as the acetylacetonates. The difficult resolution of the chelates would imply that the column surfaces were presented with an apparently similar solute, irrespective of the metal chelate, due to the high degree of fluorination encasing the chelated metal ion in an effective fluorocarbon cage.

Suggestions for future work

As already suggested from GC studies, the use of Ag(I) complexes for the resolution of olefinic complexes can be viably considered. Silica gel has been coated with $AgNO_3$ in situ, and successfully employed for the resolution of geometrical isomers of decenes, octadienes and tetradecen-1-ol (300). Assuming the metal chelates to possess an olefinic proton within the chelate, such a technique might well be utilised.

An alternative approach, as suggested in a recent paper (301), would be to immobilise β-diketones onto silica gels, and then detect the eluted metal ions by post-column reaction with eg; 4-(2-pryridylazo)-resorcinol (PAR) followed by visible absorption.

4.0

Final Conclusions

A range of novel Group I, II and divalent metal chelates and complexes of fluorinated aromatic β-diketones have been prepared, and their spectroscopic, electrochemical, thermal and chromatographic properties systematically studied. It is concluded that the four β-diketones p-Me-bta, bta, pfbtfa and pfbhfh are unlikely to provide a method for the gas and liquid chromatographic analysis of common mono and divalent metals, for a variety of reasons as discussed above.

The β-diketone ligands have been shown however to provide useful information with regard to the electronic nature of the chelate ring, and the sites at which terminal substituent effects operate within the ring.

5.0

Figures

Unless otherwise stated, the following key is used throughout:

L	Lithium
N	Sodium
K	Potassium
M	Magnesium
X	Calcium
S	Strontium
B	Barium
N	Nickel
C	Copper
Z	Zinc
P	Lead
O	Cadmium
H	Mercury
O	p-Me-bta
X	bta
*	pfbtfa
Y	pfbhfh

Figure 1

Variation in ligand acid dissociation constant with dioxan content

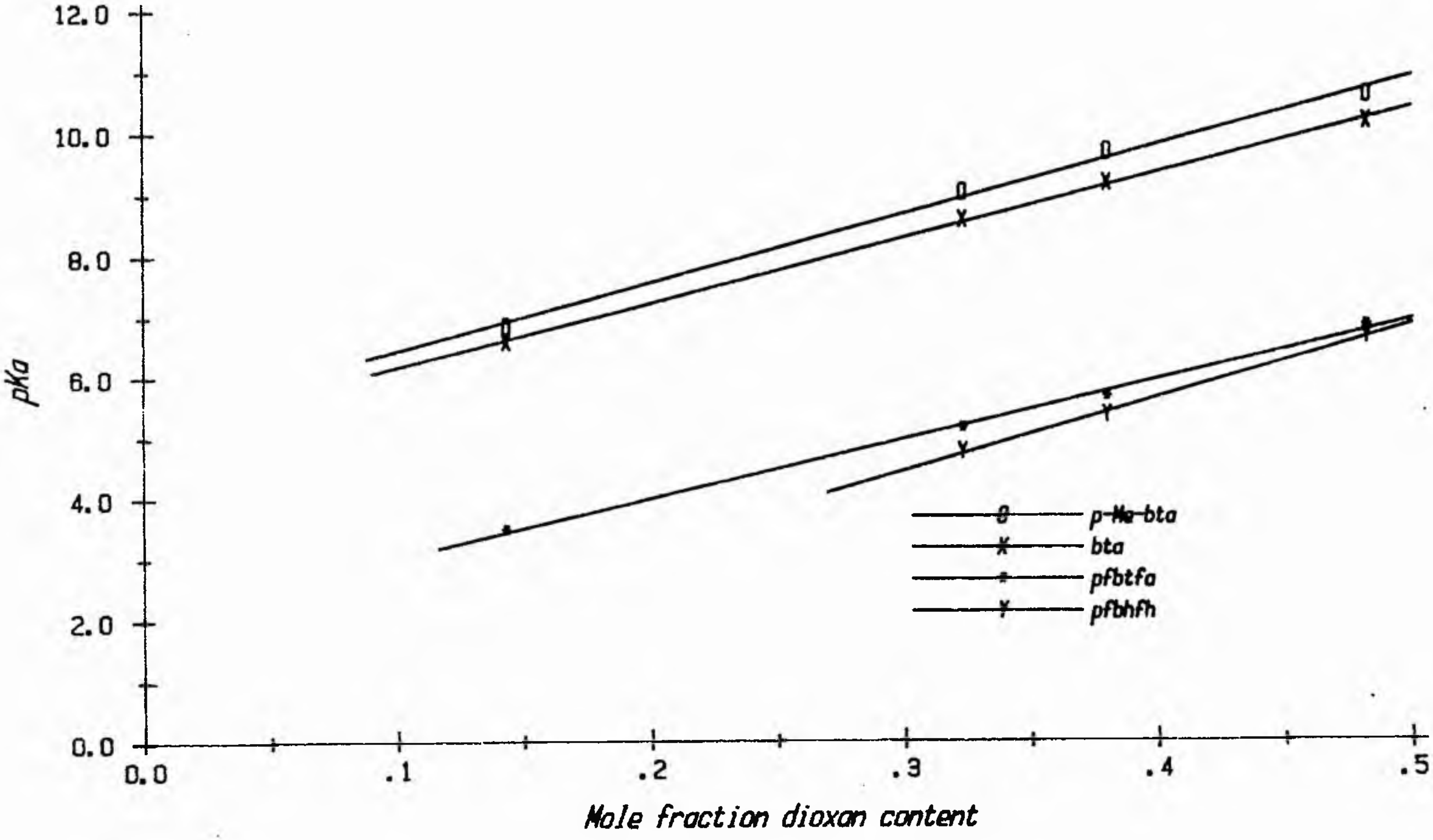

Figure **2**

Formation constant curves for GroupII chelates of p-Me-bta

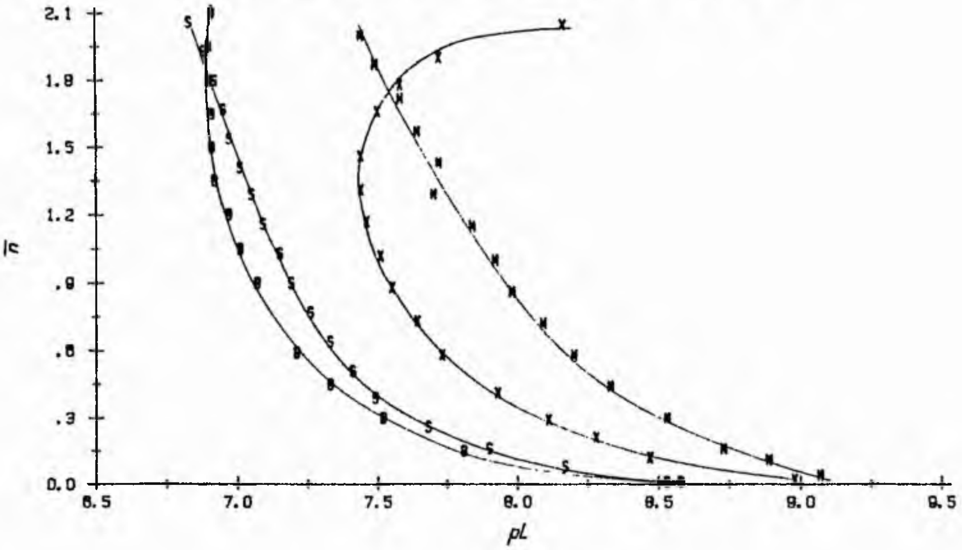

Figure **3**

Formation constant curves for GroupII chelates of bta

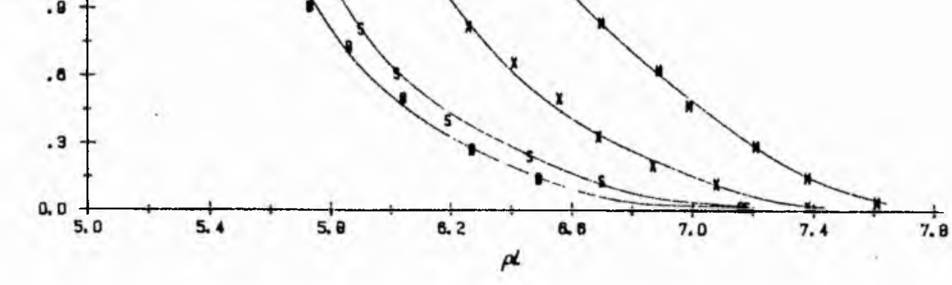

Figure 4

Formation constant curves for Group II chelates of pfbtfa

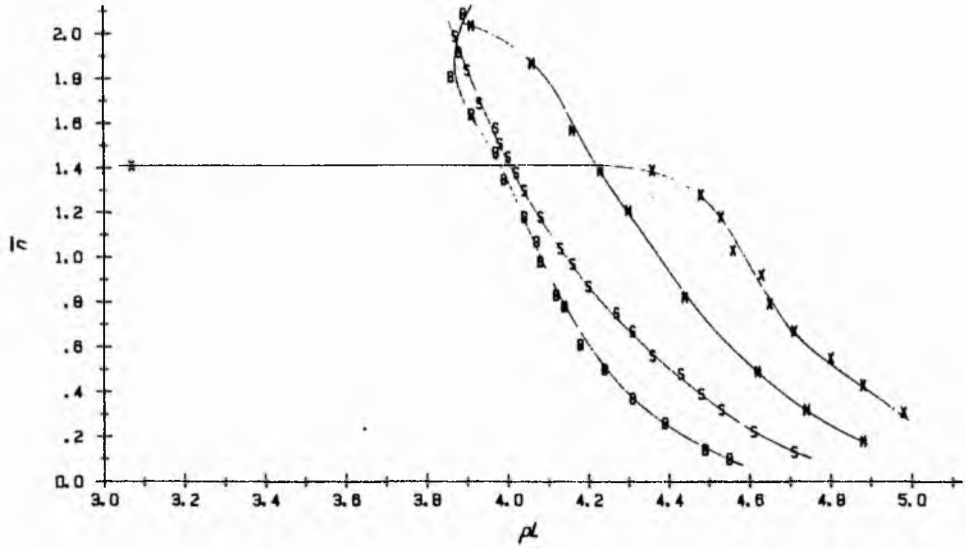

Figure 5

Formation constant curves for Group II chelates of pfbhfh

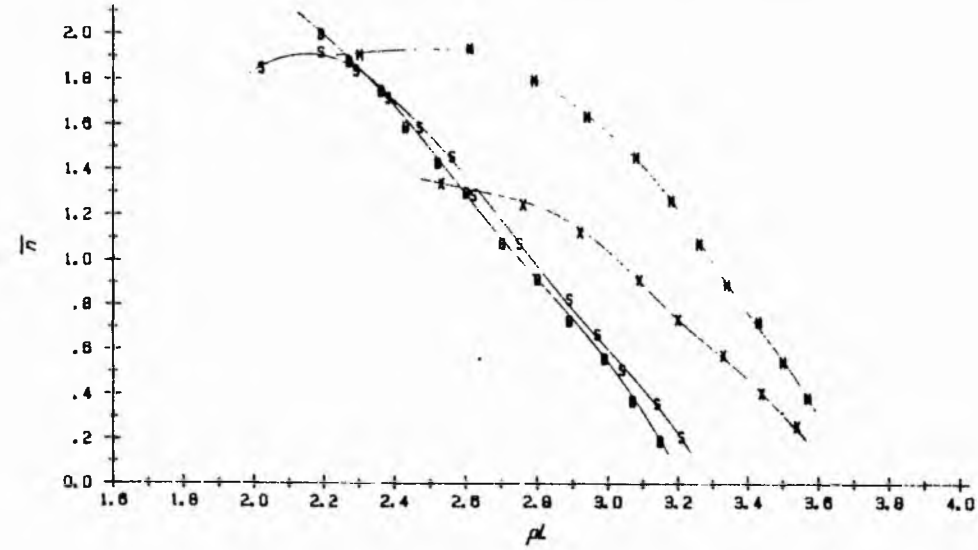

Figure 6

Formation constant curves for Ni, Cu Zn chelates of p-Me-bta

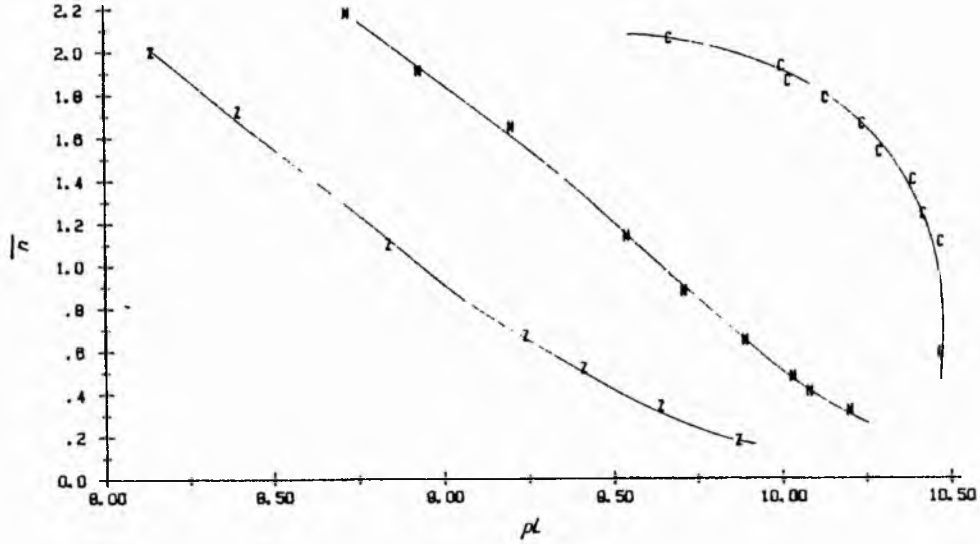

Figure 7

Formation constant curves for Ni, Cu, Zn chelates of bta

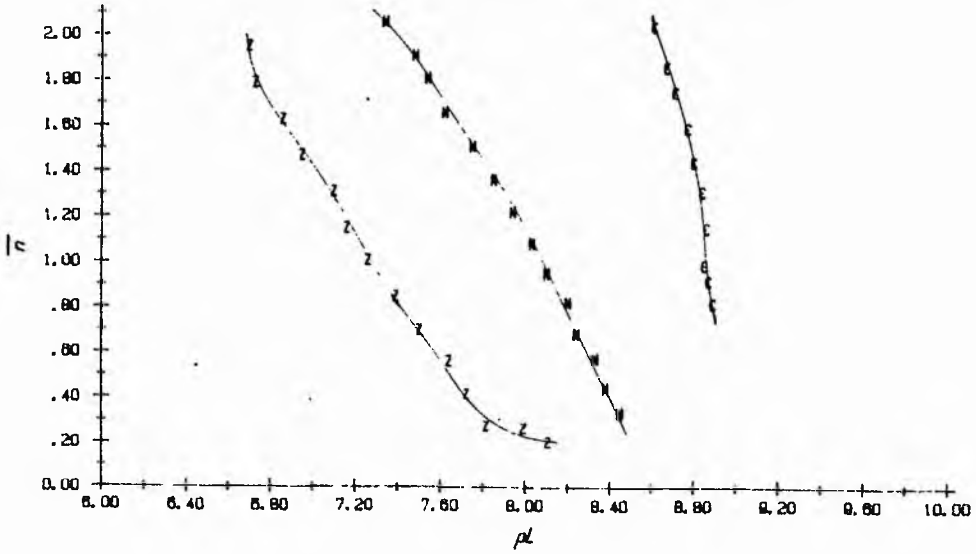

Figure 8

Formation constant curves for Ni, Cu, Zn chelates of pfbtfa

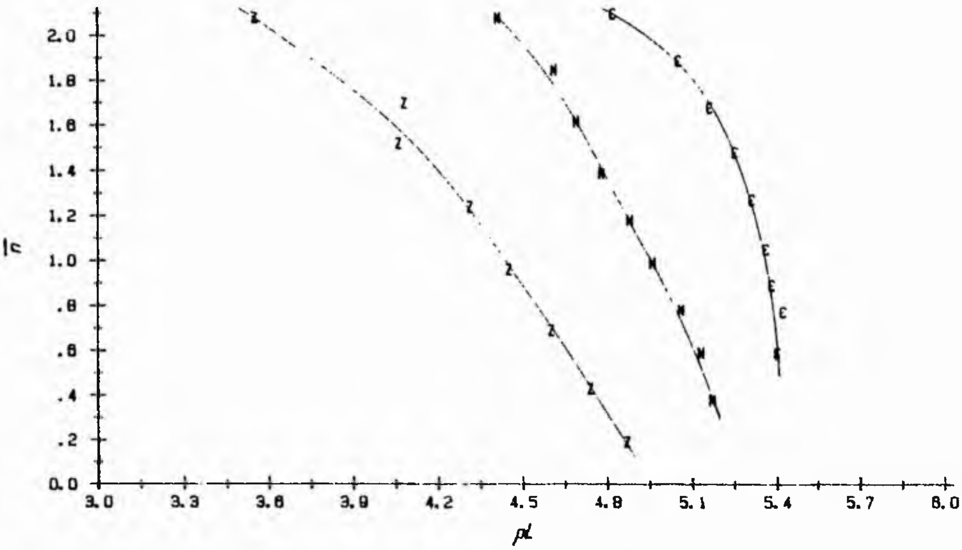

Figure 9

Formation constant curves for Ni, Cu Zn chelates of pfbhfh

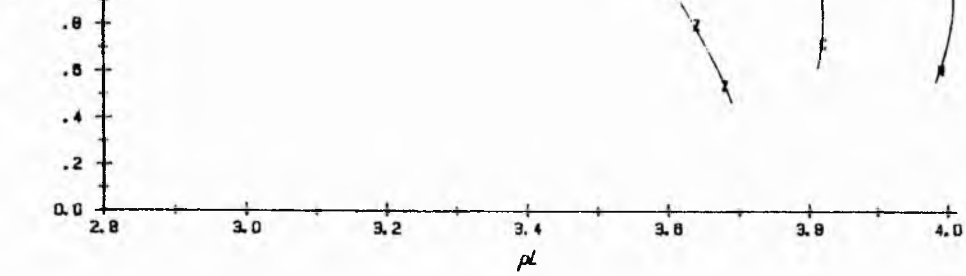

Figure **10**

Formation constant curves for Pb and Cd chelates of p-Me-bta

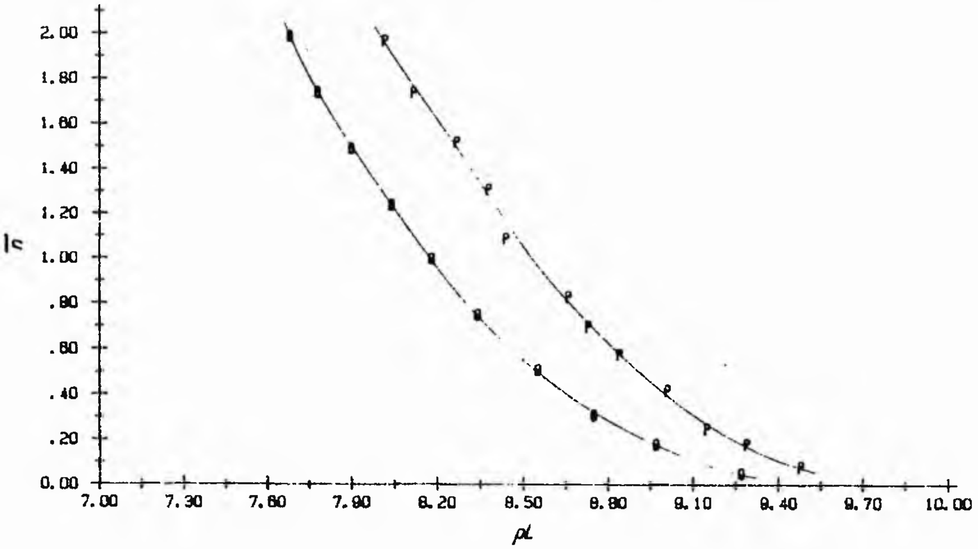

Figure **11**

Formation constant curves for Pb and Cd chelates of bta

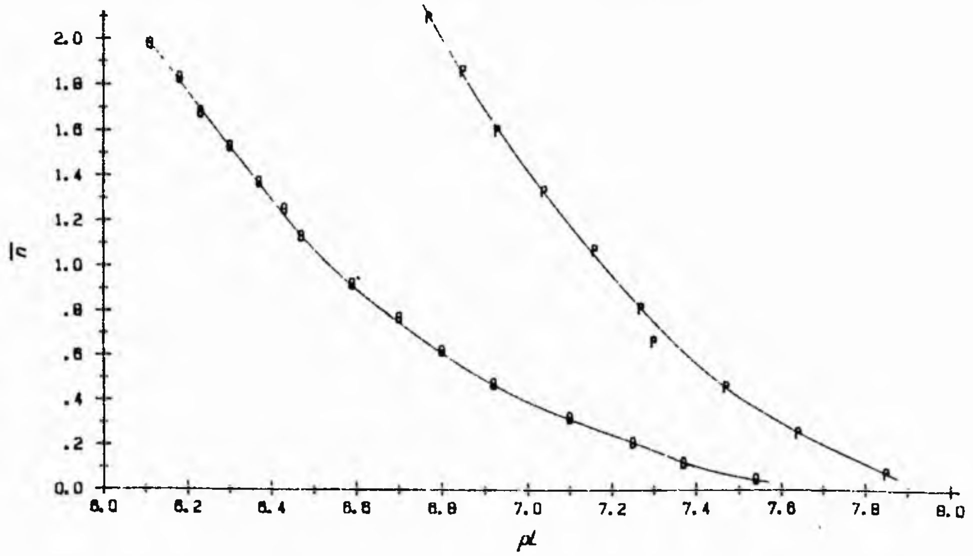

Figure 12

Formation constant curves for Pb and Cd chelates of pfbtfa

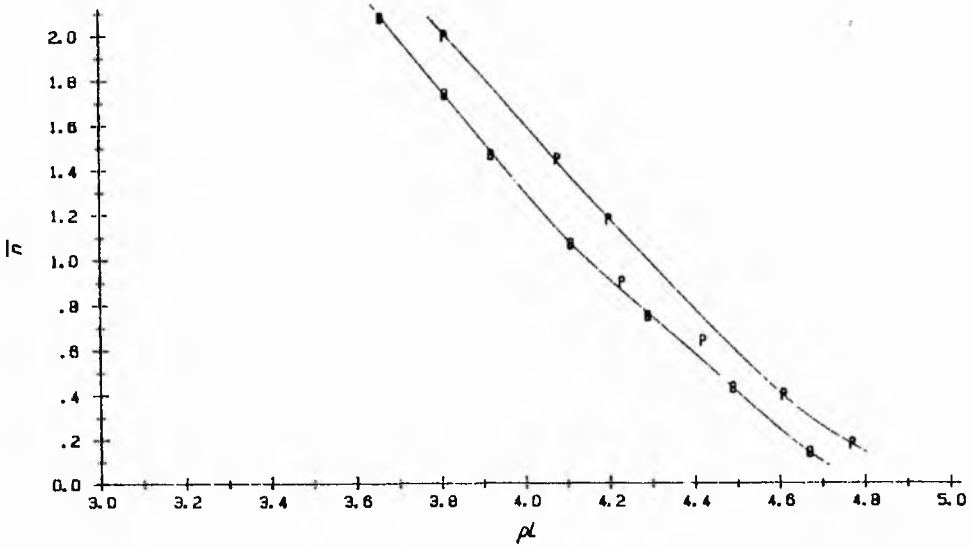

Figure 13

Formation constant curves for Pb and Cd chelates of pfbhfh

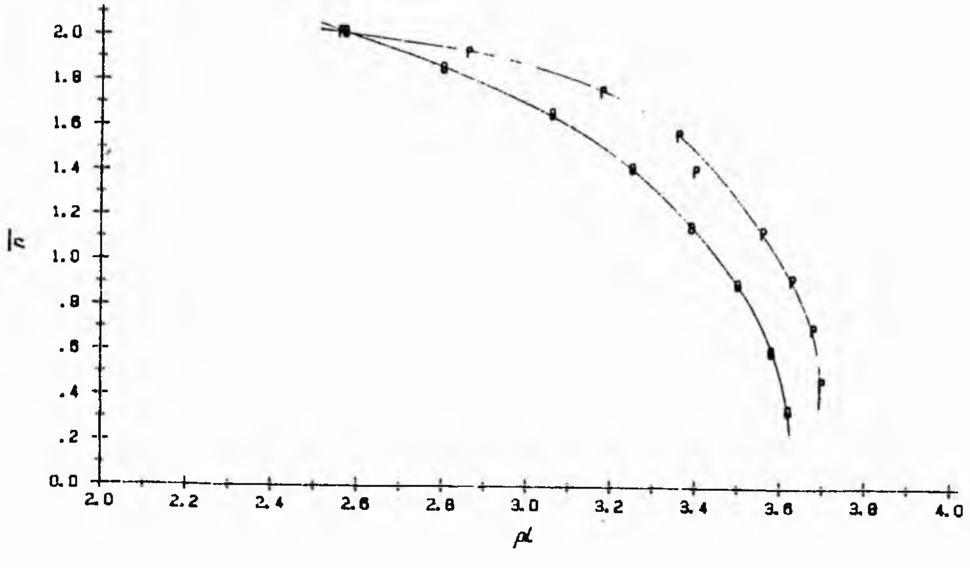

Figure **14**

Plot of log (β) : pKa for Mg, Sr, Ba chelates of the studied ligands

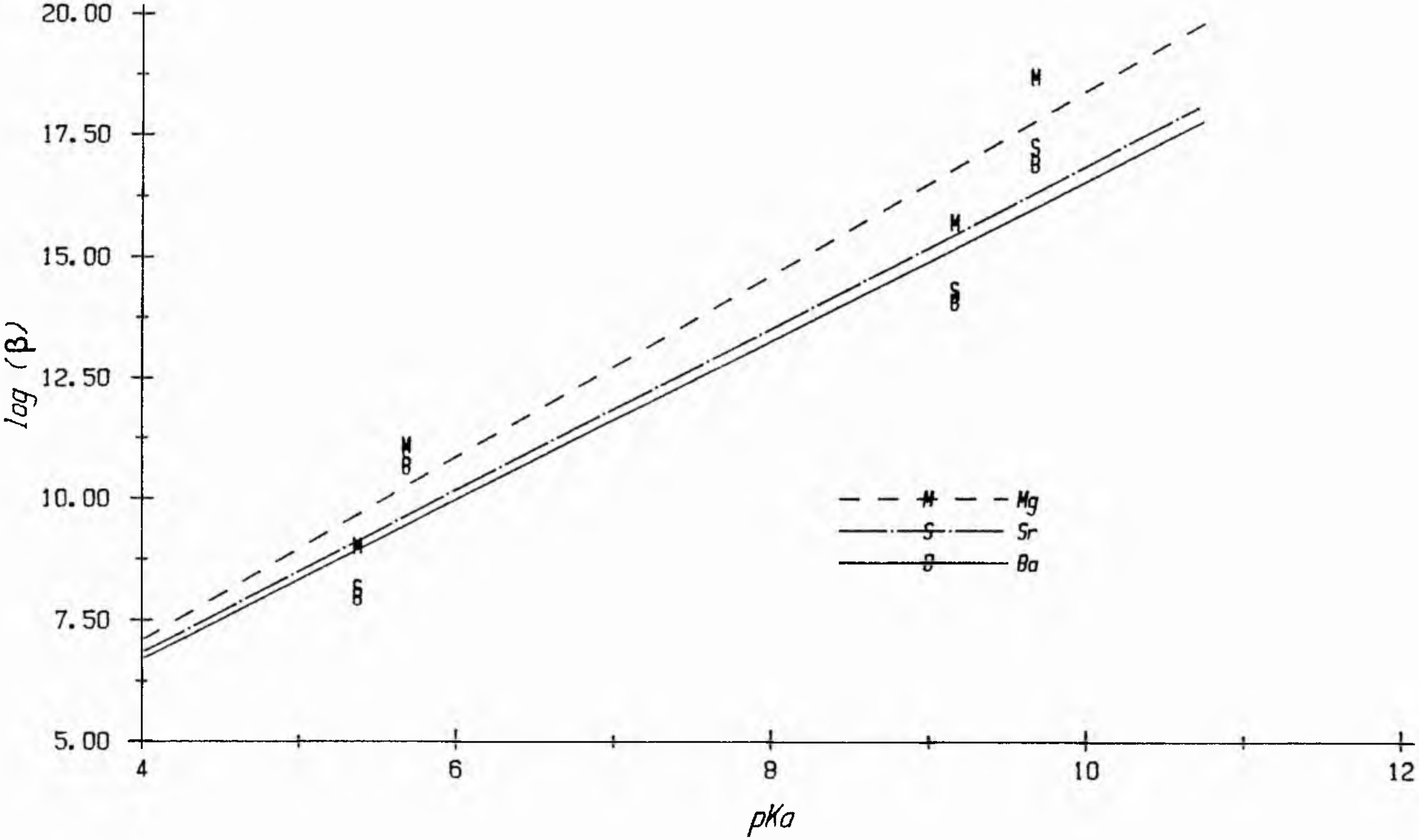

Figure 15

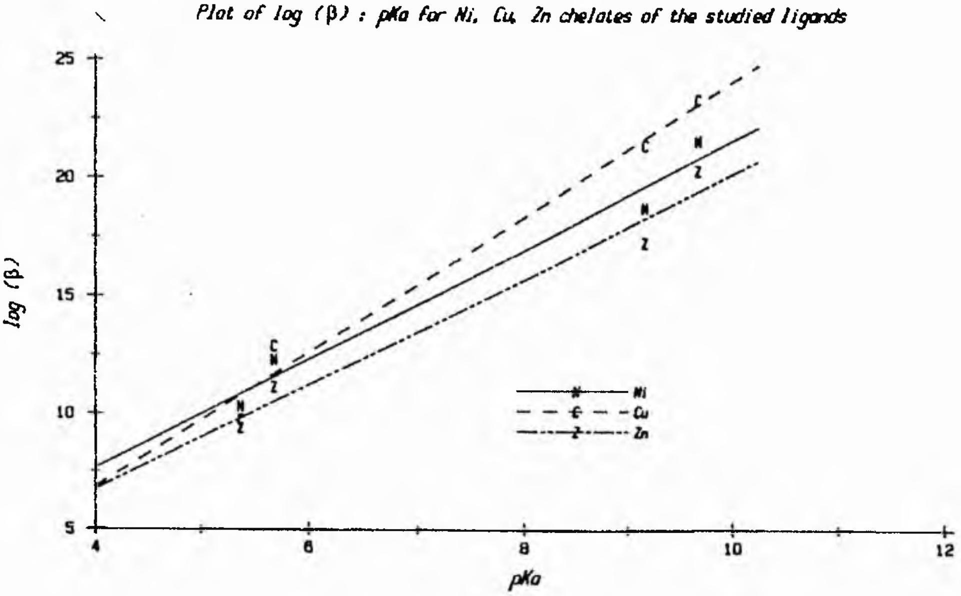
Plot of log (β) : pKa for Ni, Cu, Zn chelates of the studied ligands
log (β)
25
20
15
10
5
4
6
8
10
12
pKa
Ni
Cu
Zn
C
N
Z

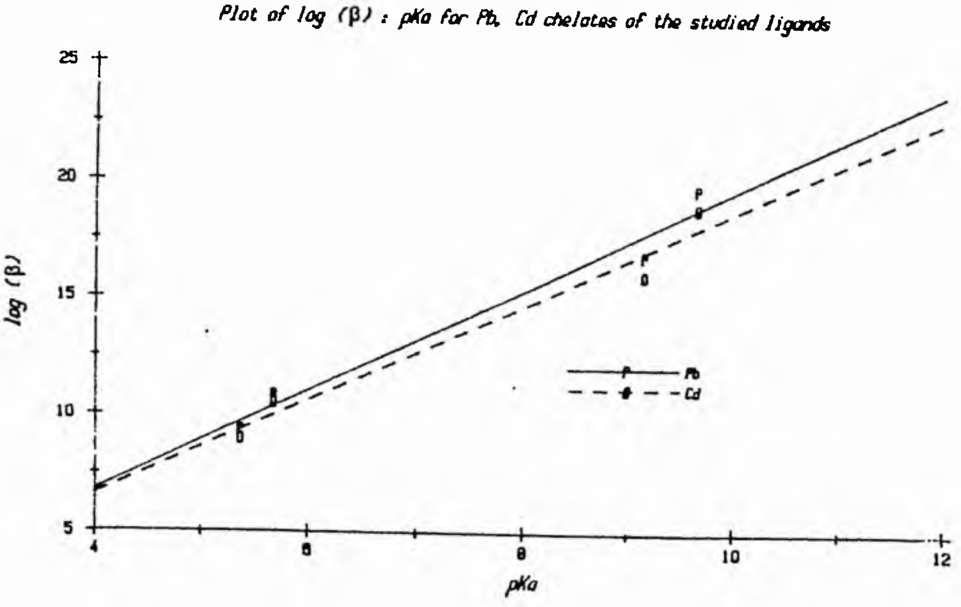
Plot of log (β) : pKa for Pb, Cd chelates of the studied ligands
log (β)
25
20
15
10
5
4
6
8
10
12
pKa
Pb
Cd
P
D

Figure **16**

Plot of log(β) : pKa for a range of copper chelates

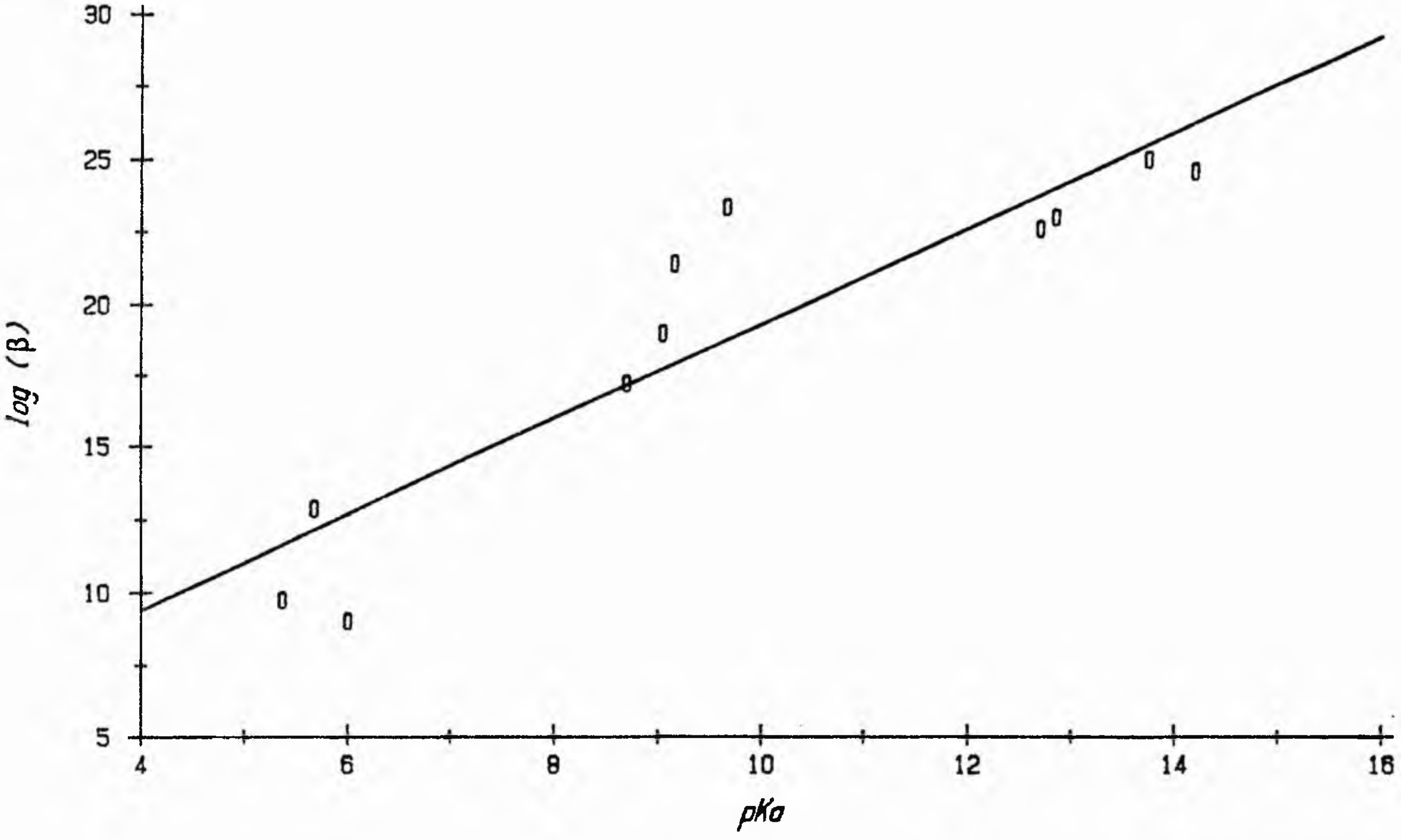

Figure 17

H NMR spectra of p-Me-bta and bta

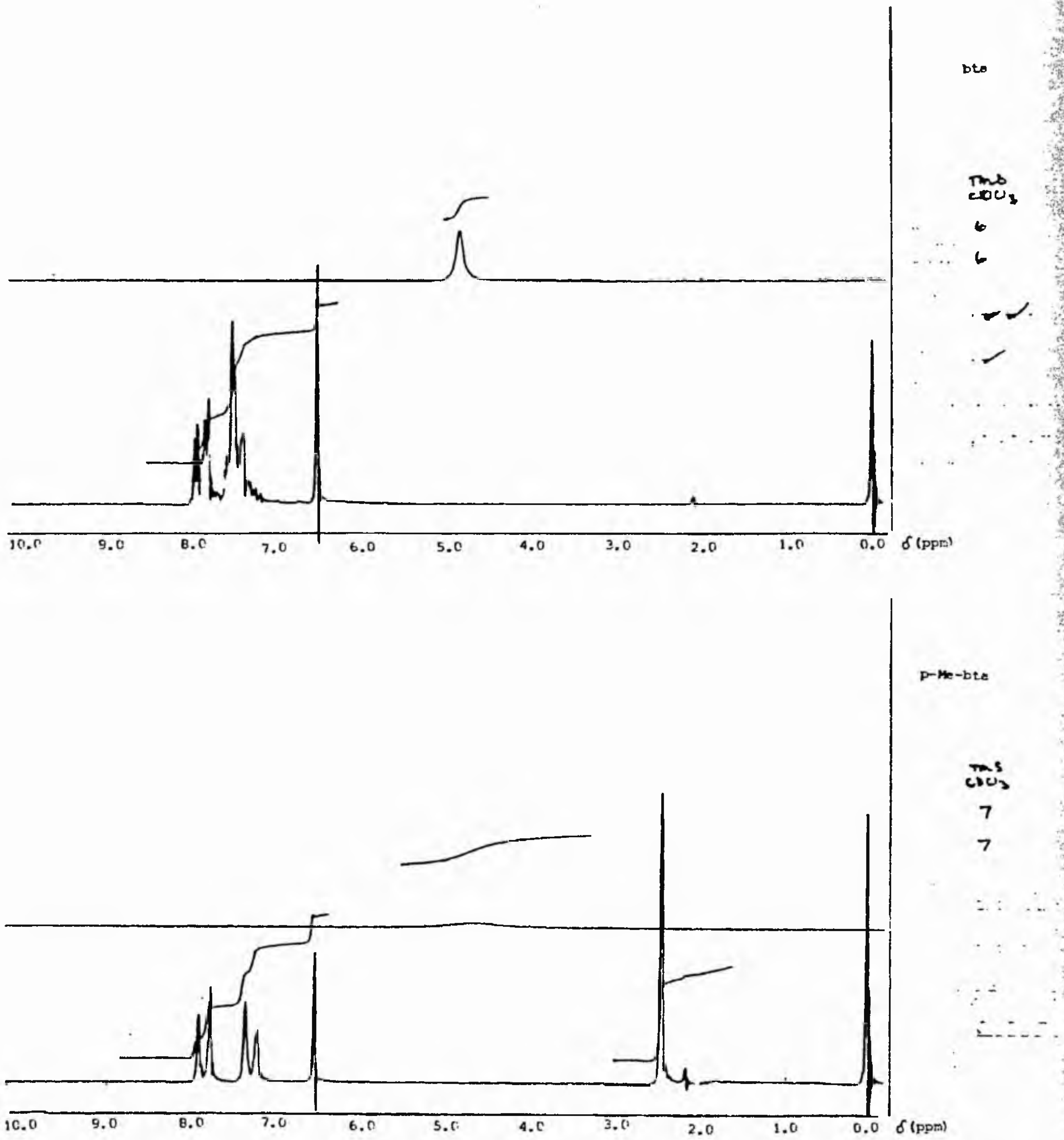

Figure 18

H NMR spectra of pfbtfa and pfbhfh

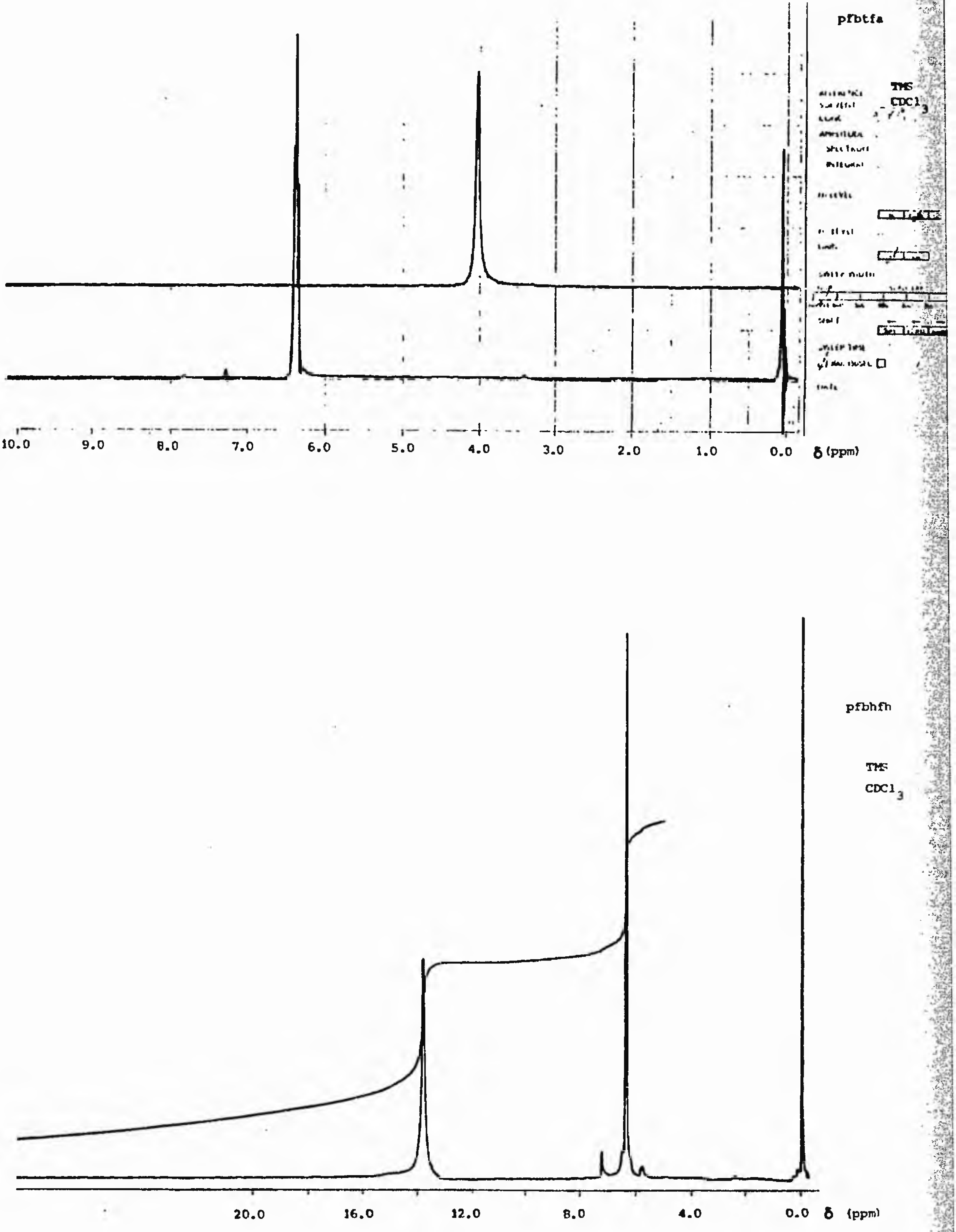

Figure 19

Plot of methine proton resonance position (in CCl_4) : β-diketone pKa

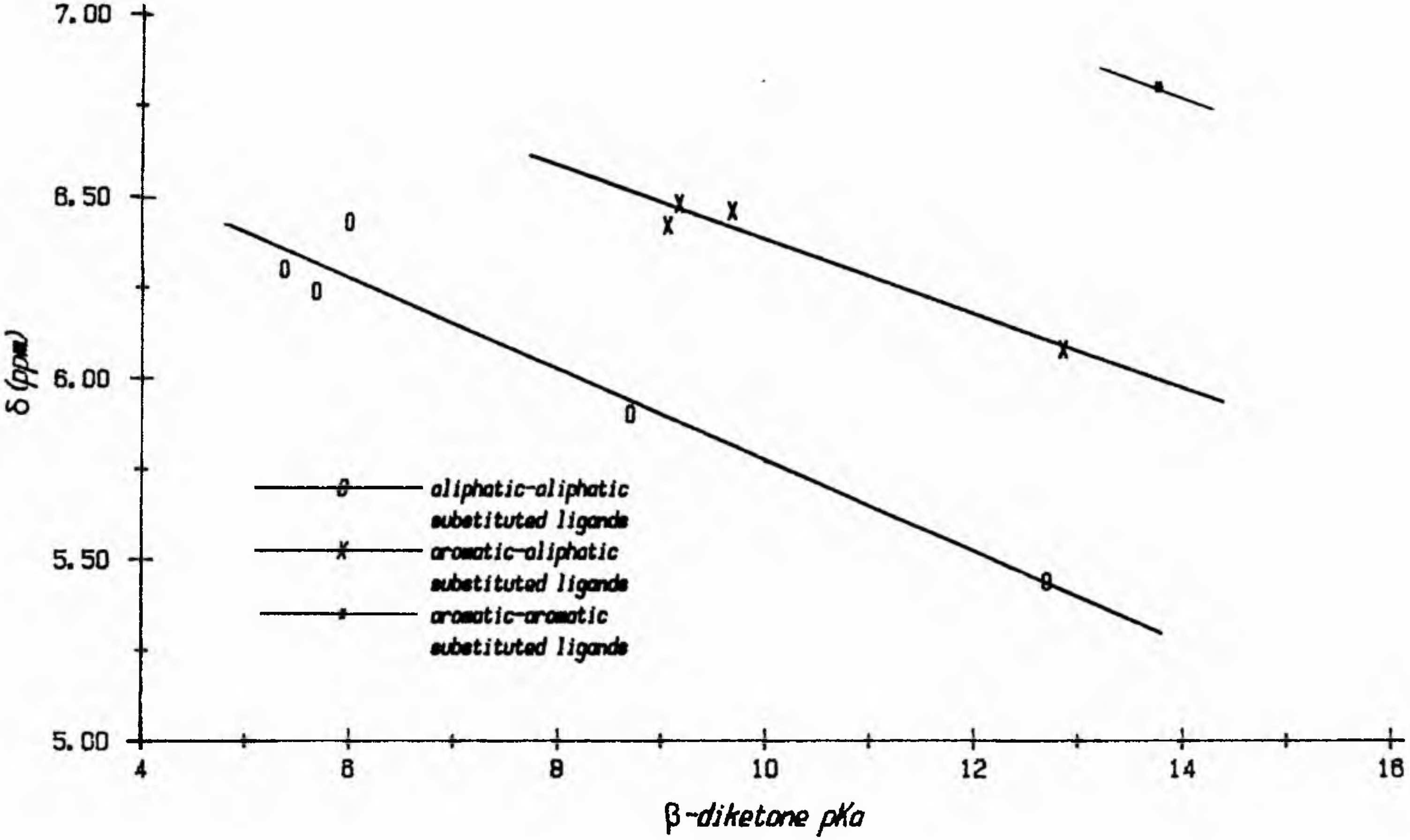

Figure **20**

Plot of metal chelate methine proton resonance : stability constant

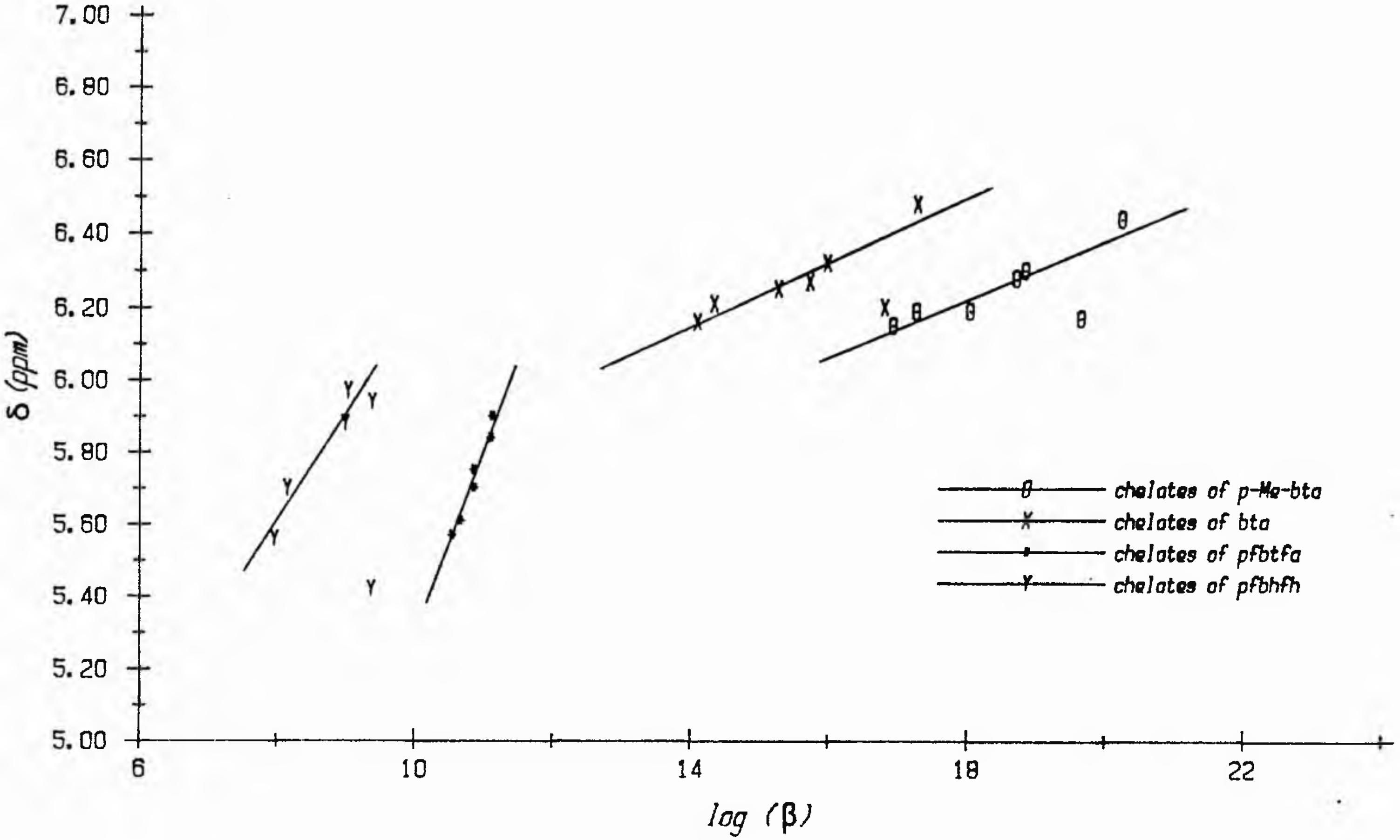

Figure 21

Polarograms of Cu(p-Me-bta)$_2$ and Zn(bza)$_2$, 75% dioxan/H$_2$O, 1M KNO$_3$, against Ag/AgCl

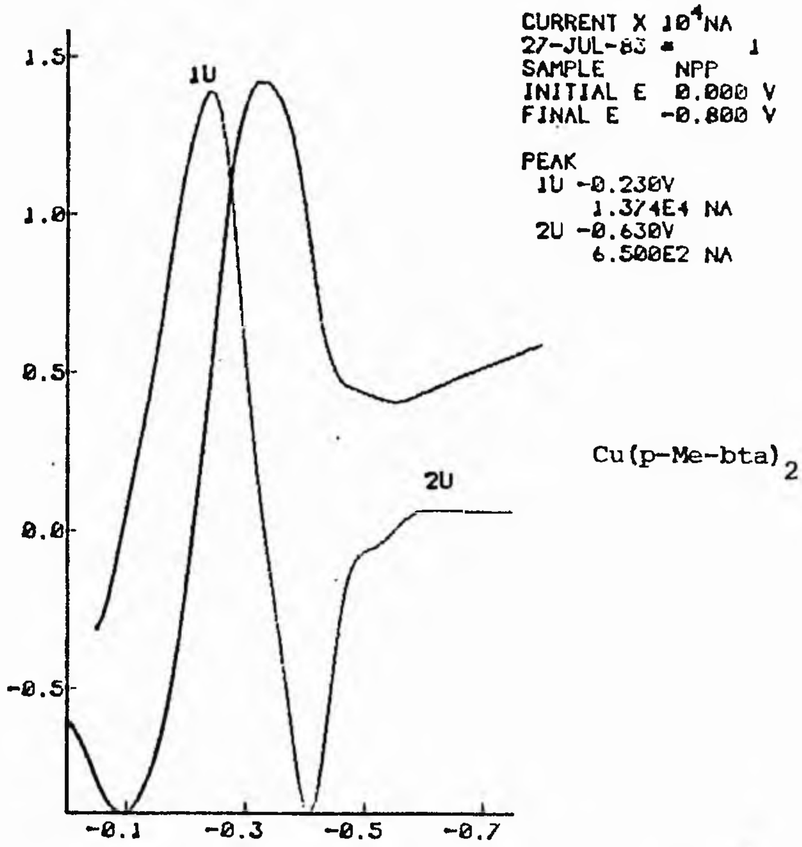

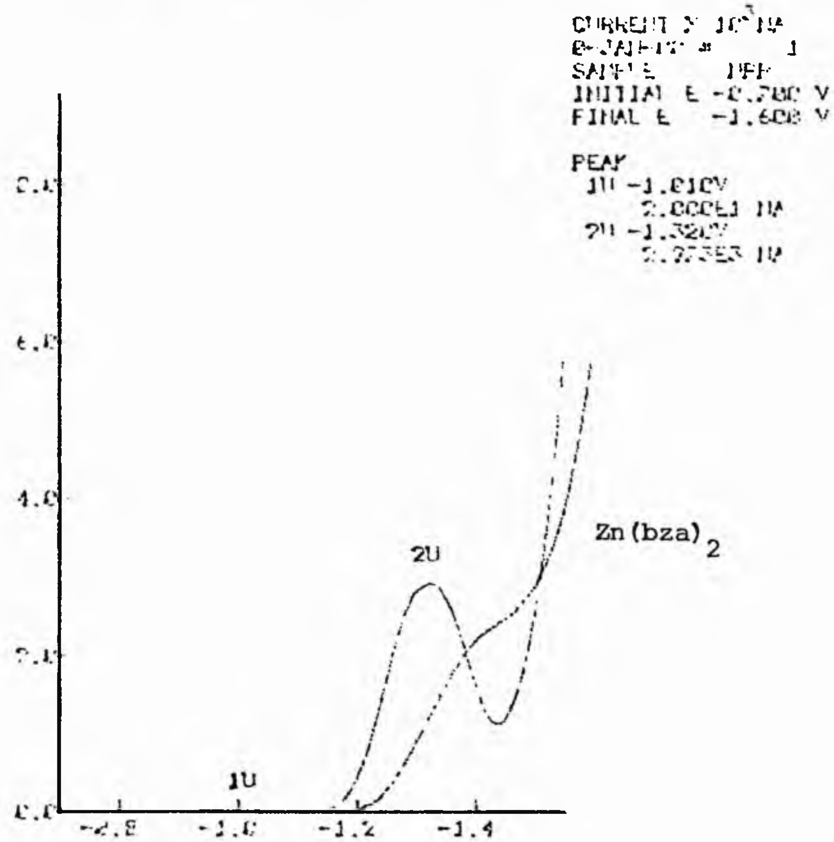

Figure 22

Plot of $E_{\frac{1}{2}}$: log (β) for the studied copper chelates

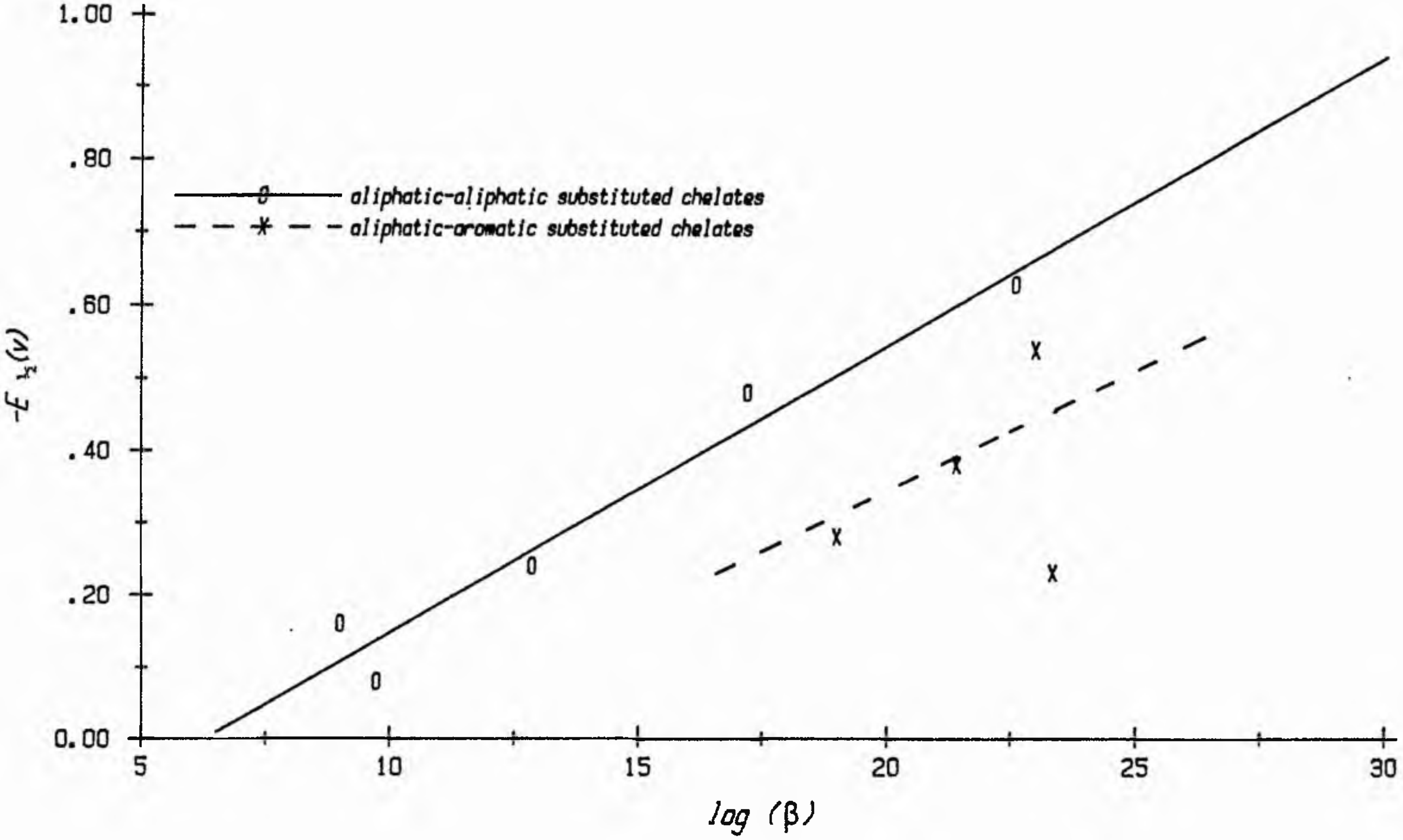

Figure 23

Plot of $E_{\frac{1}{2}}$: sum of Hammett substituent function σ_X

Plot of $\Sigma\sigma_p$ versus $E_{\frac{1}{2}}$ for the studied copper chelates

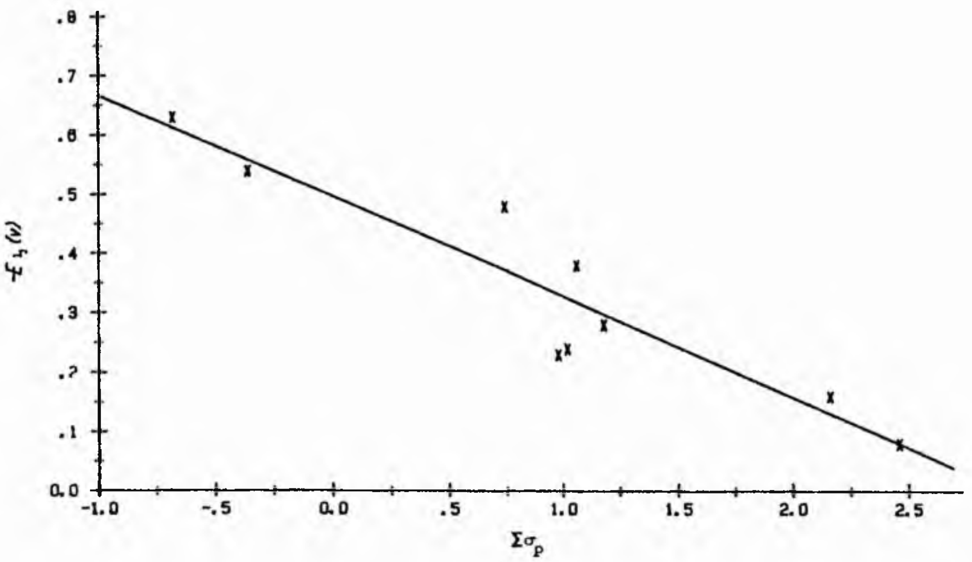

Plot of $\Sigma\sigma_m$ versus $E_{\frac{1}{2}}$ for the studied copper chelates

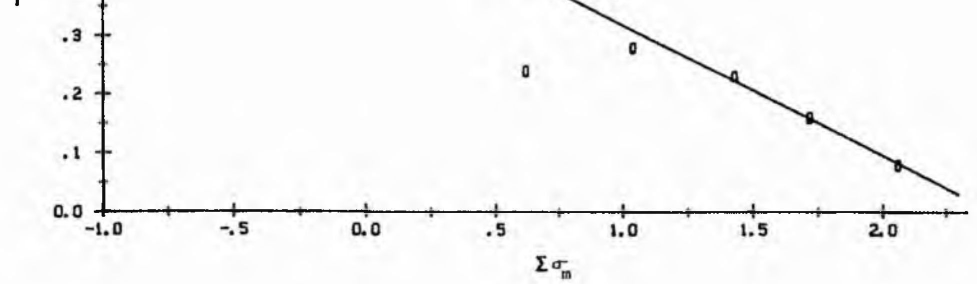

Figure 24

Plot of $E_{\frac{1}{2}}$: sum of Hammett substituent function σ_x

Plot of $\Sigma\sigma_p$ versus $E_{\frac{1}{2}}$ for the studied Ni chelates

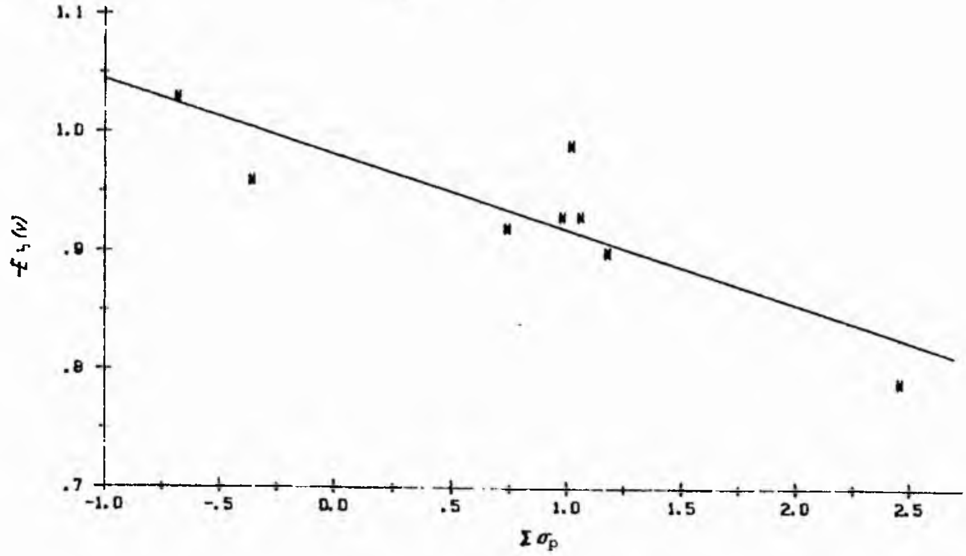

Plot of $\Sigma\sigma_m$ versus $E_{\frac{1}{2}}$ for the studied Ni chelates

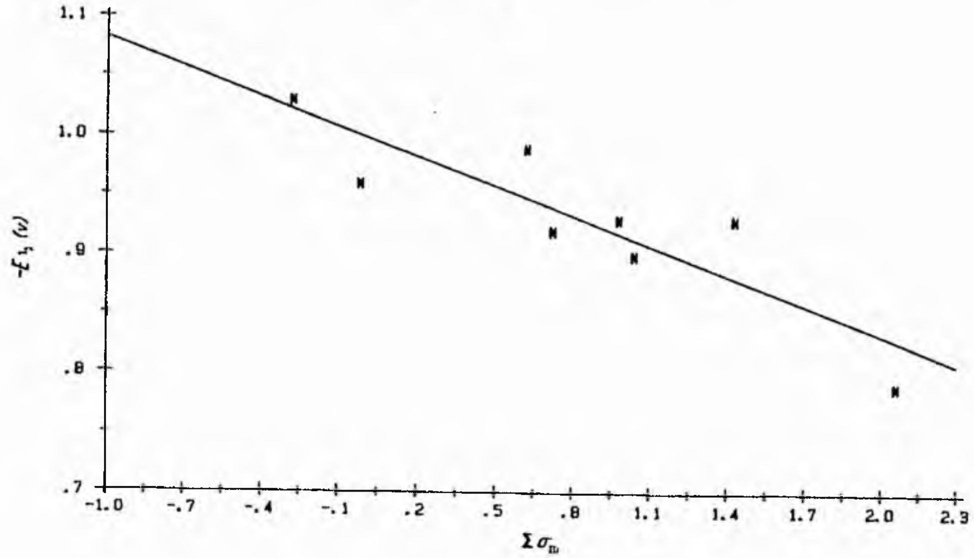

Figure 25

Plot of $E_{\frac{1}{2}}$: sum of Hammett substituent function σ_x

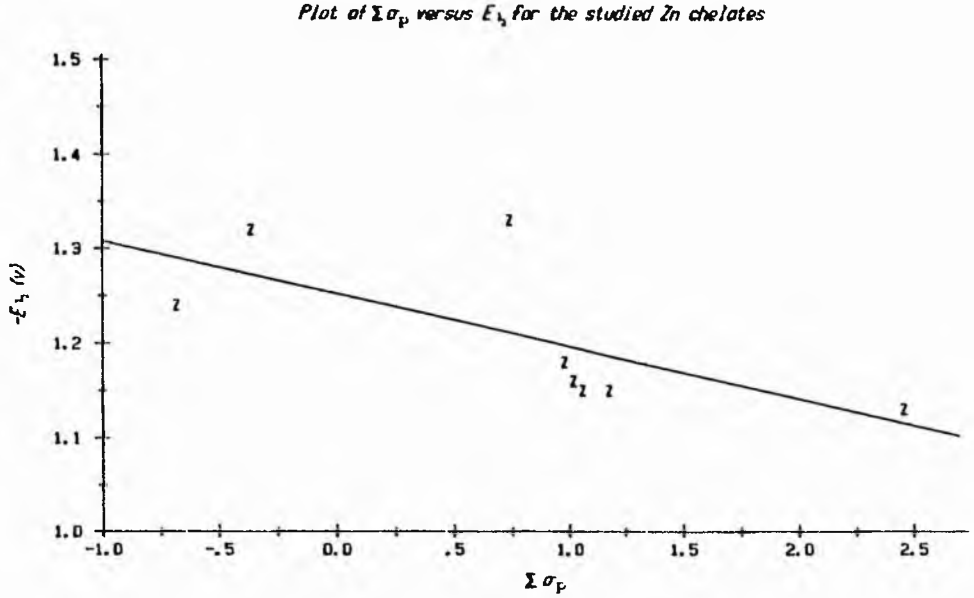

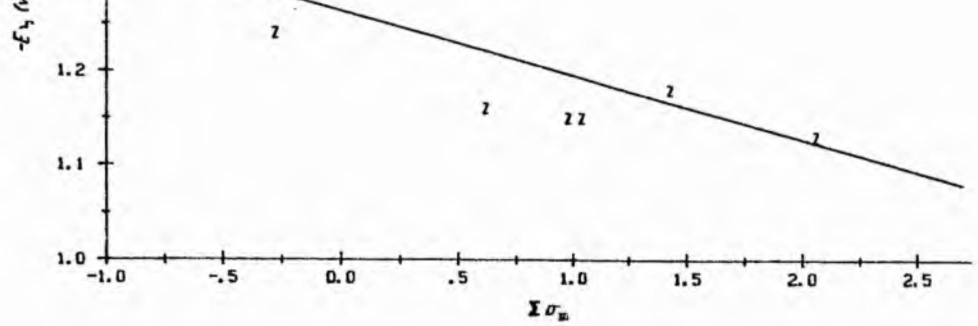

Figure 26

UV spectra of p-Me-bta and bta

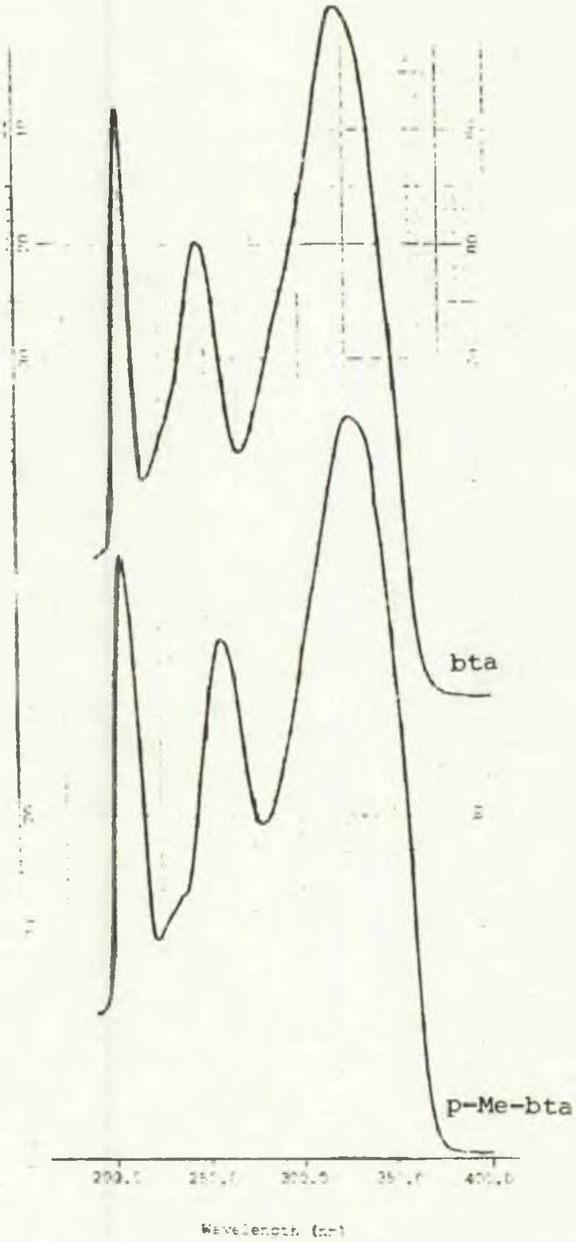

2.6 X 10^{-4} mole ml^{-1} in MeOH

Figure 27

UV spectra of pfbtfa and pfbhfh,

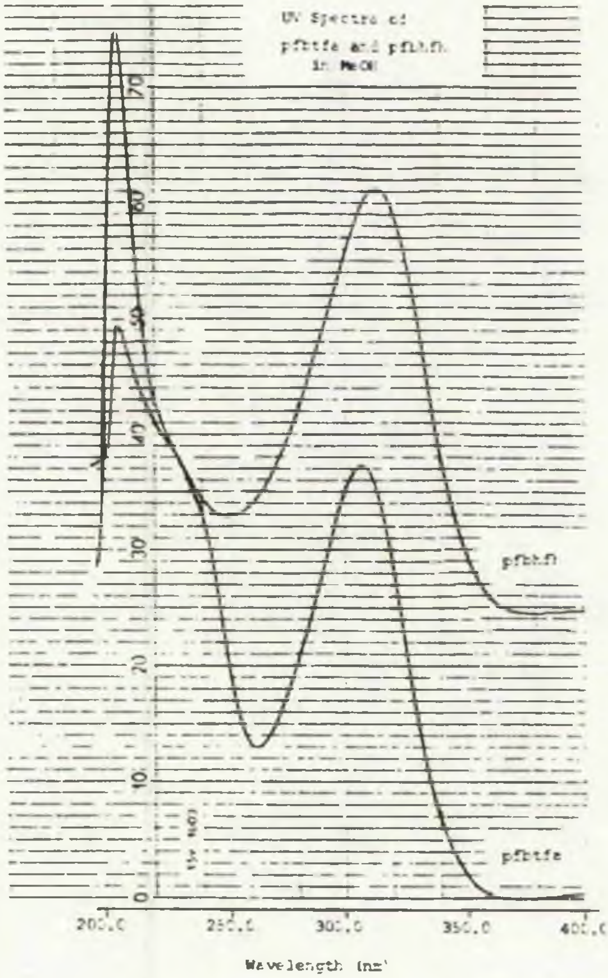

2.6 X 10^{-4} mole ml^{-1} in MeOH

Figure 28

UV spectra of $Ni(pfbtfa)_2$ and $Cu(pfbhfh)_2$.

10^{-3}M in MeOH

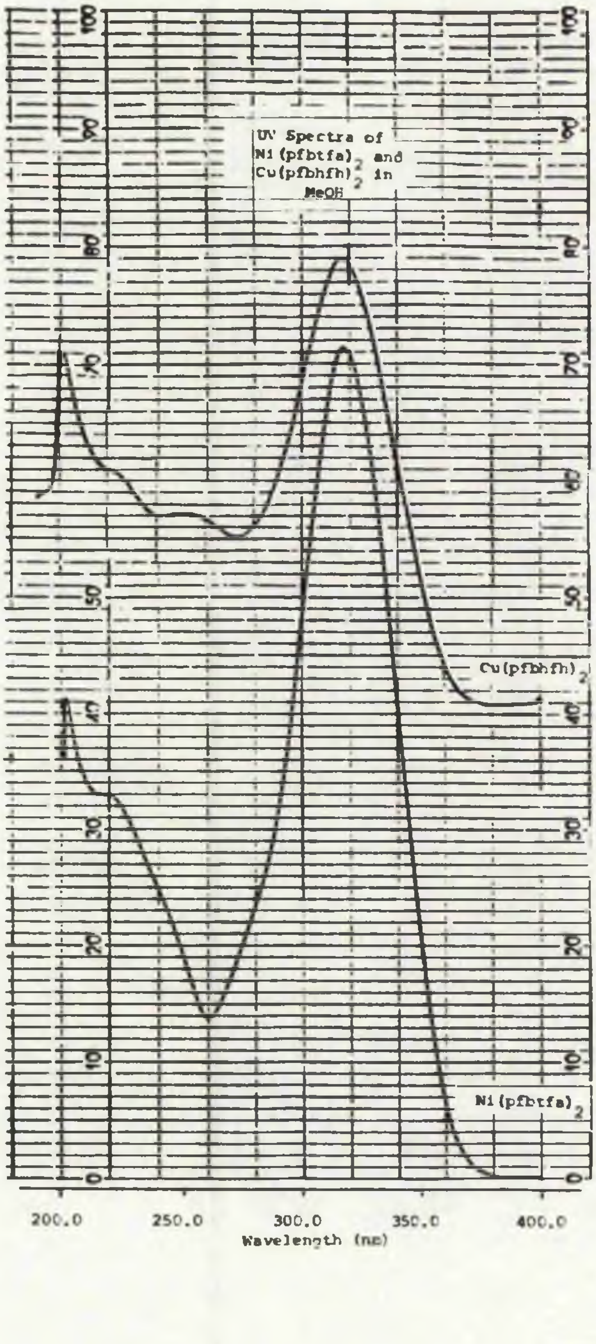

Figure 29

IR spectra of p-Me-bta and bta

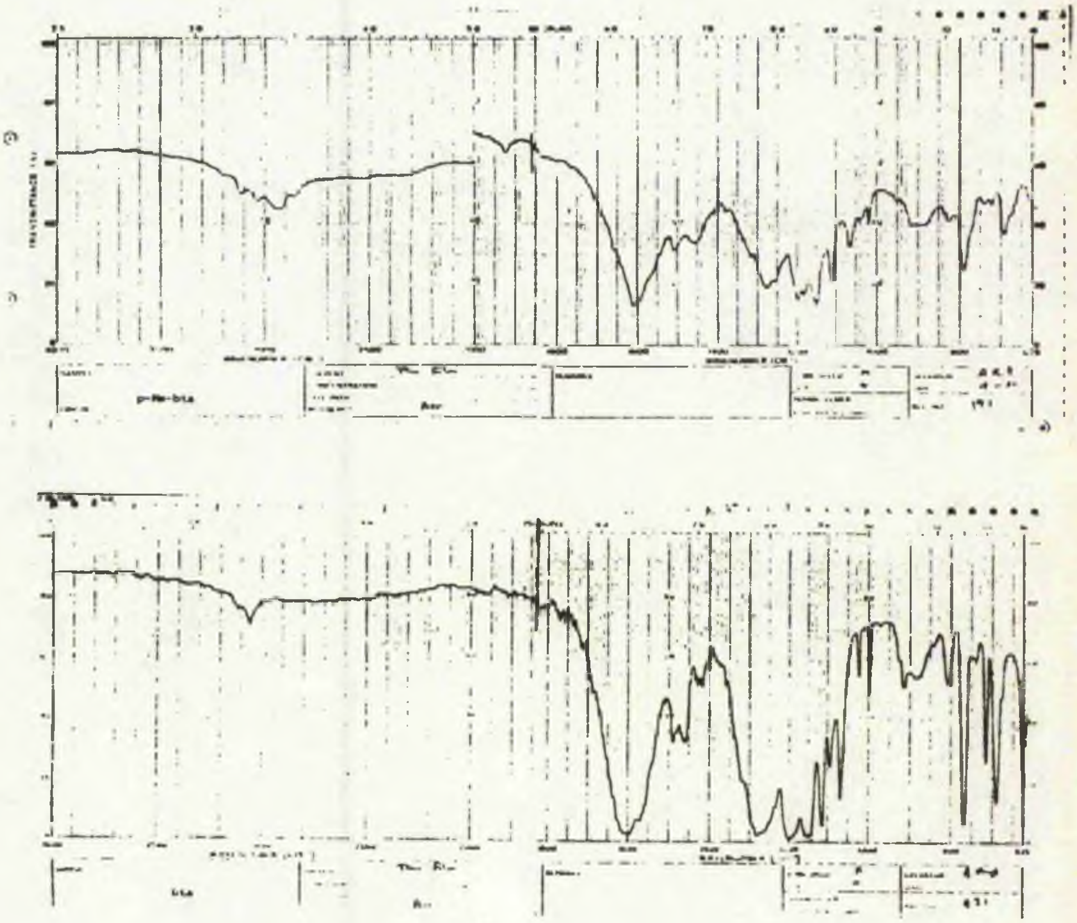

Figure 30

IR spectra of pfbtfa and pfbhfh

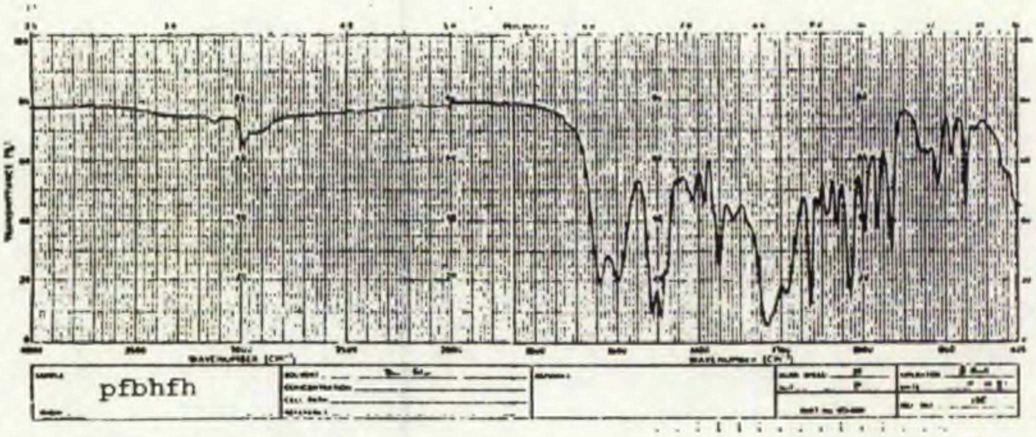

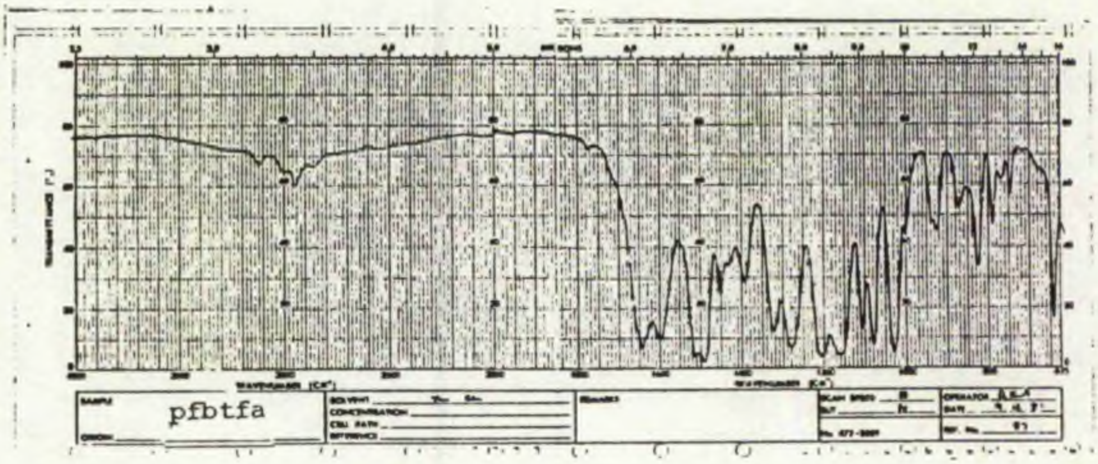

Figure 31

IR spectra of $\mathrm{Cu(pfbtfa)_2}$ and $\mathrm{Zn(pfbhfh)_2}$

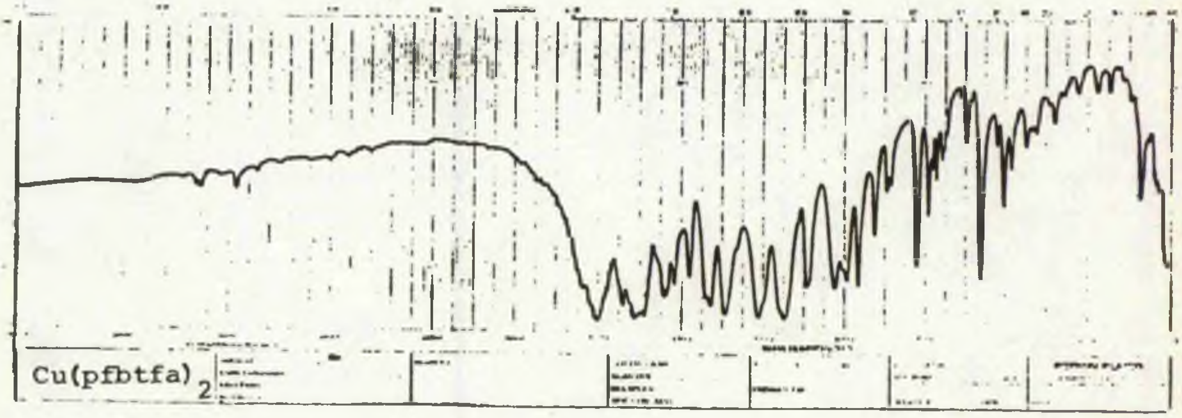

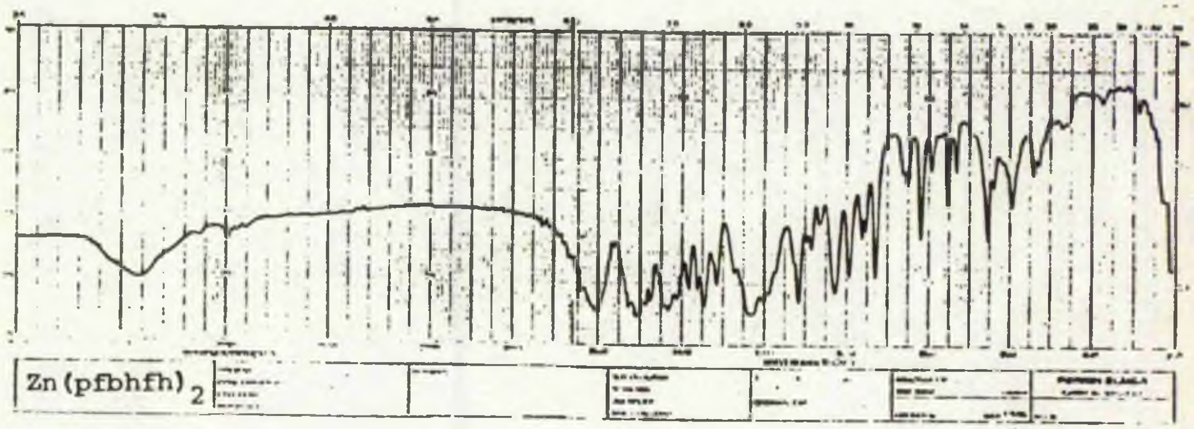

Figure **32**

Plot of ν(M-O) : log (β) for the studied Ni, Cu, Zn chelates

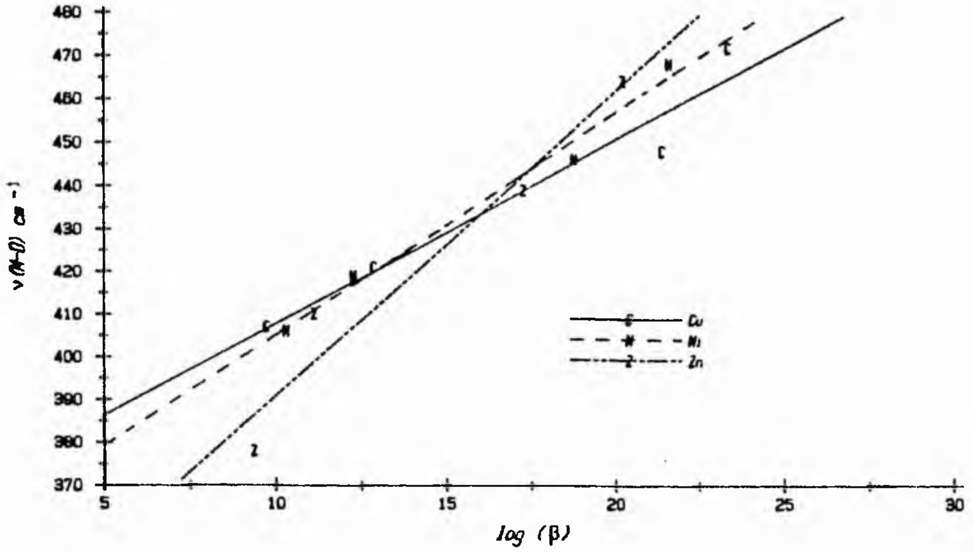

Figure **33**

Plot of ν(M-O) : log (β) for a range of copper chelates

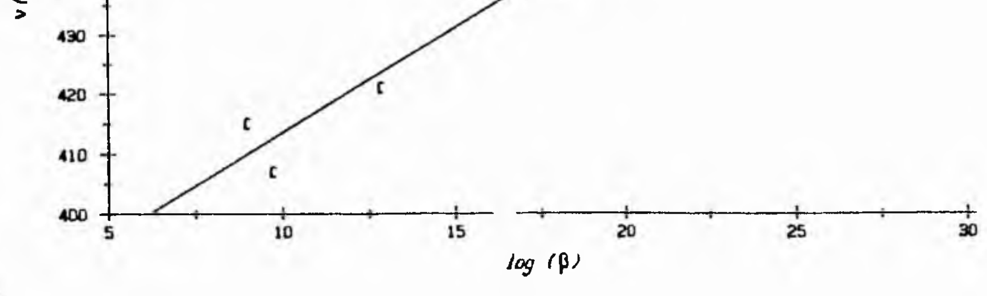

Figure 34

Thermograms for Group I chelates of p-Me-bta

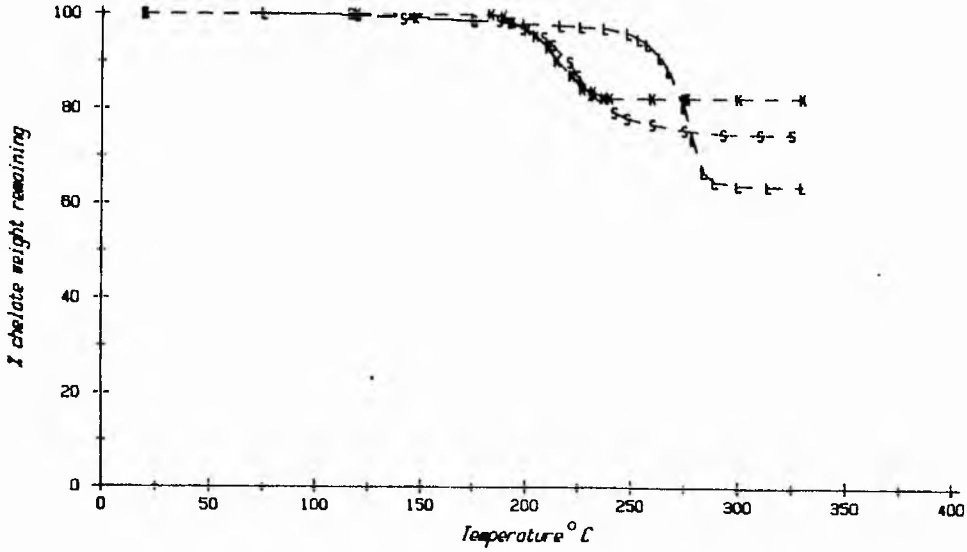

Figure 35

Thermograms for Group II chelates of p-Me-bta

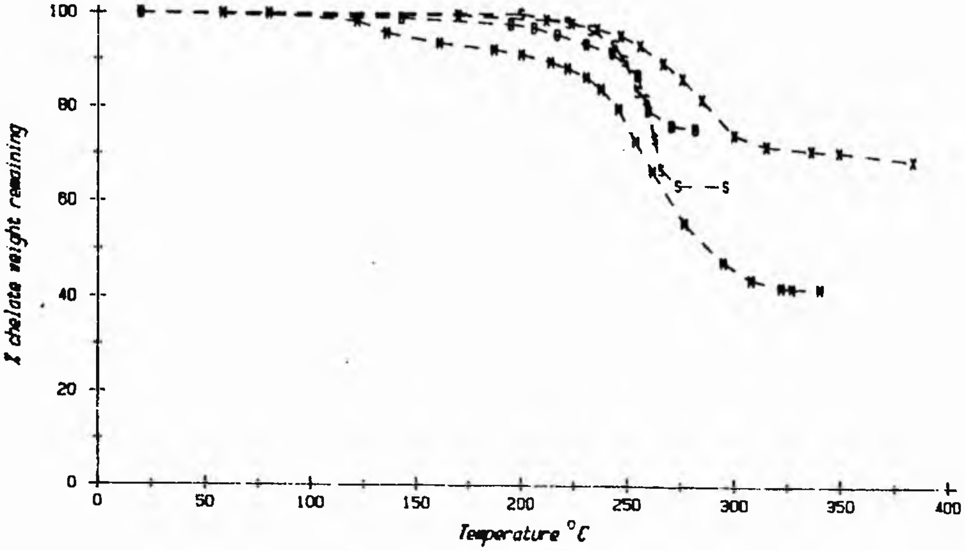

Figure 37

Thermograms for Pb, Cd, Hg chelates of p-Me-bta

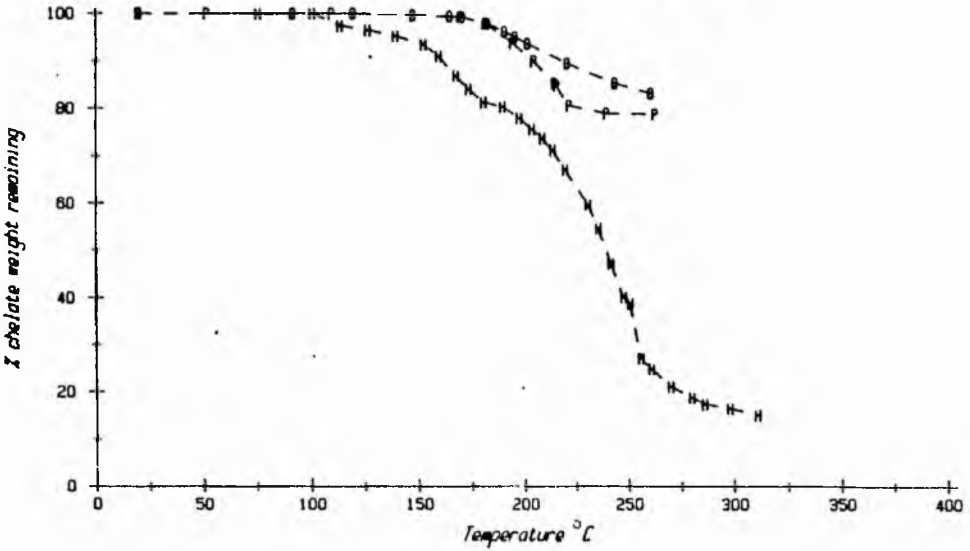

Figure 36

Thermograms for Ni, Cu, Zn, chelates of p-Me-bta

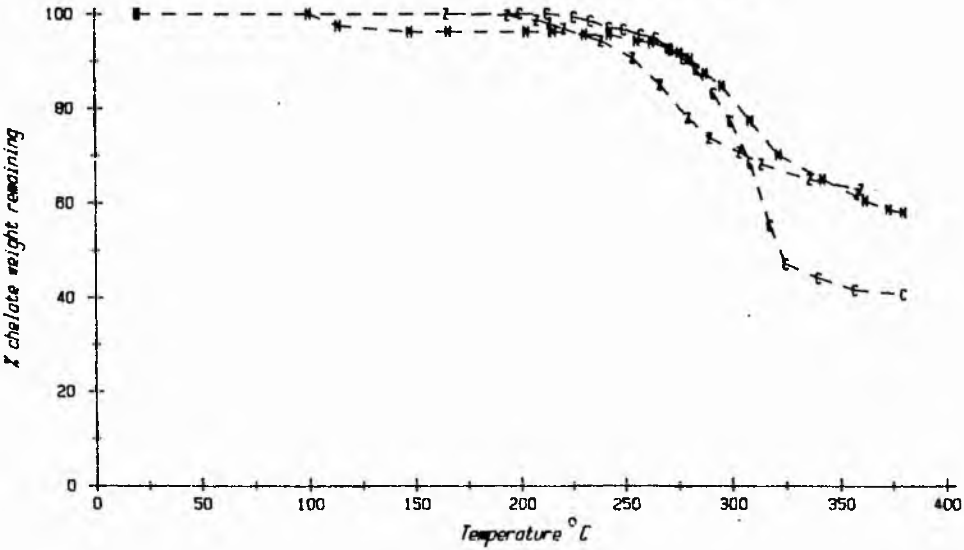

Figure **38**

Thermograms for Group I chelates of bta

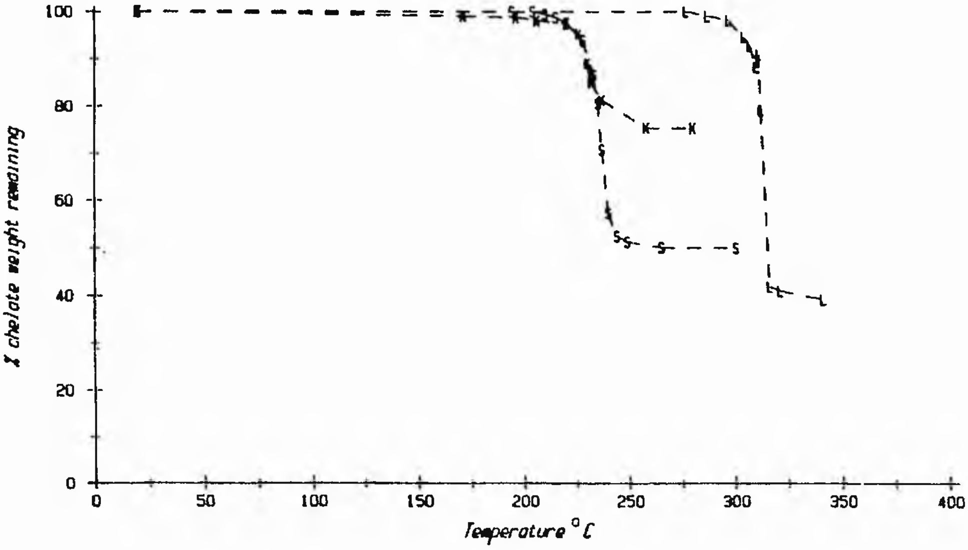

Figure **39**

Thermograms for Group II chelates of bta

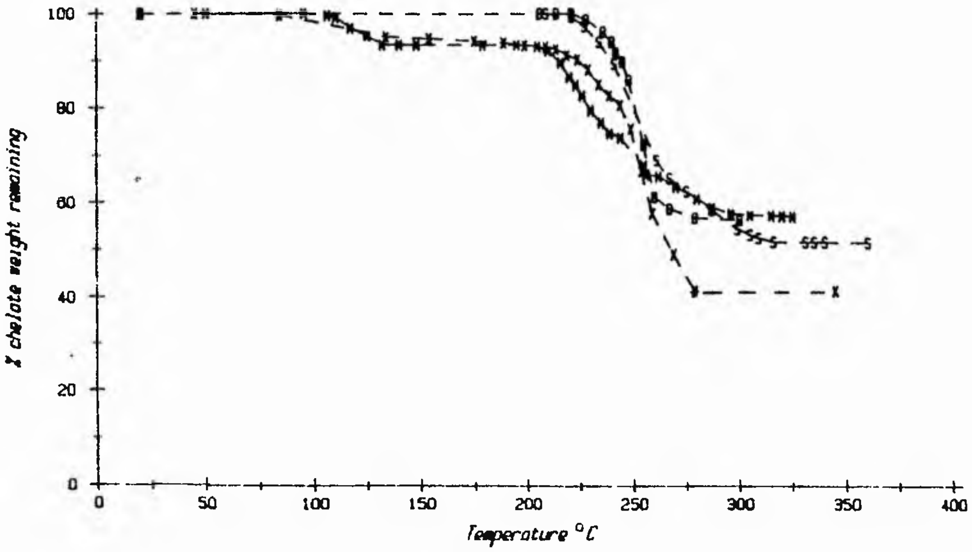

Figure **40**

Thermograms for Ni, Cu, Zn chelates of bta

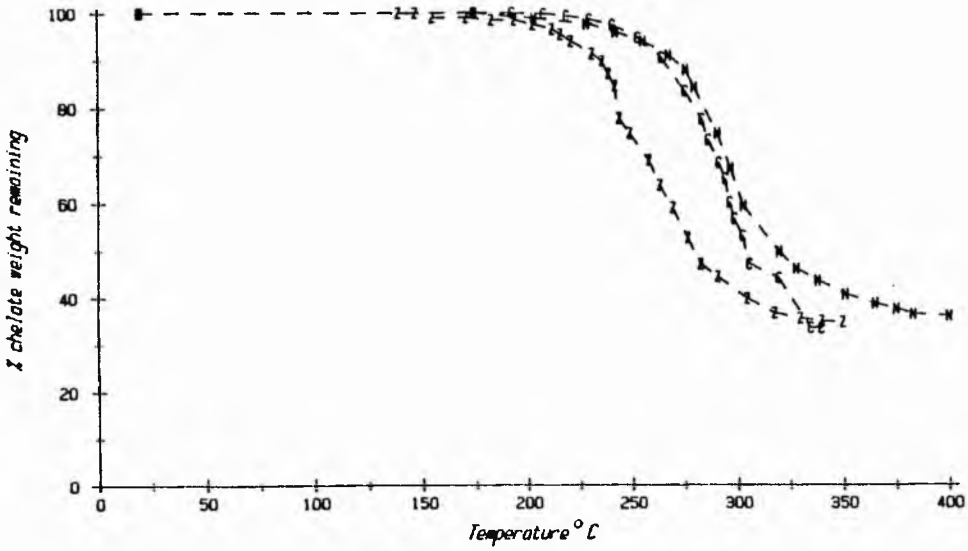

Figure **41**

Thermograms for Pb, Cd, Hg chelates of bta

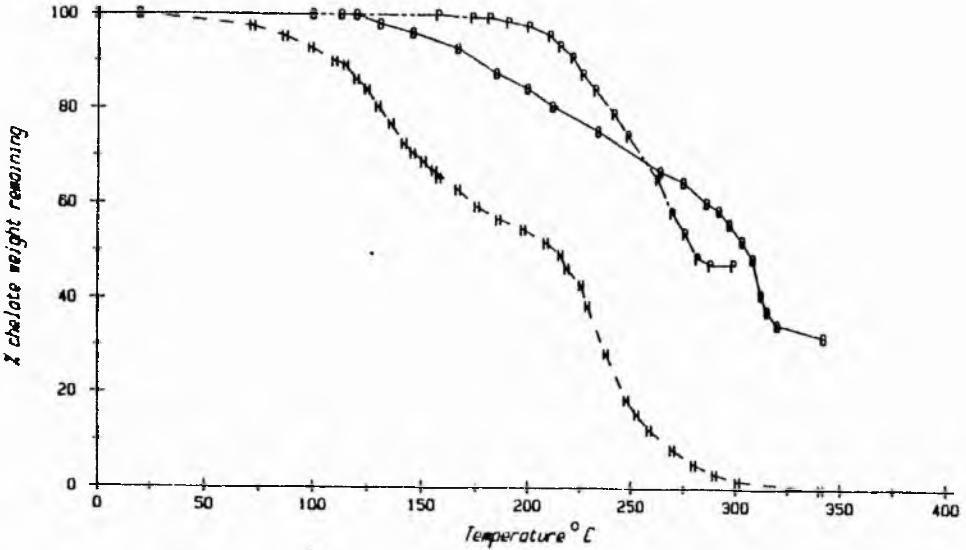

Figure 42

Thermograms for Group I chelates of pfbtfa

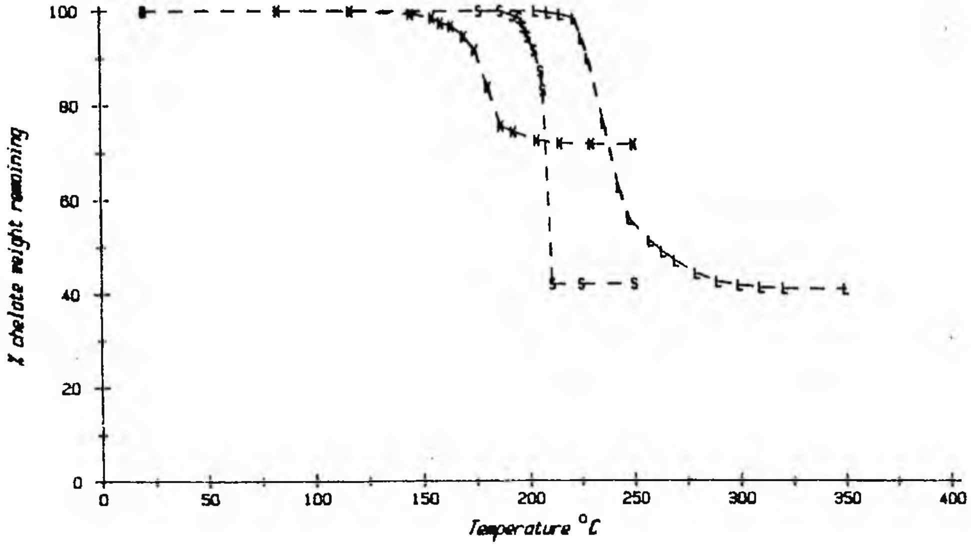

Figure 43

Thermograms for Group II chelates of pfbtfa

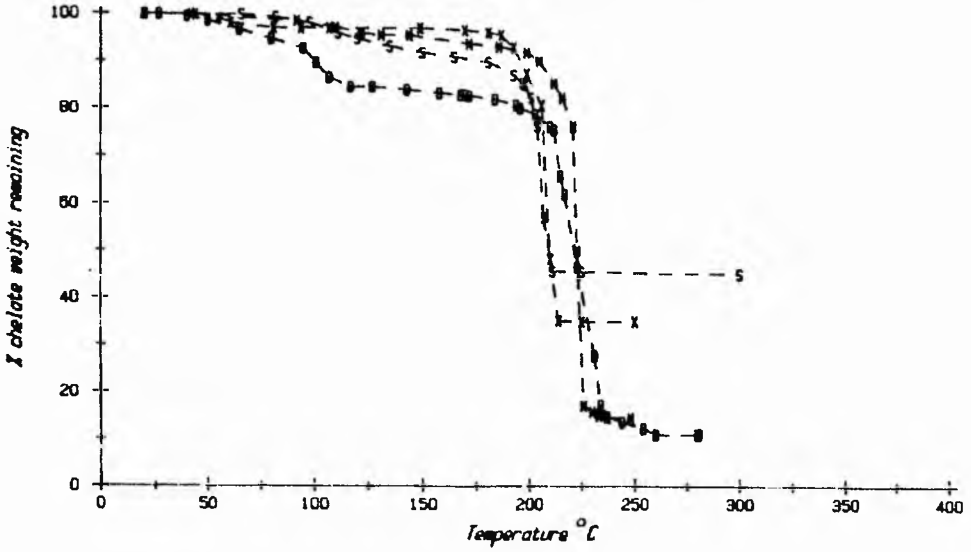

Figure **44**

Thermograms for Ni, Cu, Zn, chelates of pfbtfa

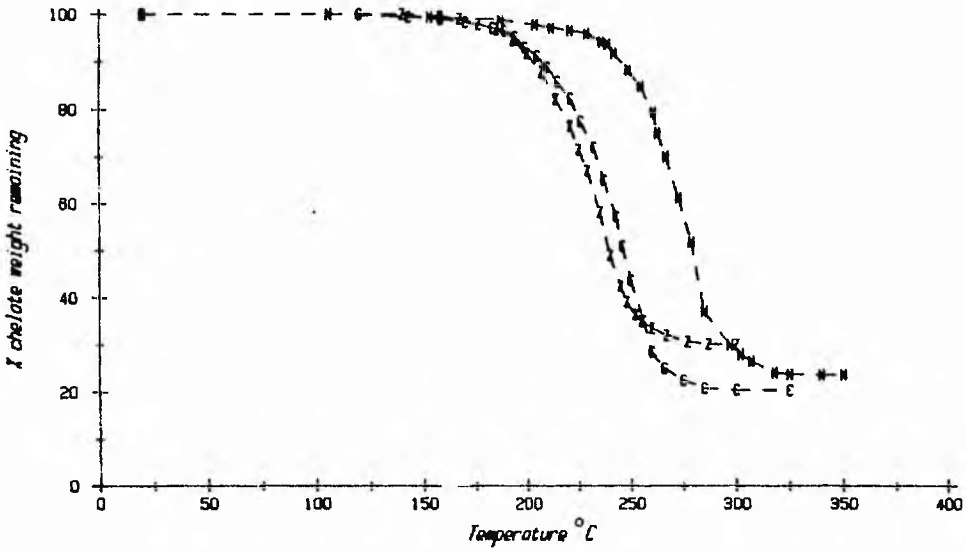

Figure **45**

Thermograms for Pb, Cd, Hg, chelates of pfbtfa

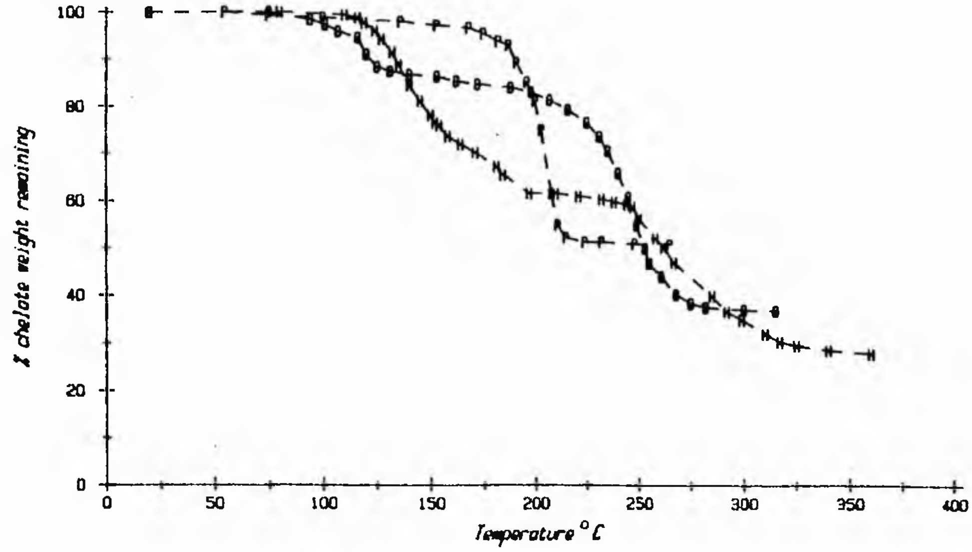

Figure 46

Thermograms for Group 1 chelates of pfbhfh

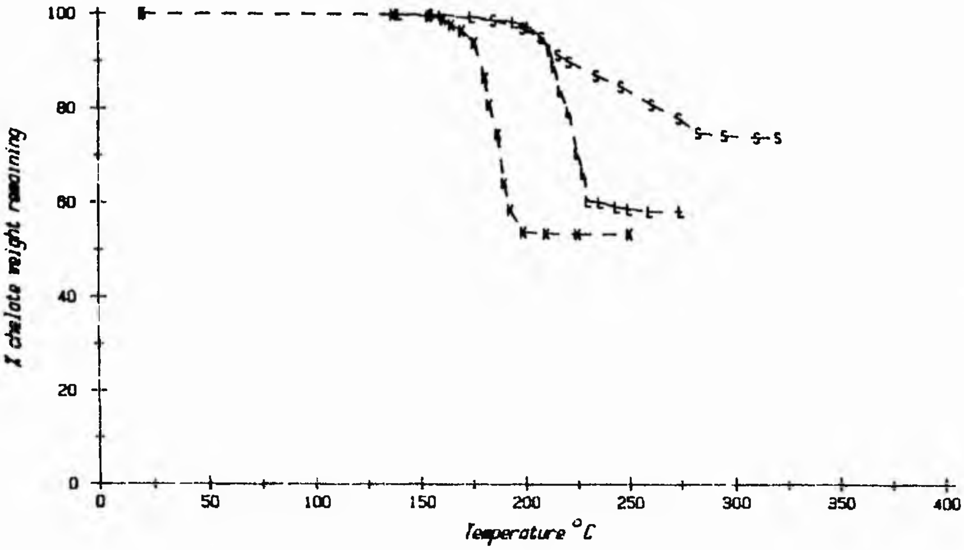

Figure 47

Thermograms for Mg, Sr, Ba, chelates of pfbhfh

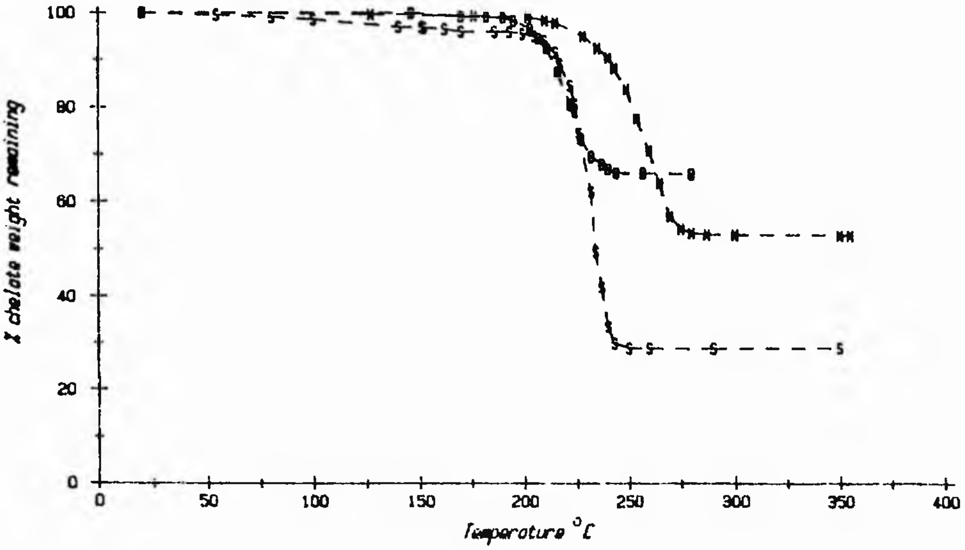

Figure 48

Thermograms for Ni, Cu, Zn, chelates of pfbhfh

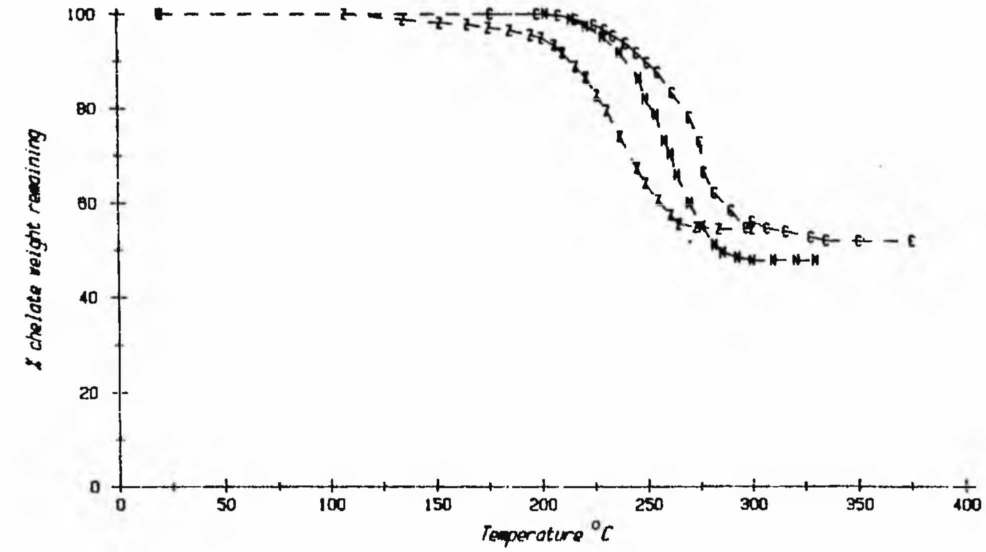

Figure 49

Thermograms for Pb, Cd, Hg, chelates of pfbhfh

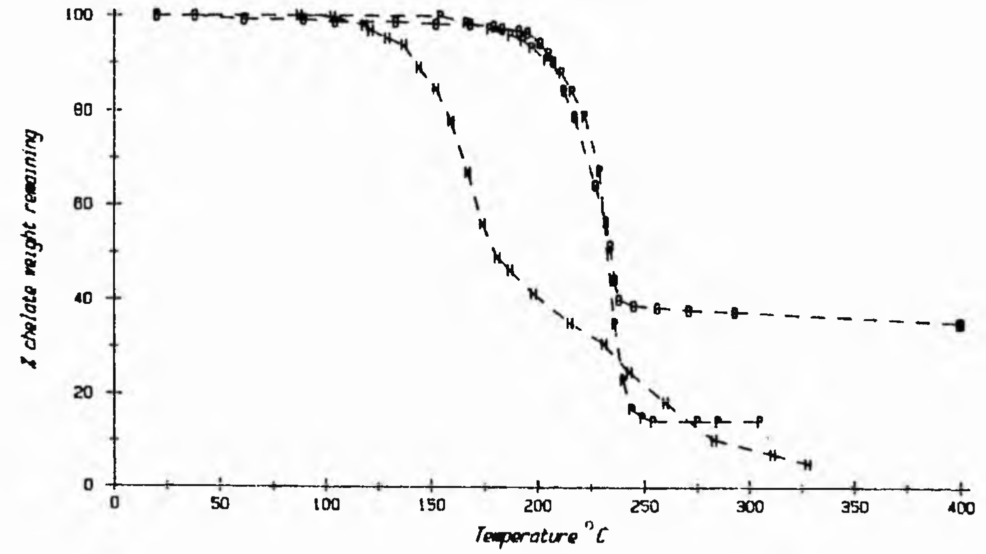

Figure 50

Clausius-Clapeyron plot for Group I complexes of p-Me-bta

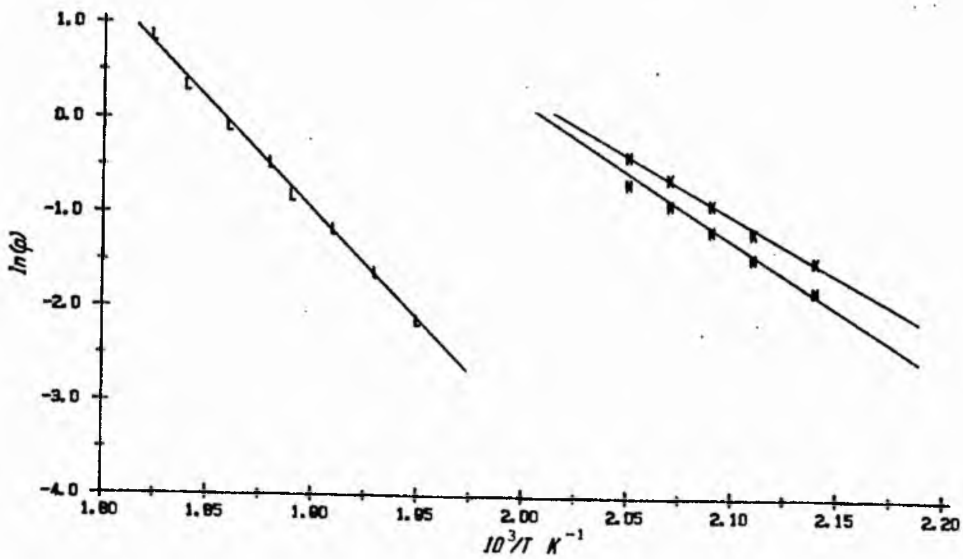

Figure 51

Clausius-Clapeyron plot for Group II chelatesof p-Me-bta

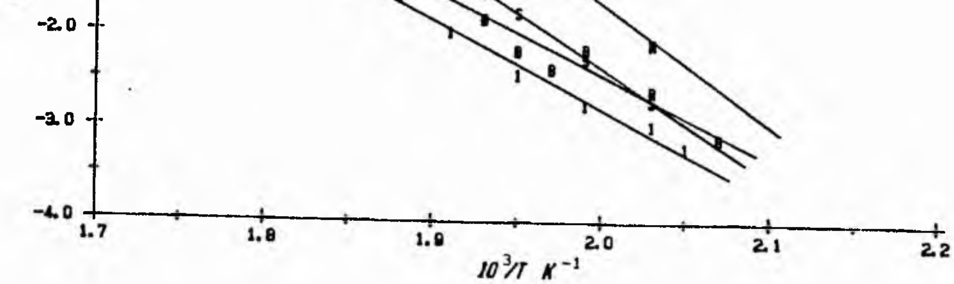

Figure 52

Clausius-Clapeyron plot for Ni, Cu, Zn chelates of p-Me-bta

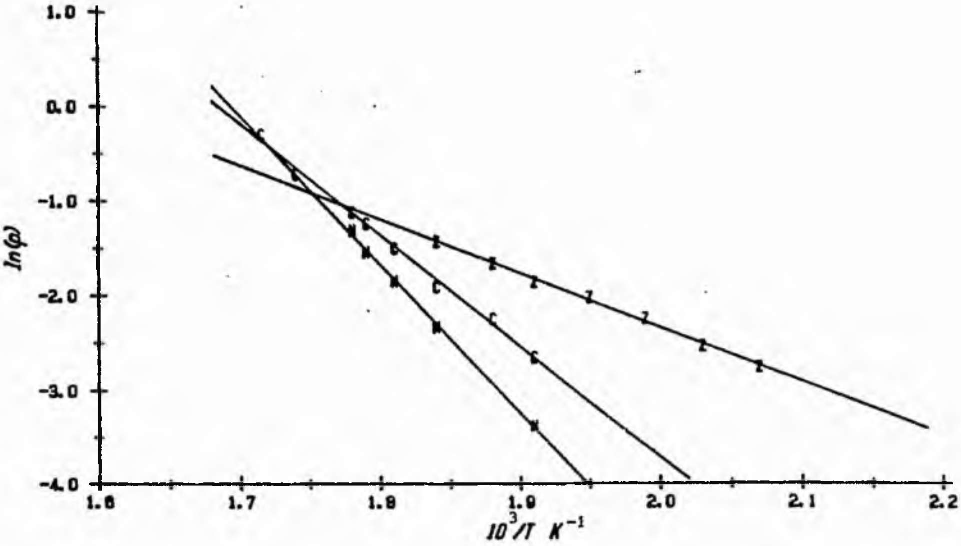

Figure 53

Clausius-Clapeyron plot for Pb, Cd, Hg chelates of p-Me-bta

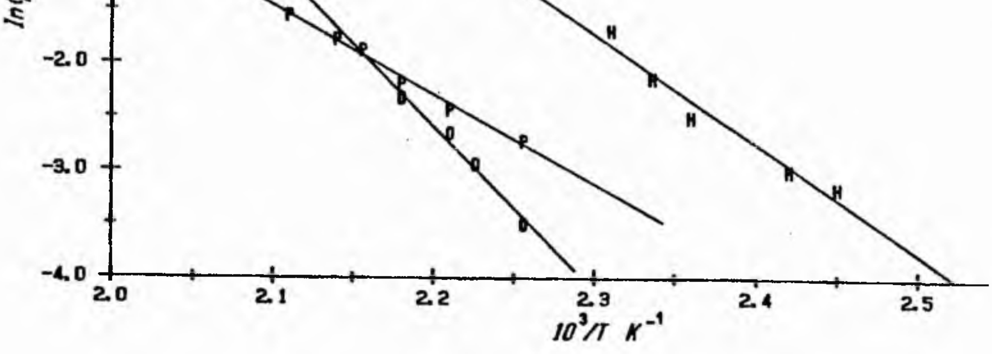

Figure 54

Clausius-Clapeyron plot for Group I complexes of bta

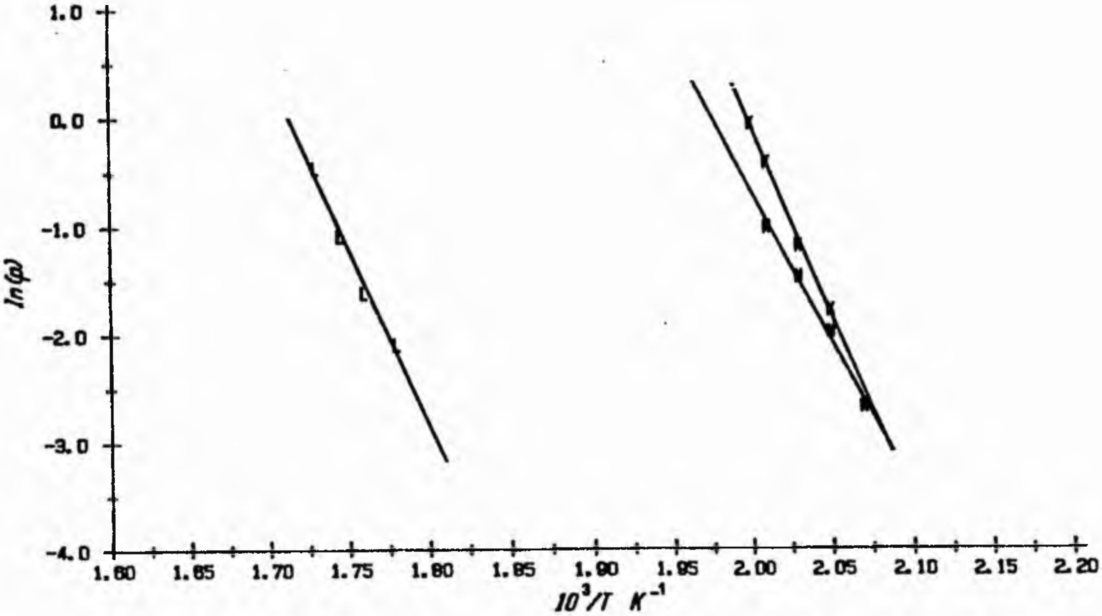

Figure 55

Clausius-Clapeyron plot for Group II chelates of bta

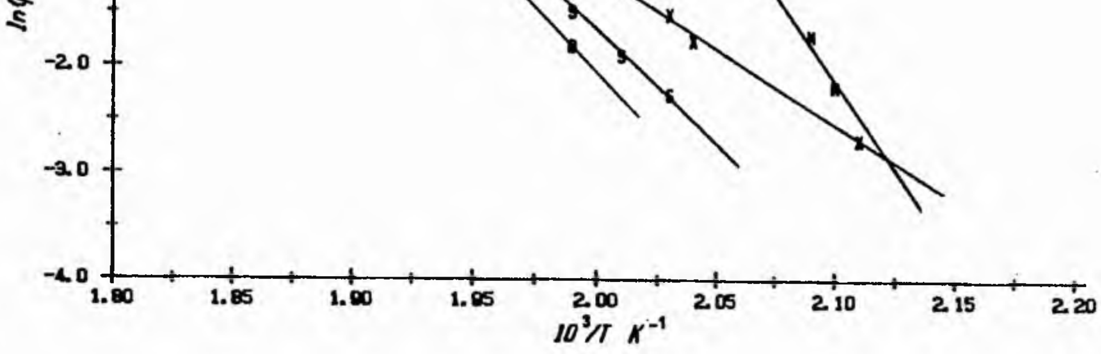

Figure 56

Clausius-Clapeyron plot for Ni, Cu, Zn chelates of bta

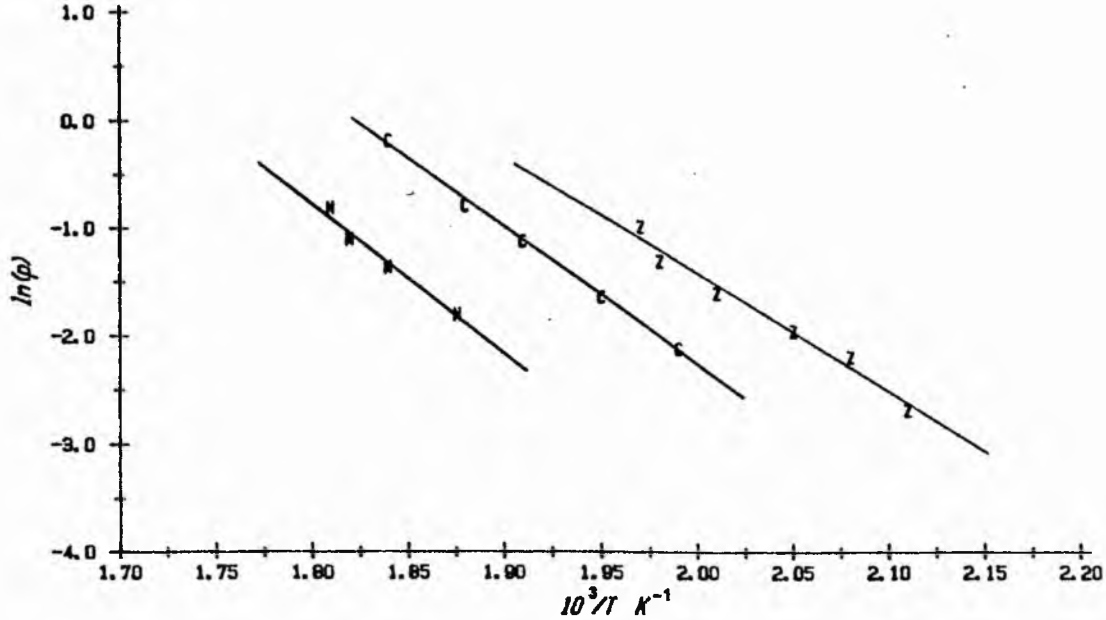

Figure 57

Clausius-Clapeyron plot for Pb and Cd chelates of bta

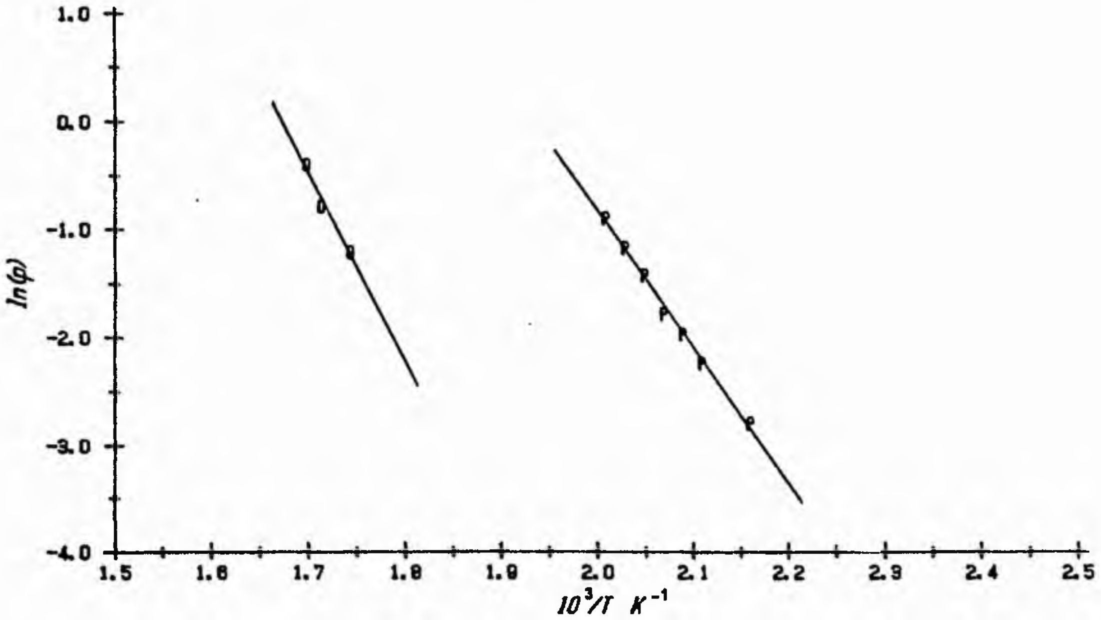

Figure 58

Clausius-Clapeyron plot for Group I complexes of pfbtfa

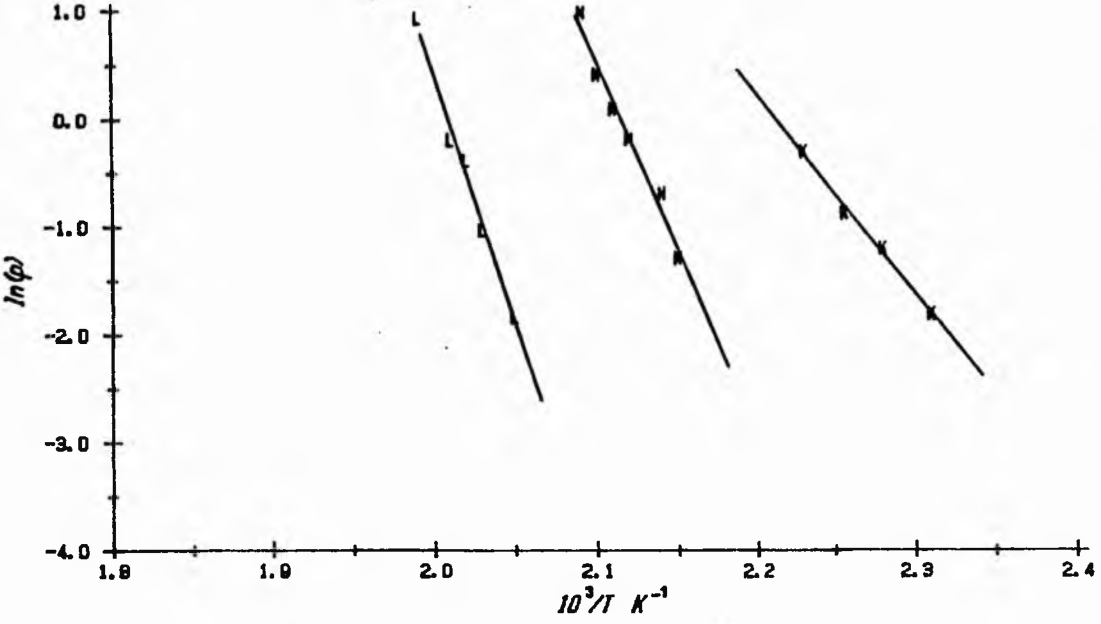

Figure 59

Clausius-Clapeyron plot for Group II chelates of pfbtfa

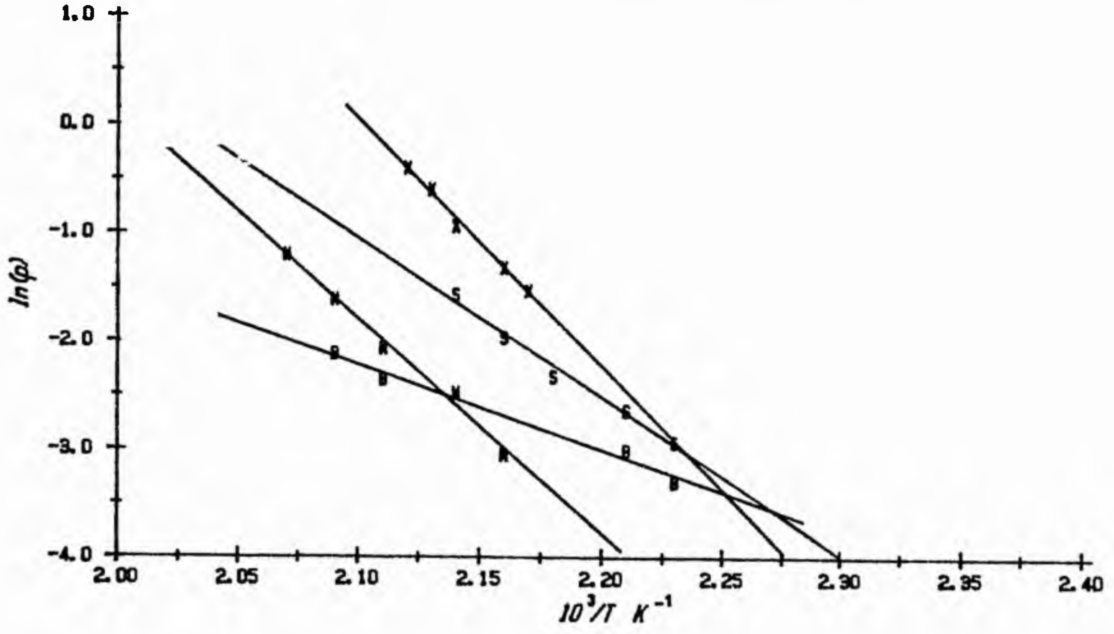

Figure 60

Clausius-Clapeyron plot for Ni, Cu, Zn chelates of pfbtfa

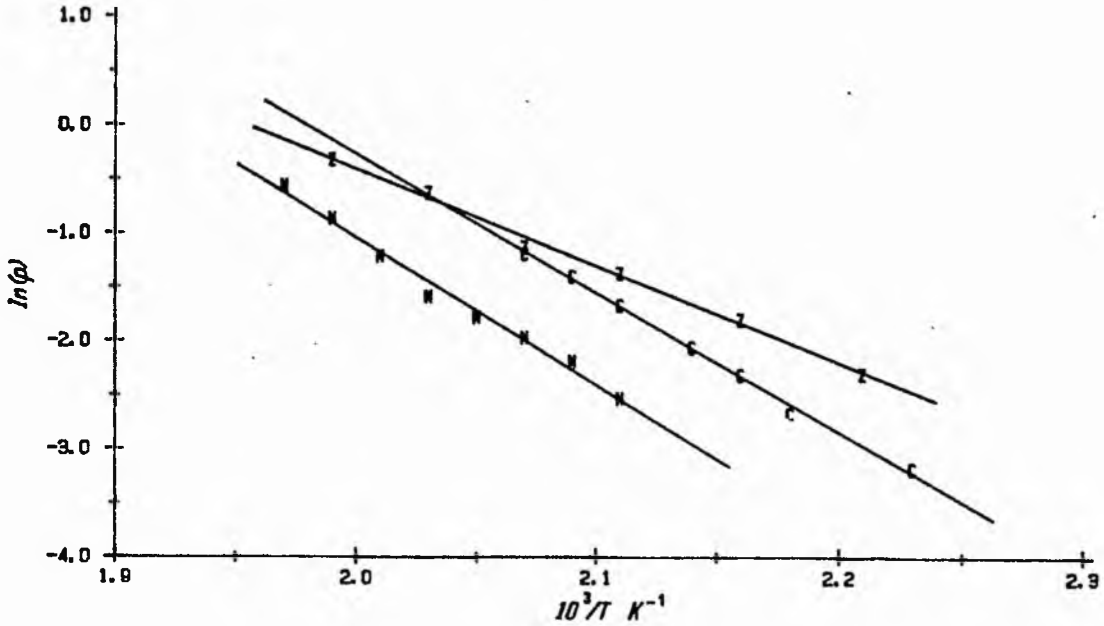

Figure 61

Clausius-Clapeyron plot for Pb, Cd, Hg chelates of pfbtfa

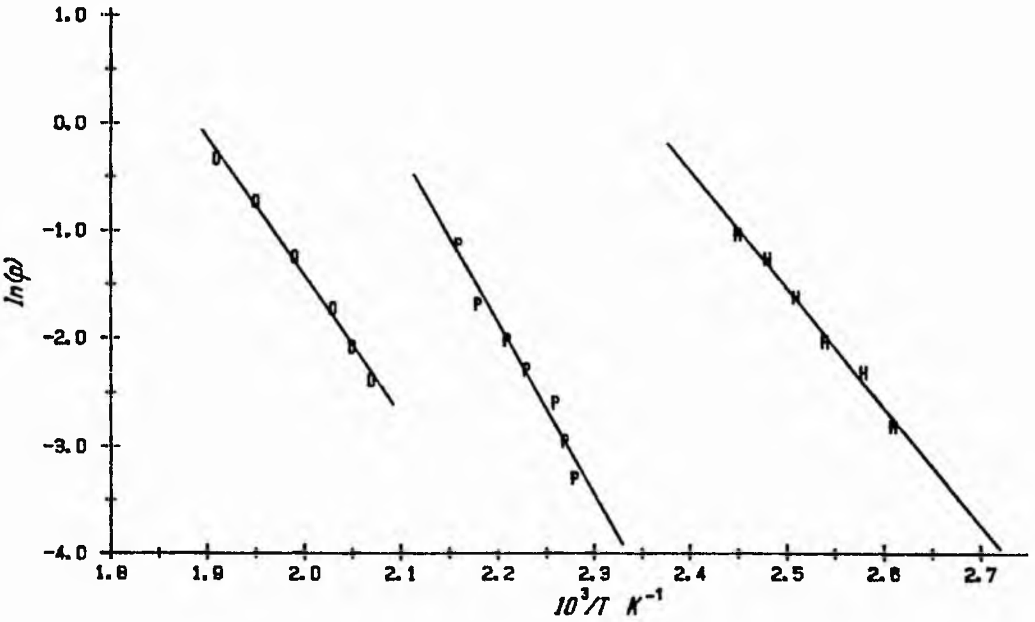

Figure 62

Clausius-Clapeyron plot for Group I complexes of pfbhfh

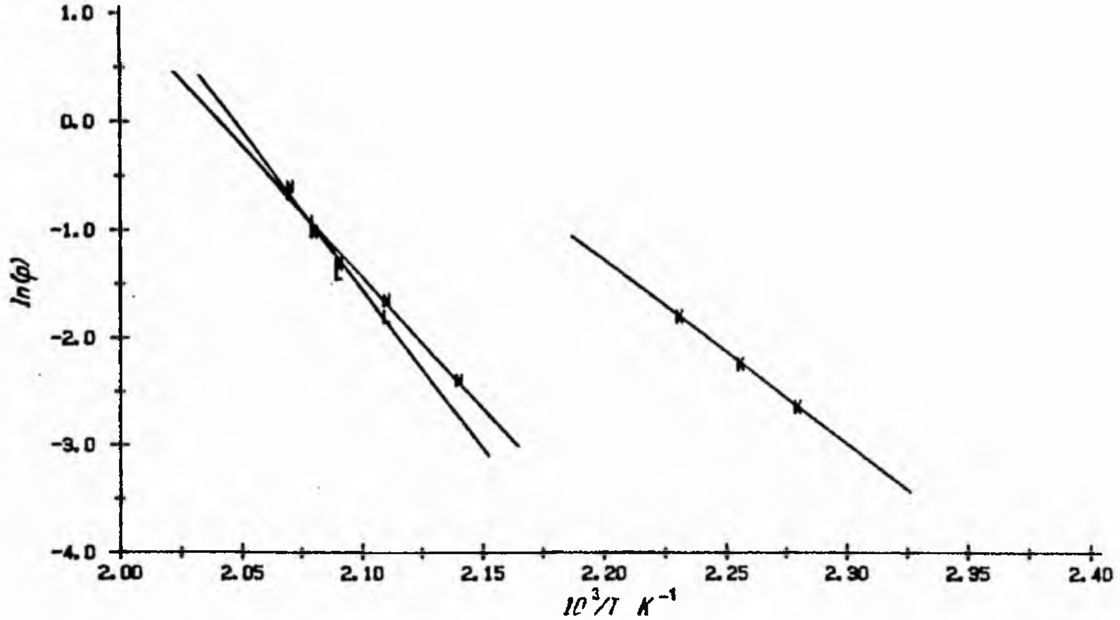

Figure 63

Clausius-Clapeyron plot for Group II chelates of pfbhfh

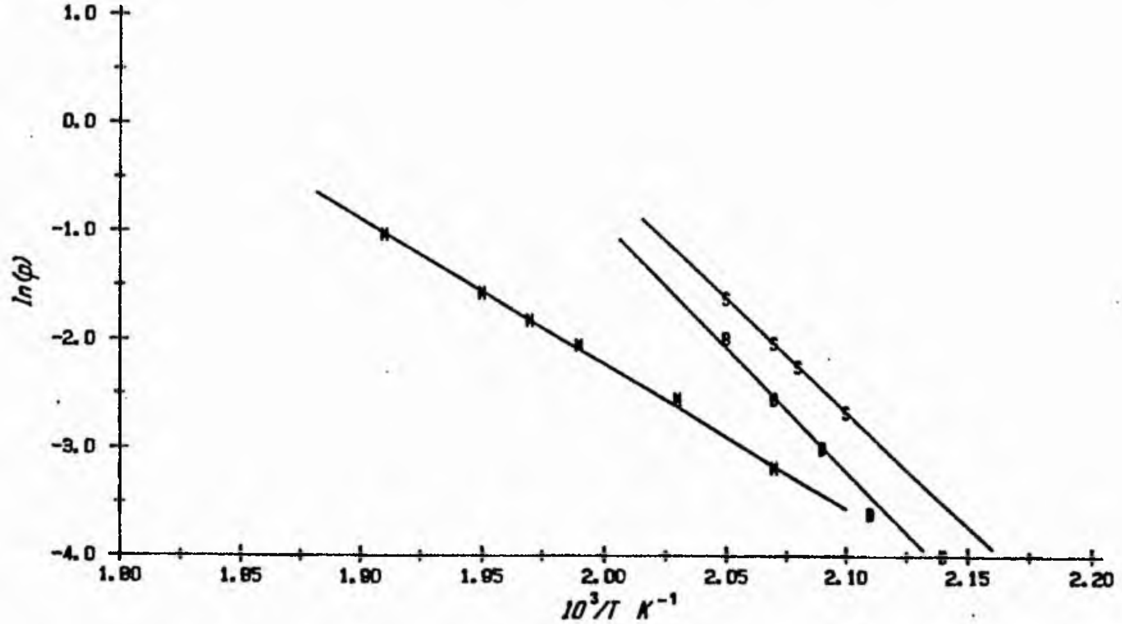

Figure 64

Clausius-Clapeyron plot for Ni, Cu, Zn chelates of pfbhfh

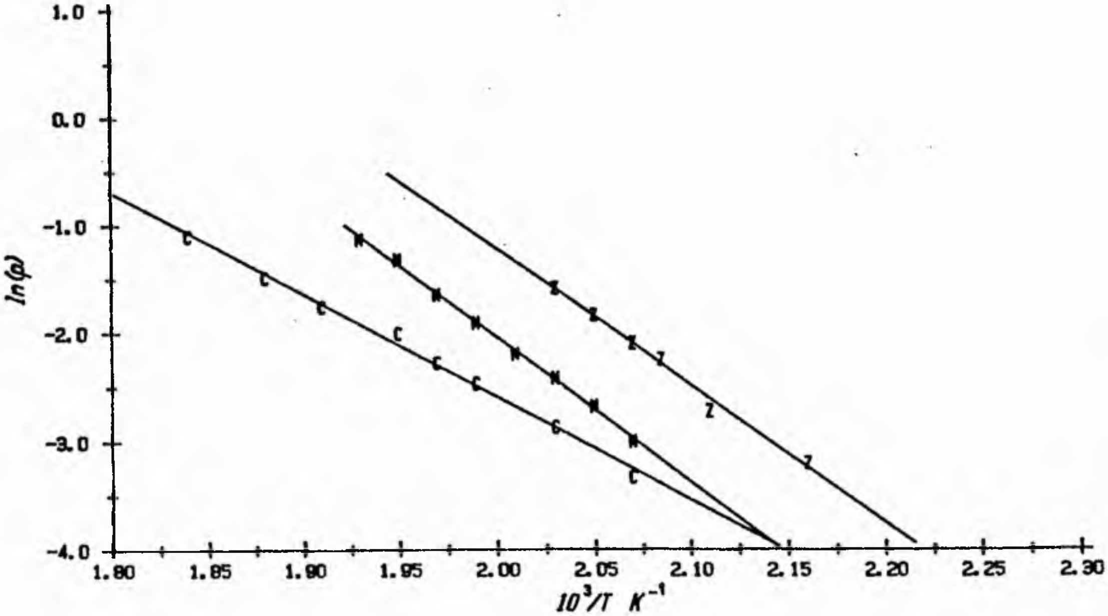

Figure 65

Clausius-Clapeyron plot for Pb, Cd, Hg chelates of pfbhfh

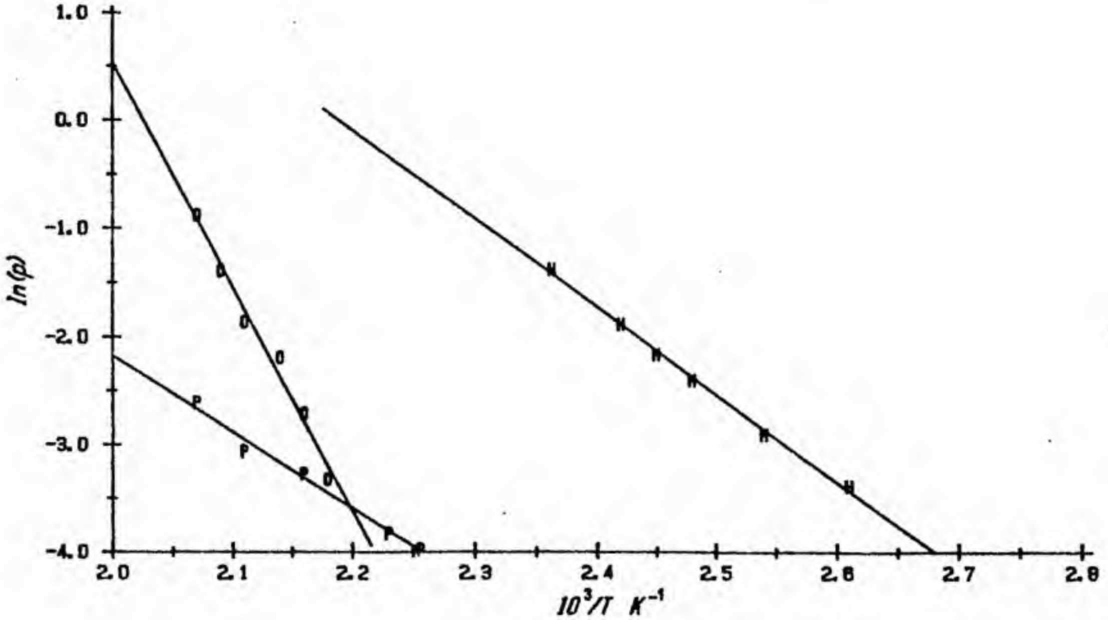

Figure 66

Comparative effect of ligand upon volatility of the Li complexes

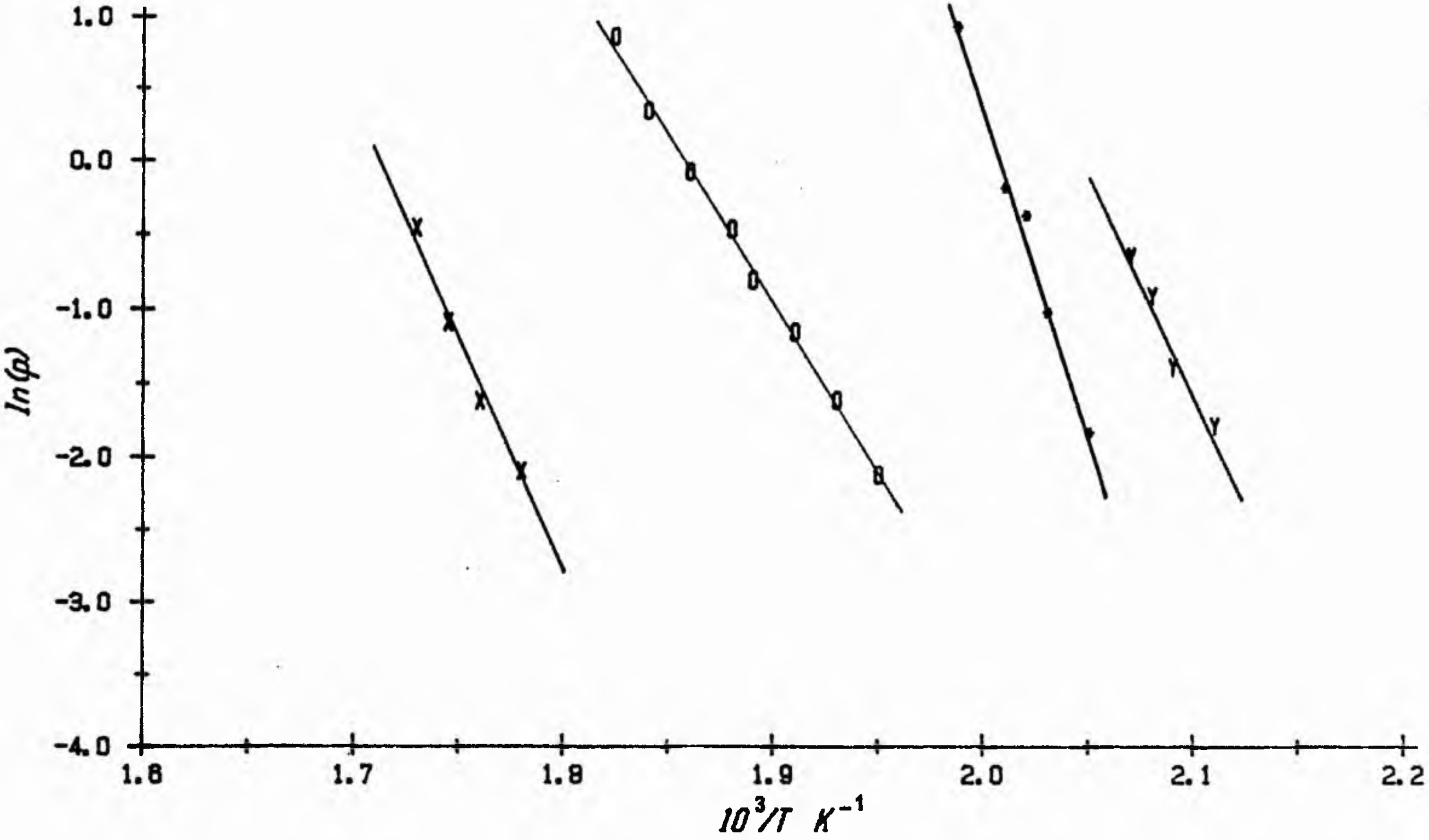

Figure 67

Comparative effect of ligand upon volatility of the Na complexes

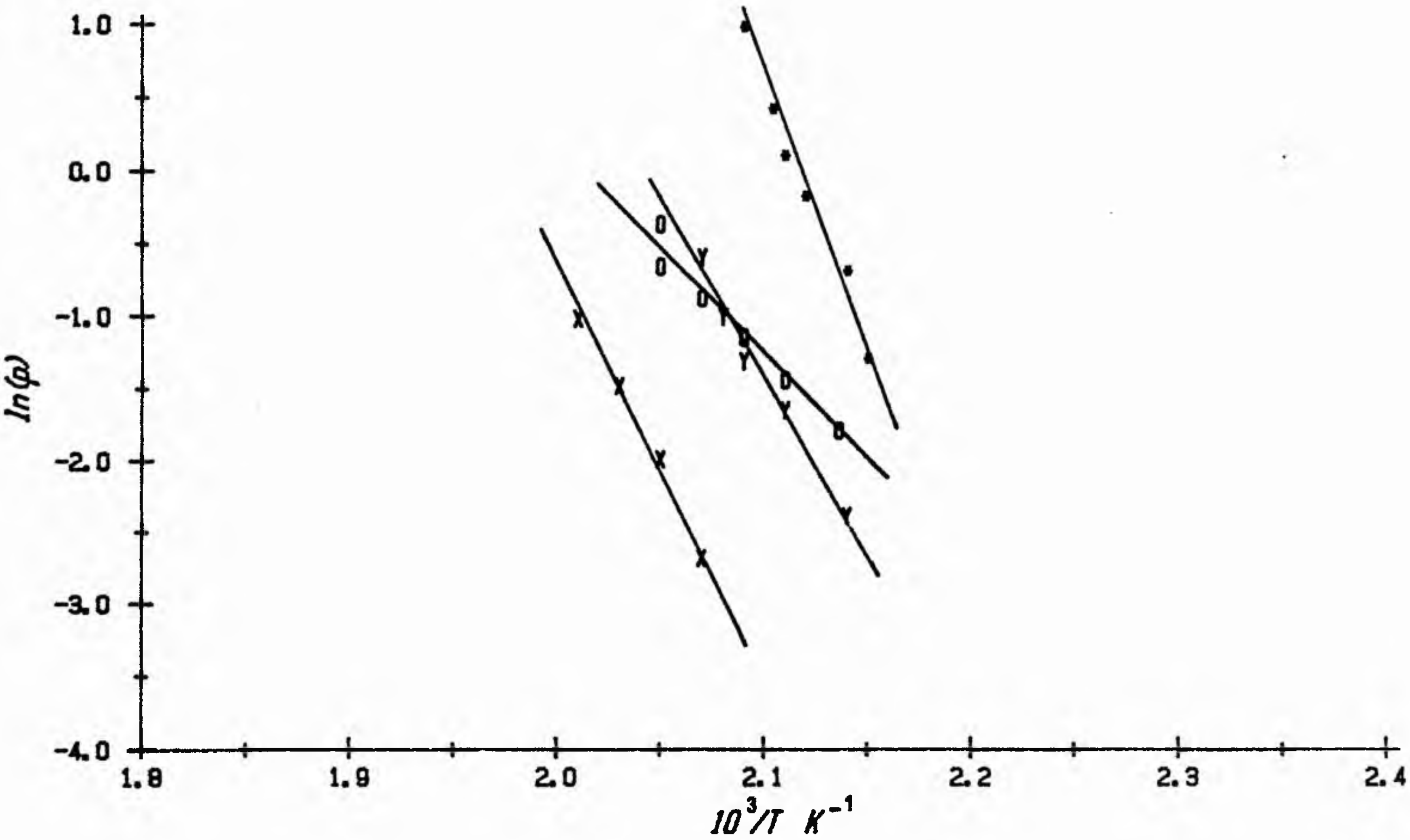

Figure **68**

Comparative effect of ligand upon volatility of the K complexes

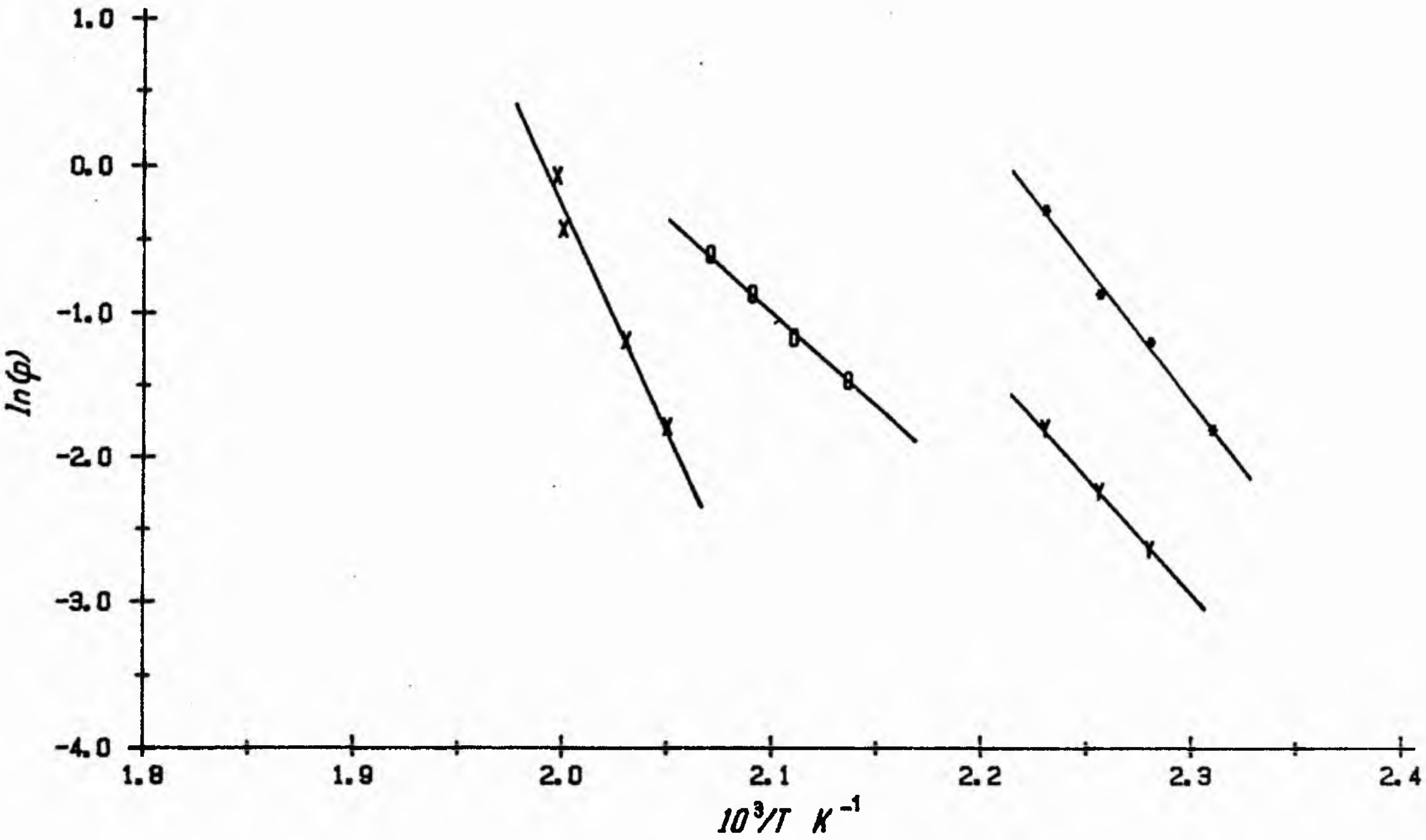

Figure 69

Comparative effect of ligand upon volatility of the Mg chelates

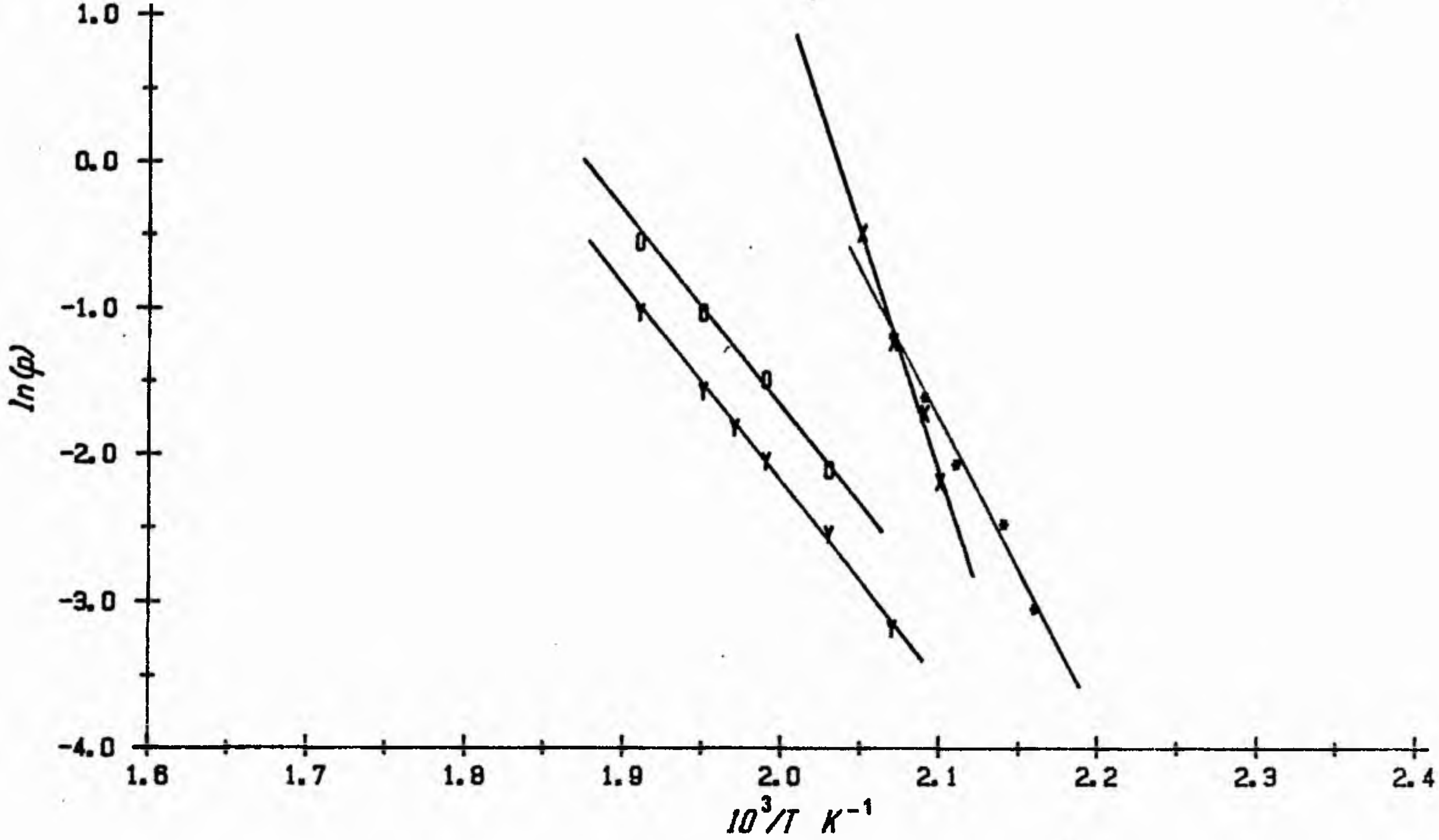

Figure 70

Comparative effect of ligand upon volatility of Ca chelates

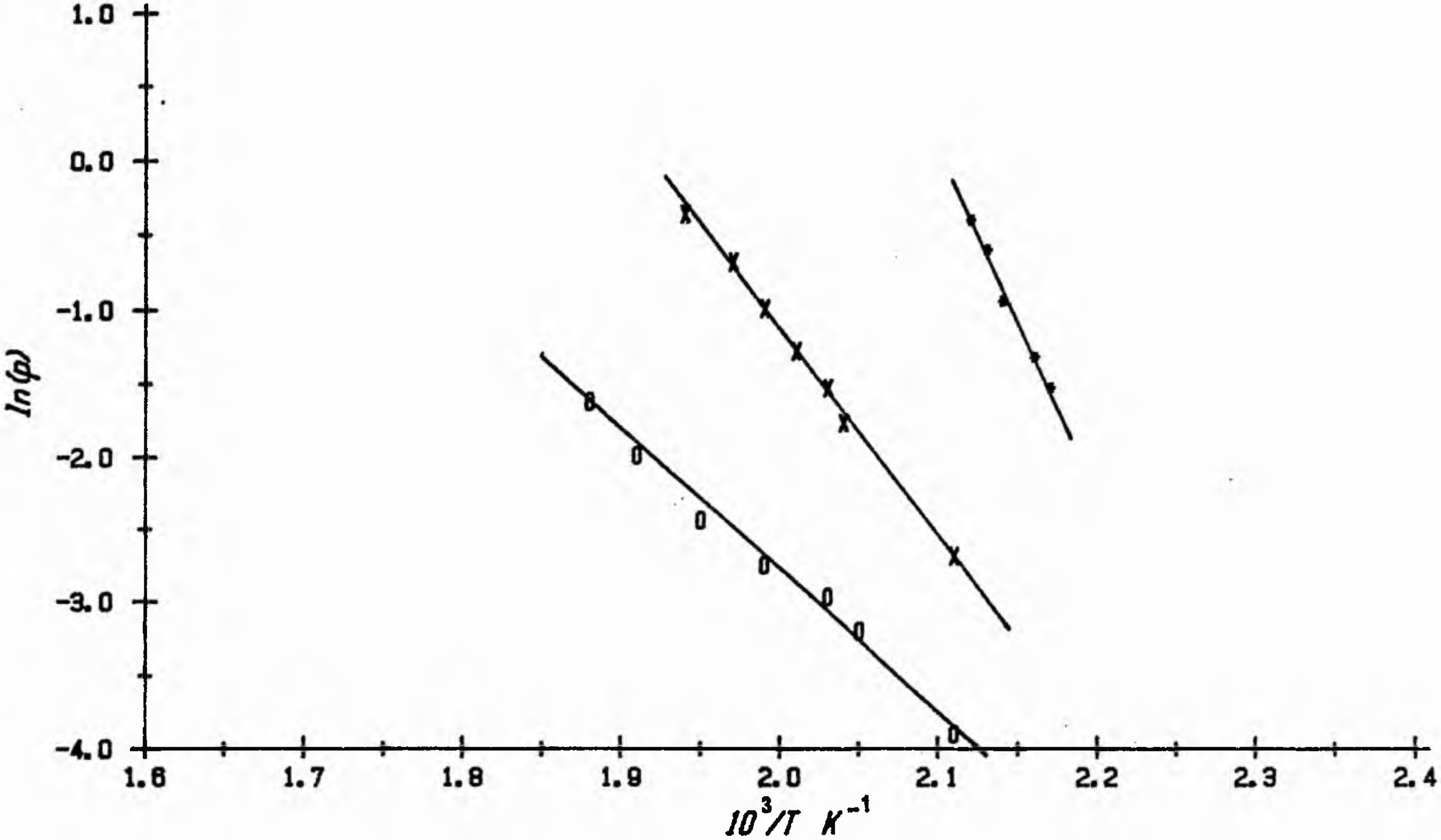

Figure 71

Comparative effect of ligand upon volatility of the Sr chelates

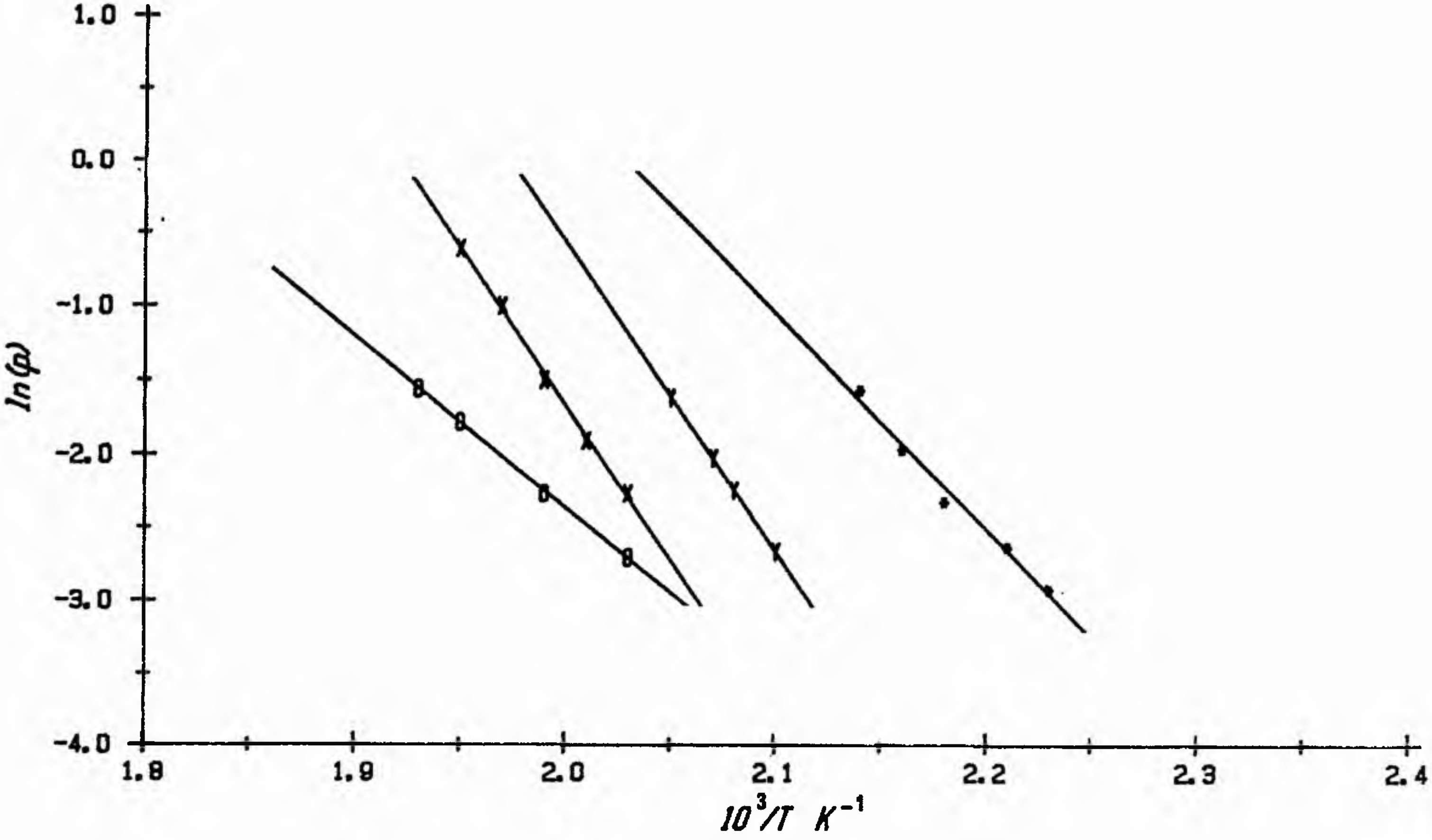

Figure 72

Comparative effect of ligand upon volatility of the Ba chelates

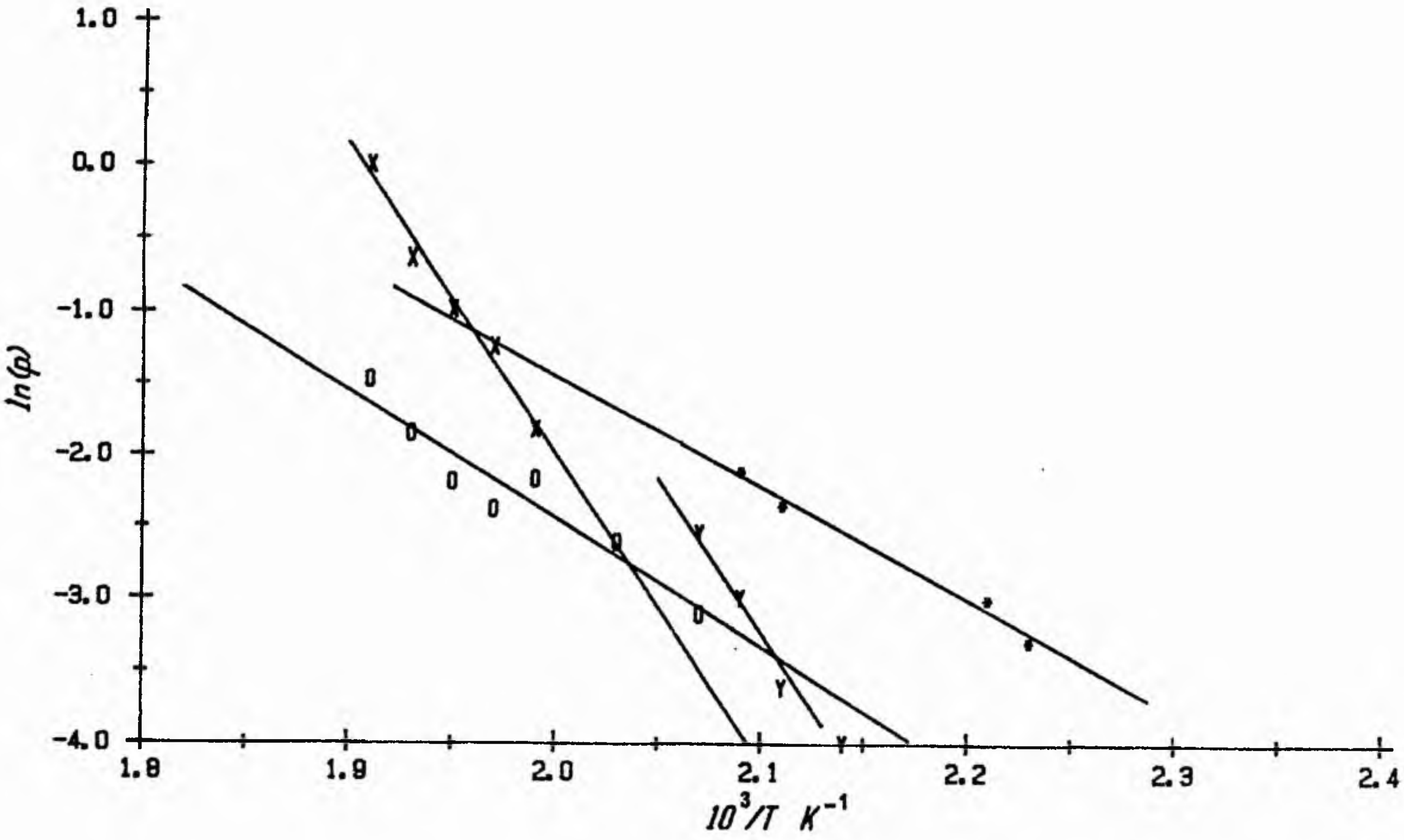

Figure 73

Comparative effect of ligand upon volatility of the Ni chelates

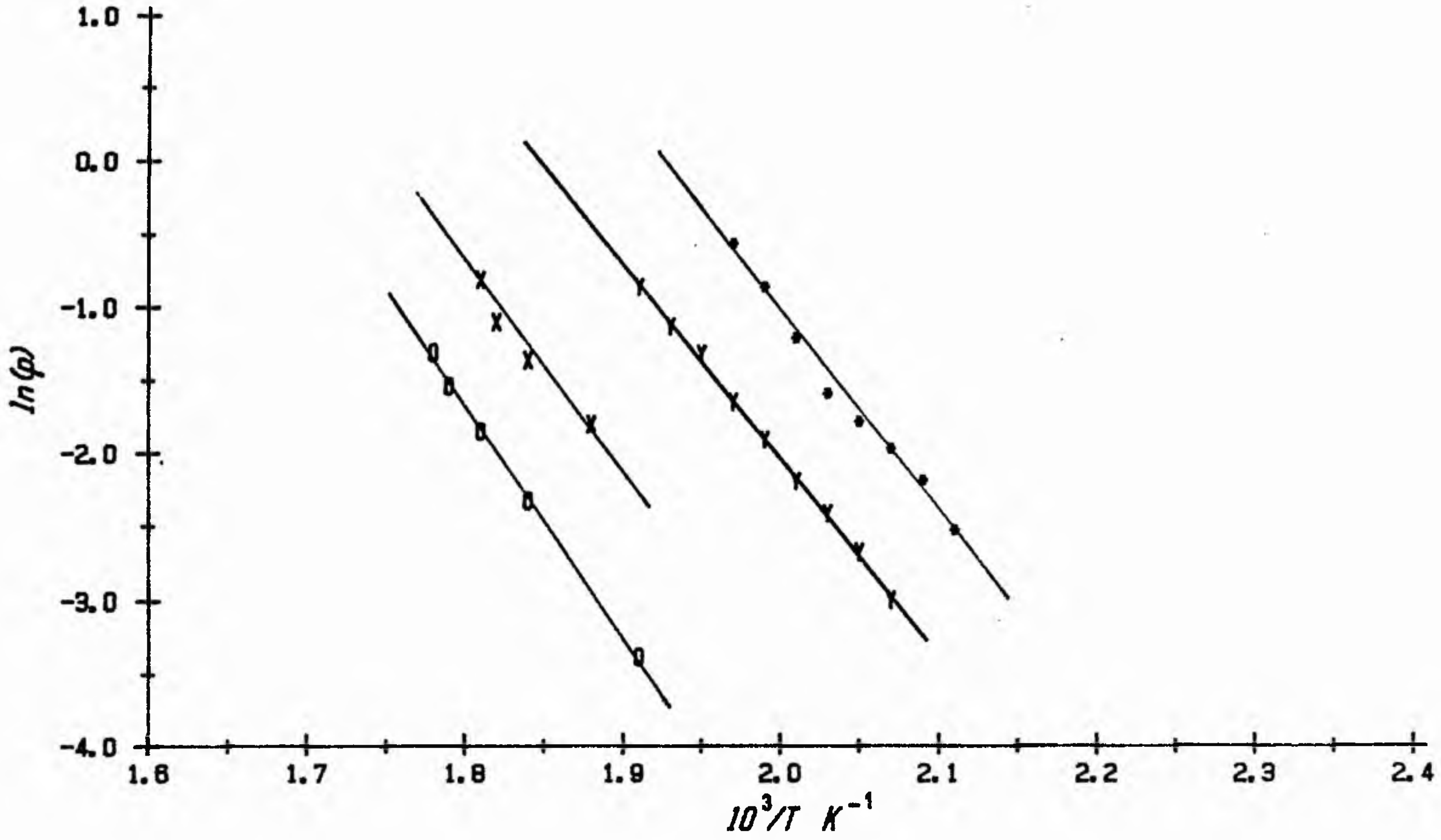

Figure 74

Comparative effect of ligand upon volatility of the Cu chelates

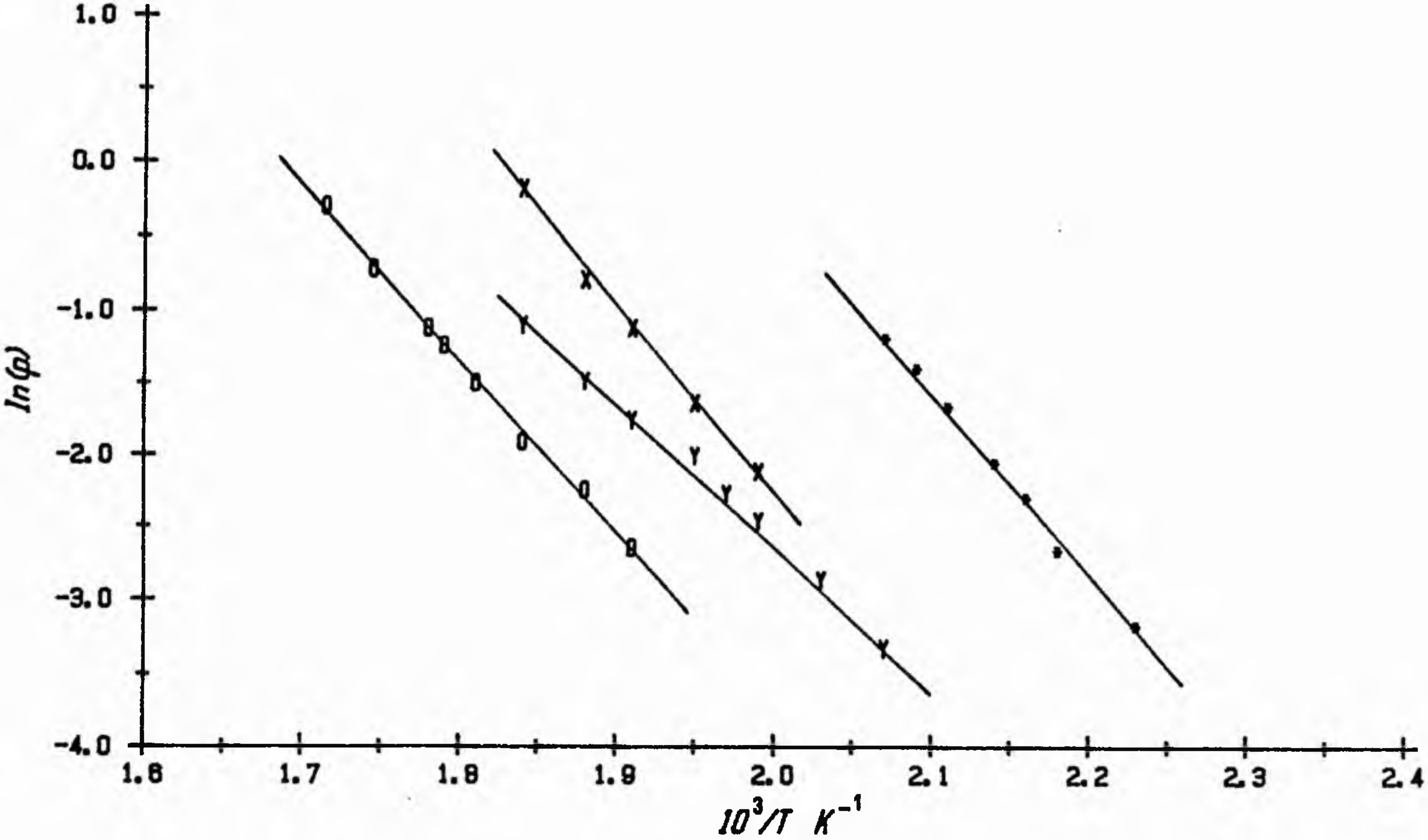

Figure 75

Comparative effect of ligand upon volatility of the Zn chelates

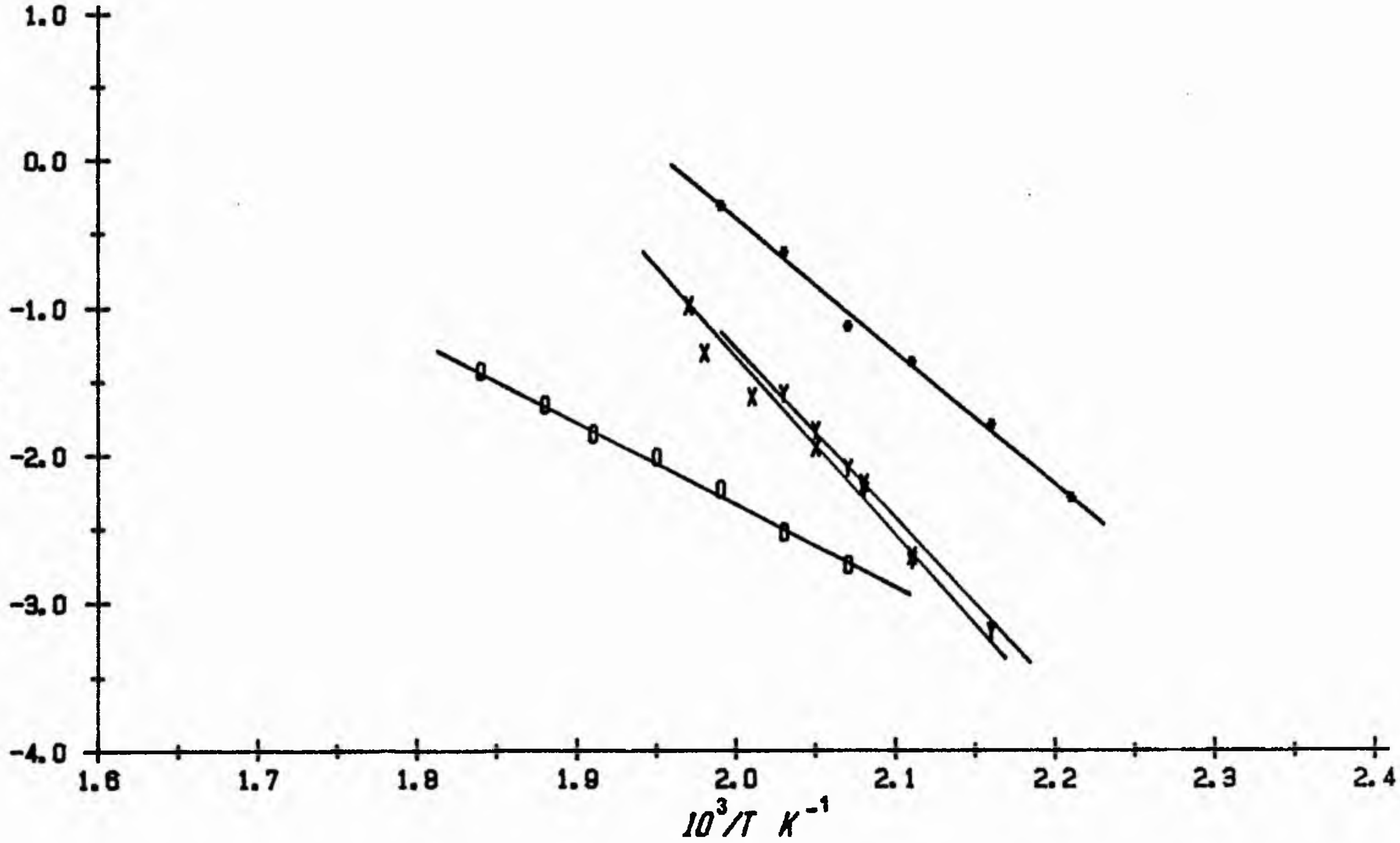

Figure 76

Comparative effect of ligand upon volatility of the Pb complexes

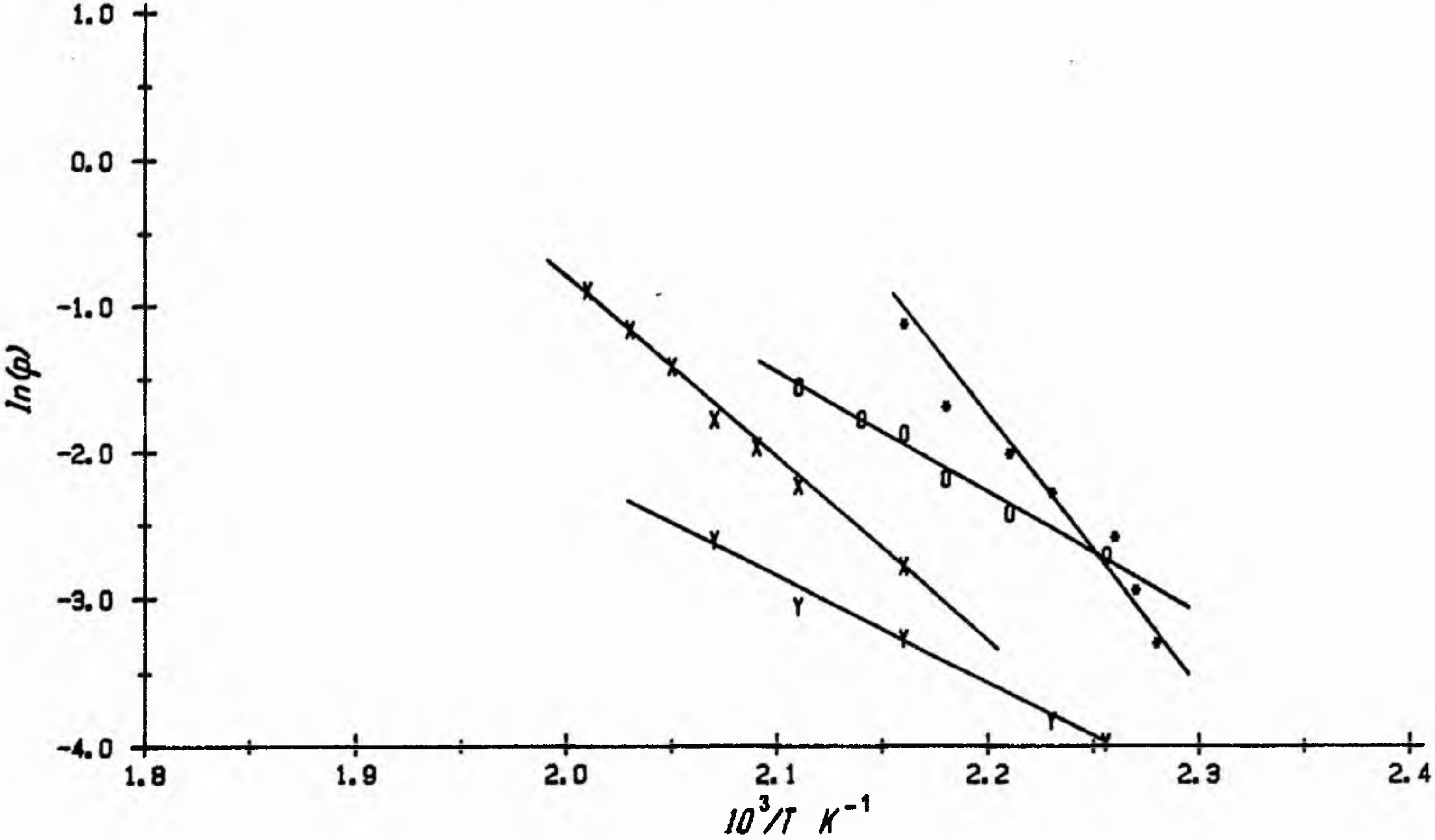

Figure 77

Comparative effect of ligand upon volatility of the Cd chelates

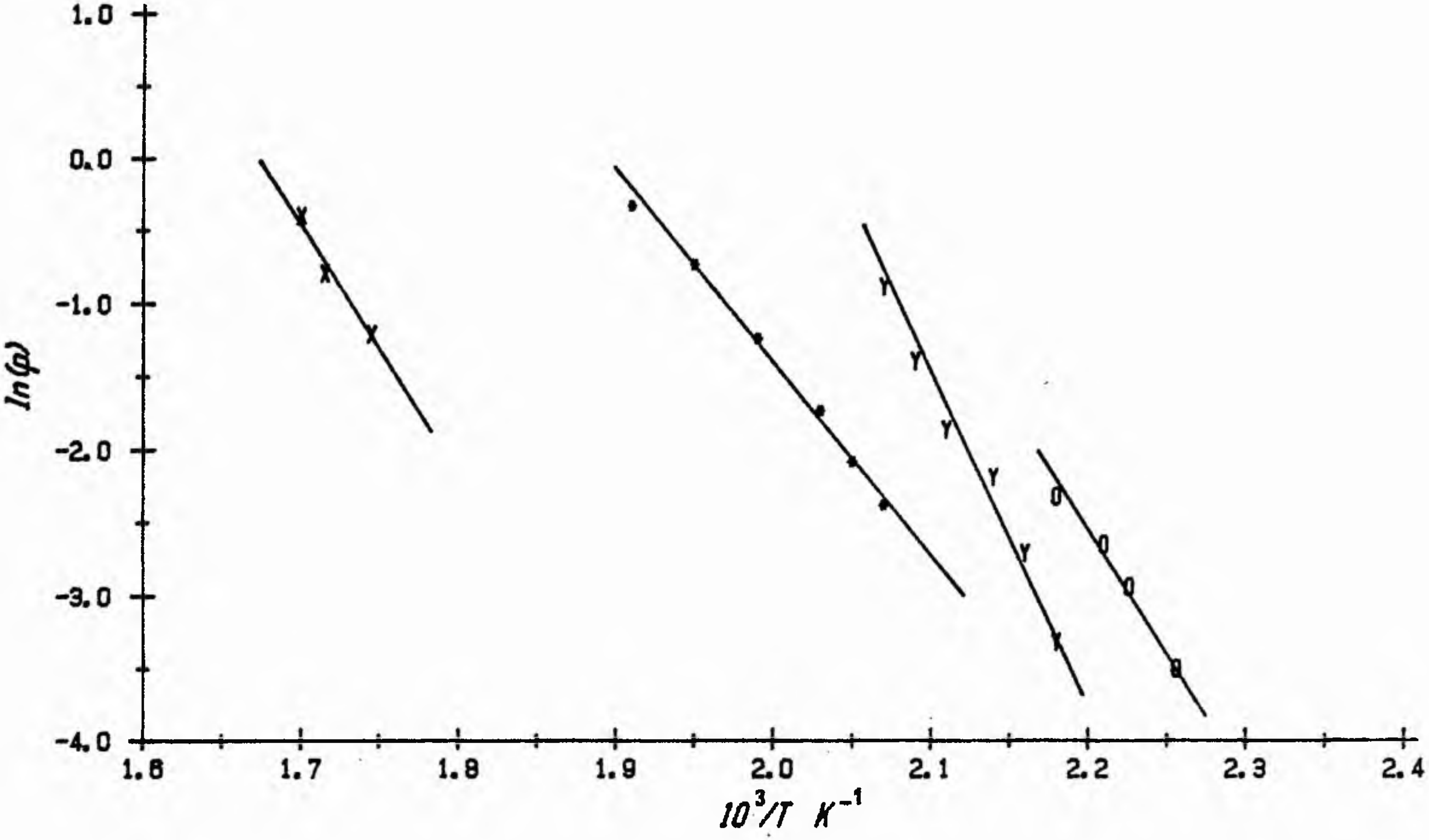

Figure 78

Comparative effect of ligand upon volatility of the Hg complexes

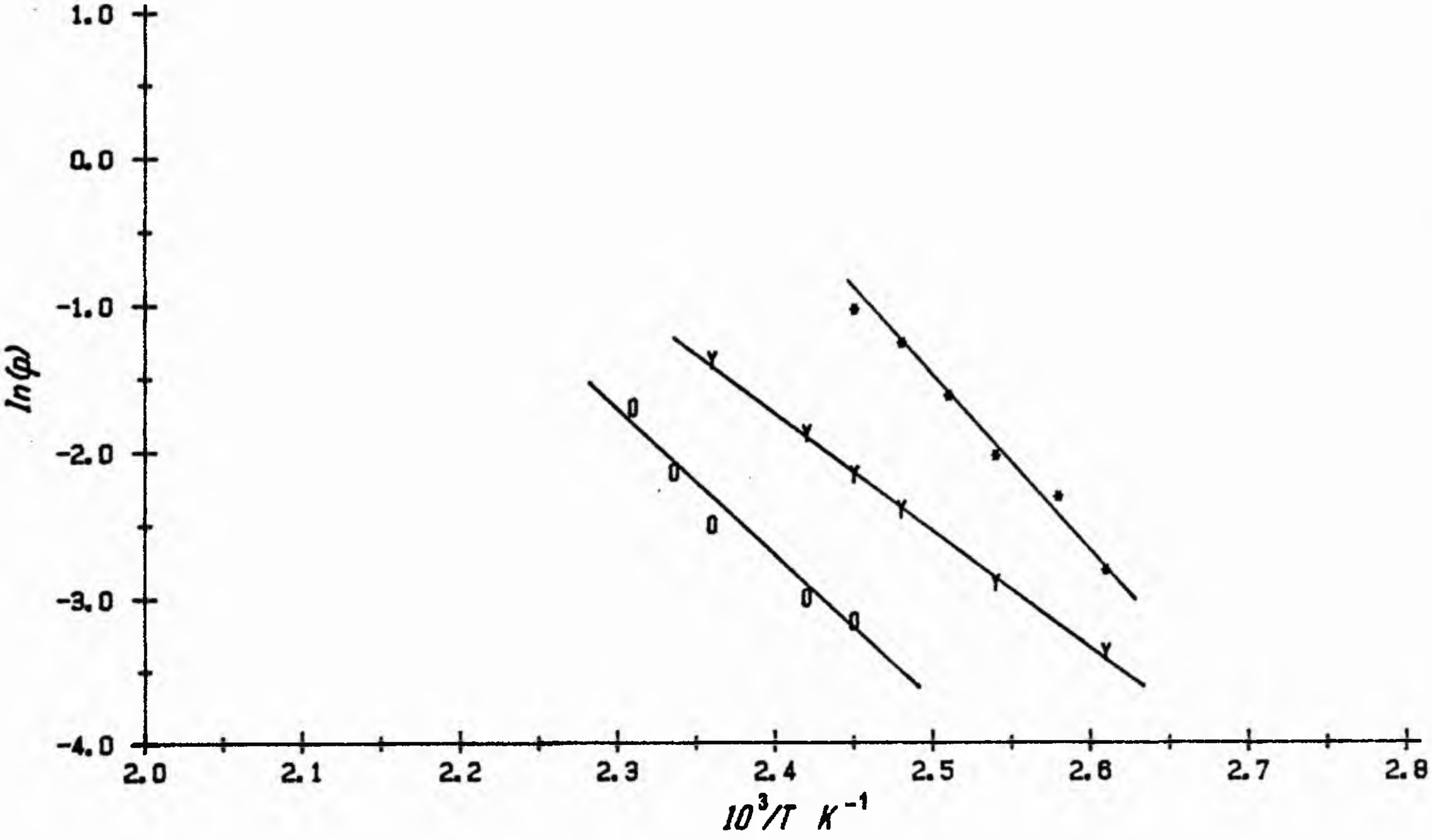

Figure 79

Chromatograms of $Mg(pfbtfa)_2$

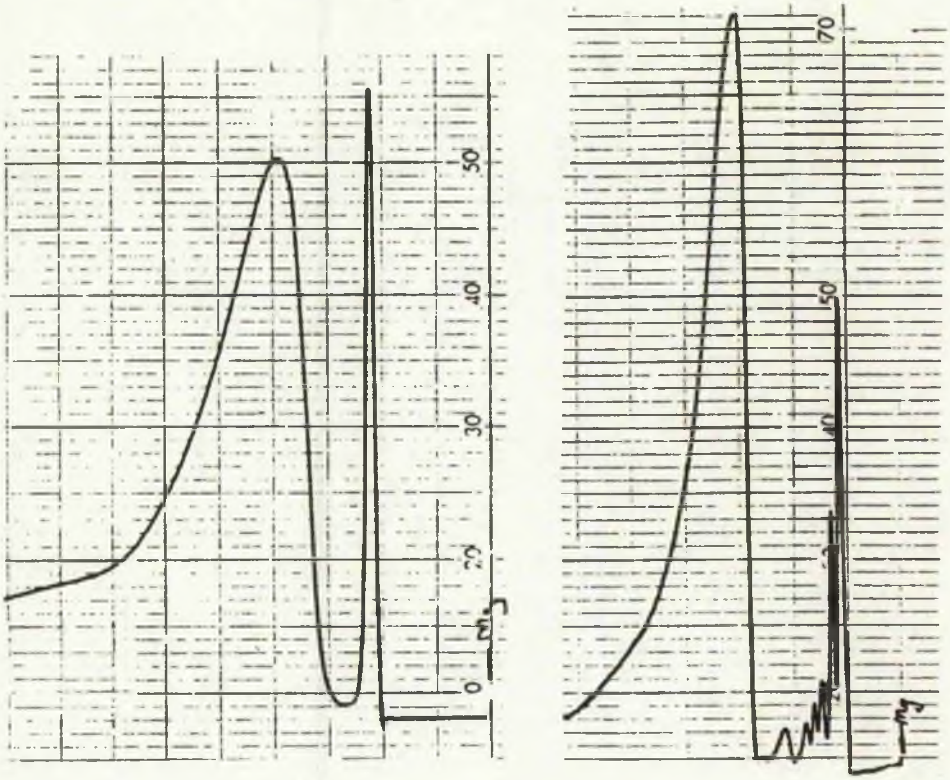

2½% OV 17 on Chromosorb G 80-100, oven 235°C, carrier 70 ml min^{-1}

10% SE 30 on Supasorb 60-80, oven 205°C, carrier 40 ml min^{-1}

Figure 80

Chromatogram of Ni(pfbtfa)$_2$

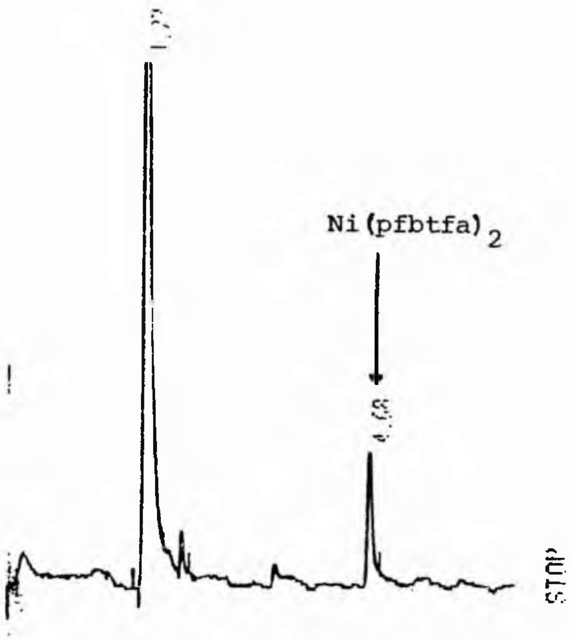

25m vitreous silica, 0.2mm id. SE 30, oven 130°C, carrier flow 25.7 cm min^{-1}, detector/injector 225°C.

Figure 81

MDQ chromatogram of $Zn(pfbtfa)_2$

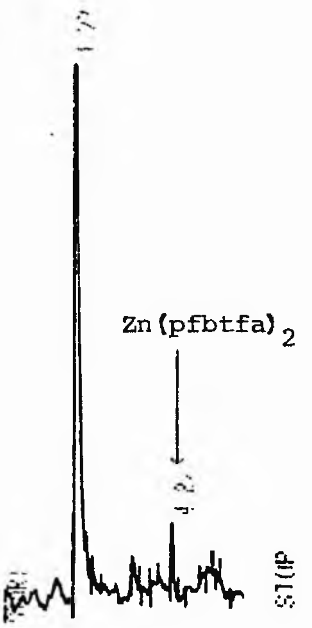

```
RUN #   26

AREA%
   RT        AREA TYPE    AR/HT      AREA%
  1.77      20305   PB    0.088     95.190
  4.27       1026   BB    0.065      4.810

TOTAL AREA=     21331
MUL FACTOR= 1.0000E+00
```

25m vitreous silica, 0.2mm i.d. SE 30, oven 130°C, carrier flow 25.7 cm min^{-1}, detector/injector 225°C.

Figure 82

Chromatograms of Cd,Hg and Ca,Ba pfbtfa chelate pairs

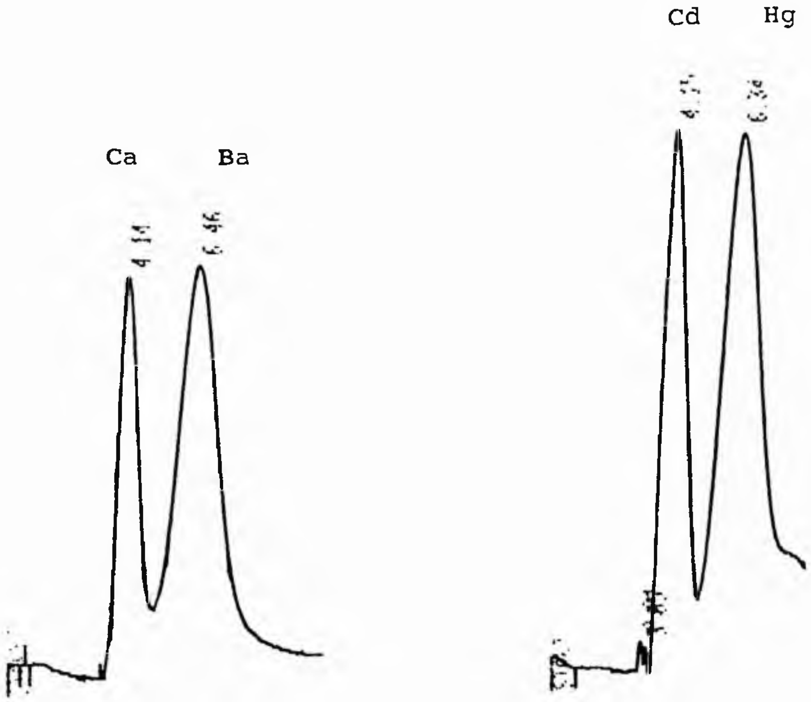

250mm Spherisorb ODS,60/40 MeOH/H_2O, 2 ml min^{-1}

TABLE 1

Essential elements for the Human diet (mg day^{-1})

Element	Deficient	Normal	Toxic
Ba	-	0.6-1.7	200
Ca	400	600-1400	-
Cd	-	0.007-0.3	3-330
Cu	0.3	0.5-6.0	-
Hg	-	0.004-0.02	0.4
K	-	1400-4700	6000
Li	-	0.1-2.0	90-200
Mg	12.0	250-300	-
Na	45.0	$(2-15)10^3$	-
Ni	0.0006	0.3-0.5	-
Pb	-	0.06-0.5	-
Se	0.006	0.006-0.2	5.0
Sr	-	0.8-5.0	-
Zn	5.0	5.0-40.0	150-600

TABLE 2

Metal content of dried Beckton sludge

Metal	Concentration (ppm)
Ca	40,089
Fe	17,005
Zn	4,705
Mg	4,151
Pb	1,450
Mn	800
Cu	780
Ni	300
Sr	175
Cd	76

Data from G.D.Christian et al Anal. Chem. 35 1128 (1963)

TABLE 3

Elements that can be directly volatilised

Matrix	Element	Temperature °C	Gas	Reference
ZnO	Cd	300/750	H_2/N_2	73
Al, Ga, In	Zn	1000/1150	H_2	279
Bauxite	Be	1000	O_2	280
Bauxite	Zn	1150	H_2	281
Cu	Se	1150	O_2	282
Rock	Bi, Cd, Tl	1000/1200	H_2/N_2	20
Si, SiO_2	B	190	HF/H_2O	25

TABLE 4

Elements that form volatile compounds with a reactant gas

Type of Compound	Elements that form volatiles (25-1000)°C
Chlorides	Ti,Zr,Hf,V,Nb,Ta Mo,W,Tc,Re,Mn,Fe,Ru,Os, Au,Zn,Pb,As,Sb,Bi,S,Se,Te,Po,Ce
Fluorides	Ti,Zr,Hf,V,Nb,Ta,Mo,W,Tc,Re,Ru,Os,Rh,Ir, Hg,Si,Ge,Sn,P,As,Sb,Bi,S,Se,Te
Oxides	S,Se, Te,Po,Tc,Re,Ru,Os,Zn,Cd,Hg
$AlCl_3$ complexes	Lanthanides, actinides, Ca,Sr,Ba,Ra,Fe, Co,Ni,Cu,Pd,Po,Mo
Hydrides	As,Se,Sn,Pb,Te,Sb,Bi
Elements	Noble gases, halogens, O,S,Se,Te,Po,N,P, As,Sb,Bi,Sn,Pb,Tl,Zn,Cd,Hg

TABLE 5

Comparison of Organic and Inorganic GC

	Organic GC	Inorganic GC
Temp. range	Up to 400°C	Up to 1000°C
Separation	Distribution, absorption	Distribution absorption (with complex formation)
Mobile phase	Inert	Reactive gases
Detector	Often non-selective	Selective
Identification	Usually retention time	Often by spectroscopy

TABLE 6

Compound	Stationary phase	Separated Elements	Detection	Ref
Fluorides	PTFE	Te,I,Mo	ECD	283
Chlorides	Fused salts $InCl_3/TlCl_3$	Te,I,Mo	ECD	283
Chlorides	Graphite LiCl/KCl	Nb,Ta,Zr,Hf	FPD	284
Bromides	Fused salts	Sn,P,Fe,Al	TCD	286
Iodides	Fused salts	Si,Ge,Ta,Nb	FPD	287
Oxides	Quartz	Ru,Te,Re,Os,Ir	Radiation	36
Metals	Charcoal	Mg,Cd,Zn	Pneumatic	285
Hydrides	Silica gel	As,Ge,Sb	PCD	34
Carbonyls	Apiezon L Squalane	Fe,Cr,W,Mo	TCD	57
$AlCl_3$-complexes	Glass	Lanthanides	Radiation	42

TABLE 7

Stationary phases for Inorganic GC

Stationary Phase	Separated Compounds	Reference
Silicone oil	$SnCl_4$,$GeCl_4$ $SiCl_4$,$TeCl_4$	288
PEG 1500	as above	"
Graphite	$NbCl_5$,$TeCl_4$	289
Quartz	$ZrCl_4$,$SbCl_3$	"
Silica Gel	$HfCl_4$,$ZrCl_4$	290
NaCl,KCl	$NbCl_5$,$TeCl_4$	289
NaBr,CsBr	$ZrBr_4$,$NbBr_5$	291
KBr/AgBr	SnBr,$TiBr_4$	287
$MgCl_2$/KCl	$BeCl_2$,$ZnCl_2$	288
$NaFeCl_4$	$SnCl_4$,$TiCl_4$	46
CdF_2 on $AlCl_3$	Aromatics Olefins	292
$MnCl_2$,$CoCl_2$ on silica gel	Aliphatics	293
NaOH on Al_2O_3	Aromatics	294

TABLE 8

Eutectic phases used in Inorganic GC

Phase			
A	B	mole % A	Temperature °C
CuCl	TlCl	60	122
TlCl	$BiCl_3$	32.5	150
$NaAlCl_4$		-	152
$NaFeCl_4$		-	158
$PbCl_3$	$FeCl_3$	37	177
$BiCl_3$	$PbCl_2$	"	215
$ZnCl_2$	AgCl	"	248
KCl	LiCl	49	352
$BaCl_2$	LiCl	33	510

TABLE 9

Enol content of some β-diketones (determined by ^1H NMR)

β-1,3-diketone	Solvent	% Enol	Reference
Acetylacetone	-	81	61
tfa	-	97	"
hfa	-	100	"
Benzoylacetone	CCl_4	100	"
Dibenzoylmethane	CCl_4	100	"
3-methylacac	-	30	68
fod	-	100	69
fhd	-	98	117
dpm	CCl_4	100	61
3-Br-acac	-	46	"
3-Cl-acac	-	94	"
tta	CS_2	100	"

TABLE 10

GC of chelates of Trifluoroacetylacetonates

Class 1	Class 2	Class 3
Be	Fe(111)	Nd(111)
Al	Mn(111)	
Ga	Zr	
Sc	Hf	
Cu	Zn	
Cr(111)		
V(1V)		
In		
Rh		

TABLE 11

Minimum detectable quantities of Al and Cr(111) chelates

Chelate	S/N Ratio	Metal detected (moles) (N_2 eluent)
$Cr(acac)_3$	10	2.5×10^{-10}
$Cr(tfa)_3$	4	1.8×10^{-13}
$Cr(hfa)_3$	7	4.9×10^{-14}
$Al(acac)_3$	17	1.6×10^{-7}
$Al(tfa)_3$	2	5.9×10^{-12}
$Al(hfa)_3$	2	7.4 x 10-13

Chelate	S/N Ratio	Metal detected (moles) (Ar eluent)
$Cr(acac)_3$	5	5.0×10^{-10}
$Cr(tfa)_3$	5	4.4×10^{-13}
$Cr(hfa)_3$	5	1.2×10^{-12}
$Al(acac)_3$	10	3.2×10^{-8}
$Al(tfa)_3$	9	2.8×10^{-11}
$Al(hfa)_3$	8	7.4×10^{-12}

TABLE 12

Comparison of FID and ECD detectors for metal chelate analysis

Chelate	FID	ECD
	Metal detected (moles) S/N 2	
$Cr(acac)_3$	1.2×10^{-10}	4.1×10^{-13}
$Cr(tfa)_3$	3.7×10^{-10}	3.1×10^{-15}
$Al(tfa)_3$	1.7×10^{-10}	1.2×10^{-13}
$Cu(tfa)_2$	1.6×10^{-10}	2.0×10^{-10}

TABLE 13

Minimum detectable quantities of chelates using capillary columns

Chelate	S/N Ratio	Metal detected (g)
$Be(tfa)_2$	2	4.0×10^{-14}
$Al(tfa)_3$	2	5.6×10^{-13}
$Cr(tfa)_3$	2	6.1×10^{-13}
$Cu(tfa)_2$	2	1.2×10^{-10}

TABLE 14

Minimum detectable quantities of selected dialkyldithiocarbamates

Chelate	ECD	NPD	FPD
Ni(DEDTC)$_2$	-	1.4	10.0
Co(DEDTC)$_3$	-	1.1	8.5
Ni(FDEDTC)$_2$	0.5	1.2	9.0
Co(FDEDTC)$_3$	0.2	0.8	7.0

Units for ECD in g x 10^{-12}

Units for NPD in gN sec^{-1} x 10^{-12}

Units for FPD in gS sec^{-1} x 10^{-11}

TABLE 15

HCl catalyst concentrations necessary for the preparation of β-thioketones

1,3-diketone	% Enol (EtOH)	Conc. of HCl at -10°C
Me-COCH$_2$CO-OEt	13	Very dilute
ϕ-COCH$_2$CO-OEt	27	"
Me-COCH$_2$CO-Me	84	dilute
ϕ-COCH$_2$CO-Me	94	Concentrated
ϕ-COCH$_2$CO-O	90 - 100	"
Thenoyltrifluoracetone	100	Supersaturated

TABLE 16

Monothio-β-diketones for the GC of metal chelates

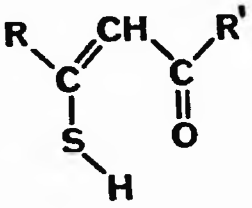

R'	R'	Name	Abbreviation
Me	Me	Monothioacetylacetone	H(t-acac)
Me	t-butyl	Monothioacetylpivalylmethane	H(t-apm)
Me	CF_3	Monothiotrifluoroacetylacetone	H(t-tfa)
CF_3	CF_3	Monothiohexafluoroacetylacetone	H(t-hfa)
CF_3	t-butyl	Monothiotrifluoroacetylpivalylmethane	H(t-tpm)

TABLE 17

Minimum detectable quantities of some monothio-β-diketonates

Chelate	Metal detected (g)
$Co(t\text{-}tfa)_2$	1.0×10^{-5}
$Ni(t\text{-}tfa)_2$	5.0×10^{-7}
$Zn(t\text{-}tfa)_2$	7.0×10^{-6}
$Pd(t\text{-}tfa)_2$	8.0×10^{-7}
$Pt(t\text{-}tfa)_2$	1.0×10^{-6}

TABLE 18

β-Ketoamines used in the GC of metal chelates

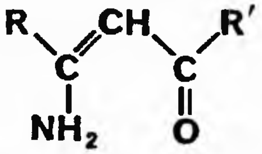

R	R'	Name	Abbreviation
Me	Me	Aminoacetylacetone	H(ap)
Me	CF_3	Aminotrifluoroacetylacetone	H(a-tfa)
Me	t-butyl	Aminoacetylpivalylmethane	H(a-apm)
CF_3	t-butyl	Aminotrifluoroacetylpivalylmethane	H(a-tpm)

TABLE 19

Tetradentate-β-Ketoamines used in metal chelate GC

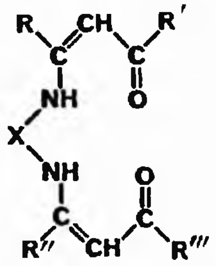

R	R'	R"	R"'	X	Abbreviation
Me	Me	Me	Me	en	H_2(en-AA_2)
Me	Me	Me	Me	pn	H_2(pn-AA_2)
Me	Me	Me	Me	bn	H_2(bn-AA_2)
CF_3	Me	Me	CF_3	en	H_2(en-TFA_2)
CF_3	Me	Me	CF_3	pn	H_2(pn-TFA_2)
CF_3	Me	Me	CF_3	bn	H_2(bn-TFA_2)
CF_3	Me	Me	Me	en	H_2(en-AA-TFA)
CF_3	Me	Me	Me	pn	H_2(pn-AA-TFA)
CF_3	Me	Me	Me	bn	H_2(bn-AA-TFA)

en = $CH_2 - CH_2$ pn = $CH(CH_3) - CH_2$ bn = $CH(CH_3) - CH(CH_3)$

TABLE 20

Chemical shifts (ppm) for some tetravalent β-diketonates

	In CCl_4			In $CDCl_3$		
Chelate	$-CH=$	$-CH_3$	$-CF_3$	$-CH=$	$-CH_3$	$-CF_3$
H(tfa)	5.88	2.21	3.89	5.92	2.22	3.93
$Zr(tfa)_4$	5.97	2.19	2.85	5.99	2.15	2.91
$Hf(tfa)_4$	5.95	2.18	3.01	5.97	2.15	3.05
$Ce(tfa)_4$	5.80	2.20	2.37	5.81	2.16	2.43
$Th(tfa)_4$	5.93	2.20	2.96	5.93	2.15	3.02
H(acac)	5.39	1.99	-	5.51	2.04	-
$Zr(acac)_4$	5.37	1.90	-	5.48	1.92	-
$Hf(acac)_4$	5.34	1.89	-	5.46	1.92	-
$Ce(acac)_4$	5.21	1.89	-	5.31	1.91	-
$Th(acac)_4$	5.34	1.91	-	5.44	1.93	-

^1H and ^{19}F shifts are relative to TMS and $Rh(tfa)_3$ respectively

TABLE 21

Values of ν(C-O), ν(C-C) and ν(M-O) for some metal chelates cm^{-1}

Chelate	ν(C-O)	ν(C-C)	ν(M-O)	Reference
Na(acac)	1622	-	405	205
K(acac)	1630	-	410	"
Cu(acac)$_2$	1540	1580	455	207
Ni(acac)$_2$	1598	1598	452	"
Na(bza)	1590	-	425	215
K(bza)	1590	-	424	"
Eu(bza)$_4$	1600	1520	400	295
Cu(bza)$_2$	1554	1520	485	207
Ni(bza)$_2$	1591	1593	455	207
Cu(dbzm)$_2$	1544	1593	462	207
Ni(dbzm)$_2$	1595	1595	458	207
Eu(dbzm)$_2$	1600	1520	405	295
Cu(tfa)$_2$	1600	1611	445	207
Ni(tfa)$_2$	1621	1639	427	207
Cu(hfa)$_2$	1614	1644	415	207
Ni(hfa)$_2$	1613	1643	397	207
Mg(acac)$_2$	1615	-	-	205
Cd(acac)$_2$	1613	-	-	"
Mn(acac)$_2$	1607	-	-	"

TABLE 22

Polarographic data for some copper chelates

Aliphatic - aliphatic terminal substitution

R'	R"	$E_{\frac{1}{2}}$(V)
CF_3	CF_3	+0.038
CH_3	CF_3	-0.169
t-butyl	CF_3	-0.346
Me	Me	-0.502
t-butyl	Me	-0.600
t-butyl	t-butyl	-0.687

Aliphatic - aromatic terminal substitution

CF_3	2-C_4H_3O	-0.130
CF_3	2-C_4H_3S	-0.137
CF_3	C_6H_5	-0.150
CH_3	2-C_4H_3O	-0.341
CH_3	2-C_4H_3S	-0.317
CH_3	C_6H_5	-0.381

Aromatic - aromatic terminal substitution

2-C_4H_3O	2-C_4H_3O	-0.288
C_6H_5	C_6H_5	-0,379

Values of $E_{\frac{1}{2}}$ measured against SCE. Solutions in 75% Dioxan/H_2O with KNO_3 support electrolyte.

TABLE 23

Polarographic data for Ruthenium chelates

Chelate	$E_{\frac{1}{2}}$(V)
$Ru(hfa)_3$	+0.726
$Ru(bta)_3$	+0.104
$Ru(tfa)_3$	-0.016
$Ru(dbzm)_3$	-0.501
$Ru(bza)_3$	-0.593
$Ru(acac)_3$	-0.728
$Ru(dpm)_3$	-1.038

Values of $E_{\frac{1}{2}}$ measured against SCE, in DMF at 25°C

TABLE 24 A

Analytical data for the p-Me-bta chelates

			Metal content %		
	M.p. °C	Colour	Calc.	Fnd.	Formula
Li	220 d	Cream	2.94	2.93	ML
Na	190 d	Cream	9.12	9.14	ML
K	150 d	Cream	14.58	14.36	ML
Mg	182	White	4.69	4.61	$ML_2.2H_2O$
Ca	163	White	7.50	7.81	$ML_2.2H_2O$
Sr	240 d	White	15.06	15.11	$ML_2.2H_2O$
Ba	215 d	White	21.75	21.63	$ML_2.2H_2O$
Ni	173	Green	10.62	10.74	$ML_2.2H_2O$
Cu	233	Green	11.40	11.59	$ML_2.2H_2O$
Zn	147	White	11.69	12.25	$ML_2.2H_2O$
Pb	206	Cream	31.15	32.0	ML_2
Cd	116	White	18.54	19.01	$ML_2.2H_2O$
Hg	104	White	43.74	44.24	$ML_2.MOAc$

TABLE 24 B

Analytical data for the bta chelates

	M.p.°C	Colour	Metal content % Calc.	Fnd.	Formula
Li	230 d	White	3.13	3.16	ML
Na	200 d	White	9.66	9.70	ML
K	205 d	Cream	15.39	15.56	ML
Mg	186	White	4.96	4.89	$ML_2.2H_2O$
Ca	126	White	7.92	8.03	$ML_2.2H_2O$
Sr	174 d	White	15.83	15.92	$ML_2.2H_2O$
Ba	221 d	White	22.76	22.52	$ML_2.2H_2O$
Ni	160	Green	11.19	11.74	$ML_2.2H_2O$
Cu	224	Green	12.00	11.90	$ML_2.2H_2O$
Zn	129	White	12.30	11.58	$ML_2.2H_2O$
Pb	188	White	32.52	32.80	ML_2
Cd	125	White	19.43	19.07	$ML_2.2H_2O$
Hg	167	White	-	33.33	-

TABLE 24 C

Analytical data for the pfbtfa chelates

	M.p.°C	Colour	Metal content % Calc.	Metal content % Fnd.	Formula
Li	238	Cream	2.22	2.22	ML
Na	206	Cream	9.66	9.70	ML
K	172	Cream	11.36	11.06	ML
Mg	153	White	3.63	3.74	$ML_2.2H_2O$
Ca	103	White	5.84	5.70	$ML_2.2H_2O$
Sr	155	White	11.94	12.00	$ML_2.2H_2O$
Ba	205	White	17.53	17.45	$ML_2.2H_2O$
Ni	152	Green	8.33	8.50	$ML_2.2H_2O$
Cu	82	Green	8.95	9.05	$ML_2.2H_2O$
Zn	113	White	10.88	10.23	$ML_2.2H_2O$
Pb	152	White	25.35	25.75	ML_2
Cd	113	White	14.82	15.10	$ML_2.2H_2O$
Hg	158	White	24.75	24.91	ML_2

TABLE 24 D

Analytical data for the pfbhfh chelates

	M.p.°C	Colour	Metal content % Calc.	Metal content % Fnd.	Formula
Li	126	White	1.68	1.69	ML
Na	150 d	White	5.37	5.45	ML
K	157 d	White	8.80	8.54	ML
Mg	146	White	2.79	2.99	$ML_2.2H_2O$
Ca	—	—	—	—	—
Sr	155	White	9.38	9.56	$ML_2.2H_2O$
Ba	200 d	White	13.97	14.14	$ML_2.2H_2O$
Ni	140	Green	6.49	6.67	$ML_2.2H_2O$
Cu	102	Green	6.99	7.15	$ML_2.2H_2O$
Zn	119	White	7.17	7.53	$ML_2.2H_2O$
Pb	224	White	20.37	20.92	ML_2
Cd	118	White	11.73	11.93	$ML_2.2H_2O$
Hg	138	White	19.85	19.63	ML_2

TABLE 25

Acid dissociation constants of p-Me-bta, bta, pfbtfa and pfbhfh at varying solution mole fraction dioxan content.

% Dioxan content (mole fraction)

1,3-diketone	82% (0.482)	75% (0.380)	70% (0.323)	45% (0.143)
p-Me-bta	10.58 ± 0.26	9.67 ± 0.06	9.02 ± 0.06	6.86 ± 0.25
bta	10.15 ± 0.32	9.16 ± 0.03	8.57 ± 0.01	6.60 ± 0.08
pfbtfa	6.85 ± 0.02	5.68 ± 0.06	5.17 ± 0.09	3.49 ± 0.03
pfbhfh	6.67 ± 0.19	5.37 ± 0.18	4.77 ± 0.19	-

TABLE 26

Regression constant data to the equation $pK_a = a(f_2) + b$

1,3-diketone	Correlation coefficient	a	b
p-Me-bta	0.997	11.11 ± 0.56	5.34 ± 0.20
bta	0.999	10.52 ± 0.23	5.13 ± 0.01
pfbtfa	0.998	9.80 ± 0.39	2.04 ± 0.14
pfbhfh	0.999	12.04 ± 0.57	0.85 ± 0.23

TABLE 27

Formation constant data for chelates of p-Me-bta

Metal	log K_1	log K_2	log β
Mg	9.62	9.08	18.70
Ca	9.18	8.85	18.03
Sr	8.82	8.44	17.26
Ba	8.62	8.30	16.92
Ni	11.13	10.47	21.60
Cu	11.66^E	11.69	23.35
Zn	10.56	9.67	20.23
Pb	10.08	9.56	19.64
Cd	9.71	9.12	18.83

E: denotes estimated value

TABLE 28

Formation constant data for chelates of bta

Metal	log K_1	log K_2	log β
Mg	8.22	7.50	15.72
Ca	7.87	7.39	15.26
Sr	7.37	6.95	14.32
Ba	7.26	6.82	14.08
Ni	9.65	9.11	18.76
Cu	11.34^{E}	10.06	21.40
Zn	8.97	8.31	17.28
Pb	8.24	7.73	15.97

E: denotes estimated value

TABLE 29

Formation constant data for chelates of pfbtfa

Metal	log K_1	log K_2	logβ
Mg	5.73	5.37	11.10
Ca	5.99	-	-
Sr	5.60	5.25	10.85
Ba	5.44	5.22	10.66
Ni	6.30	5.97	12.27
Cu	6.47^E	6.39	12.86
Zn	5.81	5.31	11.12
Pb	5.62	5.23	10.85
Cd	5.51	5.03	10.54

E: denotes estimated value

TABLE 30

Formation constant data for chelates of pfbhfh

Metal	log K_1	log K_2	logβ
Mg	4.70	4.32	9.02
Ca	4.58	-	-
Sr	4.30	3.85	8.15
Ba	4.20	3.77	7.97
Ni	5.16^E	5.14	10.30
Cu	4.86^E	4.87	9.73
Zn	4.74^E	4.63	9.37
Pb	4.79	4.58	9.37
Cd	4.64	4.34	8.98

E: denotes estimated value

TABLE 31

Methine and enolic proton resonance positions for p-Me-bta, bta, pfbtfa and pfbhfh.

β-diketone	Resonance position (ppm)					
	CCl_4		$CDCl_3$		^{6}D-Acetone	
	-CH=	-OH	-CH=	-OH	-CH=	-OH
p-Me-bta	6.46	15.04	6.50	14.62	6.89	12.12
bta	6.48	15.03	6.51	14.85	6.88	13.68
pfbtfa	6.24	14.40	6.30	13.97	6.52	12.70
pfbhfh	6.30	14.30	6.39	13.89	6.66	12.55

TABLE 32

Resonance position of metal chelate α-H (ppm) in ^{6}D-acetone

Metal	bta	p-Me-bta	pfbtfa	hfh
Li	6.26	6.19	5.63	5.76
Na	6.08	6.05	5.39	5.55
K	5.93	5.95	5.30	5.38
Mg	6.27	6.28	5.84	5.97
Ca	6.25	6.19	5.66	-
Sr	6.21	6.19	5.70	5.70
Ba	6.16	6.15	5.61	5.56
Ni	-	-	-	-
Cu	-	-	-	-
Zn	6.48	6.44	5.90	5.94
Pb	6.20	6.17	5.75	5.42
Cd	6.32	6.30	5.57	5.88

TABLE 33

Values of $E\frac{1}{2}$ for Ni, Cu, Zn chelates in 75% Dioxan-H_2O solution

	-E(V)		
Ligand	Ni	Cu	Zn
acac	1.03	0.63	1.24
tfa	0.92	0.48	1.33
hfa	-	0.16	-
bza	0.96	0.54	1.32
tta	0.90	0.28	1.15
p-Me-bta	0.93	0.23	1.18
bta	0.93	0.38	1.15
pfbtfa	0.99	0.24	1.16
pfbhfh	0.79	0.08	1.13

TABLE 34

Values of λ_{max} and ϵ_{max} for p-Me-bta, bta, pfbtfa and pfbhfh in MeOH.

β-diketone	λ_{max}(nm)	ϵ_{max}(dm^3 mol^{-1} cm^{-1})
p-Me-bta	327	9000
bta	324	10,300
pfbtfa	309	15,400
pfbhfh	314	13,300

TABLE 35

Values of λ_{max}(nm) (in MeOH) for the studied metal chelates

	p-Me-bta	bta	pfbtfa	pfbhfh
Li	324	321	309	311
Na	321	321	309	312
K	321	322	308	312
Mg	325	322	310	313
Ca	323	324	309	—
Sr	325	323	309	314
Ba	323	324	310	315
Ni	330	330	318	324
Cu	326	327	314	318
Zn	320	320	313	314
Pb	329	327	312	314
Cd	324	324	310	313
Hg	261	249	312	314

TABLE 36

Values of ϵ_{max} ($dm^3\ mol^{-1}\ cm^{-1}$) (in MeOH) for the studied metal chelates

	p-Me-bta	bta	pfbtfa	pfbhfb
Li	16,700	16,600	17,300	16,200
Na	9,200	10,800	14,200	15,000
K	16,000	12,500	14,200	16,700
Mg	36,800	32,200	32,600	31,800
Ca	35,300	21,600	17,000	—
Sr	34,700	30,500	31,500	26,600
Ba	34,500	32,200	32,500	25,700
Ni	32,700	27,400	25,500	21,800
Cu	36,200	32,100	26,400	22,200
Zn	39,100	34,600	30,400	31,200
Pb	30,300	28,900	27,200	33,900
Cd	39,200	32,500	30,500	31,600
Hg	22,100	—	25,100	17,200

TABLE 37

Positions of ν(C-O) for the studied ligands and metal chelates (cm^{-1})

	p-Me-bta	bta	pfbtfa	pfbhfh
Li	1620	1628	1635	1635
Na	1625	1625	1640	1635
K	1640	1635	1635	1640
Mg	1618	1622	1635	1615
Ca	1622	1635	1640	–
Sr	1630	1633	1635	1640
Ba	1620	1625	1635	1640
Ni	1610	1615	1620	1600
Cu	1595	1605	1602	1600
Zn	1612	1610	1635	1600
Pb	1605	1605	1610	1642
Cd	1610	1610	1620	1602
Ligand	- , 1610	- , 1605	1642, 1600	1640, 1598

TABLE 38

Positions of ν(M-O) for the Ni, Cu, Zn chelates (cm^{-1})

Ligand	Ni	Cu	Zn
p-Me-bta	468	472	464
bta	446	448	439
pfbtfa	419	421	410
pfbhfh	406	407	378

TABLE 39

Values of ΔH KCal mol^{-1}

	p-Me-bta	bta	pfbtfa	pfbhfh
Li	45.5 ± 1.1	61.8 ± 9.0	90.8 ± 5.5	58.4 ± 7.4
Na	29.2 ± 2.4	54.5 ± 3.7	68.9 ± 4.6	50.9 ± 3.6
K	26.4 ± 1.0	68.9 ± 2.6	36.6 ± 2.0	33.3 ± 0.1
Mg	25.5 ± 1.3	64.7 ± 4.7	39.2 ± 2.3	26.2 ± 0.6
Ca	18.3 ± 0.8	27.8 ± 0.7	45.2 ± 2.4	–
Sr	23.0 ± 0.4	42.0 ± 1.3	80.6 ± 1.4	41.8 ± 0.3
Ba	17.6 ± 2.5	42.6 ± 3.8	12.4 ± 7.8	46.5 ± 3.2
Ni	30.6 ± 0.3	51.5 ± 9.9	27.1 ± 1.2	26.4 ± 0.4
Cu	23.6 ± 0.5	33.4 ± 4.4	25.4 ± 0.7	18.5 ± 0.7
Zn	11.3 ± 0.3	21.6 ± 1.6	20.0 ± 6.6	25.2 ± 1.2
Pb	16.5 ± 1.1	25.3 ± 0.8	31.5 ± 2.6	14.5 ± 0.7
Cd	31.7 ± 3.9	34.6 ± 5.9	25.5 ± 1.0	41.1 ± 2.8
Hg	17.7 ± 2.1	-	21.8 ± 1.1	15.7 ± 0.5

TABLE 40

Values of ΔS Cal mol^{-1} K^{-1}

	p-Me-bta	bta	pfbtfa	pfbhfh
Li	84.5 ± 2.0	105.7 ± 15.8	182.4 ± 11.1	119.5 ± 15.5
Na	58.9 ± 5.1	107.6 ± 7.6	145.7 ± 9.8	104.0 ± 7.6
K	53.4 ± 2.1	137.6 ± 5.3	81.0 ± 4.6	70.8 ± 0.3
Mg	47.7 ± 2.5	131.6 ± 9.7	78.7 ± 4.9	48.0 ± 1.2
Ca	31.1 ± 1.6	53.3 ± 1.4	94.9 ± 5.1	-
Sr	41.3 ± 0.7	80.6 ± 2.5	72.6 ± 7.5	82.4 ± 0.7
Ba	30.4 ± 5.0	81.2 ± 7.4	21.2 ± 16.7	91.2 ± 6.7
Ni	51.8 ± 0.5	91.9 ± 18.3	52.1 ± 2.5	48.7 ± 0.8
Cu	39.8 ± 0.9	61.3 ± 8.6	50.3 ± 1.5	31.8 ± 1.4
Zn	17.9 ± 0.6	40.4 ± 3.3	39.0 ± 13.8	48.0 ± 2.5
Pb	31.7 ± 2.3	49.0 ± 1.7	65.7 ± 5.8	24.8 ± 1.6
Cd	64.4 ± 8.6	57.9 ± 10.1	48.1 ± 2.0	83.3 ± 5.9
Hg	34.5 ± 4.6	-	51.6 ± 2.9	34.1 ± 1.2

TABLE 41

Temperatures necessary to achieve a chelate vapour pressure of 0.1 mm Hg (^{o}C)

	p-Me-bta	bta	pfbtfa	pfbhfh
Li	238	287	213	198
Na	188	213	185	196
K	182	212	155	169
Mg	215	202	198	225
Ca	241	207	181	-
Sr	228	220	182	207
Ba	231	224	210	212
Ni	271	261	205	222
Cu	259	233	190	235
Zn	229	208	186	206
Pb	181	199	176	222
Cd	187	281	210	195
Hg	180	-	116	132

TABLE 42

Minimum detectable quantities (MDQ) of the pfbtfa chelates

Metal	MDQ (g of metal)
Mg	3.7×10^{-13}
Ca	3.4×10^{-11}
Sr	7.9×10^{-13}
Ba	2.7×10^{-12}
Ni	6.2×10^{-13}
Cu	5.1×10^{-13}
Zn	3.2×10^{-13}
Pb	1.5×10^{-12}
Cd	9.5×10^{-11}
Hg	5.6×10^{-13}

25m vitreous silica coated with SE30. Detector/injector 225°C, oven 130°C, N_2 carrier 25.7cm sec^{-1}, ECD detector.

7.

Bibliography

1 F.H.Nielsen et al

J Nutrition 105 1607 (1972)

2 D.L.Hachey et al

Anal Chem 52 1131 (1980)

3 T.Okajima et al

Int J Neurology 11 62 (1976)

4 R.M.Harrison and D.P.H.Laxen

Chem in Britain 16 316 (1980)

5 R.G.MacLaren et al

J Soil Science 24 172 (1973)

6 F.E.Mosey

Water Pollution Control 70 (5) (1971)

7 R.E.Brown

J Water Poll Control Fed 47 (12) (1975)

8 Water Research Centre

Research programme 1981/2

9 M.V.Chesshire et al

'The Composition of Soil Humus'

10 J.O.Evans

Compost Science 14 16 (1973)

11 A.L.Page

'Fate and effects of trace elements in sewerage sludge when applied to agricultural land' US Dept Commerce (1974)

12 H.J.M.Bowen

'Environmental chemistry of the elements'

Academic Press (London) (1979)

13 D.M.Coleman et al

Environmental Sci Technol 6 452 (1972)

14 J.M.Hemsley

Water Pollution Control 70 611 (1971)

15 J.D.Winefordner et al

Anal Chem 44 150R (1972)

16 E.B.Sandell

'Colorimetric determination of traces and metals'

Inter Science 3rd Ed. (1965)

17 J.B.Andelman

J Water Poll Control Fed 40 1844 (1968)

18 T.B.Pierce

Sel Ann Rev Anal Sci 1 133 (1971)

19 W.Geilmann

Z Anal Chem 160 410 (1958)

20 H.Heinrichs

ibid 294 345 (1979)

21 K.Bachmann

Talanta 29 1 (1982)

22 K.Bachmann et al

GSI Report J 1 - 77

23 W.Geilmann and H.Hepp

Z Anal Chem 200 291 (1964)

24 C.Spachidis and K.Bachmann

ibid 300 343 (1980)

25 C.Spachidis et al

ibid 306 268 (1981)

26 N.Ya.Chalkov et al

Zh Analit Khim 28 678 (1973)

27 G.Tolg

Inter Microchemical Sym, Graz Paper 117 (1980)

28 F.Dienstbach and K.Bachmann

Anal Chem 52 620 (1980)

29 A.Farzaneh and G.Troll

Geochem J 11 177 (1977)

30 M.Burguera and A.Townsend

Anal Chim Acta 117 247 (1980)

31 A.Farzaneh and G.Troll

Z Anal Chem 292 293 (1973)

32 M.Biehl and K.Bachmann

Mikrochim Acta 11 357 (1980)

33 E.Jackwerth and P.G.Willmer

Spectrochim Acta 33B 343 (1978)

34 R.K.Skogerboe and A.P.Bejmuk

Anal Chim Acta 94 297 (1977)

35 K.Bachmann and J.Rudolph

J Radioanal Chem 32 243 (1976)

36 A.Steffen and K.Bachmann

Talanta 25 551 (1978)

37 J.Rudolph and K.Bachmann

Microchim Acta 1 477 (1979)

38 A.G.Hamlin

Anal Chem 35 2037 (1963)

39 W.S.Pappas

Anal Chem 40 2176 (1968)

40 N.C.Agliulov et al

J Anal Chem USSR 23 486 (1968)

41 L.G.Vlasov et al

Chem Abstr 60 2530 (1964)

42 T.S.Zvarova et al

J Chromatography 44 604 (1969)

43 T.S.Zvarova et al

ibid 49 290 (1970)

44 G.Guichon and C.Pommier

'GC in inorganics and organometallics'

Ann Arbor Science (1973)

45 R.S.Juvet and F.M.Wachi

Anal Chem 32 290 (1960)

46 F.M.Zado and R.S.Juvet in

'Gas Chromatography' Ed. A.B.Littlewood (1966)

47 J.F.Ellis et al

Anal Chim Acta 22 27 (1960)

48 J.F.Ellis et al

J Inorganic Nuc Chem 16 150 (1960)

49 K.Tanikawa and K.Arakawa

Chem Pharm Bull 13 926 (1965)

50 A.N.Nessmeyanov et al

Bull Acad Sci USSR 530 (1966)

51 G.G.Devyatyk et al

ibid 207 (1969)

52 P.Longi and R.Mozzochi

Chim Ind (Milan) 48 718 (1966)

53 S.A.Estes et al

J High Res Chrom and Chrom Comm 3 472 (1980)

54 R.Dijkstra et al

Z Anal Chem 181 399 (1961)

55 L.V.Guild et al

Anal Chem 33 1156 (1961)

56 H.J.Dawson

ibid 35 542 (1963)

57 C.Pommier and G.Guiochon

J Chrom Sci 8 486 (1970)

58 G.N.Turkel'Taub et al

Khim Tekhnol 12 58 (1967)

59 C.R.Hauser et al

Organic Reactions Vol(111)

J Wiley and Sons (NY 1954)

60 G.S.Hammond et al

J Amer Chem Soc 81 4682 (1959)

61 J.L.Burdett and M.T.Rogers

ibid 86 2150 (1964)

62 J.D.Park et al

ibid 75 4754 (1953)

63 J.C.Reid and M.Calvin

ibid 75 2948 (1950)

64 K.H.Meyer

Ann Physik 380 212 (1911)

65 R.LeFevre and M.Welsh

J Chem Soc 2230 (1949)

66 P.Grossman

Z Physik Chem 109 305 (1924)

67 K.H.Meyer and F.G.Wilson

Chem Ber 47 838 (1914)

68 H.S.Jarrett et al

J Chem Phys 21 2092 (1953)

69 C.S.Springer et al
Inorg Chem 6 1105 (1967)

70 C.A.Burdett and J.S.Fritz
Anal Chem 44 1738 (1972)

71 R.Filler and S.M.Naqvi
ibid 26 2571 (1961)

72 L.W.Reeves
Canad J Chem 35 1351 (1957)

73 N.V.Sidgwick and F.M.Brewer
J Chem Soc 127 2379 (1925)

74 G.T.Morgan and R.A.S.Castell
J Chem Soc 3252 (1928)

75 D.H.Dewar et al
ibid 688 (1964)

76 K.Nakamoto et al
J Amer Chem Soc 83 1066 (1961)

77 F.Bonati and G.Minghetti
J Organometallic Chem 22 5 (1970)

78 S.Tanatar and E.Kurovskii
J Russ Phys Chem Soc 40 580 (1909)

79 G.T.Morgan and H.W.Ross
J Chem Soc 105 195 (1914)

80 A.N.Nesmeyanov et al
J Organometal Chem 12 187 (1968)

81 G.S.Hammond et al
Inorg Chem 2 73 (1963)

82 R.Allman and H.Musso
Chem Ber 106 3001 (1973)

83 R.Allman et al

ibid 105 30 (1972)

84 R.H.Fish

J Amer Chem Soc 96 6664 (1974)

85 R.C.Meyrota et al

'Metal β-diketonates and allied derivatives'

Academic Press (London) 1978 p202

86 R.C.Mehrota et al

ibid p7

87 M.Lederer

Nature 176 462 (1955)

88 W.J.Biermann and H.Gesser

Anal Chem 32 1525 (1960)

89 A.A.Duswalt Jnr

Doctoral Diss Purdue Univ (1958)

90 R.D.Hill

M Sc Thesis Univ Manitoba (1962)

91 J.Janak

'Gas Chromatography' p306

Ed.R.P.W.Scott Butterworths (1960)

92 R.W.Moshier and R.E.Sievers

'Gas Chromatography of metal chelates'

Pergamon Press (1965)

93 R.G.Charles and M.A.Pawlikowski

J Phy Chem 62 440 (1958)

94 J.Von Hoene et al

ibid 62 1098 (1958)

95 K.Yamakawa et al

Chem Pharm Bull (Tokyo) (11) 11 1405 (1963)

96 C.G.MacDonald and J.S.Shannon

Australian J Chem 19 1545 (1966)

97 W.R.Wolf et al

Anal Chem 44 616 (1972)

98 W.G.Baldwin

M Sc Thesis Univ Manitoba (1961)

99 W.D.Ross

Anal Chem 35 1596 (1963)

100 R.E.Sievers et al

Inorg Chem 2 693 (1963)

101 J.C.Goan et al

ibid 2 1078 (1963)

102 R.E.Sievers et al

ibid 1 966 (1962)

103 R.Fontaine

Doctoral Diss Paris Univ (1972)

104 W.R.Wolf et al

Inorg Chem 11 1995 (1972)

105 W.D.Ross and G.Wheeler

Anal Chem 36 266 (1964)

106 M.Tanaka et al

Nippon Kag Zasshi 89 669 (1969)

107 G.P.Cartoni et al

'Gas Chromatography'

Butterworths p273

108 R.Kownatski et al

Fres Z Anal Chem 301 179 (1980)

109 K.S.Hui et al

Neurochem Research 2 495 (1977)

110 W.D.Ross et al
'Proc 8th Int Symp on GC' p369

111 W.D.Ross and R.E.Sievers
J Environ Sci Tech 3 927 (1969)

112 K.H.Eisentraut et al
Anal Chem 43 2003 (1971)

113 R.E.Sievers
Chem and Eng News 41 41 (July1963)

114 B.G.Schult and E.M.Larsen
J Amer Chem Soc 71 3250 (1949)

115 M.L.Morris et al
Inorg Chem 2 411 (1963)

116 C.A.Burdett and J.S.Fritz
Talanta 20 363 (1973)

117 R.W.Moshier and R.E.Sievers
'Gas Chromatography of metal chelates' p51
Pergamon Press (1965)

118 E.W.Berg and J.J.Chiang
Anal Chim Acta 40 101 (1968)

119 E.W.Berg and N.M.Herrera
ibid 60 117 (1972)

120 K.J.Eisentraut
J Amer Chem Soc 87 5254 (1965)

124 M.Tanaka et al
Anal Chim Acta 43 157 (1968)

125 P.C.Uden and C.R.Jenkins
Talanta 16 893 (1969)

126 W.D.Ross et al
'Gas Chromatography' p381
Ed. R.Stock (1970)

127 J.E.Schwarberg et al
Talanta 11 1213 (1964)

128 D.K.Albert
Anal Chem 36 2034 (1964)

129 R.D.Hill and H.Gesser
J Gas Chrom 1 11 (Oct1963)

130 R.Belcher et al
Anal Chim Acta 60 109 (1972)

131 T.Fujinaga and Y.Ogino
Bull Chem Soc Japan 40 434 (1967)

132 L.Sucre and W.Jennings
J High Res Chrom and Chrom Comm 3 452 (1980)

133 R.S.Juvet and R.Durbin
J Gas Chrom 1 14 (Dec1963)

134 Y.Talmi and A.W.Andren
Anal Chem 46 2122 (1974)

135 R.J.Lloyd
Doctoral Diss Univ Mass (1977)

136 S.Ahrland et al
Quart Rev Chem Soc 12 265 (1958)

137 E.Fromm and P.Zierch
Chem Ber 39 3599 (1906)

138 Z.Reyes and R.M.Silverstein
J Amer Chem Soc 80 6367 (1958)

139 S.E.Livingstone et al
Australian J Chem 19 1179 (1966)

140 S.E.Livingstone et al
ibid 21 1781 (1968)

141 S.H.H.Chaston et al
ibid 18 673 (1965)

142 E.Uhlemann et al
J Prack Chem 34 180 (1966)

143 A.Yokoyama et al
Chem Pharm Bull (Tokyo) 15 540 (1967)

144 G.Klose et al
Tetrahedron 22 2695 (1966)

145 K.Arnold and G.Klose
ibid 25 3775 (1969)

146 F.Duus and S.O.Lawesson
Ark Kemi 29 127 (1968)

147 R.Belcher et al
J Inorganic Nuc Chem 34 1017 (1972)

148 M.Cox and J.Darken
Coord Chem Rev 7 29 (1971)

149 S.E.Livingstone
ibid 7 59 (1971)

150 R.Belcher et al
J Inorganic Nuc Chem 33 1851 (1971)

151 R.Ho et al
Australian J Chem 19 1179 (1966)

152 P.C.Uden and D.E.Henderson
Analyst 102 889 (1977)

153 R.S.Barratt et al
Anal Chim Acta 59 59 (1972)

154 N.H.Cromwell

Chem Rev 38 83 (1946)

155 R.H.Holm et al

Prog Inorg Chem 7 83 (1966)

156 D.M.Parees

Doctoral Diss Univ Mass (1976)

157 M.Miyazaki et al

Chem Pharm Bull 14 117 (1966)

158 R.Belcher et al

Anal Chem 45 1197 (1973)

159 R.Belcher et al

Chem Comm 41 (1971)

160 P.C.Uden and K.Blessel

Inorg Chem 12 352 (1973)

161 P.C.Uden and D.E.Henderson

J Chrom 99 309 (1974)

162 S.Dilli and E.Patsalides

ibid 130 251 (1977)

163 R.Belcher et al

J Inorganic Nuc Chem 35 1127 (1973)

164 P.J.Clark

Doctoral Diss Univ Mass (1977)

165 P.C.Uden et al

J Chrom Sci 12 591 (1974)

166 P.C.Uden and B.A.Waldman

Anal Lett 8 91 (1975)

167 T.J.Cardwell et al

Inorg Nuc Chem Lett 10 3283 (1974)

168 N.M.Karrayannis and A.H.Corwin
Anal Biochem 26 34 (1968)

169 N.M.Karrayannis and A.H.Corwin
J Chrom 47 247 (1970)

170 O.Samuelson
'Ion exchange separations in Analytical Chemistry'
J.Wiley and Sons (NY) (1963)

171 U.A.Th.Brinkman and G.deVries
J Chrom 85 187 (1973)

172 H.Veening et al
Chem Comm 1305 (1969)

173 J.F.K.Huber et al
Anal Chem 44 1554 (1972)

174 C.A.Tollinche and T.H.Risby
J Chrom Sci 16 448 (1978)

175 M.Lohmuller et al
J Chrom 137 165 (1977)

176 J.W.O'Laughlin and T.R.O'Brien
Anal Lett (All) 829 (1978)

177 E.Gaetani et al
Anal Chem 48 1725 (1976)

178 E.B.Edward-Inatimi et al
Anal Proc 40 (Feb1980)

179 T.Tande et al
Chromatographia 13 607 (1980)

180 O.Liska et al
J Chrom 171 145 (1979)

181 O.Liska et al
ibid 172 379 (1979)

182 O.Liska et al

ibid 172 384 (1979)

183 E.Gaetani et al

Annali di Chim 69 181 (1979)

184 F.Walters

Doctoral Diss Univ Mass (1976)

185 L.B.Hilliard and H.Freiser

Anal Chem 24 752 (1952)

186 C.S.Hambali and P.R.Haddad

Chromatographia 14 341 (1981)

187 R.E.Majors

Inter Lab 7 (10) 11 (1975)

188 V.Rehak and E.Smolkova

Chromatographia 9 219 (1976)

189 L.C.Hansen and R.E.Sievers

J Chrom 99 123 (1974)

190 P.C.Uden et al

Anal Chim Acta 101 99 (1978)

191 G.Schwedt

Fres Z Anal Chem 295 382 (1979)

192 J.M.Hill

J Chrom 76 455 (1973)

193 A.J.Baumann et al

Anal Chem

194 A.Haas et al

Chromatographia 14 341 (1981)

195 R.C.Mehrota et al

'Metal β-diketonates and allied derivatives'

Academic Press (London) (1978) pp 141 - 190

196 M.Calvin and K.W.Wilson
J Amer Chem Soc 67 2003 (1945)

197 J.P.Collman et al
Chem and Ind 1213 (1960)

198 J.P.Collman et al
Inorg Chem 1 704 (1962)

199 J.P.Collman
'Transition metal chemistry' p 1,35
Marcel Dekker (NY)(1966) Vol 2

200 R.L.Belford et al
J Inorganic Nuc Chem 2 11 (1956)

201 R.H.Holm and F.A.Cotton
J Amer Chem Soc 80 5658 (1958)

202 J.P.Fackler et al
Inorg Chem 2 97 (1963)

203 P.R.Singh and R.Sahai
J Indian Chem Soc 46 945 (1969)

204 P.R.Singh and R.Sahai
Australian J Chem 22 1169 (1969)

205 F.A.Matesen
'Technique of organic chemistry'
InterScience (NY)(1957) p 686

206 L.Wish and R.A.Bolomey
J Amer Chem Soc 72 4486 (1950)

207 T.Sasaki et al
J Org Chem 33 680 (1968)

208 J.A.S.Smith and J.D.Thawaites
Disc Faraday Soc 34 143 (1962)

209 R.G.Linck and R.E.Sievers
Inorg Chem 5 806 (1966)

210 J.A.S.Smith and E.J.Wilkins
J Chem Soc (A) 1749 (1966)

211 T.J.Pinnavaia and R.C.Fay
Inorg Chem

212 S.Chattoraj et al
ibid 7 2501 (1968)

213 D.R.Eaton
J Amer Chem Soc 87 3097 (1965)

214 M.Raban et al
ibid 99 6527 (1977)

215 H.G.Brittain
Inorg Chem 14 2858 (1975)

216 E.Isfan and A.Barabas
Revue Rom de Chemie 18 667 (1973)

217 F.H.Brain and C.S.Gibson
J Chem Soc 762 (1939)

218 J.C.Hammel and J.A.S.Smith
ibid 1855 (1970)

219 A.Trestianu et al
Tetrahedron 24 2499 (1966)

220 R.C.Fay and T.S.Piper
J Amer Chem Soc 84 2303 (1962)

221 J.LeComte
Disc Faraday Soc 9 125 (1950)

222 L.J.Bellamy and R.F.Branch
J Chem Soc 4491 (1954)

223 H.F.Holtzclaw and J.P.Collman

J Amer Chem Soc 79 3318 (1957)

224 K.Nakamoto and E.Martel

J Chem Phys 32 558 (1960)

225 K.Nakamoto et al

ibid 66 346 (1962)

226 M.Mikami et al

Spectnochim Acta A23 1037 (1967)

227 S.Pinchas et al

J Chem Phys 46 1506 (1965)

228 G.T.Behnke and K.Nakamoto

Inorg Chem 6 433 (1967)

229 G.T.Behnke and K.Nakamoto

ibid 6 440 (1967)

230 K.C.Joshi and V.N.Pathak

Indian J Chem 10 485 (1972)

231 K.C.Joshi and V.N.Pathak

J Inorganic Nuc Chem 35 3161 (1973)

232 R.West amd R.Riley

ibid 5 295 (1958)

233 E.Boschmann

Proc Indiana Acad Sci 80 151 (1970)

234 Grove and Willis

J Chem Soc 877 (1951)

235 L.J.Bellamy and L.Beecher

ibid 4487 (1954)

236 M.L.Eidenoff

J Amer Chem Soc 67 2072 (1945)

237 L.G.Van Uitert and W.C.Fernelius
ibid 76 5887 (1954)

238 H.S.Harned and B.B.Owen
Physical Chemistry of Electrolyte Solutions
Reinhold. (NY) 1950 p548

239 B.P.Block and G.H.McIntyre Jnr
J Amer Chem Soc 75 5667 (1953)

240 D.E.Goldberg
J Chem Educ 7 341 (1963)

241 W.C.Fernelius and L.G.Van Uitert
Acta Chem Scand 8 1726 (1954)

242 W.C.Fernelius et al
J Phys Chem 58 1133 (1954)

243 L.G.Van Uitert and W.C.Fernelius
J Amer Chem Soc 75 2736-3862 (1953)

244 V.E.Uhlemann and E.Frank
Z Anorg Allg Chem 340 319 (1965)

245 G.A.Gutter and G.S.Hammond
J Amer Chem Soc 81 4686 (1959)

246 W.C.Fernelius et al
J Phys Chem 59 80 (1955)

247 R.L.Lintvedt et al
Inorg Chem 5 1603 (1960)

248 L.G.Van Uitert
J Amer Chem Soc 75 457 (1953)

249 R.F.Handy and R.L.Lintvedt
Inorg Chem 13 893 (1947)

250 R.C.Larsen and R.T.Iwamoto
J Amer Chem Soc 82 3526 (1960)

251 H.Taube
Canadian J Chem 37 129 (1959)

252 G.S.Patterson and R.H.Holm
Inorg Chem 11 2285 (1972)

253 K.J.Eisentraut and R.E.Sievers
J Inorganic Nuc Chem 29 1931 (1967)

254 E.W.Berg
J Phys Chem 64 487 (1960)

255 K.Utsunomiya
Bull Chem Soc Japan 44 2688 (1971)

256 E.W.Berg and J.T.Truemper
Anal Chim Actc 32 245 (1965)

257 A.Smith and A.Menzies
J Amer Chem Soc 32 1412 (1910)

258 H.S.Booth and H.S.Halbedel
ibid 68 2652 (1946)

259 J.L.Wood and M.M.Jones
Inorg Chem 3 1553 (1964)

260 J.L.Wood and M.M.Jones
J Inorganic Nuc Chem 32 113 (1i67)

261 G.K.Schweitzer
Anal Chim Acta 43 332 (1968)

262 W.A.Frankhauser
M.Sc Thesis Air Force Inst Tech (1965)

263 R.A.Shulstad
M.Sc Thesis Air Force Inst Tech (1968)

264 J.E.Sicre et al
J Amer Chem Soc 91 3476 (1969)

265 H.A.Swain and D.G.Karraker
J Inorganic Nuc Chem 33 2851 (1971)

266 H.A.Swain and D.G.Karraker
Inorg Chem 9 1766 (1970)

267 H.G.Weidemann
Thermochim Acta 3 355 (1972)

268 S.J.Ashcroft
ibid 2 512 (1971)

269 T.Fujinaga et al
Talanta 18 429 (1971)

270 T.Fujinaga et al
Anal Chim Acta 71 141 (1974)

271 T.Fujinaga et al
Talanta 28 295 (1981)

272 K.Neeb
Z Anal Chem 194 255 (1963)

273 W.Geilmann et al
ibid 190 60 (1962)

274 W.Geilmann
Ang Chem 67 26 (1955)

275 A.Meyer et al
Z Anal Chem 281 201 (1976)

276 O.Pitak
Chromatographia 2 304 (1969)

277 C.Pommier et al
Bull Soc Chim France 1401 (1969)

278 D.N.Sokolov and N.A.Vakin

J Chrom Sci 10 417 (1972)

279 R.S.Juvet and R.L.Fisher

Anal Chem 37 1752 (1965)

280 S.N.Chesler and R.S.Juvet

J Chrom Sci 11 320 (1973)

281 I.Tohyama and K.Otzhi

Z Anal Chem 262 246 (1972)

282 J.Rudolph and K.Bachmann

J Chrom 187 319 (1980)

283 U.Hamm and K.Bachmann

Z Anal Chem 306 183 (1981)

284 S.Tsalas and K.Bachmann

Talanta 27 201 (1980)

285 S.Moriguchi and S.Takei

Chromatographia 7 49 (1974)

286 E.F.Barry and N.H.C.Cooke

J Chrom 104 161 (1974)

287 F.Vernon

ibid 60 406 (1971)

288 C.Y.Liang et al

J Inorganic Nuc Chem 32 811 (1970)

289 .Koshy et al

J Chrom Soc 13 97 (1975)

290 T.Nambara et al

J.Chrom 114 81 (1975)

291 M.N.Bochkarev et al

ibid 170 53 (1979)

292 W.I.Stephen

Proc. Soc. Anal Chem 137 (1972)

293 Personal Communication

B.Oliver, CHN Analysis Ltd.,

Loughborough, Leics.

294 Titration in Non-Aqueous Media

I.Gyenes. Illiffe Books Ltd. (1967)

295 R.L.Lintvedt and H.F.Holtzclaw Jnr.

J.Amer. Chem. Soc 88 2713 (1966)

296 S.F.Spencer

Anal Chem 35 592 (1963)

297 L.R.Snyder

J Chrom Sci 16 137 (1978)

298 Principles of Adsorption Chromatography

L.R.Snyder. Marcel Dekker, N.Y. (1968)

299 Du Pont Technical Report

Non-Aqueous Reversed Phase Chromatography

300 R.R.Heath and P.E.Sonnet

J Liquid Chrom 3 1129 (1980)

301 K.T.DenBleyker et al

Chromatographia 17 449 (1983)

Appendix 1

```
 3 PRINT"THIS PROGRAM CALCULATES PK VALUES"
 4 PRINT"FROM PH TITRATIONS"
 5 PRINT"INPUT INITIAL SOLN VOLUME"
 10 INPUT I
 15 PRINT"HOW MANY READINGS ?"
 17 INPUT R
 18 PRINT"LIGAND CONCENTRATION IN MMOLES ?"
 20 INPUT L
 25 PRINT"MOLARITY OF BASE TITRANT ?"
 26 INPUT M
 27 FOR C=1 TO R
 30 PRINT"TITRE VALUE ?"
 35 INPUT T
 37 REM  E= MOLE FRACTION DIOXAN
 40 E=0.34/(0.34+((10+T)/18))
 50 U=(5.1*E)-0.876
 80 Z=L/(T+I)
 90 X=(T*M)/(T+I)
 100 PRINT"CONCN OF OH =",X
 110 PRINT"VALUE OF LOG(1/G) ?"
 120 INPUT G
 140 PRINT"EXPERIMENTAL PH ?"
 150 INPUT B
 170 P=B+U-G
 180 H=10↑(-P)
 190 N=(Z-X-H)/Z
 195 IF N>=1 THEN 500
 200 Q=N/(H-H*N)
 210 A=LOG(Q)/2.303
 220 K=A+(2*G)
 225 OPEN2,4
 227 CMD2
 230 PRINT
 240 PRINT"N=",N
 245 PRINT
 250 PRINT"PK=",K
 260 PRINT
 300 PRINT"CALCULATED PH=",P
 320 PRINT
 350 PRINT"EXPERIMENTAL PH=",B
 400 PRINT
 410 PRINT#2
 420 CLOSE2
 470 NEXT C
 500 END
READY.
```

Appendix 2

```
10 PRINT"THIS PROGRAM CALCULATES "
20 PRINT"PARAMETERS FOR FORMATION "
25 PRINT"CONSTANT CURVES "
30 PRINT"INITIAL SOLUTION VOLUME ?"
40 INPUT I
50 PRINT"HOW MANY READINGS ?"
60 INPUT R
70 PRINT"MOLARITY OF BASE TITRANT ?"
80 INPUT M
90 PRINT"LIGAND CONCN IN MMOLES ?"
100 INPUT L
150 PRINT"METAL CONCN IN MMOLES ?"
160 INPUT C
170 PRINT"VALUE OF LIGAND PK ?"
180 INPUT K
200 FOR J=1 TO R
210 PRINT"EXPERIMENTAL PH ?"
220 INPUT B
230 PRINT"TITRE VALUE ?"
240 INPUT T
241 REM E=MOLE FRACTION DIOXAN
243 E=0.34/(0.34+((10+T)/18))
245 U=(5.1*E)-0.876
250 REM CONCN OF BASE = X
260 X=(T*M)/(T+I)
270 REM SOLUTION CONCN LIGAND=Z
280 Z=L/(T+I)
290 REM SOLN CONCN OF METAL = D
300 D=C/(T+I)
310 REM MEAN MOLARITY = F
320 F=1.59*(D-X)+(2*X)
330 PRINT"MEAN SOLUTION ION ACTIVITY=",F
340 PRINT"VALUE OF LOG(1/G) ?"
350 INPUT G
370 REM P=CALCULATED PH
380 P=B+U-G
390 REM HYDROGEN ION CONCN = H
400 H=10↑(-P)
430 S=K-(G*2)
440 W=10↑(S)
445 REM Y=FREE LIGAND ANION CONCN
450 Y=(Z-X-H)/(W*H)
455 REM N=AV. NO. H IONS PER ANION
460 N=(Z-((W*H)+1)*Y)/D
480 OPEN 2,4
490 CMD2
500 PRINT"VALUE OF LOG(1/G)=",G
505 PRINT
510 PRINT"CALCULATED PH=",P
520 PRINT
530 PRINT"EXPERIMENTAL PH=",B
535 PRINT
540 PRINT"N=",N
542 PRINT
545 PRINT"-LOG(FREE ANION CONCN)=",-(LOG(Y))/2.303
550 PRINT#2
555 CLOSE2
700 NEXT J
900 END
READY.
```